

SANDIA REPORT

SAND94-0308 • UC-722

TTC-1294

Unlimited Release

Printed May 1994

AD-A279 915



Impact Testing of the H1224A Shipping/Storage Container

D. C. Harding, J. G. Bobbe, D. R. Stenberg, M. Arviso

Prepared by
Sandia National Laboratories
Albuquerque, New Mexico 87185 and Livermore, California 94550
for the United States Department of Energy
under Contract DE-AC04-94AL85000

Approved for public release; distribution is unlimited.

O
DTIC
ELECTED
JUN 02 1994
S G D

231 94-16309



DTIC QUALITY INSPECTED 1

Issued by Sandia National Laboratories, operated for the United States Department of Energy by Sandia Corporation.

NOTICE: This report was prepared as an account of work sponsored by an agency of the United States Government. Neither the United States Government nor any agency thereof, nor any of their employees, nor any of their contractors, subcontractors, or their employees, makes any warranty, express or implied, or assumes any legal liability or responsibility for the accuracy, completeness, or usefulness of any information, apparatus, product, or process disclosed, or represents that its use would not infringe privately owned rights. Reference herein to any specific commercial product, process, or service by trade name, trademark, manufacturer, or otherwise, does not necessarily constitute or imply its endorsement, recommendation, or favoring by the United States Government, any agency thereof or any of their contractors or subcontractors. The views and opinions expressed herein do not necessarily state or reflect those of the United States Government, any agency thereof or any of their contractors.

Printed in the United States of America. This report has been reproduced directly from the best available copy.

Available to DOE and DOE contractors from
Office of Scientific and Technical Information
PO Box 62
Oak Ridge, TN 37831

Prices available from (615) 576-8401, FTS 626-8401

Available to the public from
National Technical Information Service
US Department of Commerce
5285 Port Royal Rd
Springfield, VA 22161

NTIS price codes
Printed copy: A11
Microfiche copy: A01

SAND94-0308
TTC-1294
Unlimited Release
Printed May 1994

Distribution
Category UC-722

Impact Testing of the H1224A Shipping/Storage Container*

D. C. Harding, J. G. Bobbe, D. R. Stenberg, and M. Arviso
Transportation Systems Technology and Development Departments 6642 and 6643
Sandia National Laboratories**
Albuquerque, NM 87185

Abstract

H1224A weapons containers have been used for years by the Departments of Energy and Defense to transport and store W78 warhead midsections. Although designed to protect these midsections only in low-energy handling drop and impact accidents, a recent transportation risk assessment effort has identified a need to evaluate the container's ability to protect weapons in higher-energy environments. Four impact tests were performed on H1224A containers with W78 Mod 6c mass mockup midsections inside, onto an essentially unyielding target. Dynamic acceleration and strain levels were recorded during the side-on and end-on impacts, each at 12.2 m/s (40 ft/s) and 38.1 m/s (125 ft/s). Measured peak accelerations experienced by the midsections during lower velocity impacts ranged from 250 to 600 Gs for the end-on impact and 350 to 600 Gs for the side-on impact. Measured peak accelerations of the midsections during the higher velocity impacts ranged from 3,000 to 10,000 Gs for the end-on impact and 8,000 to 10,000 Gs for the side-on impact. Deformations in the H1224A container ranged from minimal to severe buckling and weld tearing. At higher impact velocities, the H1224A container may not provide significant energy absorption for the re-entry vehicle midsection but can provide some confinement of potentially damaged components.

* This work was performed at Sandia National Laboratories, Albuquerque, New Mexico, and sponsored by the Defense Nuclear Agency under DNA MIPR #93-837 Work Unit #00165.

** A U. S. Department of Energy Facility

Acknowledgments

Thanks to J. Calderone and L. A. Abeyta (2761) for test support. W. L. Uncapher (6642) and M. Hankinson (6642) provided data acquisition and reduction support, and Glenn Hohnstreiter (6642) provided management support throughout this investigation. Program management was provided by P. E. D'Antonio (12324), C. G. Shirley (12333) and J. D. Pierce (6642). C. L. Carrington (7432) assisted with security issues. Thanks also to D. J. Ammerman (6642) and P. E. McConnell (6643) for their draft document review.

Table of Contents

List of Figures	4
List of Tables	6
Nomenclature	7
1. Introduction.....	8
2. Impact Test Parameters	10
3. Test Hardware and Inspections.....	14
4. Instrumentation	21
5. Results.....	41
5.1 Longitudinal Low Velocity.....	41
5.2 Horizontal Low Velocity	48
5.3 Longitudinal High Velocity	56
5.4 Horizontal High Velocity.....	65
6. Conclusions.....	73
References.....	74
Appendix A. LLV Accelerometer and Strain Gage Data: Raw, Filtered, and Reduced...76	
Appendix B. HLV Accelerometer and Strain Gage Data: Raw, Filtered, and Reduced 109	
Appendix C. LHV Accelerometer and Strain Gage Data: Raw, Filtered, and Reduced 139	
Appendix D. HHV Accelerometer and Strain Gage Data: Raw, Filtered, and Reduced 172	
Appendix E. Inspection Reports	201
Distribution	228

Accesion For	
NTIS	CRA&I
DTIC	TAB
Unannounced	
Justification _____	
By _____	
Distribution / _____	
Availability Codes	
Dist	Avail and/or Special
A-1	

List of Figures

1.1	W78 midsection inside H1224A shipping/storage container.....	9
2.1	Longitudinal (end-on) container impact test set-up	11
2.2	Horizontal (side-on) container impact test set-up	12
2.3	Low-velocity impact target.....	13
2.4	High-velocity impact target	13
3.1	H1224 / H1224A container body photograph.....	15
3.2	H1224A lower flexible foam insert and plywood load spreader	16
3.3	RV midsection with threaded fore plate and aft cover	16
3.4	RV midsection inside inner container and foam and H1224A outer shell	17
3.5	Mk12a Mod6c schematic with internal weight plates	17
3.6	H1224A container body measurement locations	18
3.7	H1224A inner container measurement locations	19
3.8	Mk12A midsection and fore and aft cover measurement locations.....	20
4.1	Strain gage locations for longitudinal impact tests	23
4.2	Strain gage locations for horizontal impact tests	25
4.3	Accelerometer locations for longitudinal impact tests.....	27
4.4	Accelerometer locations for horizontal impact tests.....	30
4.5	LLV mounting locations for A1, A2, S1, S15, S16, and terminal strips	33
4.6	LLV mounting location for A4	33
4.7	LLV mounting location for A6 and A12	34
4.8	LLV mounting locations for A8, A9, A13, and S14.....	34
4.9	LLV mounting locations for A10 and A11	35
4.10	LLV mounting location for S4 and S5.....	35
4.11	LLV mounting location for S6 and S7	36
4.12	LLV mounting location for S12 and S13.....	36
4.13	HLV mounting locations for A1, A2, A3, and some terminal strips	37
4.14	HLV mounting location for A5.....	37
4.15	HLV mounting location for A6, A7, and A15.....	38
4.16	HLV mounting location for A12 and A13.....	38
4.17	HLV mounting locations for S2, S4, and S6	39
4.18	HLV mounting location for more terminal strips	40
4.19	HLV mounting location for S7	40
5.1.1	LLV impact test pre-drop.....	42
5.1.2	LLV H1224A post-test deformation	43
5.1.3	LLV H1224A weld crack.....	44
5.1.4	LLV upper foam insert joint separation	45
5.1.5	LLV inner container weld tears	45
5.1.6	LLV fore plate bending.....	46
5.1.7	LLV H1224A bottom pan deformation	46
5.1.8	LLV fore plate (nose end, RV) accelerations	47
5.1.9	LLV aft cover (tail end, RV) accelerations.....	47

5.2.1	HLV impact test pre-drop	49
5.2.2	HLV H1224A top-end post-test deformation	50
5.2.3	HLV H1224A bottom-end post-test deformation	51
5.2.4	HLV inner container bending	52
5.2.5	HLV H1224A outer shell mid-body bending	52
5.2.6a	HLV Mk12a Mod6c cracking	53
5.2.6b	HLV Mk12a Mod6c cracking	53
5.2.7	HLV RV weight plate bolt shearing	54
5.2.8	HLV aft cover (tail end, RV) accelerations (2 kHz filter)	55
5.2.9	HLV fore plate (nose end, RV) accelerations (2 kHz filter)	55
5.3.1	LHV impact test pre-drop	57
5.3.2a	LHV H1224A post-test deformation	58
5.3.2b	LHV H1224A post-test deformation	59
5.3.2c	LHV H1224A post-test deformation	59
5.3.3	LHV inner container buckling	60
5.3.4	LHV aft cover below top level of inner container	60
5.3.5	LHV Mk12a Mod6c aeroshell fracture and weight plate detachment	61
5.3.6	LHV RV carbon phenolic aeroshell fracture	62
5.3.7	LHV RV aeroshell nose-end fracture and impact onto accelerometers	63
5.3.8	LHV fore plate deformation	63
5.3.9	LHV fore plate (nose end, RV) accelerations	64
5.3.10	LHV aft cover (tail end, RV) accelerations	64
5.4.1	HHV impact test pre-drop	66
5.4.2a	HHV H1224A post-test deformation	67
5.4.2b	HHV H1224A post-test deformation	67
5.4.2c	HHV H1224A post-test deformation	68
5.4.3	HHV fore plate deformation and bolt shearing	69
5.4.4	HHV inner container and aft cover deformation	69
5.4.5	HHV H1224A outer shell deformation	70
5.4.6	HHV Mk12a Mod6c aeroshell fracture and detached weight plates	70
5.4.7	HHV RV carbon phenolic aeroshell fracture	71
5.4.8	HHV fore plate (nose end, RV) accelerations	72
5.4.9	HHV aft cover (tail end, RV) accelerations	72

List of Tables

2.1	Test Matrix for H1224A Impact Testing	10
4.1	Longitudinal Impact Instrumentation Requirements--Strain Gages.....	24
4.2	Horizontal Impact Instrumentation Requirements--Strain Gages.....	26
4.3a	Longitudinal 40 ft/sImpact Instrumentation Requirements--Accelerometers	28
4.3b	Longitudinal 125 ft/sImpact Instrumentation Requirements--Accelerometers ..	29
4.4a	Horizontal 40 ft/sImpact Instrumentation Requirements--Accelerometers	31
4.4b	Horizontal 125 ft/sImpact Instrumentation Requirements--Accelerometers	32
E 1.1	LLV H1224A Container Body Inspection Data	201
E 1.2	LLV Inner Container Inspection Data	205
E 1.3	LLV RV, Fore, and Aft Cover Inspection Data.....	206
E 2.1	HLV H1224A Container Body Inspection Data.....	207
E 2.2	HLV Inner Container Inspection Data.....	211
E 2.3	HLV RV, Fore, and Aft Cover Inspection Data	212
E 3.1	LHV H1224A Container Body Inspection Data.....	214
E 3.2	LHV Inner Container Inspection Data.....	217
E 3.3	LHV RV, Fore, and Aft Cover Inspection Data	219
E 4.1	HHV H1224A Container Body Inspection Data	220
E 4.2	HHV Inner Container Inspection Data	224
E 4.3	HHV RV, Fore, and Aft Cover Inspection Data	225

Nomenclature

LLV	Longitudinal Low-Velocity impact test
HLV	Horizontal Low-Velocity impact test
LHV	Longitudinal High-Velocity impact test
HHV	Horizontal High-Velocity impact test
RV	Re-entry Vehicle midsection mass mock-up
WR	War Reserve
STS	Stockpile-to-Target Sequence
G	Acceleration of Gravity
ms	milliseconds
m	Mass
V	Velocity

Impact Testing of the H1224A Shipping/Storage Container

1. Introduction

Based on the results of recent Congressional and Department of Defense studies [1-3], the Defense Nuclear Agency (DNA) has commenced a program to assess the safety of the Minuteman III/W78/W87 weapon system in the form of a probabilistic risk assessment. The Minuteman III Weapon System Safety Assessment (WSSA) requires determination of the potential physical environments surrounding the W78 and W87 re-entry vehicles caused by credible accidents during air and ground transportation. Impact testing of the H1224A storage/shipping container is necessary to quantify the impact mitigation provided by the structure and determine boundary conditions for analytical modelling of weapon response during potential C-141 aircraft and ground transportation accident scenarios associated with the W78's Stockpile-to-Target Sequence (STS) [4].

The aluminum H1224A storage/shipping container is approximately 1.4 m (54 in.) high and 0.82 m (33 in.) in diameter with a flexible polyurethane foam lining for cushioning (see Figure 1.1). The H1223B consists of an internal container and fore and aft threaded covers for the re-entry vehicle (RV) midsection. The H1224A container's original design intent was to protect W78 RV midsections from relatively light loadings associated with vibrations during shipping and handling, as well as providing protection against weather during storage. Previous testing of H1224A containers encompassed only vibration and minor handling drops [5-14]. Although not designed to provide significant RV impact mitigation during higher-speed accidents, the WSSA requires quantification of load levels during extreme accident conditions. Specifically, Weidlinger Associates (a contractor to DNA for this study) required RV and H1224A container acceleration histories during four different impact conditions to validate analytical predictions they were tasked to perform.

A series of four container impact tests (two impact orientations, each at low and high velocities) onto an essentially unyielding surface have been conducted to determine warhead midsection loadings during postulated severe accident conditions and to validate finite element model predictions. Accelerometers, strain gages, and photometric instrumentation were used to record container deformations and loads transmitted to the container and re-entry vehicle during impact testing. Computer modelling will be used to predict weapon response throughout the range of accident conditions, including impact, puncture, and crush environments.

Test results are described in terms of measured container and RV deceleration histories for each of the four impact tests and subsequent structural deformations. Raw and reduced acceleration and strain data are included with deformation measurements in the appendices.

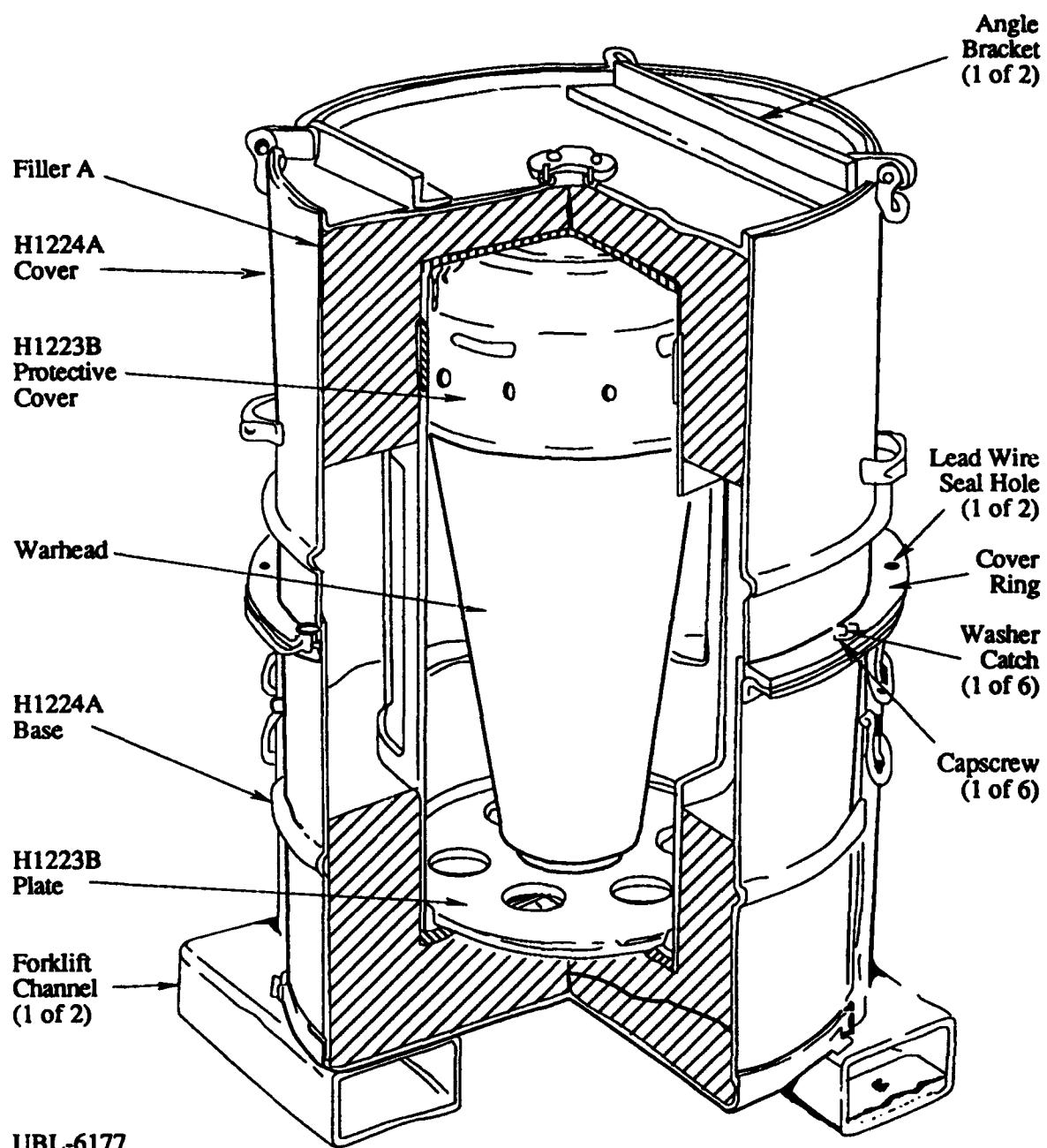


Figure 1.1 W78 midsection inside H1224A shipping/storage container

2. Impact Test Parameters

Impact test velocities were determined jointly with Weidlinger Associates (Los Altos, California), to encompass a wide range of impact energies and validate analytical model predictions. Impacts at 12.2 m/s (40 ft/s) and 38.1 m/s (125 ft/s) in both end-on and side-on orientations onto an essentially unyielding target were selected. To ensure flat impacts in these two orientations, two parallel cables were used to guide the container to a point just above the target surface, where the container was released to continue freely toward impact, as shown schematically in Figures 2.1 and 2.2. The four impact tests are outlined below in Table 2.1.

Table 2.1 Test Matrix for H1224A Impact Testing

<u>Test</u>	<u>Container Orientation</u>	<u>Impact Velocity</u>	<u>Drop Height</u>
1	Longitudinal (end-on) (LLV)	12.2 m/s (40 ft/s)	8.2 m (27 ft)
2	Horizontal (side-on) (HLV)	12.2 m/s (40 ft/s)	7.9 m (26 ft)
3	Longitudinal (end-on) (LHV)	38.1 m/s (125 ft/s)	86 m (283 ft)
4	Horizontal (side-on) (HHV)	38.1 m/s (125 ft/s)	88 m (288 ft)

Two different targets were used to conduct container impact tests, each essentially unyielding. The two lower-velocity drop tests were conducted at the 185-ft drop tower of Sandia National Laboratories, consisting of a steel plate grouted to two concrete blocks, as shown in Figure 2.3. The steel is 91 cm x 244 cm x 13 cm (3 ft x 8 ft x 5 in) and provides the smooth target surface. The bottom concrete block is 168 cm x 332 cm x 61 cm (5.5 ft x 11 ft x 2 ft) of 5000 lb/in² reinforced concrete. The top concrete block is the same material but only 30.5 cm (12 in) thick. The overall mass of the target is over 10,000 kg (22,000 lb).

The two higher-velocity drop tests were conducted at Sandia's Aerial Cable Facility in Coyote Test Field, consisting of a 1520 m (5000 ft) long wire rope suspended across a mountain canyon. The target consists of 910,000 kg (2,000,000 lb) of reinforced concrete and steel, partially resting on bedrock. A battleship armor plate 3 m x 8.5 m and 10 cm to 20 cm thick is welded to the concrete reinforcing members and coupled to the concrete by a high-strength grout. The dimensions and construction of this target are shown in Figure 2.4.

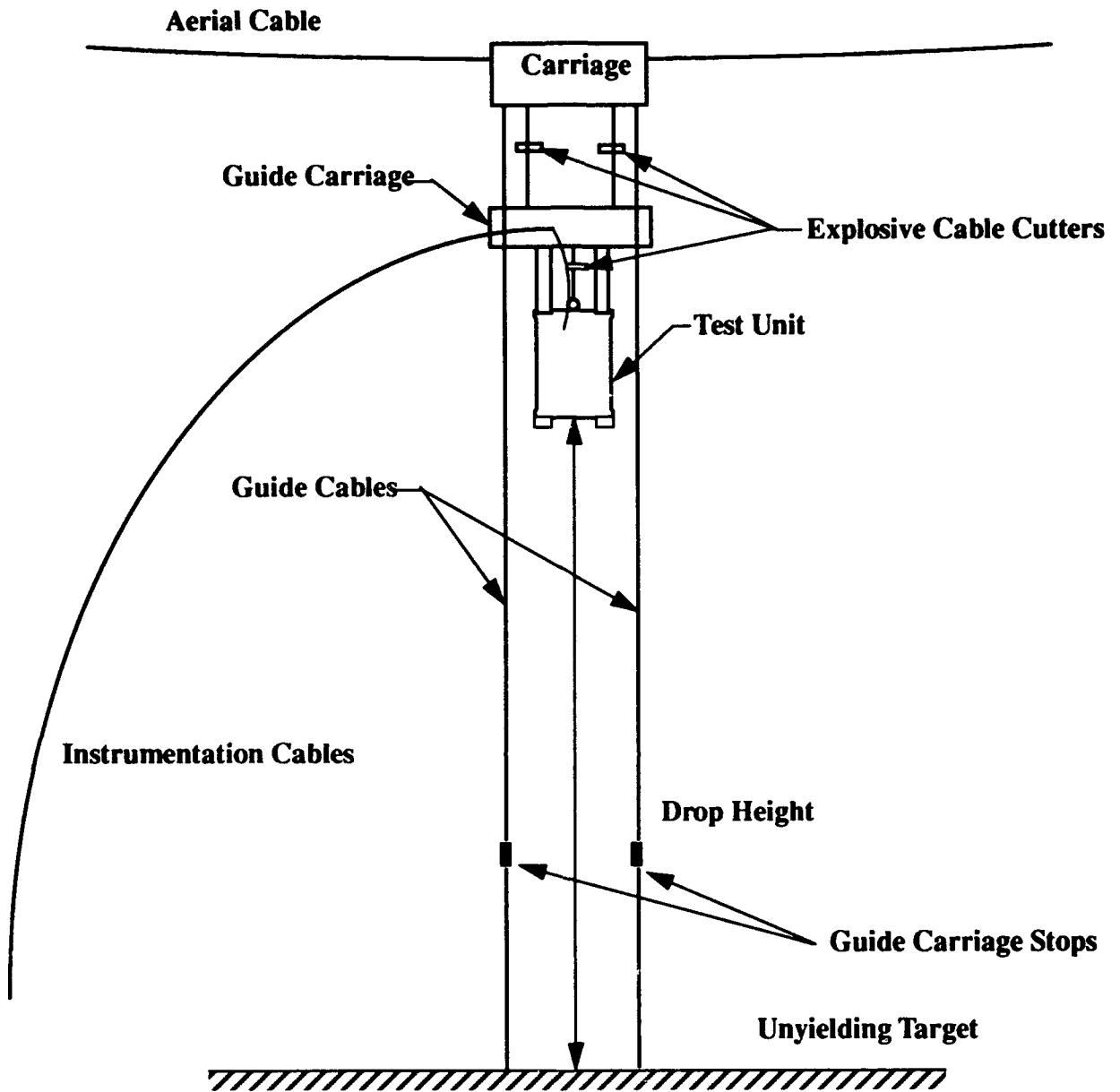


Figure 2.1 Longitudinal (end-on) container impact test set-up

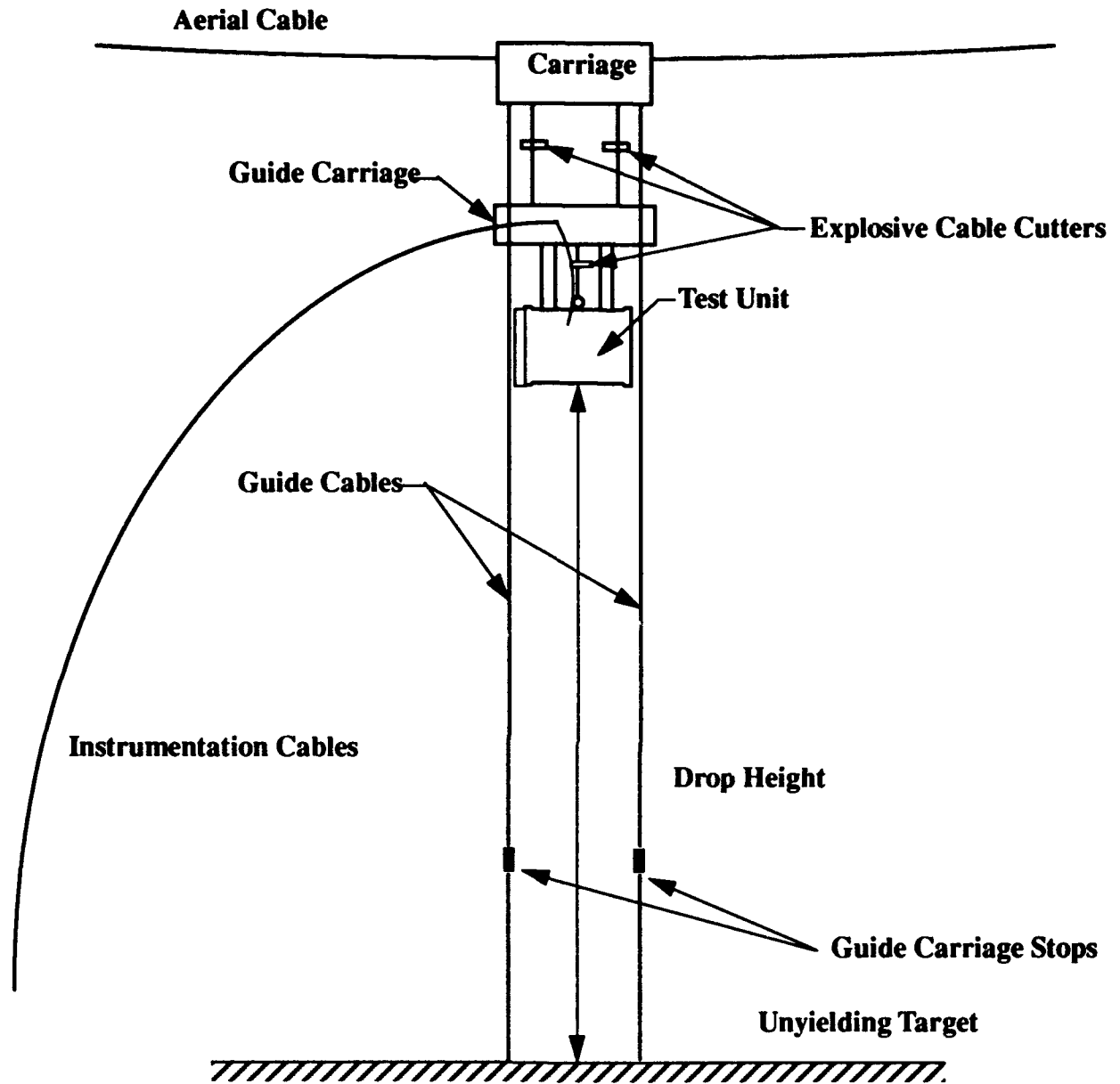


Figure 2.2 Horizontal (side-on) container impact test set-up



Figure 2.3 Low-velocity impact target

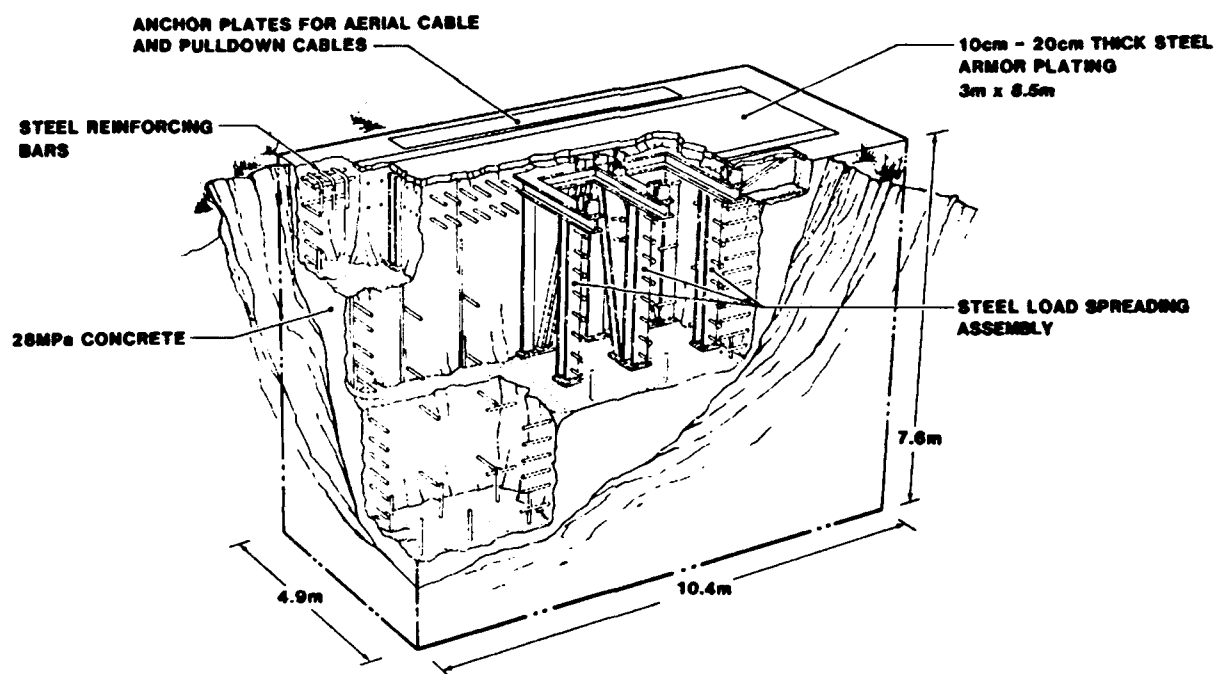


Figure 2.4 High-velocity impact target

3. Test Hardware and Inspections

The H1224A shipping/storage container basically consists of a 2.3 mm (0.091 in.) thick 6061-T4 aluminum cylindrical outer shell approximately 1.4 m (54 in.) high and 0.82 m (33 in.) in diameter with a flexible polyurethane foam lining for RV cushioning [15] (see Figures 1.1 and 3.1). Fork lift channels are welded to the base for ease of handling. Its weight is approximately 145 kg (320 lb) without the RV inside. Flexible polyurethane foam vibration and light shock isolation is provided by the approximately 0.12 m (4.8 in.) thick General Plastics Last-a-Foam TF-5070 inserts, which can deform and "bounce back" elastically.

The H1224A's cylindrical outer container shell is assembled in two halves, the base and the cover, by tightening bolts around a thin steel flange at the mid-body level. A thin silicone rubber gasket provides a light weather seal between the base and cover outer shell sections. Filler A and filler B denote the upper and lower foam inserts, the lower of which is 20 mm (0.8 in.) thicker than the upper. A 3.2 mm (0.125 in.) thick cylindrical aluminum inner container assembly holds the RV midsection and assists with load spreading to the flexible foam inserts. The inner container assembly includes a 3.2 mm (0.125 in.) aluminum bottom plate welded circumferentially to the cylinder, but is open at the top end for insertion of the RV midsection and has open cut-outs or windows for heat dissipation along its mid plane longitudinally. A 19 mm (0.75 in.) thick plywood load spreader rests between the lower foam insert and the inner container assembly (see Figure 3.2).

The H1223B is an assembly which includes the RV midsection aft protective cover and fore (nose end) plate (with necessary threaded rings and bolts). The 13 mm (0.5 in.) 6064-T6 aluminum fore plate is threaded into the nose of the RV midsection acting as a load spreader and a balance. The aft protective cover is 7 mm (0.28 in.) thick forged 6061-T6 aluminum and threads onto the aft end of the RV midsection protecting critical components, as shown in Figure 3.3 and partially assembled into the container in Figure 3.4.

The H1224A container is actually a modification to the original H1224 container designed for the W62 warhead midsection. Most parts internal to the outer container shell are different, but the only outer container shell difference is the addition of four tie-down loops (just below the original H1224 loops) and 9.5 x 76 x 178 mm (0.375 x 3 x 7 in.) reinforcements inside the ends and at the bottom of the aluminum forklift channels. For impact testing purposes, therefore, H1224 container outer shells are essentially identical to H1224A outer shells and were used interchangeably in these tests due to limited availability of the newer H1224A outer shells for testing. Most of the test units arrived at Sandia with a number of small dents, which were "hammered out" in order to better replicate the performance of actual WR (war reserve) dent-free units.

The W78 warhead midsection was simulated using a Mk12a Mod6c midsection. The aeroshell/heatshield consists of an approximately 13 mm (0.5 in.) carbon fiber reinforced phenolic over a thin aluminum substrate. A series of fore and aft weighted plates simulate the mass properties of a W78 physics package, bolted to the aeroshell at points shown in Figure 3.5.

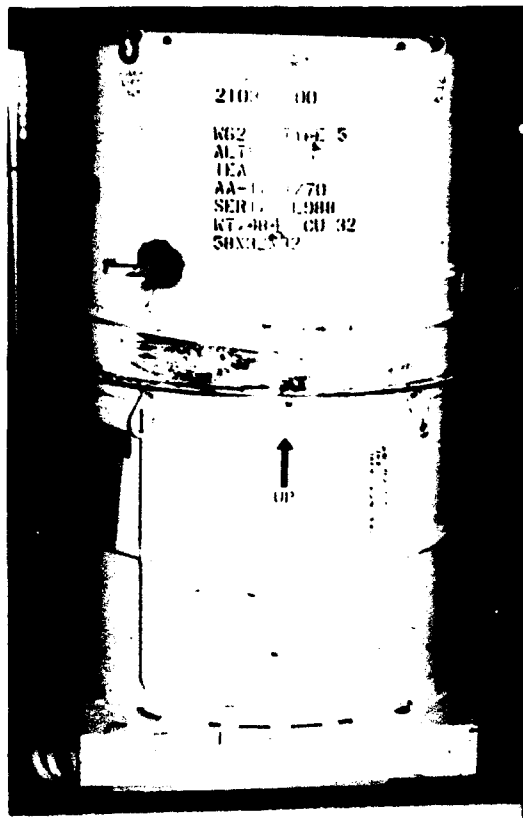


Figure 3.1 H1224 / H1224A container body photograph

Quantification of H1224A deformations resulting from impact tests was performed using detailed pre- and post-test measurements. On the outer container shell, length and diametral measurements were recorded at locations indicated in Figure 3.6, at each 45° angular increment. Deformations in the internal container assembly were recorded as lengths and diameters at locations indicated in Figure 3.7, at each 60° angular increment. And finally, deformations of the carbon phenolic aeroshell, fore end plate, and aft cover were recorded as pre- and post-test lengths, outer diameters, and inner diameters as indicated in Figure 3.8, at each 60° angular increment.

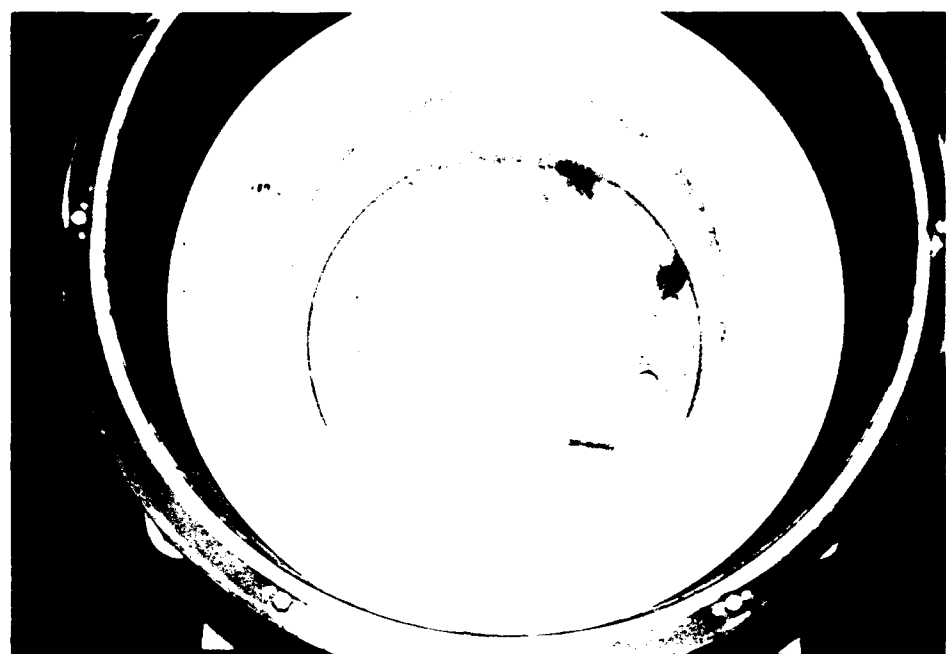


Figure 3.2 H1224A lower flexible foam insert and plywood load spreader



Figure 3.3 RV midsection with threaded fore plate and aft cover

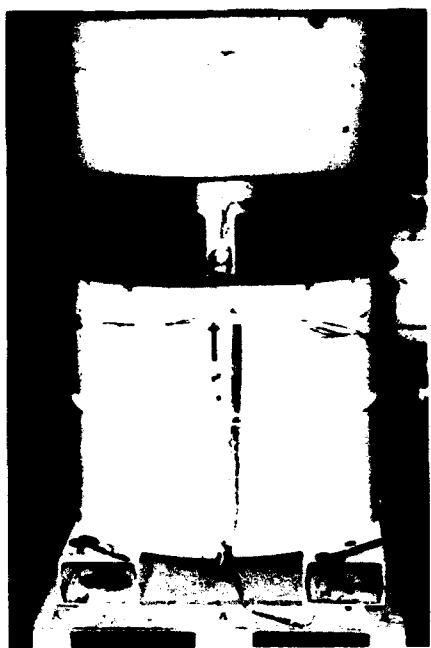


Figure 3.4 RV midsection inside inner container and foam and H1224A outer shell

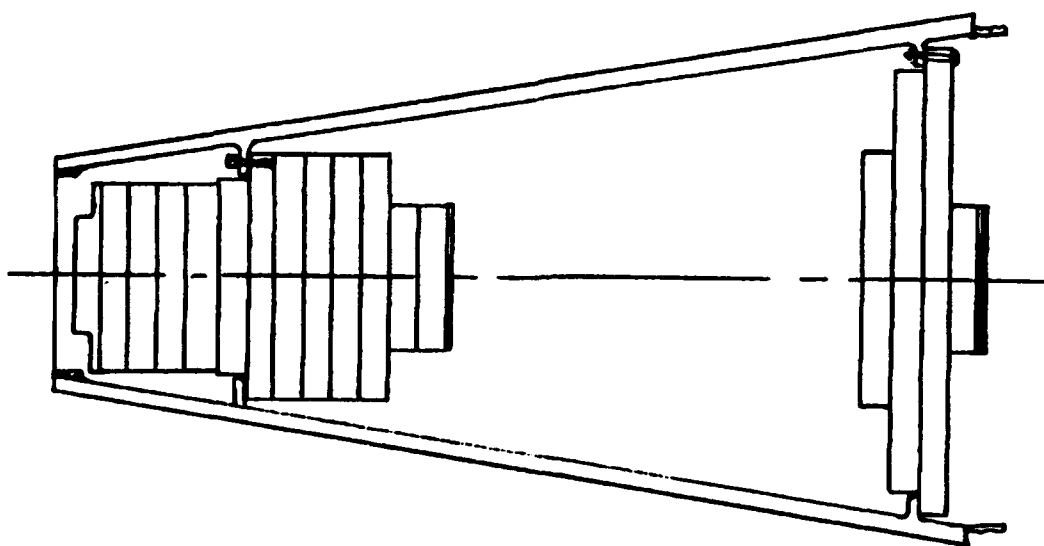


Figure 3.5 Mk12a Mod6c schematic with internal weight plates

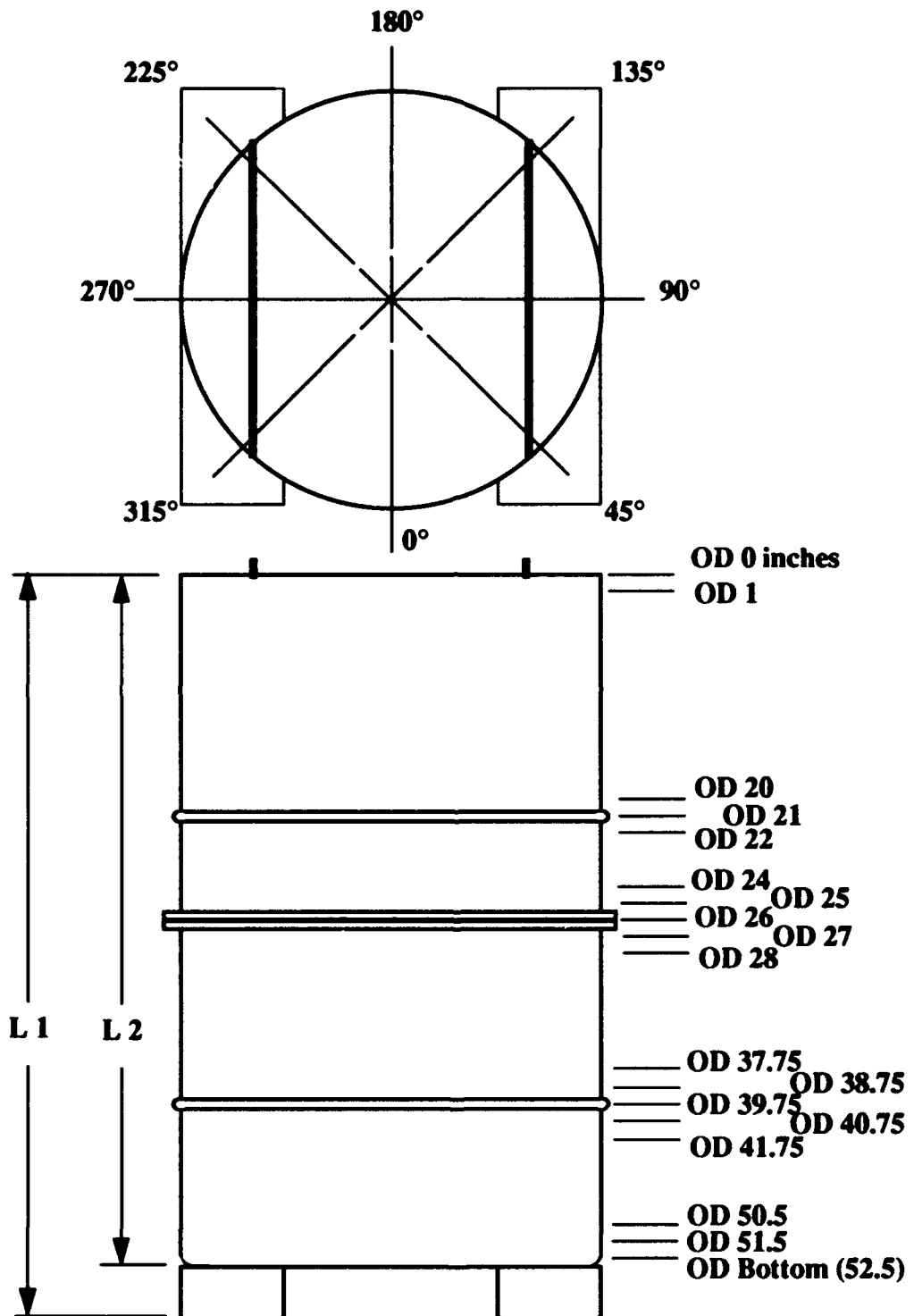


Figure 3.6 H1224A container body measurement locations

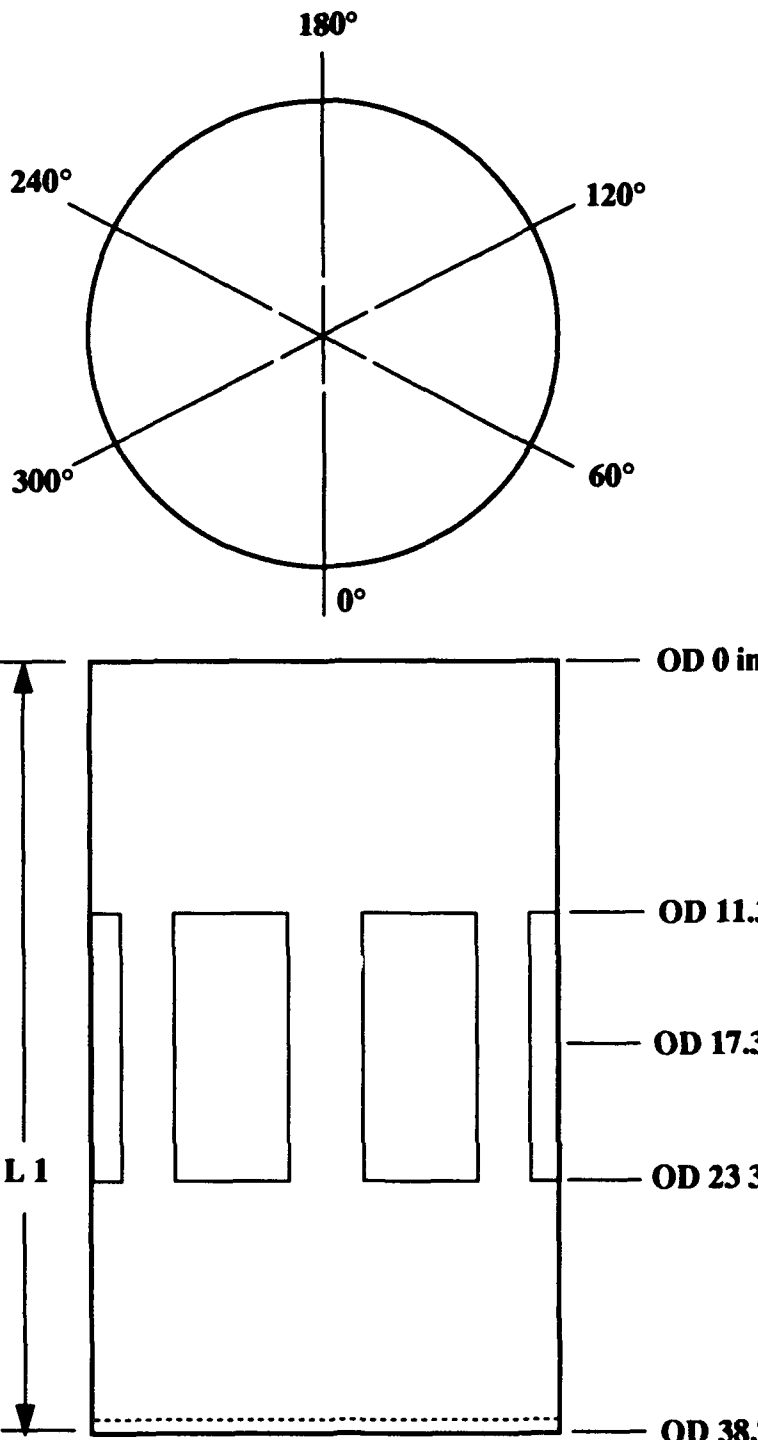


Figure 3.7 H1224A inner container measurement locations

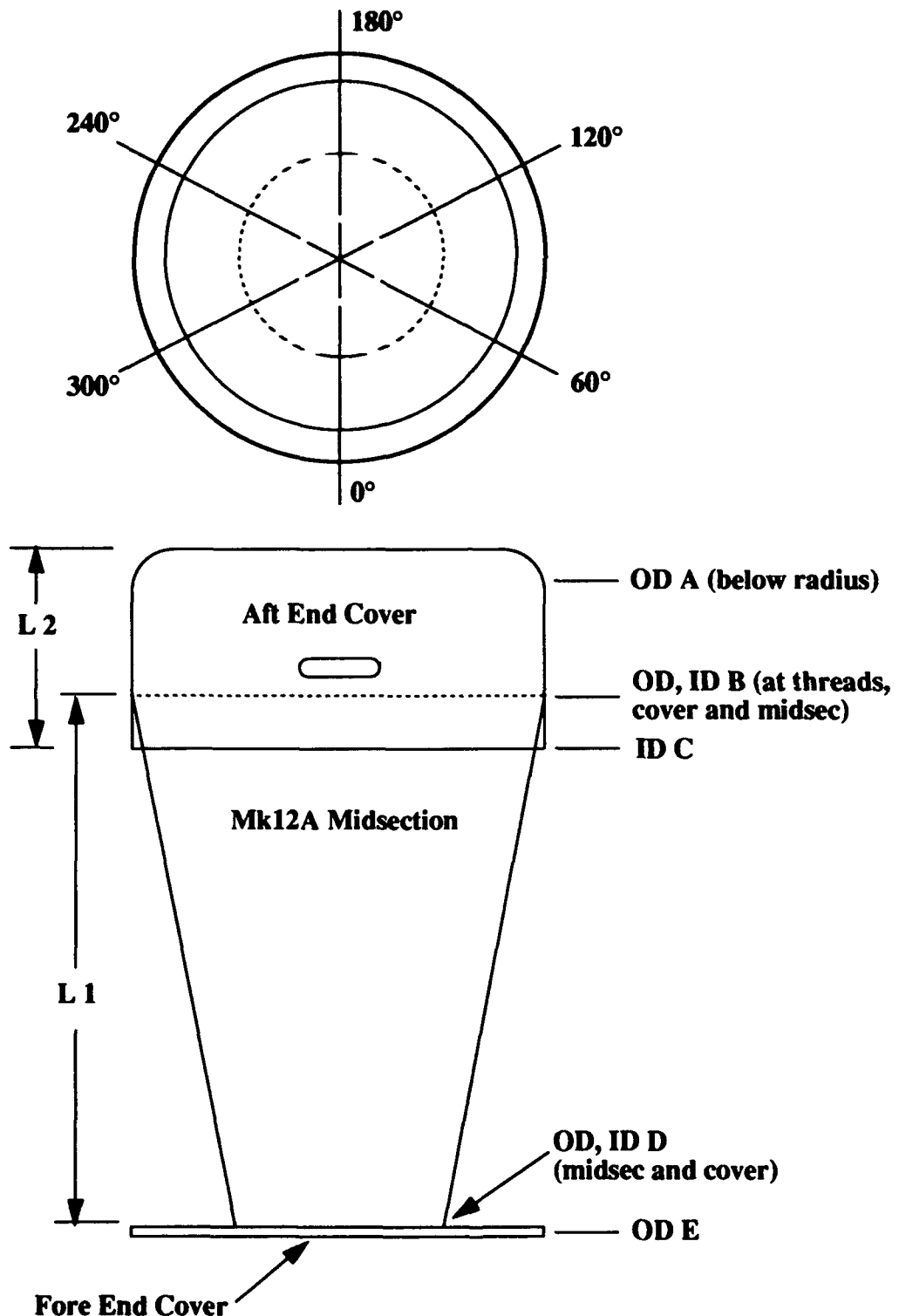


Figure 3.8 Mk12A midsection and fore and aft cover measurement locations

4. Instrumentation

Accelerometers, strain gages, and photometrics were used in each of the four impact tests to provide quantitative experimental data necessary for determining overall structural response of the H1224A shipping/storage container and to validate analytical model predictions.

Accelerometers and strain gages were monitored through instrumentation cables attached to the container. Each impact test was sequenced by a microprocessor providing event signals for the explosive cable cutters, instrumentation, and high-speed photometrics. Instrumentation data acquisition was provided by Sandia's MIDAS system [16,17], a self-contained mobile data collection and processing facility. This data acquisition system included signal conditioners that supplied input voltage, bridge balance, and shunt calibration capabilities. Electrical signals proportional to acceleration and strain at specific locations on the container were amplified, passed through a voltage-controlled oscillator, and recorded digitally through primary and secondary devices. The digital backup (secondary) recorder provided the capability of linearly recording data with amplitudes two-and-a-half times the value of the calibration signal. The secondary data was sampled at a rate of 500,000 samples per second, then transferred to a computer workstation for data analysis and reduction, including filtering, integrating, and displaying in the form of plots. Fast Fourier transforms (FFTs) were performed on each data set to analyze amplitude information in the frequency domain. All raw and reduced data plots are included in the Appendices.

The uncertainty band associated with this accelerometer and strain gage data is approximately 15 percent [18]. The primary contributors to the uncertainty include the accelerometers and strain gages themselves including their attachment method, accuracy of the data acquisition system, and the ability to record and reduce this data.

Strain gage instrumentation was used to quantify dynamic strains at key locations for future validation with analytical model predictions. Eighth-inch 5-percent-strain Micro Measurements CEA-series axial and biaxial constantan gages, compatible with the aluminum H1224A container in terms of thermal expansion, were mounted as per manufacturer's specifications [19] as shown in Figures 4.1 and 4.2 as well as Tables 4.1 and 4.2. After installation, each gage was coated with a thin layer of RTV 3145 for protection. "Dummy" strain gage channels with impedance similar to active channels, were used to characterize background noise and any other potential spurious voltage signals acquired during the impact tests.

Dynamic accelerations throughout the container and RV during impact tests were recorded using Endevco 7270A 2,000-g, 6,000-g, and 20,000-g piezoresistive accelerometers [20]. "Dummy" accelerometers, whose physical appearance and impedance are identical to active units, were used to characterize background noise and any other potential spurious voltage signals acquired during the impact tests. Accelerometers for each test were bolted to the container body screwed to mounting blocks (glued and screwed) at mounting locations shown in Figures 4.3 and 4.4 and in Tables 4.3a, 4.3b, 4.4a, and 4.4b. These miniature units are only 14.2 mm (0.56 in.) x 7.1 mm (0.28 in.) x 2.8 mm (0.11 in.) thick, adding virtually zero mass and thus not affecting the dynamic response of the measurement location. High resonant frequencies (90 to 350 kHz) and zero damp-

ing also allow the accelerometers to respond accurately to fast rise time, short duration shock motion all the way down to dc or steady state accelerations. The flat amplitude frequency response ($\pm 5\%$ max) for these accelerometers extends to 10 to 50 kHz, depending on the acceleration limit, providing linearity below these limits. Container structural response was separated from the accelerometer response using IIR 6-stage Butterworth (low-pass) filters with cutoff frequencies of 2 kHz and 250 Hz, bracketing the internationally recommended range to eliminate high-frequency noise [21]. Prior to and after each impact test, each accelerometer was calibrated using drop ball, shaker, and centrifuge methods [22-24] by Sandia's Measurement Standard Department. Post-test calibration ensures that the transducer has not been damaged during testing.

The tests were recorded photometrically by orthogonal high-speed motion-picture cameras, operating at 400 frames/s and 2000 frames/s to capture detailed deformation histories. Each camera also recorded a synchronized 1000 Hz IRIG timing signal to verify velocity measurements. Gridded stadia-board backgrounds aided displacement and velocity determination from the high-speed films.

Photographs showing more detailed mounting locations of strain gages, accelerometers, and terminal strips for the Longitudinal Low Velocity (LLV), Horizontal Low Velocity (HLV), Longitudinal High Velocity (LHV), and Horizontal High Velocity (HHV) impact tests are presented in Figures 4.5 through 4.19. As shown in some of these photographs, strain relief was designed into placement of instrumentation lead wires and cables in order to minimize the chance of overstressing these wires and losing test data.

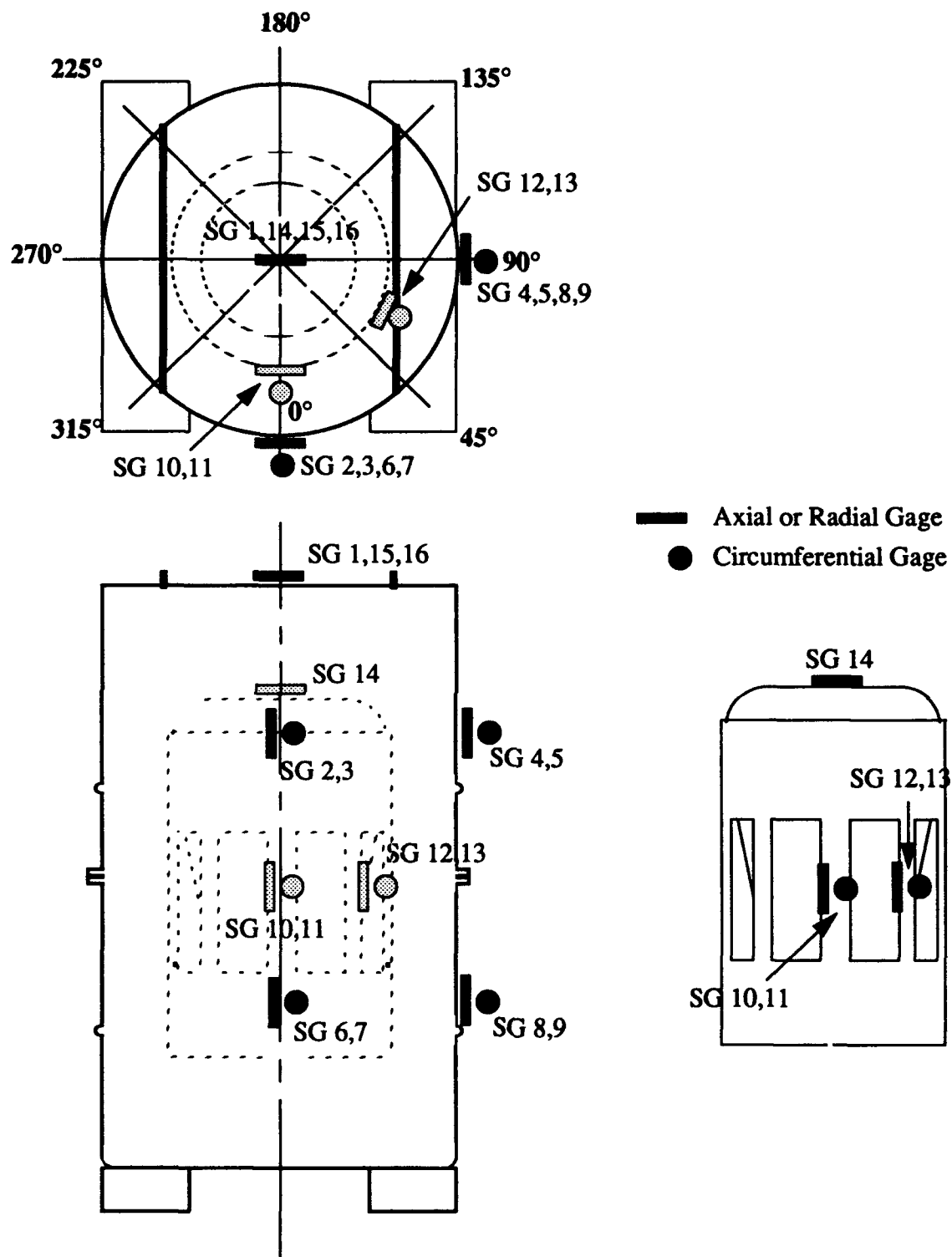


Figure 4.1 Strain Gage Locations for Low and High Velocity Longitudinal Impact Tests

TABLE 4.1
LONGITUDINAL IMPACT INSTRUMENTATION REQUIREMENTS - STRAIN GAGES

<u>Strain Desig.</u>	<u>Type/Catalog Number</u>	<u>Location</u>	<u>Direction</u>
SG1	CEA-13-125UW-350	Top, Off-Center (3" toward 0°)	radial
SG2	CEA-13-125UT-350	13" Down, Side, 0°	axial
SG3	CEA-13-125UT-350	13" Down, Side, 0°	circumferential
SG4	CEA-13-125UT-350	13" Down, Side, 90°	axial
SG5	CEA-13-125UT-350	13" Down, Side, 90°	circumferential
SG6	CEA-13-125UT-350	37" Down, Side, 0°	axial
SG7	CEA-13-125UT-350	37" Down, Side, 0°	circumferential
SG8	CEA-13-125UT-350	37" Down, Side, 90°	axial
SG9	CEA-13-125UT-350	37" Down, Side, 90°	circumferential
SG10	CEA-13-125UT-350	19.38" Down, Inner, 0°	axial
SG11	CEA-13-125UT-350	19.38" Down, Inner, 0°	circumferential
SG12	CEA-13-125UT-350	19.38" Down, Inner, 60°	axial
SG13	CEA-13-125UT-350	19.38" Down, Inner, 60°	circumferential
SG14	CEA-13-125UW-350	Top of 1223B, Center	radial
SG15	7270A-R / GW	Top, Center	N/A
SG16	7270A-R / RB	Top, Center	N/A

NOTE:

1. Strain gages 15 and 16 are dummy gages
2. Axial direction refers to along the length of the container axis

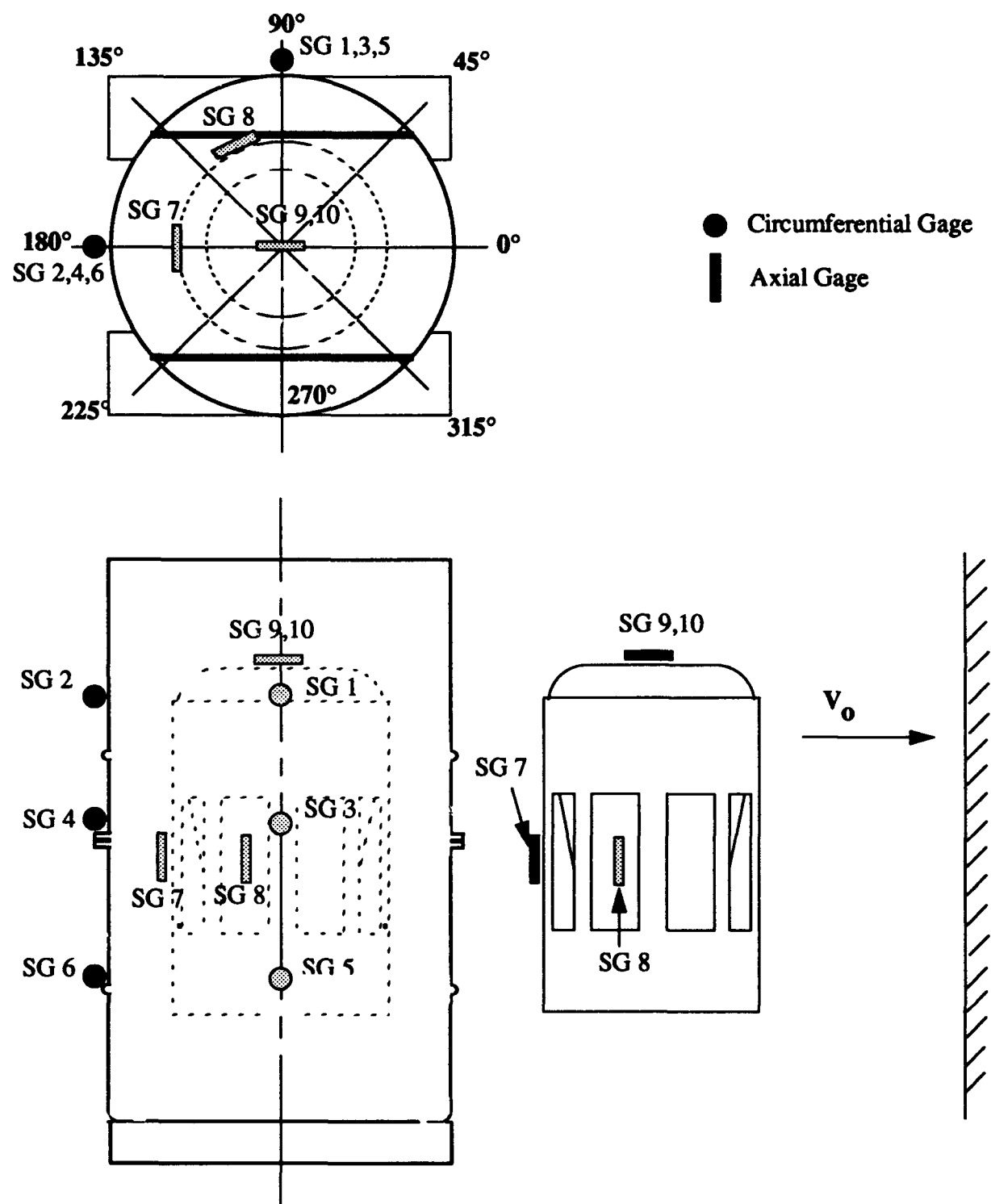


Figure 4.2 Strain Gage Locations for Low and High Velocity Horizontal Impact Tests

TABLE 4.2
HORIZONTAL IMPACT INSTRUMENTATION REQUIREMENTS - STRAIN GAGES

<u>Strain Desig.</u>	<u>Type/Catalog Number</u>	<u>Location</u>	<u>Direction</u>
SG1	CEA-13-125UW-350	13" Down, Side, 90°	circumferential
SG2	CEA-13-125UW-350	13" Down, Side, 180°	circumferential
SG3	CEA-13-125UW-350	22.75" Down, Side, 90°	circumferential
SG4	CEA-13-125UW-350	22.75" Down, Side, 180°	circumferential
SG5	CEA-13-125UW-350	37" Down, Side, 90°	circumferential
SG6	CEA-13-125UW-350	37" Down, Side, 180°	circumferential
SG7	CEA-13-125UW-350	19.38" Down, Inner Container, 120°	axial
SG8	CEA-13-125UW-350	19.38" Down, Inner Container, 180°	axial
SG9	7270A-R / GW	1223B, Side, 180° (on A8&9 block)	N/A
SG10	7270A-R / RB	1223B, Side, 180° (on A8&9 block)	N/A

NOTE:

1. Strain gages 9 and 10 were dummy gages
2. Axial direction refers to along the length of the container axis

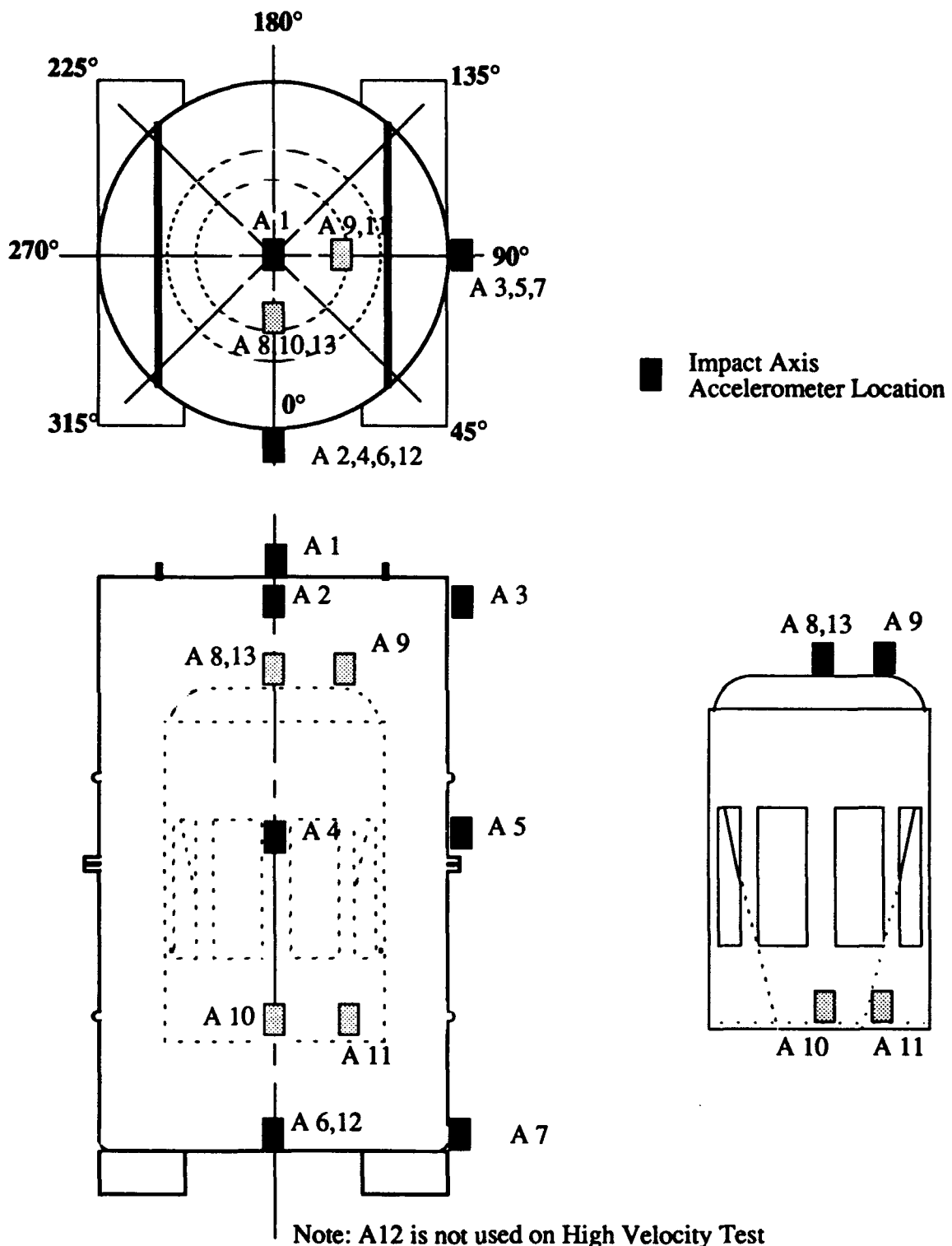


Figure 4.3 Accelerometer Locations for Low and High Velocity Longitudinal Impact Tests

TABLE 4.3a
LONGITUDINAL 40 FT/S IMPACT INSTRUMENTATION REQUIREMENTS -
ACCELEROMETERS

<u>Accel. Desig.</u>	<u>Type/Catalog Number</u>	<u>Location</u>	<u>Direction</u>
A1	7270A-2K	Top, Center	Impact Axis
A2	7270A-2K	Top, Side, 0°	Impact Axis
A3	7270A-2K	Top, Side, 90°	Impact Axis
A4	7270A-2K	24.5" Down, Side, 0°	Impact Axis
A5	7270A-2K	24.5" Down, Side, 90°	Impact Axis
A6	7270A-6K	Bottom, Side, 0°	Impact Axis
A7	7270A-6K	Bottom, Side, 90°	Impact Axis
A8	7270A-2K	1223B Top, End, 0°	Impact Axis
A9	7270A-2K	1223B Top, End, 90°	Impact Axis
A10	7270A-2K	Fore Mount Plate, 1/2" From Inner Edge, 0°	Impact Axis
A11	7270A-2K	Fore Mount Plate, 1/2" From Inner Edge, 90°	Impact Axis
A12	7270A-20K	Bottom, Side, 0°	Impact Axis
A13	7270A-Z	1223B Top, End, 0°	N/A

Note:

1. A13 was a dummy accelerometer

TABLE 4.3b
LONGITUDINAL 125 FT/S IMPACT INSTRUMENTATION REQUIREMENTS -
ACCELEROMETERS

<u>Accel. Desig.</u>	<u>Type/Catalog Number</u>	<u>Location</u>	<u>Direction</u>
A1	7270A-20K	Top, Center	Impact Axis
A2	7270A-20K	Top, Side, 0°	Impact Axis
A3	7270A-20K	Top, Side, 90°	Impact Axis
A4	7270A-20K	24.5" Down, Side, 0°	Impact Axis
A5	7270A-20K	24.5" Down, Side, 90°	Impact Axis
A6	7270A-20K	Bottom, Side, 0°	Impact Axis
A7	7270A-20K	Bottom, Side, 90°	Impact Axis
A8	7270A-20K	1223B Top, End, 0°	Impact Axis
A9	7270A-20K	1223B Top, End, 90°	Impact Axis
A10	7270A-20K	Fore Mount Plate, 1/2" From Inner Edge, 0°	Impact Axis
A11	7270A-20K	Fore Mount Plate, 1/2" From Inner Edge, 90°	Impact Axis
A13	7270A-Z	1223B Top, End, 0°	N/A

Note:

1. A13 was a dummy accelerometer

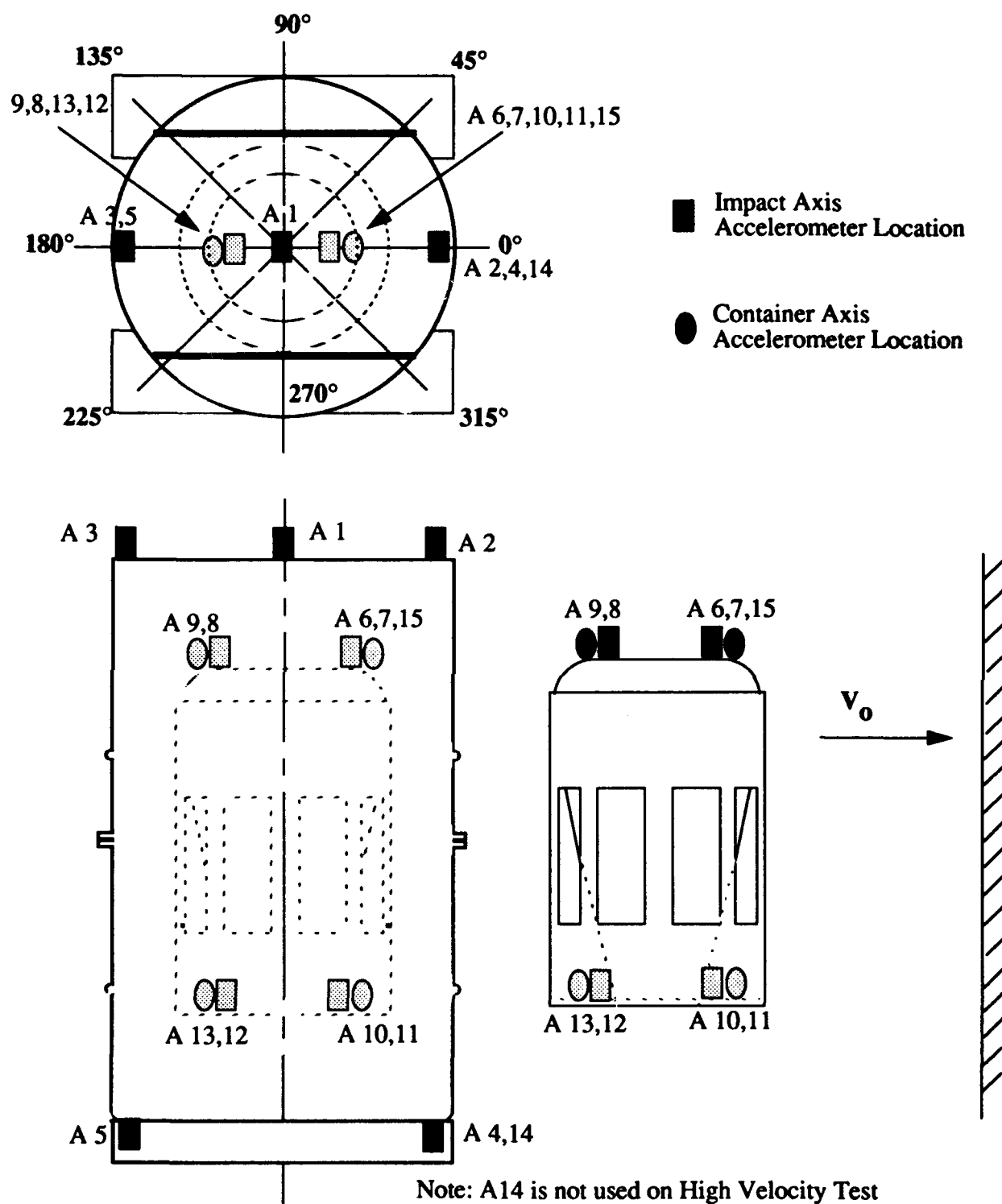


Figure 4.4 Accelerometer Locations for Low and High Velocity Horizontal Impact Tests

TABLE 4.4a
HORIZONTAL 40 FT/S IMPACT INSTRUMENTATION REQUIREMENTS -
ACCELEROMETERS

<u>Accel. Desig.</u>	<u>Type/Catalog Number</u>	<u>Location</u>	<u>Direction</u>
A1	7270A-2K	Top, Center	Impact Axis
A2	7270A-6K	Top, End, 0°	Impact Axis
A3	7270A-2K	Top, End, 180°	Impact Axis
A4	7270A-6K	Bottom, End, 0°	Impact Axis
A5	7270A-2K	Bottom, End, 180°	Impact Axis
A6	7270A-2K	1223B Top, End, 0°	Impact Axis
A7	7270A-2K	1223B Top, End, 0°	Container Axis
A8	7270A-2K	1223B Top, End, 180°	Impact Axis
A9	7270A-2K	1223B Top, End, 180°	Container Axis
A10	7270A-2K	Fore Mount Plate, 1/2" From Inner Edge, 0°	Impact Axis
A11	7270A-2K	Fore Mount Plate, 1/2" From Inner Edge, 0°	Container Axis
A12	7270A-2K	Fore Mount Plate, 1/2" From Inner Edge, 180°	Impact Axis
A13	7270A-2K	Fore Mount Plate, 1/2" From Inner Edge, 180°	Container Axis
A14	7270A-20K	Bottom, End, 0°	Impact Axis
A15	7270A-Z	1223B Top, End, 180°	N/A

Note:

1. A15 was a dummy accelerometer

TABLE 4.4b
HORIZONTAL 125 FT/S IMPACT INSTRUMENTATION REQUIREMENTS -
ACCELEROMETERS

<u>Accel. Desig.</u>	<u>Type/Catalog Number</u>	<u>Location</u>	<u>Direction</u>
A1	7270A-20K	Top, Center	Impact Axis
A2	7270A-20K	Top, End, 0°	Impact Axis
A3	7270A-20K	Top, End, 180°	Impact Axis
A4	7270A-20K	Bottom, End, 0°	Impact Axis
A5	7270A-20K	Bottom, End, 180°	Impact Axis
A6	7270A-20K	1223B Top, End, 0°	Impact Axis
A7	7270A-20K	1223B Top, End, 0°	Container Axis
A8	7270A-20K	1223B Top, End, 180°	Impact Axis
A9	7270A-20K	1223B Top, End, 180°	Container Axis
A10	7270A-20K	Fore Mount Plate, 1/2" From Inner Edge, 0°	Impact Axis
A11	7270A-20K	Fore Mount Plate, 1/2" From Inner Edge, 0°	Container Axis
A12	7270A-20K	Fore Mount Plate, 1/2" From Inner Edge, 180°	Impact Axis
A13	7270A-20K	Fore Mount Plate, 1/2" From Inner Edge, 180°	Container Axis
A15	7270A-Z	1223B Top, End, 180°	N/A

Note:

1. A15 was a dummy accelerometer

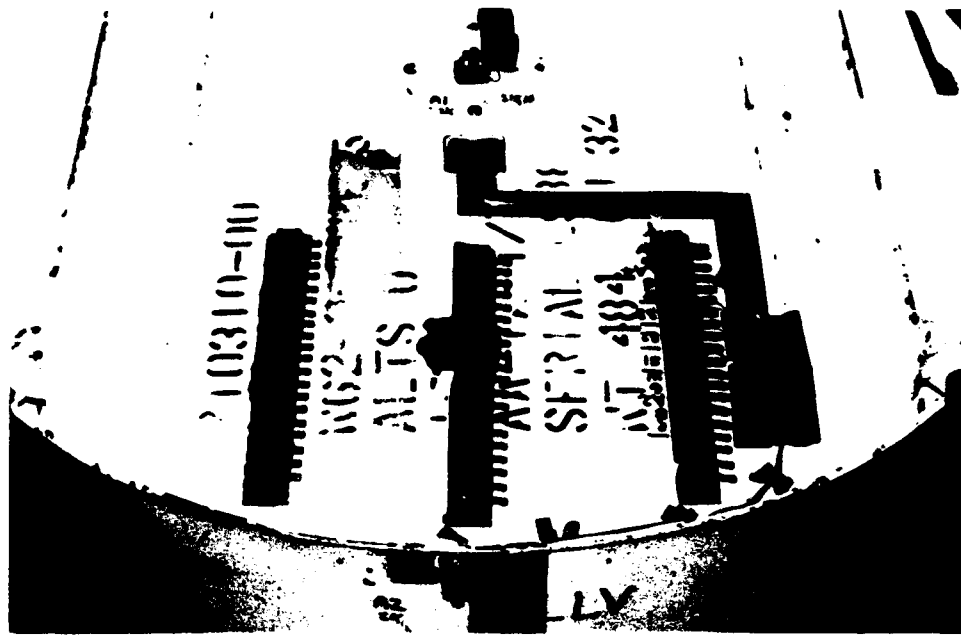


Figure 4.5 LLV mounting locations for A1, A2, S1, S15, S16, and terminal strips

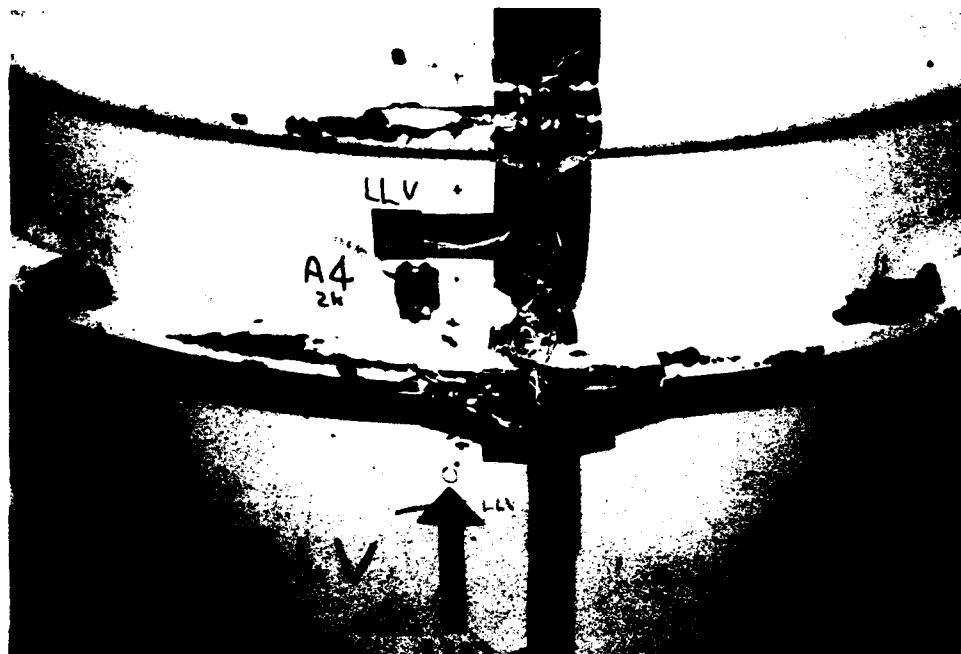


Figure 4.6 LLV mounting location for A4

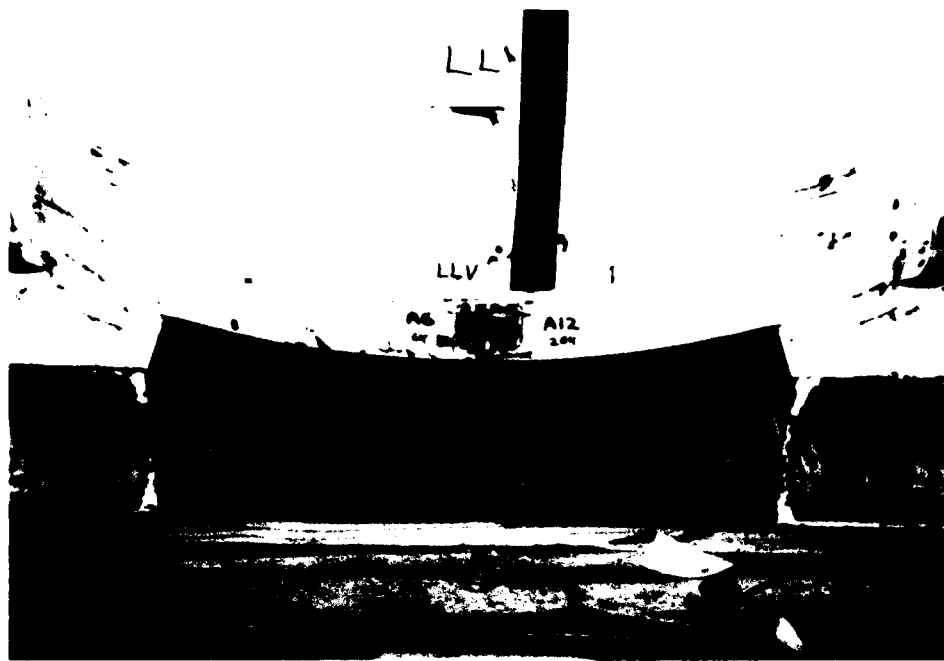


Figure 4.7 LLV mounting location for A6 and A12



Figure 4.8 LLV mounting locations for A8, A9, A13, and S14

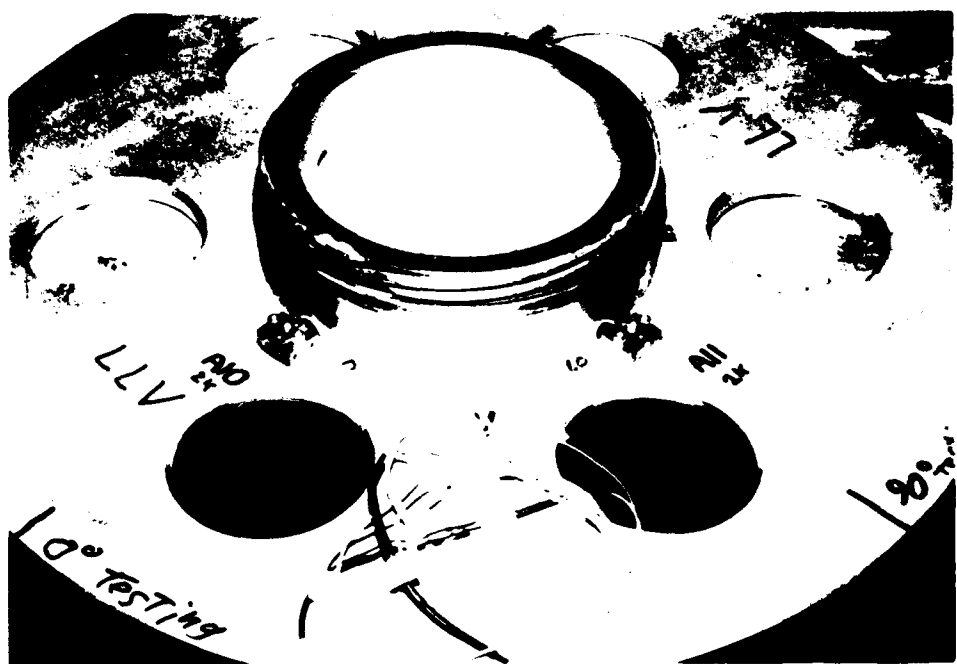


Figure 4.9 LLV mounting locations for A10 and A11

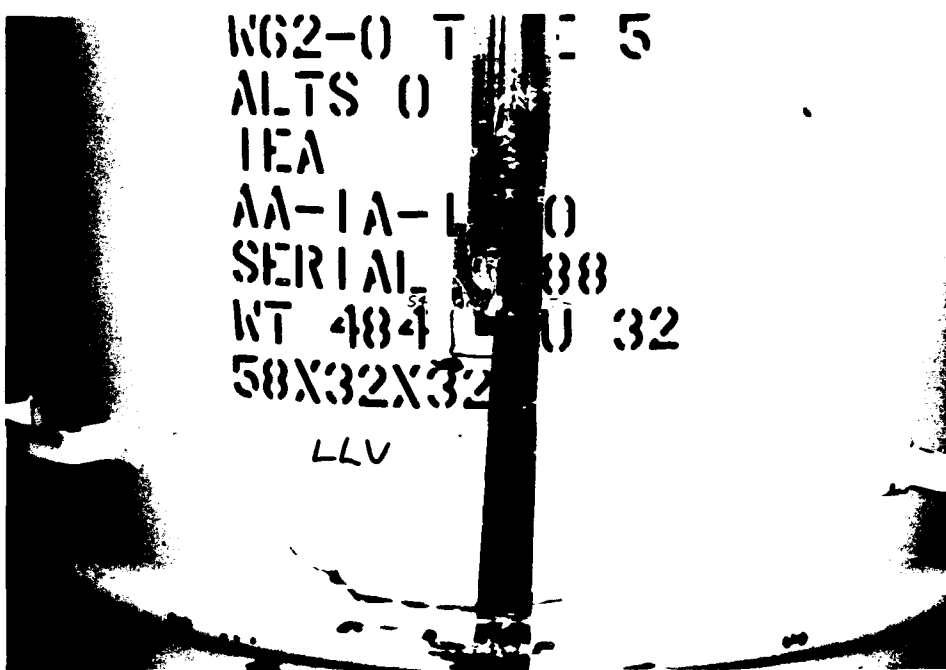


Figure 4.10 LLV mounting location for S4 and S5

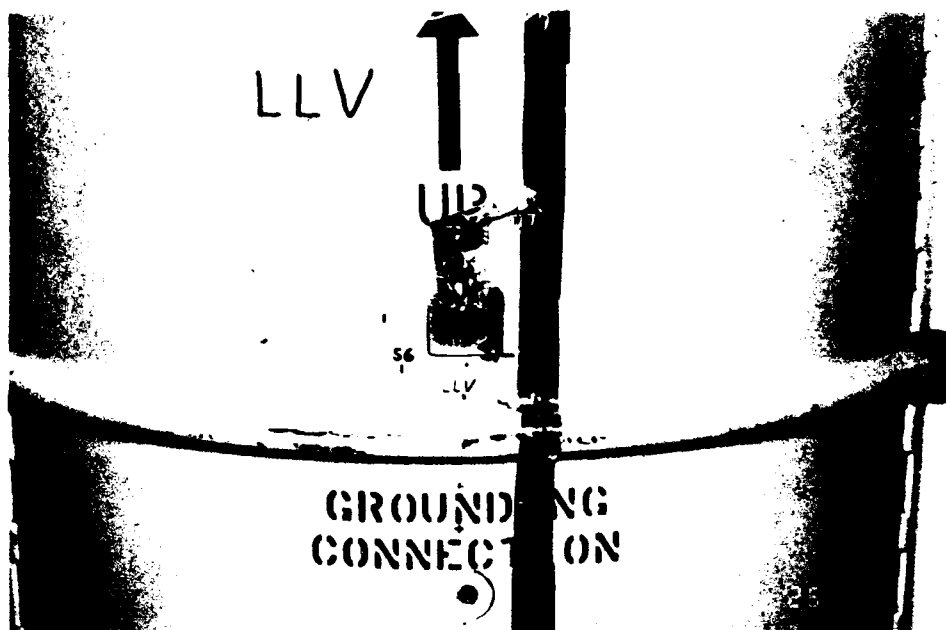


Figure 4.11 LLV mounting location for S6 and S7

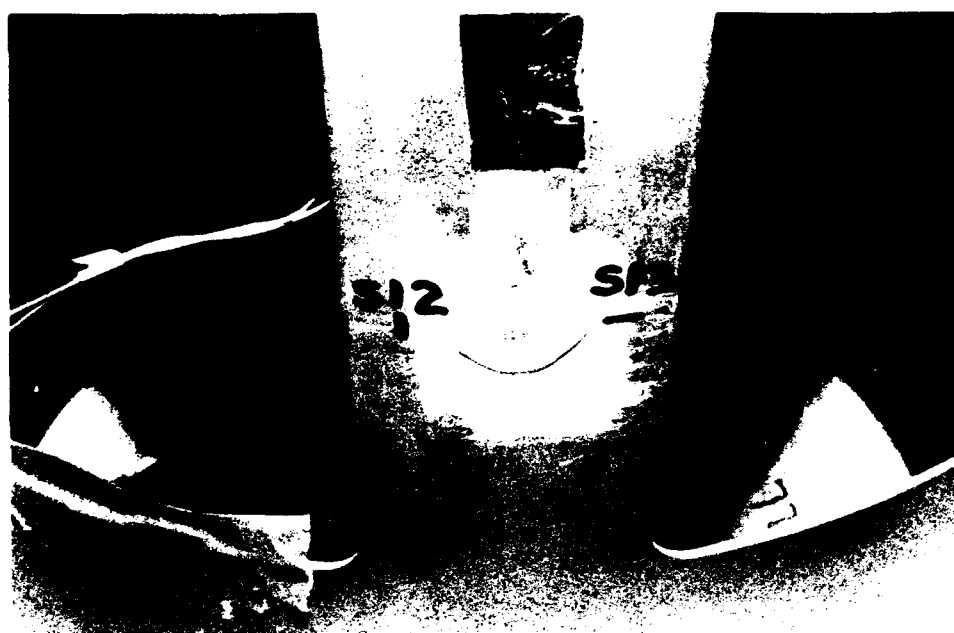


Figure 4.12 LLV mounting location for S12 and S13



Figure 4.13 HLV mounting locations for A1, A2, A3, and some terminal strips

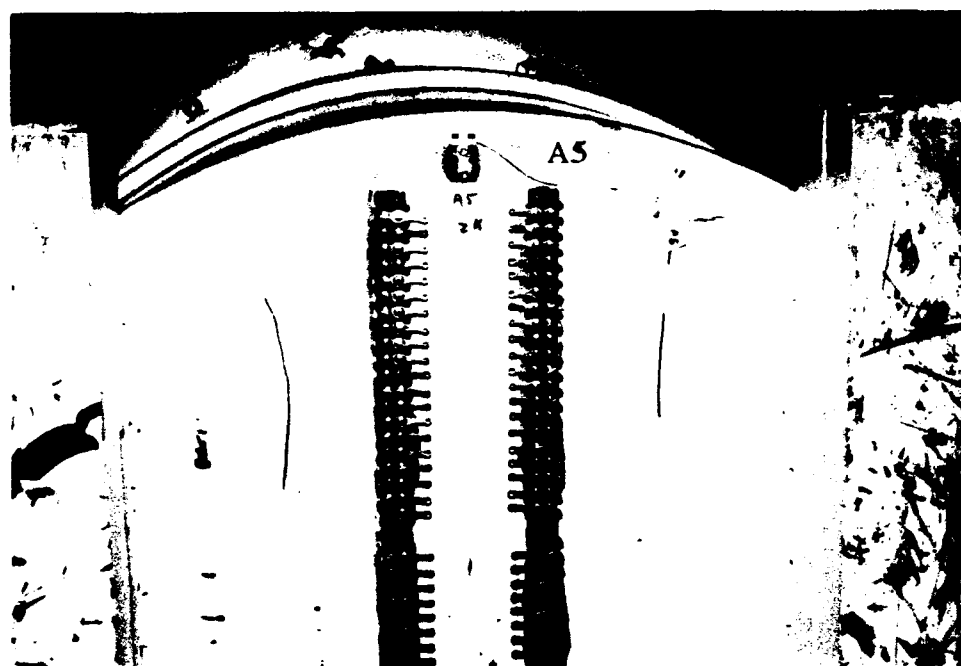


Figure 4.14 HLV mounting location for A5

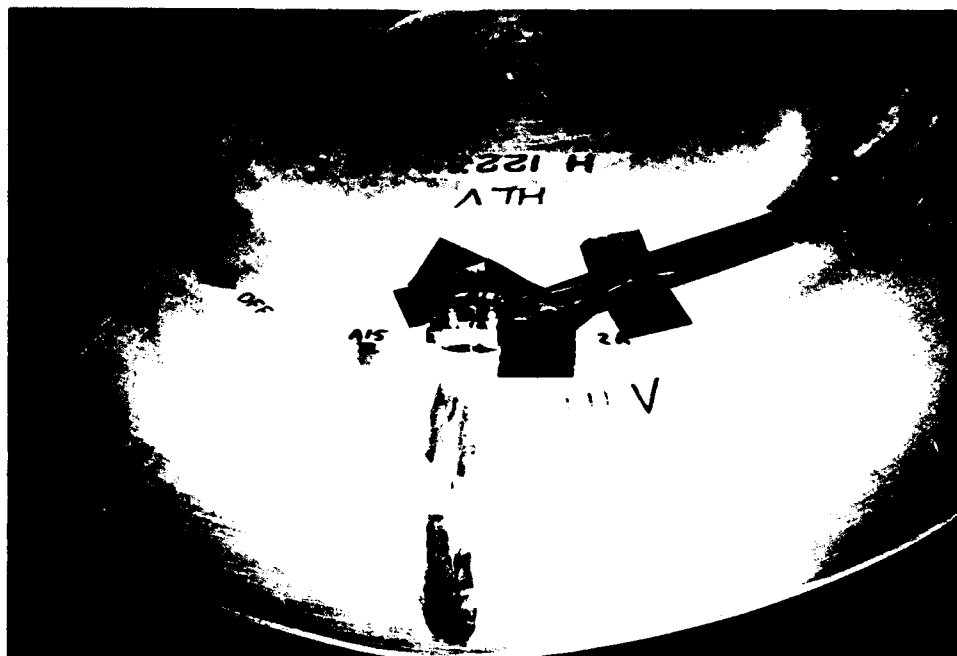


Figure 4.15 HLV mounting location for A6, A7, and A15



Figure 4.16 HLV mounting location for A12 and A13

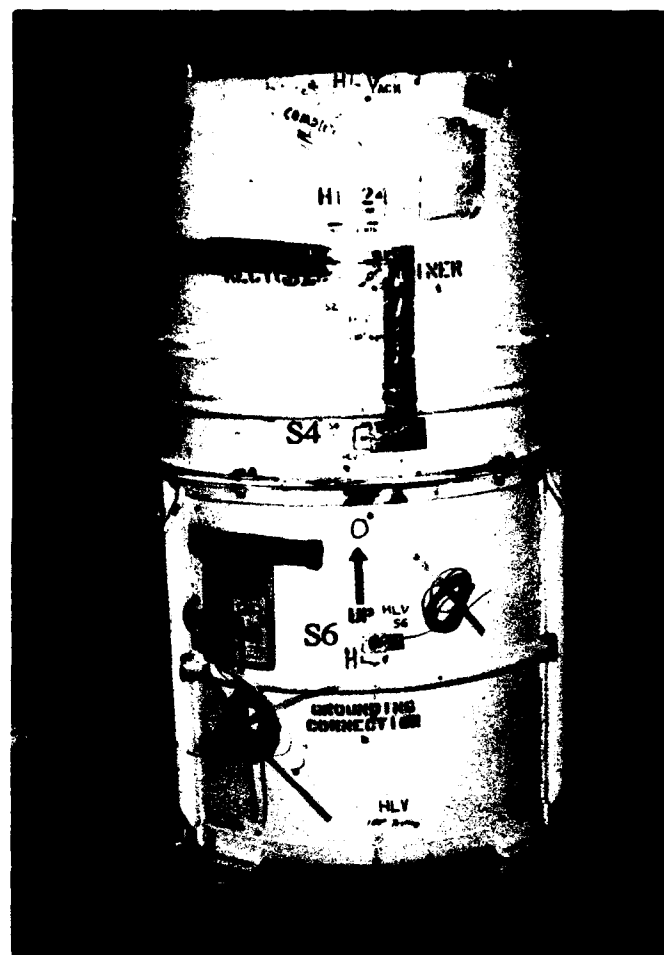


Figure 4.17 HLV mounting locations for S2, S4, and S6

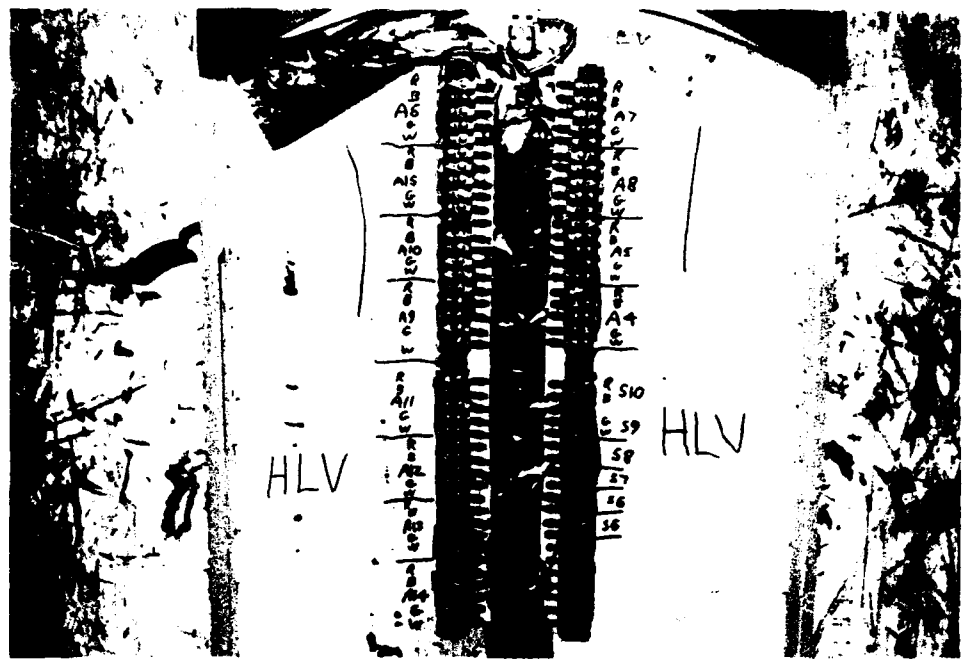


Figure 4.18 HLV mounting location for more terminal strips

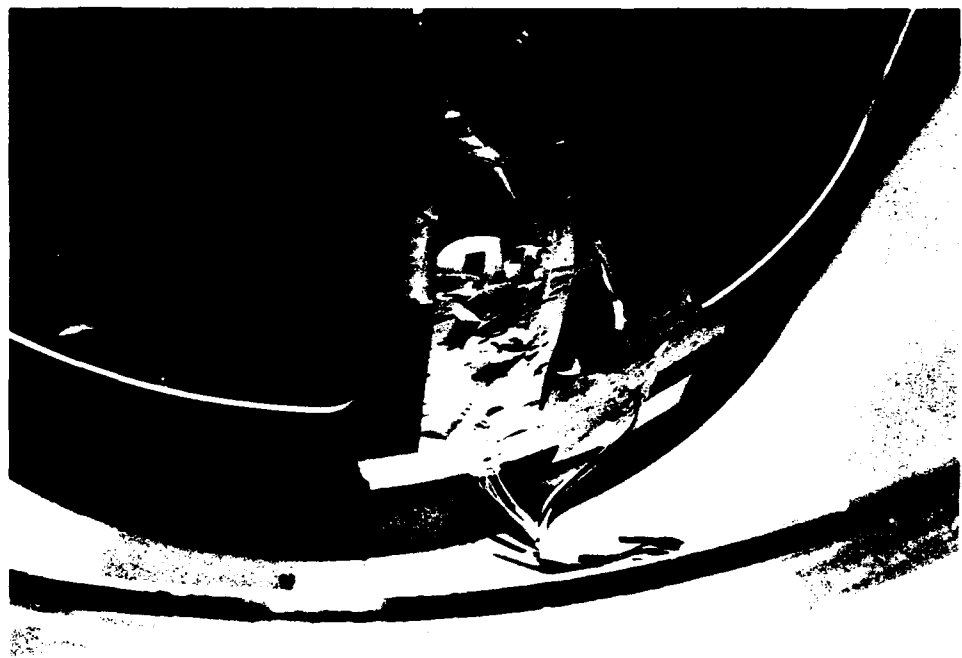


Figure 4.19 HLV mounting location for S7

5. Results

5.1 Longitudinal Low Velocity

The longitudinal low-velocity (LLV) impact test was performed on June 29, 1993 at the 185-ft drop tower of Sandia National Laboratories. The container drop height was 8.2 m (27 ft) along a high-tension cable guided path which controlled impact orientation (see Figure 5.1.1). Analysis of high-speed films yielded an impact velocity of 12.3 m/s (40.5 ft/s) at an impact angle of 1.7° from perfectly upright. After impact, the test unit rebounded approximately 1.2 m (4 ft) from the unyielding target, tilting slightly in mid-air causing the unit to fall from the raised target after the second impact.

H1224A outer shell deformation resulting from the 12.3 m/s longitudinal impact was minimal, as shown in Figure 5.1.2. The lower longitudinal stiffeners buckled slightly at the container's lower circumferential bulge, reducing the container's overall length by up to 31 mm (1.22 in.) on the side shown in Figure 5.1.2, or 0° circumferentially (see Appendix E: Inspection Data, Table E 1.1). On the opposite side of the container, slight weld tearing occurred in the joints between the container's bottom pan and its fork lift channels, as shown in Figure 5.1.3.

Inside the container, the upper foam insert glue joint partially separated (see Figure 5.1.4) due to deceleration of its own mass. Weld tearing along the bottom of the inner container (see Figure 5.1.5) occurred where it was unsupported by the fork lift channels. Similar deformation to the RV's threaded fore plate is shown in Figure 5.1.6, where the bending moment was provided by asymmetric loading through the fork lift channels. Bulging of the outer container's bottom pan between the fork lift channels can be seen in Figure 5.1.7. Container deformations for the LLV impact test are quantified in Tables E 1.1, E 1.2, and E 1.3 of Appendix E, from measurement locations specified in Figures 3.6, 3.7, and 3.8.

Accelerations measured (and low-pass filtered to 2 kHz) at the fore and aft ends of the RV midsection are presented in Figures 5.1.8 and 5.1.9. The accelerometers in each figure were located 90° apart and show similar acceleration peaks of approximately 600 Gs at the nose or fore end and 250 Gs at the aft end. Since the carbon phenolic aeroshell is not a rigid body, some attenuation of the impact loading occurs through the RV. As identified by the time of peak acceleration and by the time of zero velocity in the integrated acceleration plots of Appendix A, the RV mid-section began rebounding approximately 14 to 16 milliseconds after container impact began.

Note that dynamic strain histories, as well as all raw and filtered data, FFTs and integrated accelerations are presented for the LLV impact test in Appendix A.



Figure 5.1.1 LLV impact test pre-drop



Figure 5.1.2 LLV H1224A post-test deformation



Figure 5.1.3 LLV H1224A weld crack

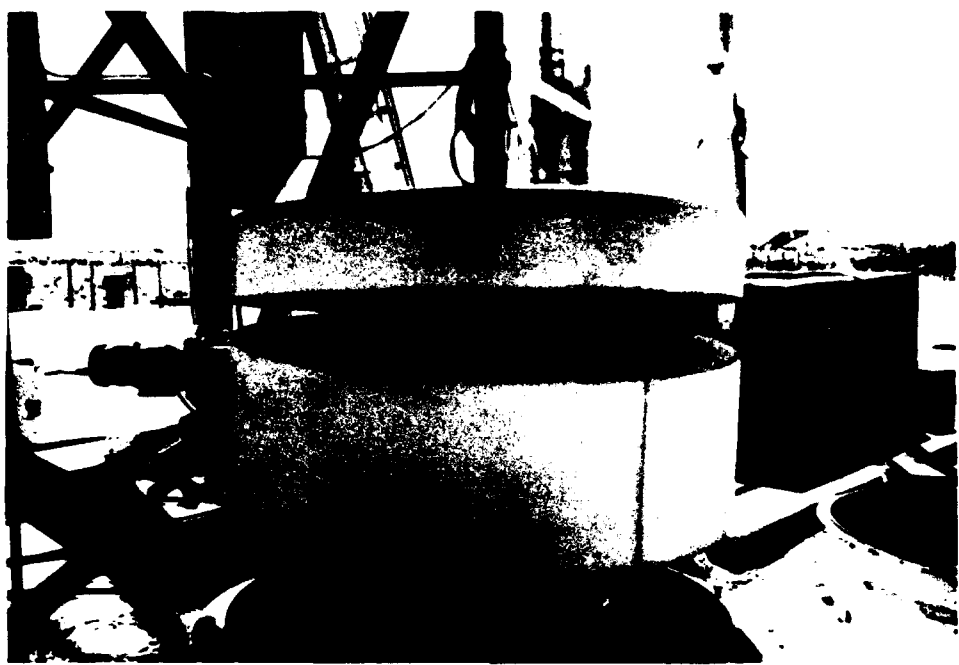


Figure 5.1.4 LLV upper foam insert joint separation

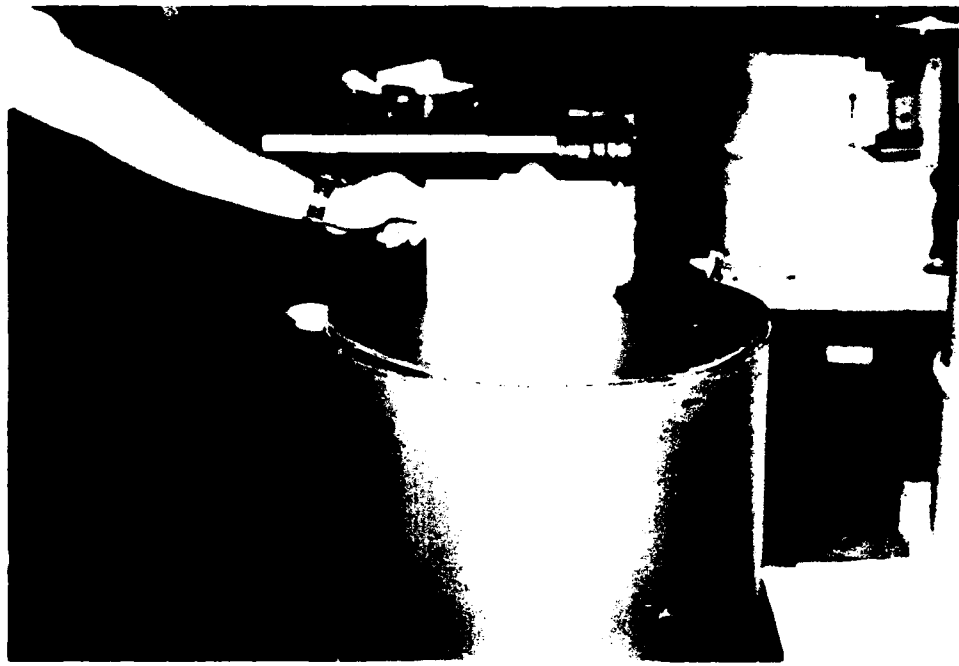


Figure 5.1.5 LLV inner container weld tears

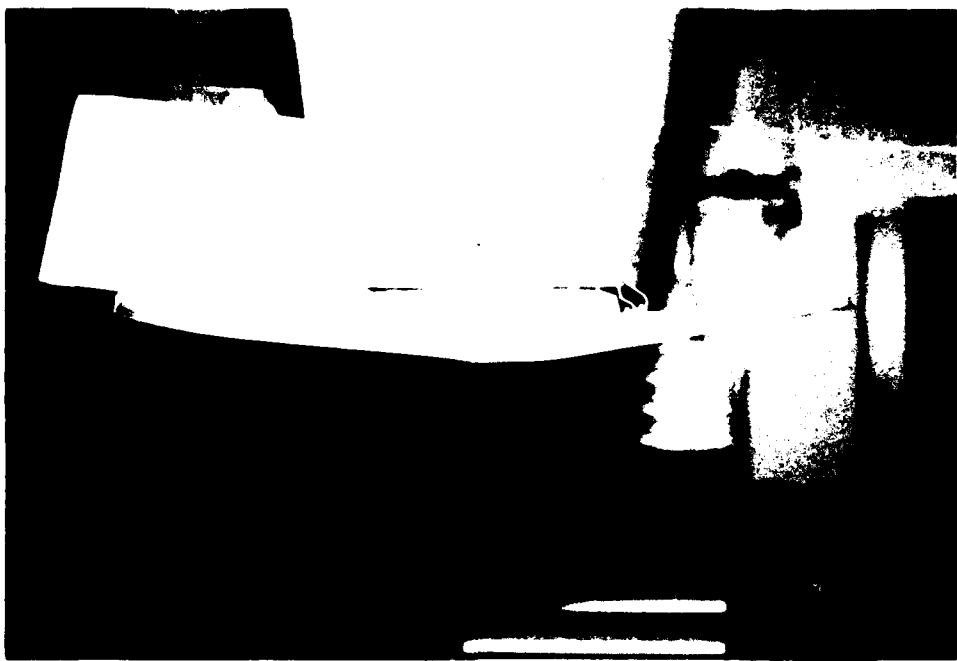


Figure 5.1.6 LLV fore plate bending

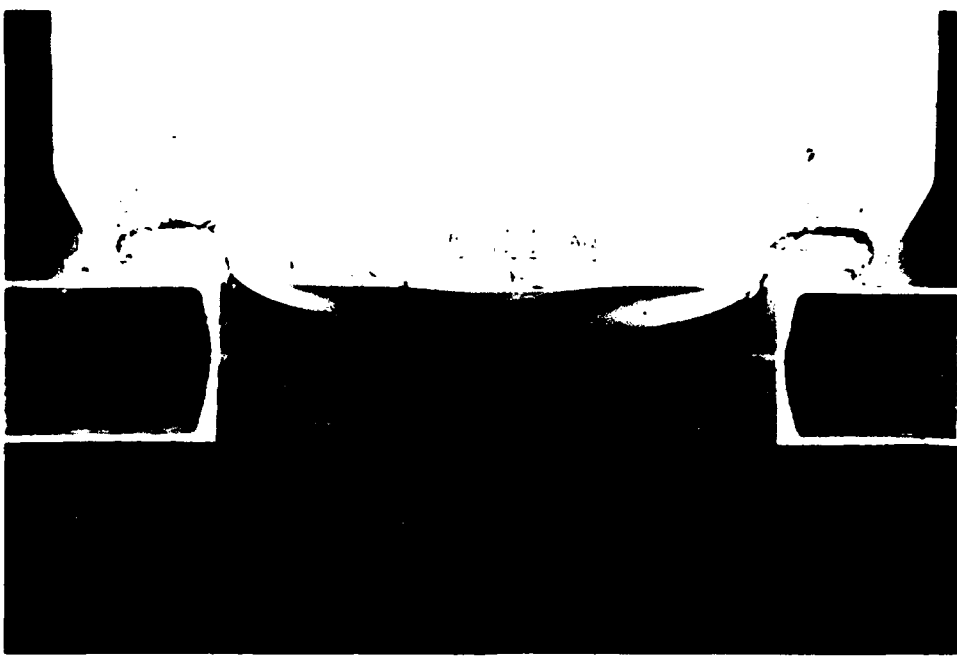


Figure 5.1.7 LLV H1224A bottom pan deformation

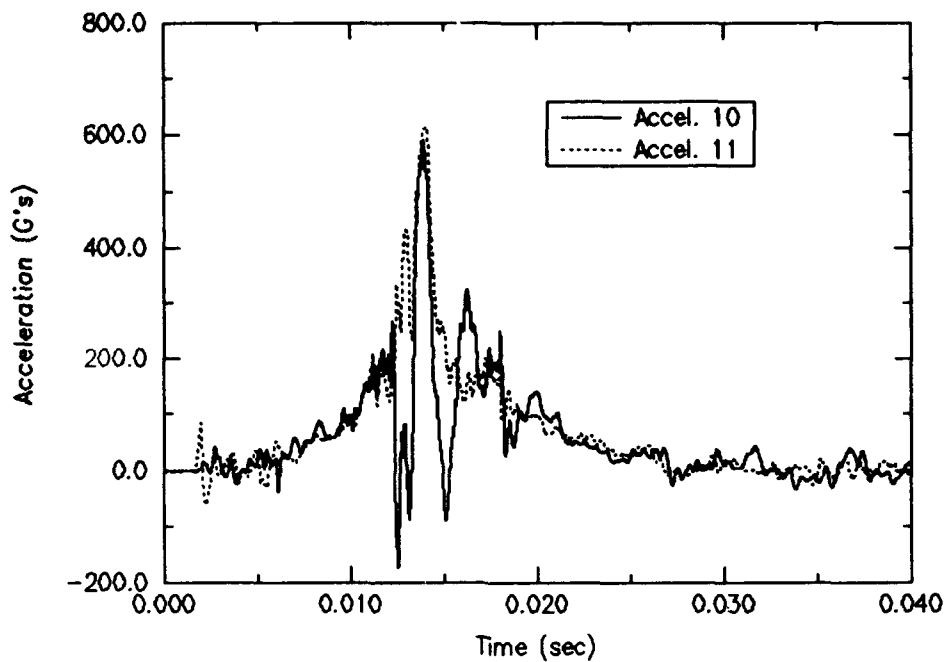


Figure 5.1.8 LLV fore plate (nose end, RV) accelerations (2 kHz filter)

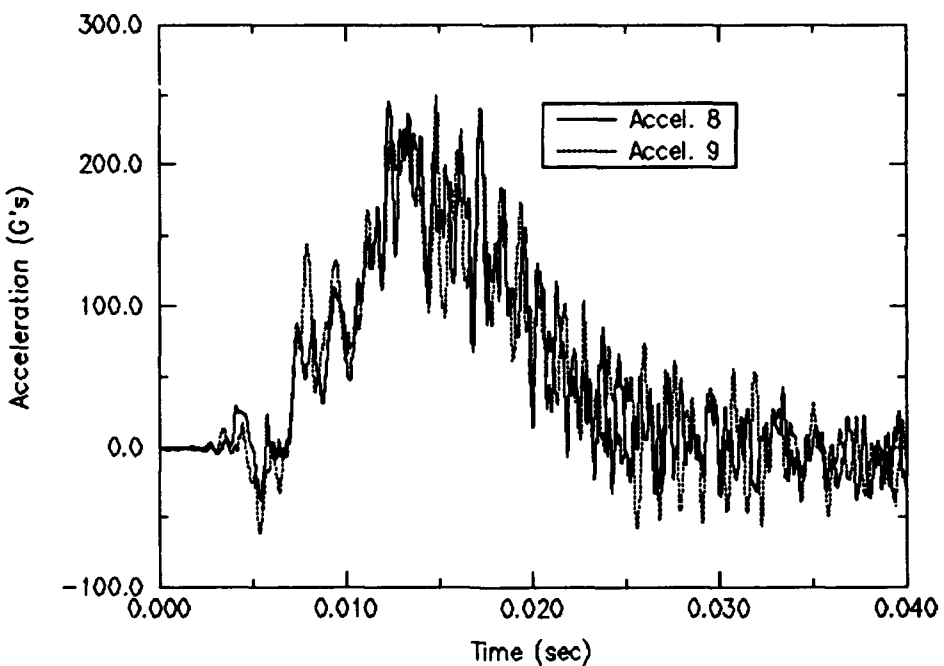


Figure 5.1.9 LLV aft cover (tail end, RV) accelerations (2 kHz filter)

5.2 Horizontal Low Velocity

The horizontal low-velocity (HLV) impact test was performed on June 30, 1993 at the 185-ft drop tower of Sandia National Laboratories. The container drop height was 7.9 m (26 ft) along a high-tension cable guided path which controlled impact orientation (see Figure 5.2.1). Analysis of high-speed films yielded an impact velocity of 12.1 m/s (39.8 ft/s) at an impact angle of 3.3° from perfectly horizontal. After impact, the test unit rebounded approximately 1.2 m (4 ft) from the unyielding target, tilting in mid-air toward the fork lift channel end, and impacting lightly at approximately 30° to horizontal after rebounding.

H1224A outer shell deformation resulting from the 12.1 m/s horizontal impact was greatest at the top end, as shown in Figure 5.2.2. The flexible foam inserts helped force the upper container shell back out to nearly its original diameter at the top end. The diameter at the container's outer shell midsection was reduced by approximately 82 mm (3.2 in.) at 0° circumferentially (see Appendix E: Inspection Data, Table E 2.1, and Figure 5.2.5). On the opposite end of the container near the fork lift channels, no deformation is visible, as shown in Figure 5.2.3.

Inside the container, the inner container diameter was decreased at its midsection slightly, as shown in Figure 5.2.4, due to contact with the outer shell during impact. The bending moment through the RV midsection due to support only at its ends during the side-on impact caused slight fracture of the carbon phenolic aeroshell at its midpoint and fore end (0° circumferentially), as shown in Figures 5.2.6a and 5.2.6b. The rapid loading of the RV after the flexible foam "bottomed out" caused bolts on the fore-most fore end weight plate to shear, as shown in Figure 5.2.7. No deformation was visible on the fore plate and aft cover. Container and RV deformations for the HLV impact test are quantified in Tables E 2.1, E 2.2, and E 2.3 of Appendix E, from measurement locations specified in Figures 3.6, 3.7, and 3.8.

Accelerations measured (and low-pass filtered to 2 kHz) at the aft and fore ends of the RV midsection are presented in Figures 5.2.8 and 5.2.9. The accelerometers in each figure were located 90° apart and show similar acceleration peaks of approximately 350 Gs at the aft end and 600 Gs at the nose or fore end. As identified by the time of peak acceleration and by the time of zero velocity in the integrated acceleration plots of Appendix B, the RV midsection aft end began rebounding approximately 15 milliseconds after container impact began and the fore end approximately 19 milliseconds after impact. The time delay between RV aft and fore end rebound is due in part to the slightly off-horizontal container impact.

Dynamic strain histories, as well as all raw and filtered data, FFTs and integrated accelerations are presented for the HLV impact test in Appendix B.



Figure 5.2.1 HSV impact test pre-drop



Figure 5.2.2 HLV H1224A top-end post-test deformation



Figure 5.2.3 HLV H1224A bottom-end post-test deformation



Figure 5.2.4 HLV inner container bending



Figure 5.2.5 HLV H1224A outer shell mid-body bending



Figure 5.2.6a HLV Mk12a Mod6c cracking

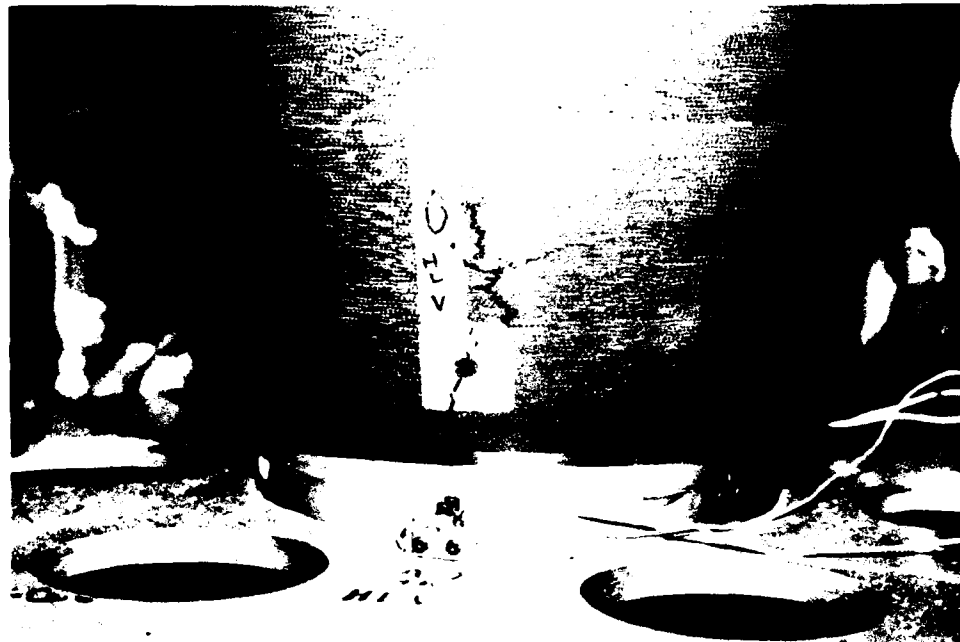


Figure 5.2.6b HLV Mk12a Mod6c cracking

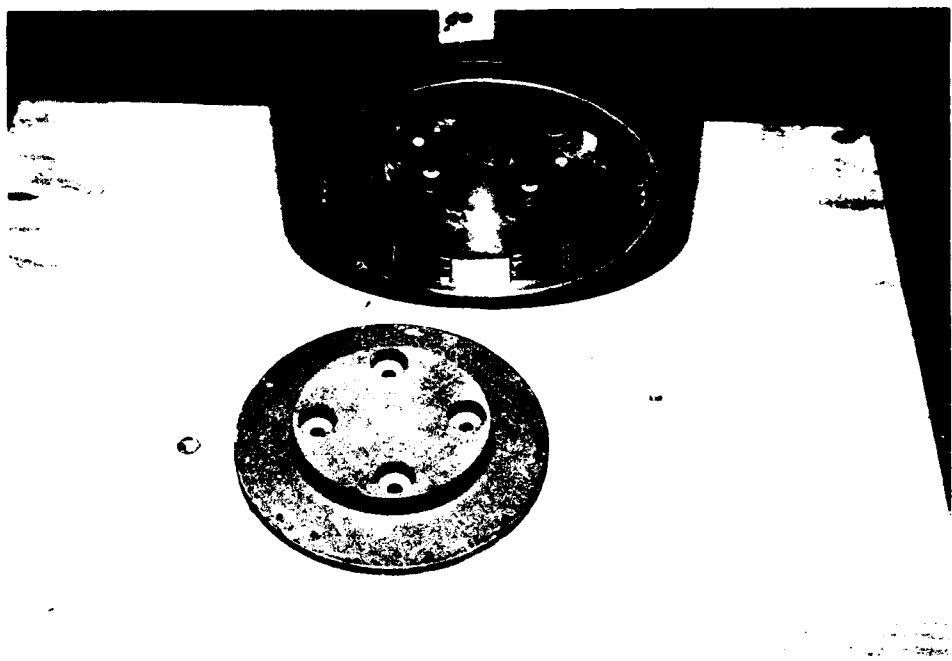


Figure 5.2.7 HLV RV weight plate bolt shearing

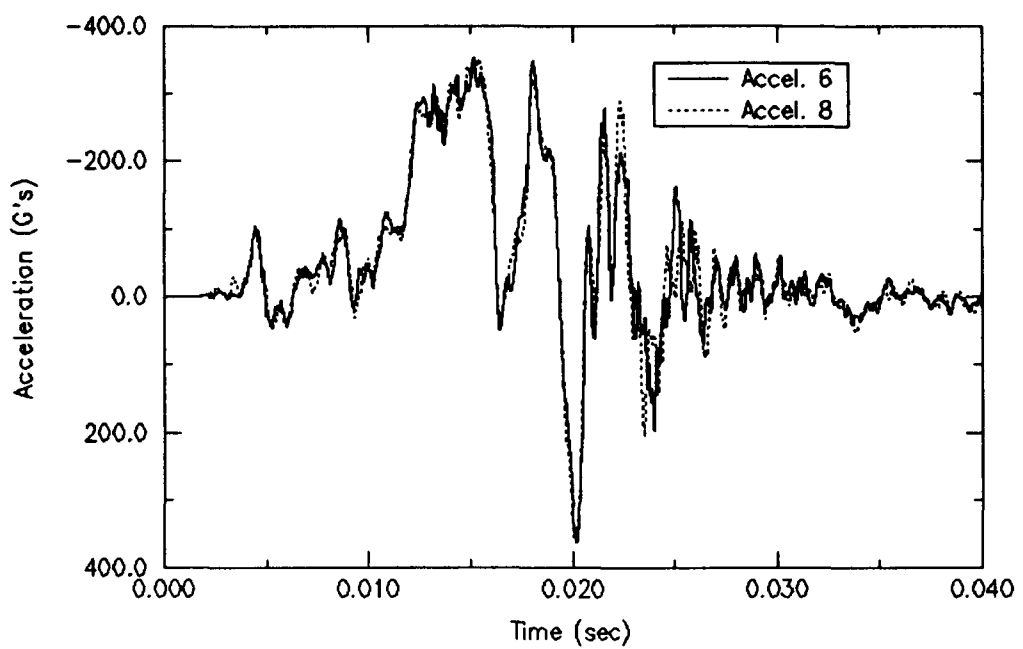


Figure 5.2.8 HLV aft cover (tail end, RV) accelerations (2 kHz filter)

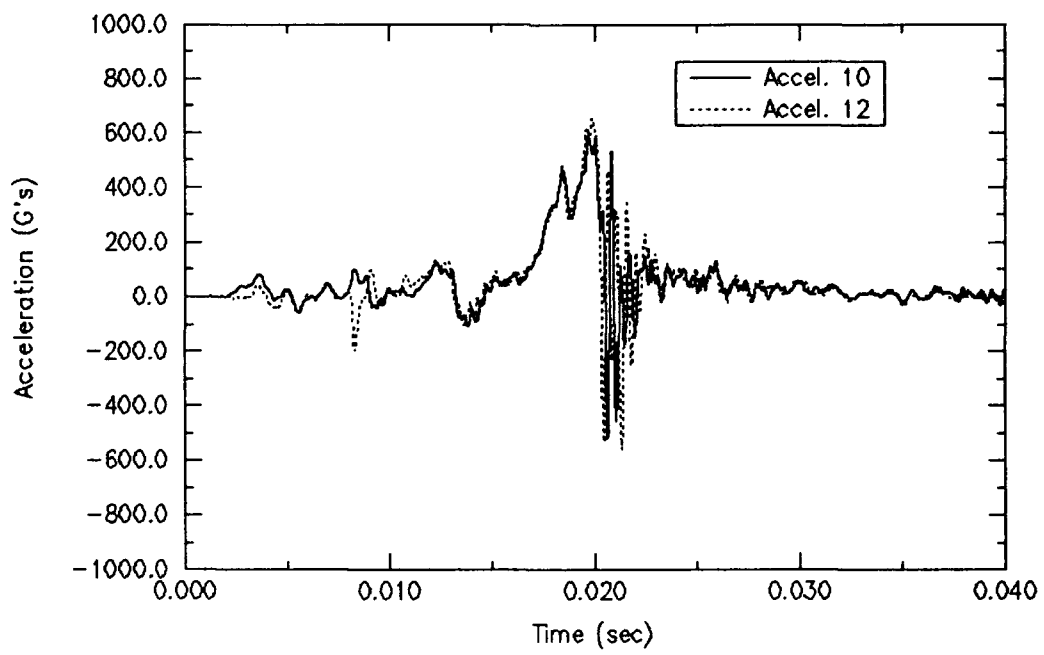


Figure 5.2.9 HLV fore plate (nose end, RV) accelerations (2 kHz filter)

5.3 Longitudinal High Velocity

The longitudinal high-velocity (LHV) impact test was performed on August 12, 1993 at the Aerial Cable Facility of Sandia National Laboratories. The container drop height was 86 m (283 ft) along a high-tension cable guided path which controlled impact orientation (see Figure 2.1). The LHV test unit is shown in Figure 5.3.1 before impact. Analysis of high-speed films yielded an impact velocity of 38.0 m/s (124.7 ft/s) at an impact angle of 0.7° from perfectly upright. After impact, the test unit rebounded about 10 cm (4 in.) at most from the unyielding target, tilting in mid-air very slightly toward the 0° circumferential axis.

H1224A outer shell deformation resulting from the 38.0 m/s longitudinal impact was greatest at the bottom end and in the fork lift channels, as shown in Figure 5.3.2a, 5.3.2b, and 5.3.2c. Buckling in the container's lower half of the outer shell was not significantly greater than that observed in the LLV impact test, but fork lift channel weld fracture and bending was incomparable. The upper half of the outer container shell suffered no visible deformation but, similar to the LLV impact tests, lower longitudinal stiffeners buckled at the container's lower circumferential bulge combining with fork lift channel deformation to reduce the container's overall length by up to 180 mm (7.1 in.) at 225° circumferentially (see Appendix E: Inspection Data, Table E 3.1).

Inside the container, the inner container buckled severely, as shown in Figure 5.3.3, reducing its overall length by up to 170 mm (6.8 in.). Extreme deformation of the carbon phenolic aeroshell, however, caused the aft cover to end up below the top level of the inner container, as shown in Figure 5.3.4. Both fore and aft RV weight plate groups sheared their mounting flanges and many inter-weight-plate bolts sheared during the severe impact. Weight plate deceleration led to severe fracture in the RV midsection aeroshell carbon phenolic and aluminum substrate, as shown in Figures 5.3.5 and 5.3.6. Severe bending in the fore plate can also be seen in Figure 5.3.5 and Figure 5.3.8. About 7.5 milliseconds after initial impact, the crushed aeroshell's nose or fore end came into contact with the fore accelerometers and their lead wires, yielding spurious results, as shown in Figures 5.3.7 and 5.3.9. Container and RV deformations for the LHV impact test are quantified in Tables E 3.1, E 3.2, and E 3.3 of Appendix E, from measurement locations specified in Figures 3.6, 3.7, and 3.8.

Accelerations measured (and low-pass filtered to 2 kHz) at the fore and aft ends of the RV midsection are presented in Figures 5.3.9 and 5.3.10. The accelerometers in each figure were located 90° apart and show similar acceleration peaks of approximately 10,000 Gs at the fore end (before the signal became faulty due to aeroshell fracture) and 2,000 Gs at the aft end. As identified by the time of peak acceleration and by the time of zero velocity in the integrated acceleration plots of Appendix C, the RV midsection fore end began rebounding approximately 6.3 milliseconds after container impact began and the aft end approximately 7.5 milliseconds after impact. The time delay between RV fore and aft end peak decelerations is due to energy loss associated with aeroshell fracture.

Dynamic strain histories, as well as all raw and filtered data, FFTs and integrated accelerations are presented for the LHV impact test in Appendix C.

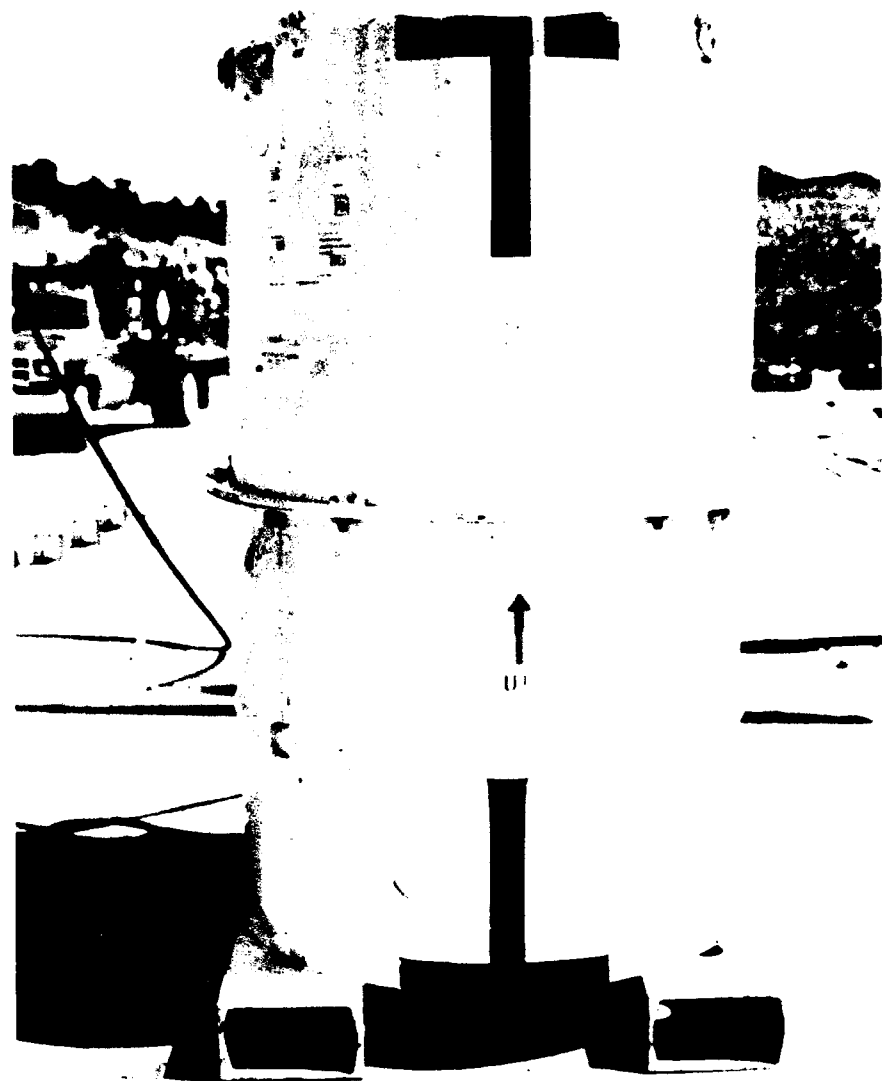


Figure 5.3.1 LHV impact test pre-drop



Figure 5.3.2a LHV H1224A post-test deformation

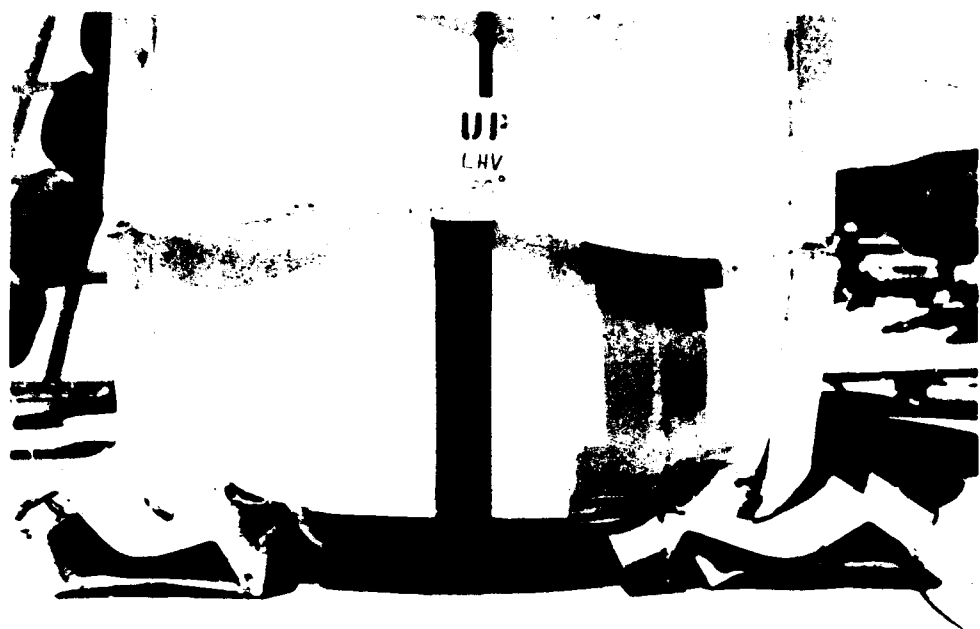


Figure 5.3.2b LHV H1224A post-test deformation



Figure 5.3.2c LHV H1224A post-test deformation



Figure 5.3.3 LHV inner container buckling



Figure 5.3.4 LHV aft cover below top level of inner container



Figure 5.3.5 Mk12a Mod6c aeroshell fracture and weight plate detachment



Figure 5.3.6 LHV RV carbon phenolic aeroshell fracture



Figure 5.3.7 LHV RV aeroshell nose-end fracture and impact onto accelerometers



Figure 5.3.8 LHV fore plate deformation

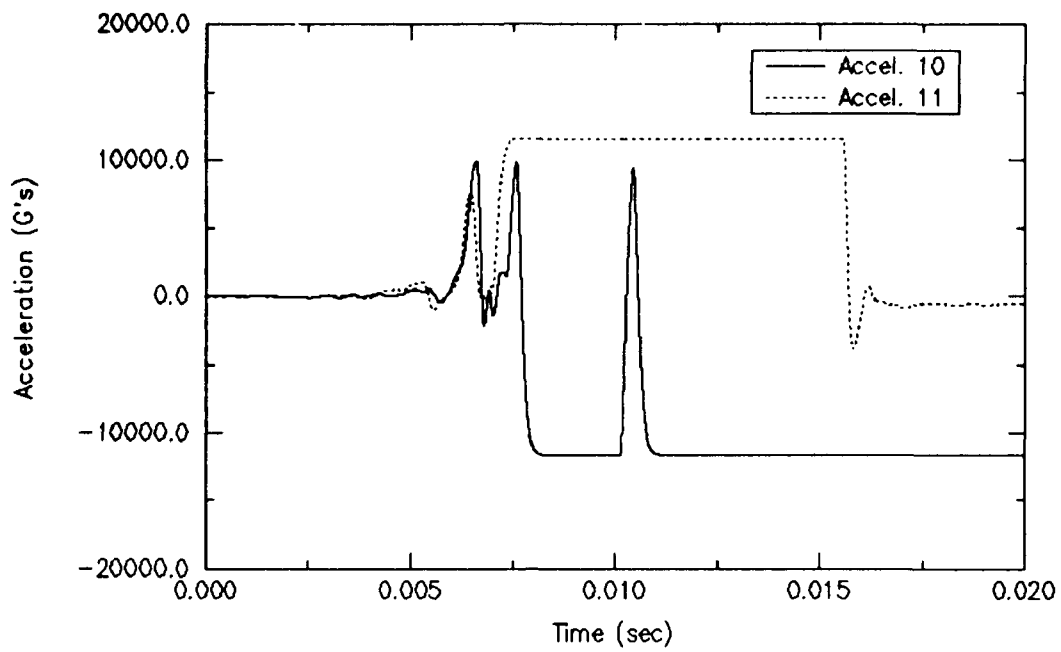


Figure 5.3.9 LHV fore plate (nose end, RV) accelerations (2 kHz filter)

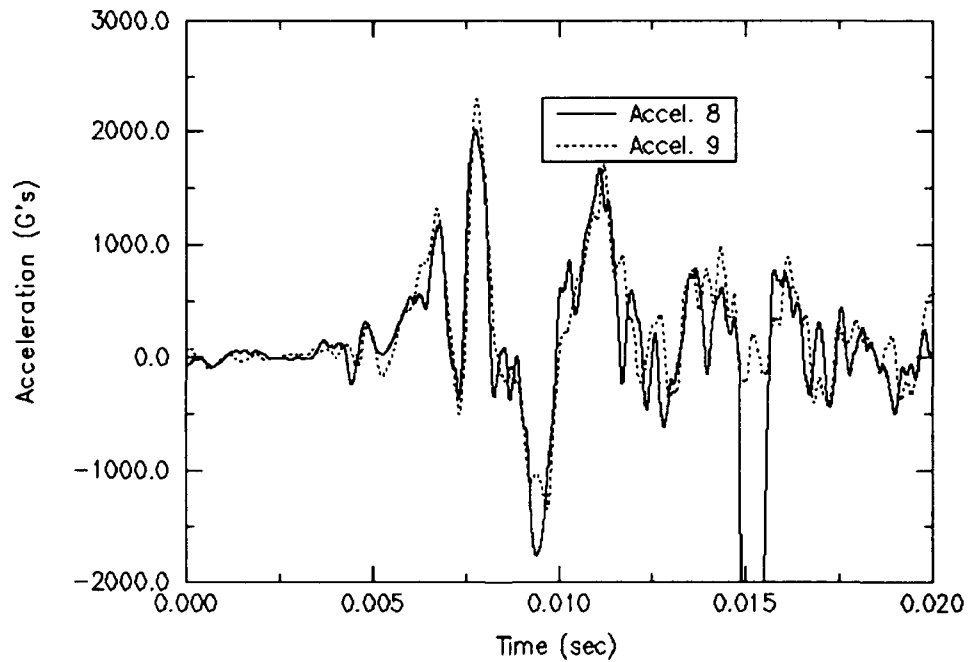


Figure 5.3.10 LHV aft cover (tail end, RV) accelerations (2 kHz filter)

5.4 Horizontal High Velocity

The horizontal high-velocity (HHV) impact test was performed on August 13, 1993 at the Aerial Cable Facility of Sandia National Laboratories. The container drop height was 88 m (288 ft) along a high-tension cable guided path which controlled impact orientation (see Figure 2.2). The HHV test unit is shown in Figure 5.4.1 before impact. Analysis of high-speed films yielded an impact velocity of 38.2 m/s (125.3 ft/s) at an impact angle of 1.1° from perfectly horizontal. After impact, the test unit rebounded about 1.5 m (5 ft) from the unyielding target, rotating longitudinally about 120° impacting partially on its bottom (fork lift channel) side after rebound.

H1224A outer shell deformation resulting from the 38.2 m/s horizontal impact is shown in Figure 5.4.2a, 5.4.2b, and 5.4.2c. Similar to the HLV impact test results, the top container shell returned nearly to its undeformed diameter at the top surface (Figure 5.4.2b) and remained deformed at its midsection (Figure 5.4.2c) by as much as 235 mm (9.2 in.) (see Appendix E: Inspection Data, Table E 4.1). But the fork lift channel, bottom pan, and inner container lower plate weld joints all sheared and tore, along with the lower foam insert glue joint, exposing the fore plate and RV aeroshell, as shown in Figure 5.4.2a.

Inside the container, the fore plate bolts (attaching it to its threaded ring) sheared upon impact and prevented severe deformation of the fore plate, as shown in Figure 5.4.3. The aft cover deformed severely (reducing its diameter by 49 mm [1.9 in.]), tearing the inner container, as shown in Figure 5.4.4. Ovalization of the outer container shell midsection is shown in Figure 5.4.5. Large bending loads in the RV midsection caused severe fracture in the aeroshell's carbon phenolic outer layer and aluminum substrate, as shown in Figures 5.4.6 and 5.4.7, releasing most of the weight plates and shearing some of the inter-plate bolts. Container and RV deformations for the HHV impact test are quantified in Tables E 4.1, E 4.2, and E 4.3 of Appendix E, from measurement locations specified in Figures 3.6, 3.7, and 3.8.

Accelerations measured (and low-pass filtered to 2 kHz) at the fore and aft ends of the RV midsection are presented in Figures 5.4.8 and 5.4.9. The accelerometers in each figure were located 90° apart and show rather dissimilar acceleration histories. Acceleration pulses from accelerometers 6, 8, 10, and 12 (fore and aft ends of the mass mock-up midsection, in the impact axis appeared to be much longer in duration than comparable acceleration pulse histories from the high speed end-on impact. Also, integration of these pulses showed that only a much shorter duration pulse was necessary to slow the re-entry vehicle midsection velocity from 125 ft/s to approximately -20 ft/s (negative denoting upward after downward impact).

After reviewing high-speed film views of the impact event, dummy accelerometer output, and the post-test accelerometer calibrations, the cause of the abnormal acceleration histories was determined. During impact, separation of the welded joint between the H1224A lower cylinder and the bottom pan caused stretching of accelerometer and strain gage channel wires. Before the wires completely failed, the stretching caused resistance changes thus inducing spurious accelerations. From high-speed films, stretching appears to begin occurring at about 2.5 to 3 milliseconds into the impact event, thus the acceleration data from these four accelerometers is suspect after

this point in time. The dummy channel (A15 in Appendix D, full scale output equals 0.05 Volts) indicates that wire stretching may have begun as early as 1.25 ms into the impact event. This is also approximately the time at which the re-entry vehicle midsection has zero velocity (see integrated velocity histories). Since the instantaneous rebound velocity of the relatively rigid attachment points for the accelerometers is much greater than zero, actual peak acceleration magnitudes should be greater than those shown in the data plots at approximately 3 ms.

It is estimated that valid acceleration data was recorded up through about peaks of approximately 8,000 Gs at the fore end and 10,000 Gs at the aft end. As identified by the time of peak acceleration and by the time of zero velocity in the integrated acceleration plots of Appendix D, the RV midsection began rebounding approximately 3 milliseconds after container impact began. This lesser peak RV deceleration time compared to the LHV test results is justified by the reduced effective container thickness in this impact orientation, since the fork lift channels have no influence.

Dynamic strain histories, as well as all raw and filtered data, FFTs and integrated accelerations are presented for the HHV impact test in Appendix D.

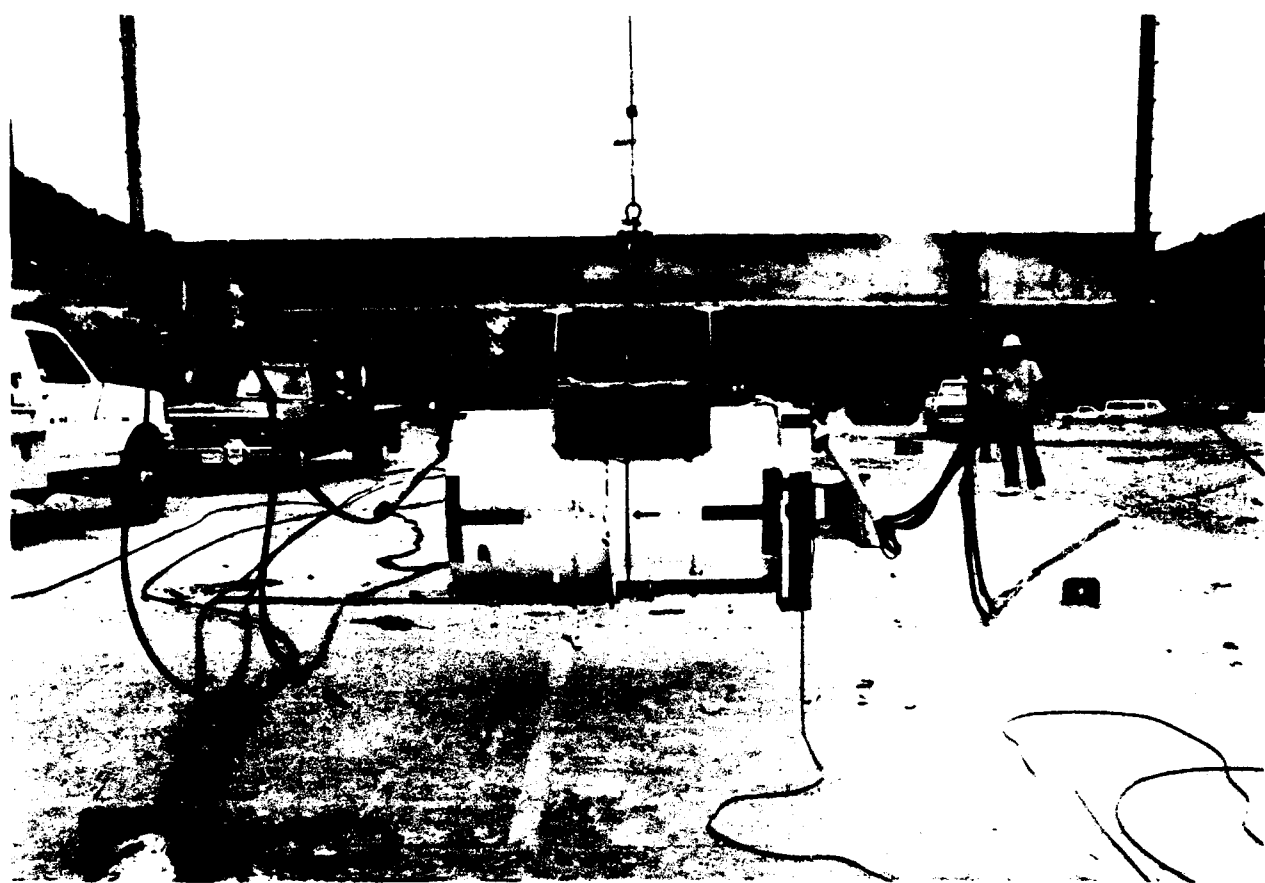


Figure 5.4.1 HHV impact test pre-test



Figure 5.4.2a HHV H1224A post-test deformation



Figure 5.4.2b HHV H1224A post-test deformation



Figure 5.4.2c HHV H1224A post-test deformation

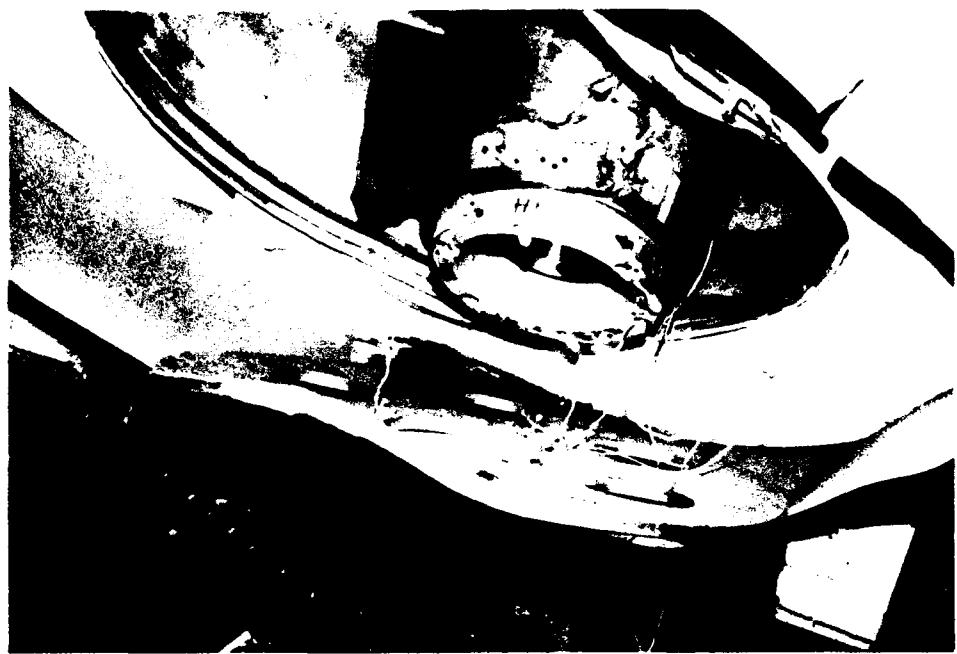


Figure 5.4.3 HHV fore plate deformation and bolt shearing



Figure 5.4.4 HHV inner container and aft cover deformation



Figure 5.4.5 HHV H1224A outer shell deformation



Figure 5.4.6 HHV Mk12a Mod6c aeroshell fracture and detached weight plates



Figure 5.4.7 HHV RV carbon phenolic aeroshell fracture

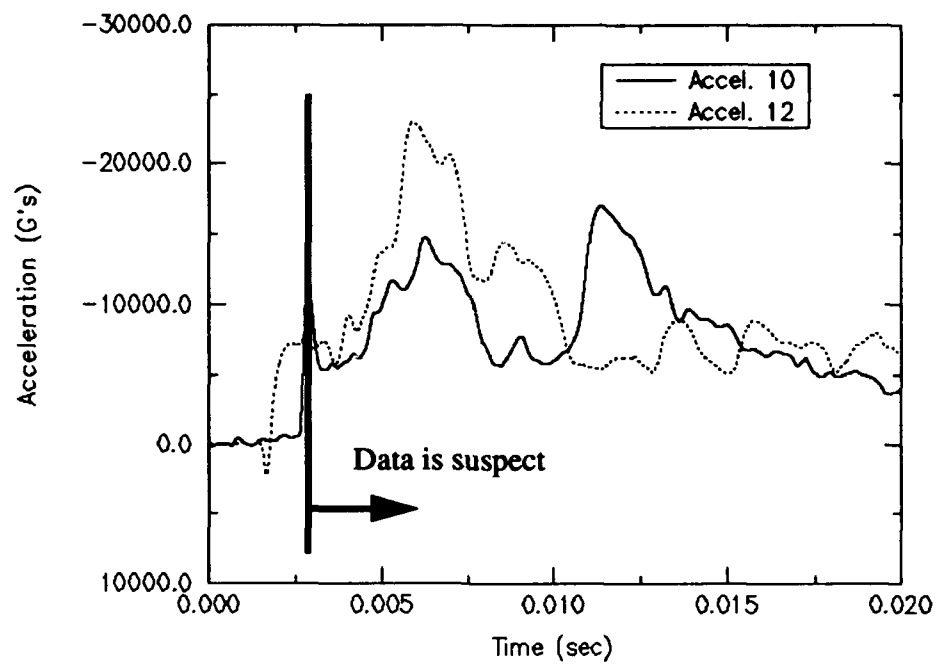


Figure 5.4.8 HHV fore plate (nose end, RV) accelerations

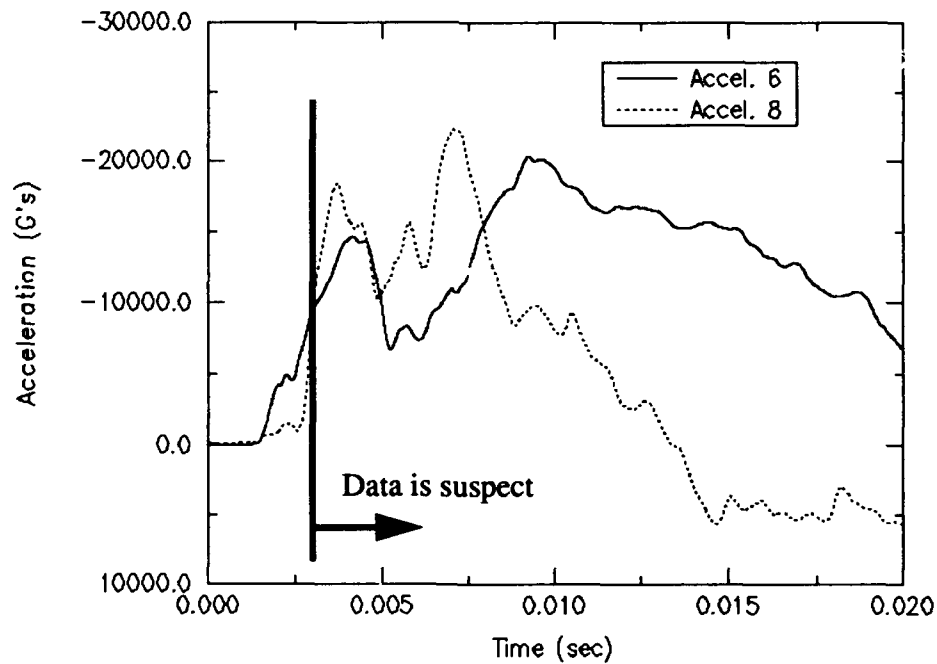


Figure 5.4.9 HHV aft cover (tail end, RV) accelerations

6. Conclusions

Sandia National Laboratories has performed four impact tests of the H1224A shipping/storage container for the Mk12a W78 warhead midsection. The 12.2 m/s (40 ft/s) and 38.1 m/s (125 ft/s) impact velocities onto unyielding targets encompass a range of potential accident conditions associated with the weapon's STS. Acceleration and deformation results should be useful in validating analytical models, which can be used to predict weapon response throughout the range of accident conditions.

Some acceleration and strain data was lost during the HHV impact test. Post-test review of the test unit, accelerometer and strain gage output histories, dummy channel output histories, and high-speed films indicated that unanticipated container deformations led to stretching and even severing of transducer lead wires. The wire stretching resulted in spurious transducer output histories at approximately 2.5 to 3 milliseconds after initial impact, limiting the usefulness of data after this point. For accelerations on the fore and aft end of the RV, however, most of the downward kinetic energy was absorbed at the time of wire stretching and can be used to partially benchmark analytical predictions.

Accelerations measured at points on the Mk12a Mod6c's fore plate and aft cover during impact tests are point measurements on a *test* unit, which may differ significantly from accelerations experienced by an actual WR Mk12a midsection under identical conditions. Dissimilar accelerations measured at opposite ends of the RV prove the non-rigidness of the body during longitudinal impact tests. Thus, modelling the RV as a rigid body should yield different results than those measured. Similarly, although mass properties are identical for undeformed WR Mk12a and Mk12a Mod6c midsections, mass distributions and interactions with the support structure of the aeroshell during severe impacts are very different. Thus, RV accelerations measured during these impact tests may only approximate those experienced by WR hardware in identical impact conditions.

Deformations in the RV midsection aeroshells during impact tests can be misleading. They are caused not only by interactions with the container and the impact surface, but also interactions with masses inside. The severe fracture patterns of RV aeroshells and aluminum substrates observed in the high-speed impact tests are unique to these test units with extremely dense, steel weight plate mass simulators at each end. The sharp cylindrical edges may aide in the fracture process as compared to an actual physics package which could deform and absorb more of its own kinetic energy upon impact. The distinction between WR and tested RV midsections is important not only for use in proper application of RV loads during accident modelling, but also in assumed levels of aeroshell deformation for containment of potentially hazardous materials.

Acknowledging differences between the tested Mk12a Mod6c midsection and a WR Mk12a, acceleration and strain results obtained during this series of low and high velocity impact tests should prove useful in approximating W78 midsection load levels and validating finite element model results for similar accident conditions.

References

- [1] Report on the Panel on Nuclear Weapon Safety on the Committee on Armed Forces, House of Representatives, One Hundred First Congress, Second Congressional Session: December 1990. (also known as "Drell Report" or "Report of Drell Panel")
- [2] Review of Drell Panel Recommendations for ICBM Systems, TRW Ogden Engineering Operations for the Department of the Air Force, Aug. 9, 1991.
- [3] Department of Defense and Department of Energy Study on the Logistic Transportation of Nuclear Weapons, Sept. 1991.
- [4] Stockpile to Target Sequence for the Mk12a (W78), Air Force Weapon Laboratory, Sept.27, 1976.
- [5] "Mk 12A/JMTP-2D Rail-ATMX Humping Shock Test," Sandia Report # R705129, April 27, 1979.
- [6] "Mk 12A/LTU-3 Simulated ATMX Railroad Humping Shock at High and Low Temperatures," Sandia Report # R705151, February 22, 1978.
- [7] "Mk 12A/LTU-3 Handling and Transportation at High and Low Temperature," Sandia Report # R705152, March 20, 1978.
- [8] "Transportation Vibration Test of the Mk 12A LTU-3," Sandia Report # R705152-1, March 17, 1978.
- [9] "Mk12A-LTU-3A Handling and Transportation Vibration," Sandia Report # R705207-1, February 18, 1979.
- [10] "Mk 12A/JMTP-2D Handling and Transportation Tests," Sandia Report # R705129, January 17, 1979.
- [11] "Final Sandia Laboratories Test Report, Mk 12A/JMTP-7B Handling, Transportation, and Flight Environments," Sandia Report #s R705211, 212, 213, 214, 216, 217, 218, March 4, 1980.
- [12] "Final Sandia Laboratories Test Report, Mk 12A/JMTP-3B, Handling, Transportation, and Flight Environments," Sandia Report #s R705138, 139, 201, 202, 203, 204, 205, 206, March 4, 1980.
- [13] "Final Sandia Laboratories Test Report, Mk 12A/JMTP-2D Handling, Transportation, and Flight Environments," Sandia Report #s R705121, 122, 123, 124, 125, 126, 128, 129, 130, September 12, 1979.
- [14] "Final Test Report, Mk 12A/JMTP-2B Transportation and Handling Tests," Sandia Report

#s R705118, 119, July 8, 1978.

[15] SNL drawing #'s AY316847, AY288436, AY288437, AY327291, AY273717, AY273718, AY273719, 273720, AY316848, AY326801, AY326802, AY326803, AY326805, and AY326806.

[16] "The Mobile Instrumentation Data Acquisition System (MIDAS)," SAND90-2916, 1990.

[17] Uncapher, W. L., Dickinson, J. R., Althaus, B. L., and Holten, J. R., "The Development of a Mobile Instrumentation Data Acquisition System for Use in Cask Testing," Presented at PATRAM '89, September 1989.

[18] Madsen, M. M., Uncapher, W. L., Stenberg, D. R., and Baynes, E. E., "Testing the Half-Scale Model of the Defense High Level Waste Transportation Cask," SAND86-1130, TTC-0662, August 1987.

[19] Measurements Group Strain Gage Mounting Specifications Reference Documents B-129, B-137-13, and TT-609.

[20] Endevco Corporation, 1992 Dynamic Instrumentation Catalog

[21] International Atomic Energy Agency, Safety Series No. 37 (Advisory Material for the IAEA Regulations for the Safe Transport of Radioactive Material), Paragraph A-601.14, 1990.

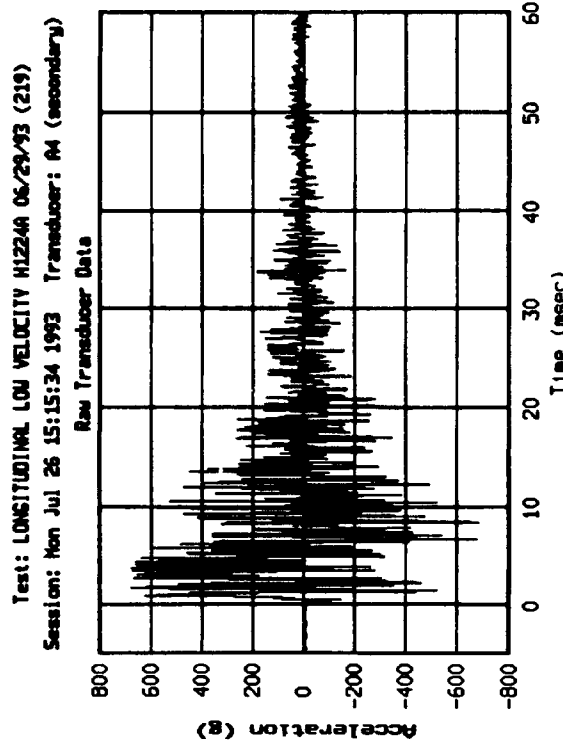
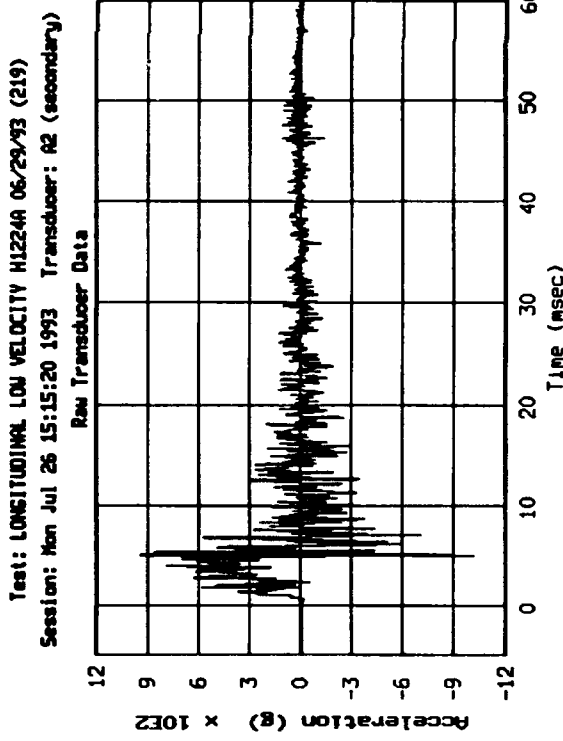
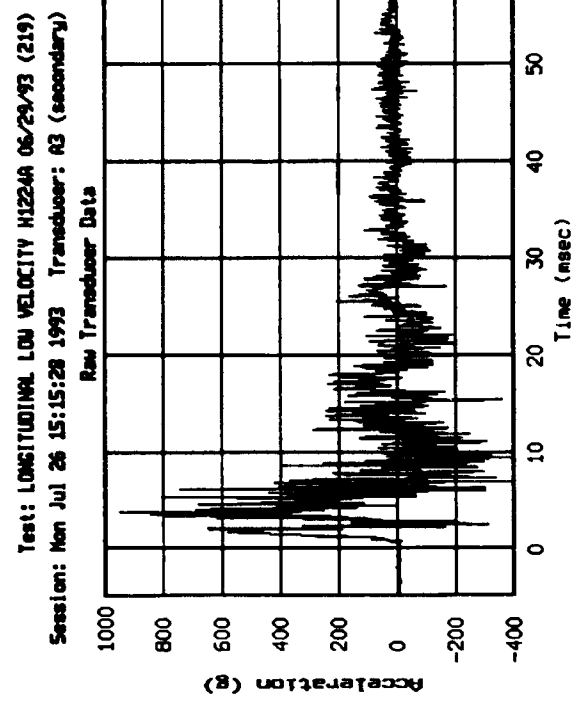
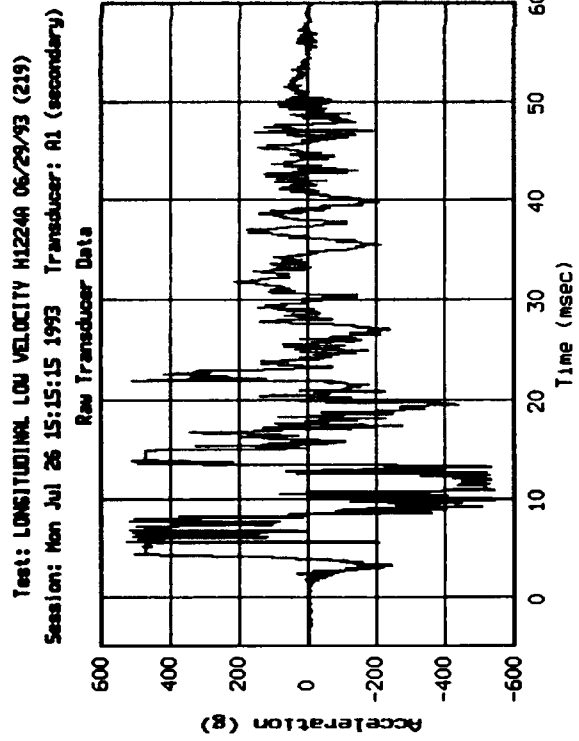
[22] F. N. Rebarchik, "Calibration of Accelerometers at the Drop Ball Station," SAND93-1232, August 1993.

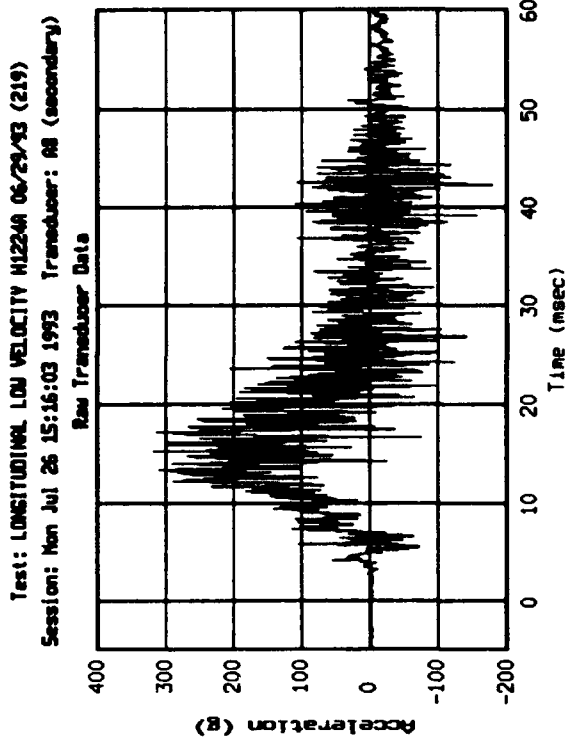
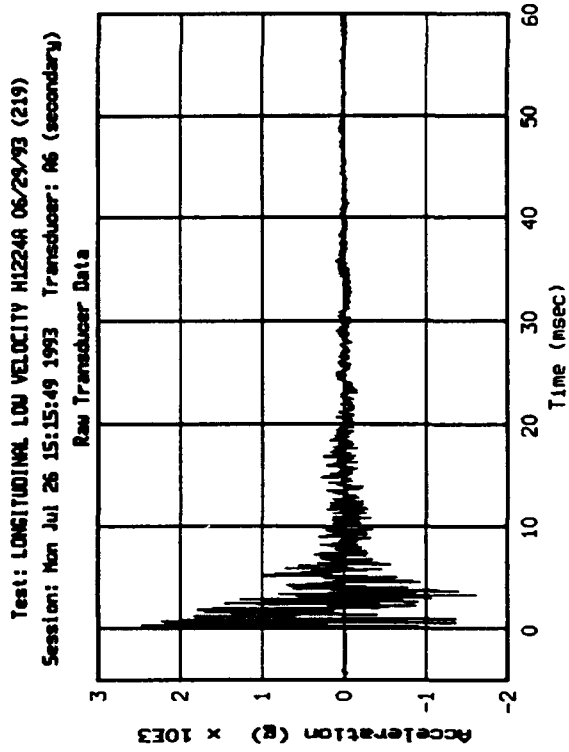
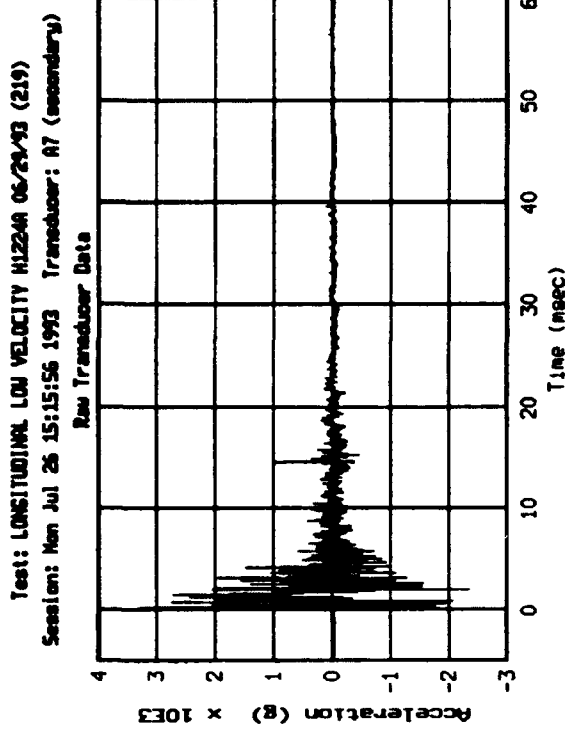
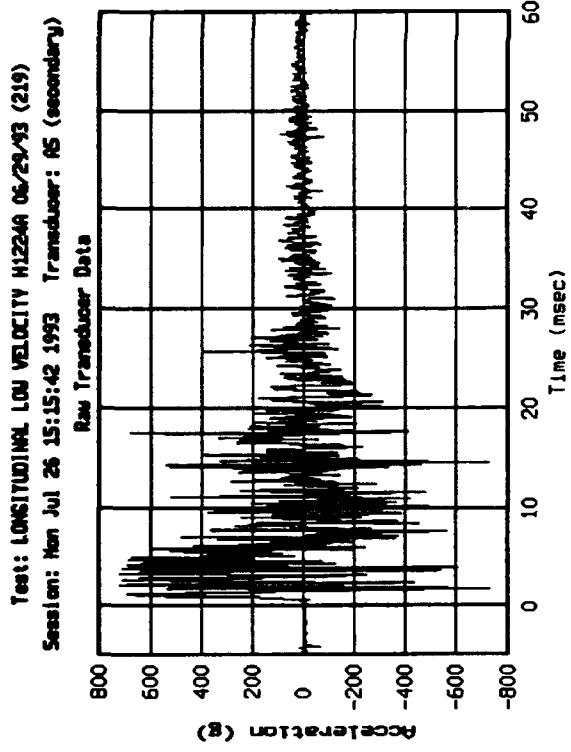
[23] F. N. Rebarchik, "Calibration of Accelerometers on the 5,000-G Centrifuge," SAND92--321, May 1992.

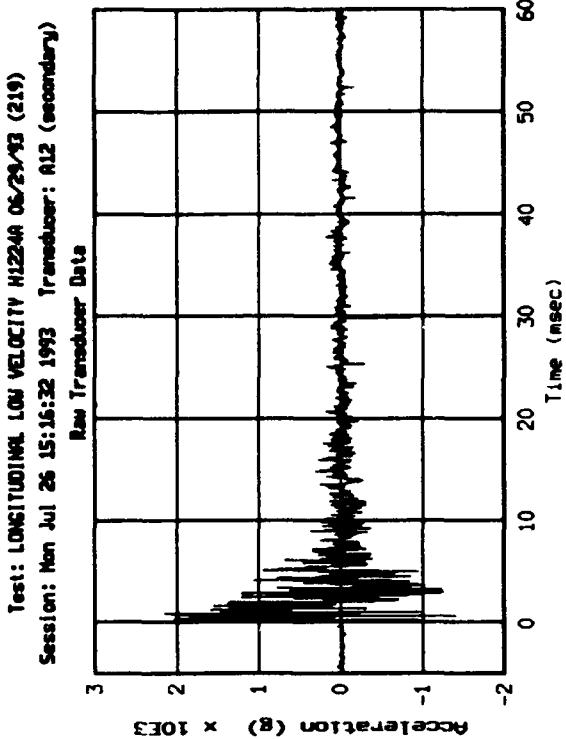
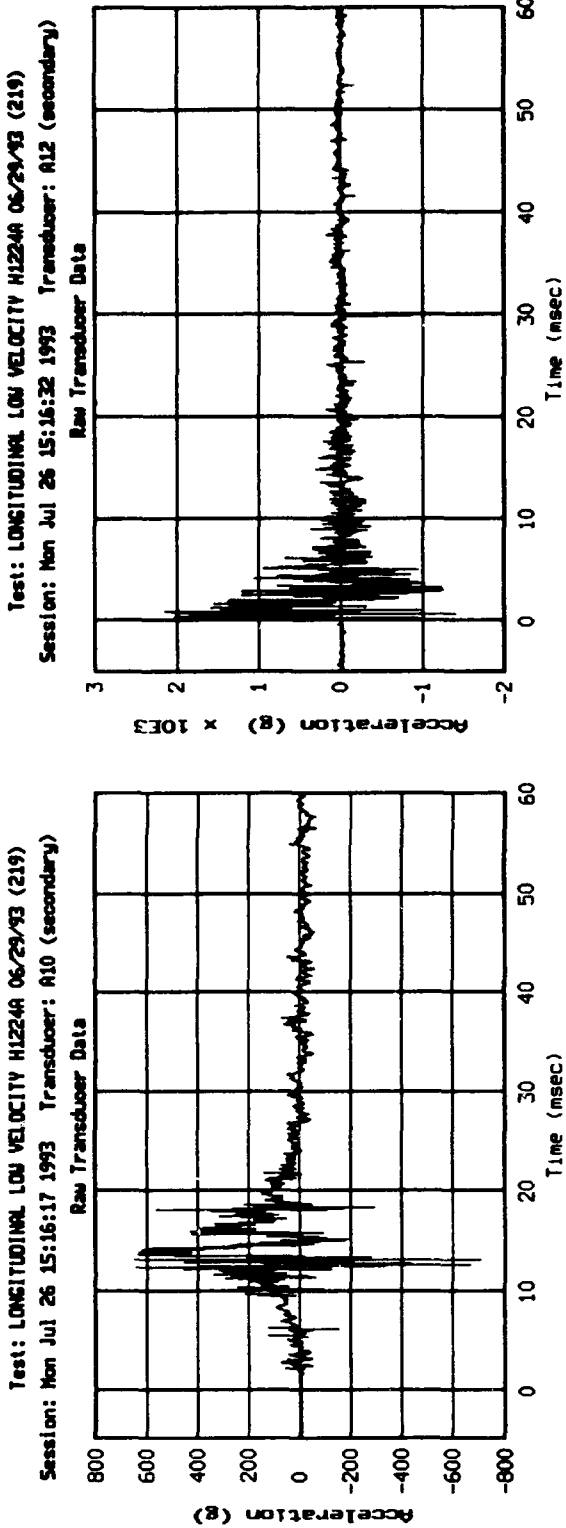
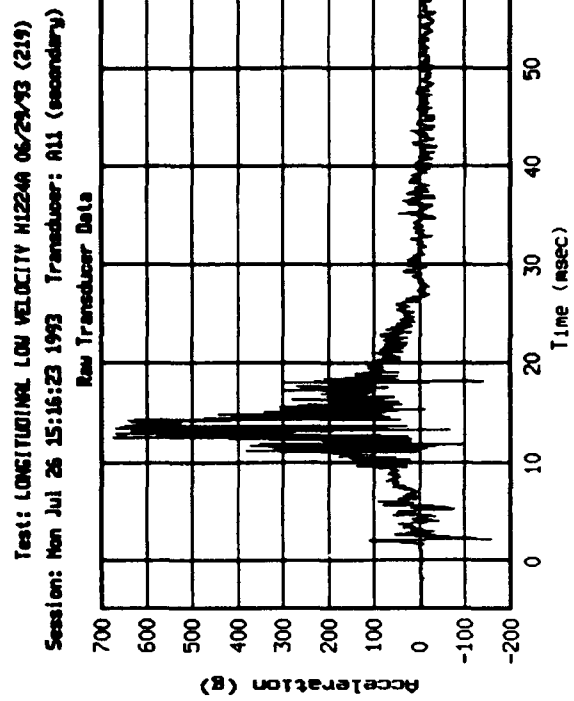
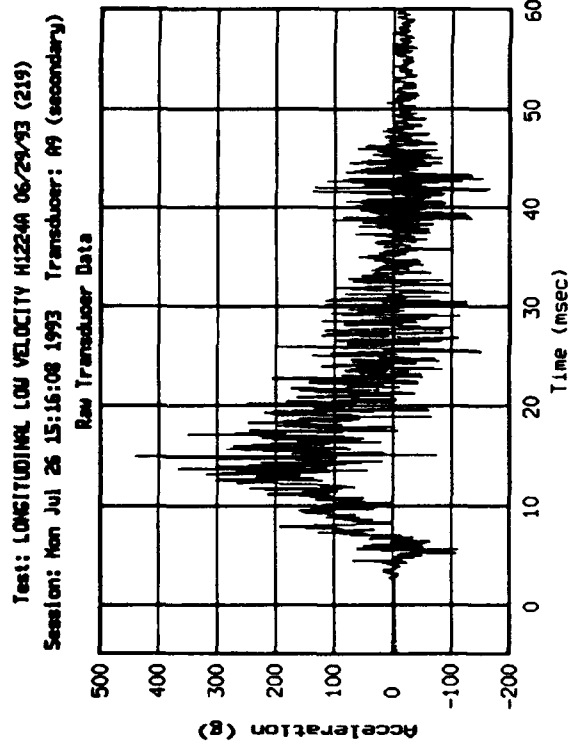
[24] F. N. Rebarchik, "Operating Procedures for Calibration of Accelerometers on the Unholtz-Dickie 100-G Shaker," Sandia Labs Internal Memorandum RS7241/89/00004, March 1989.

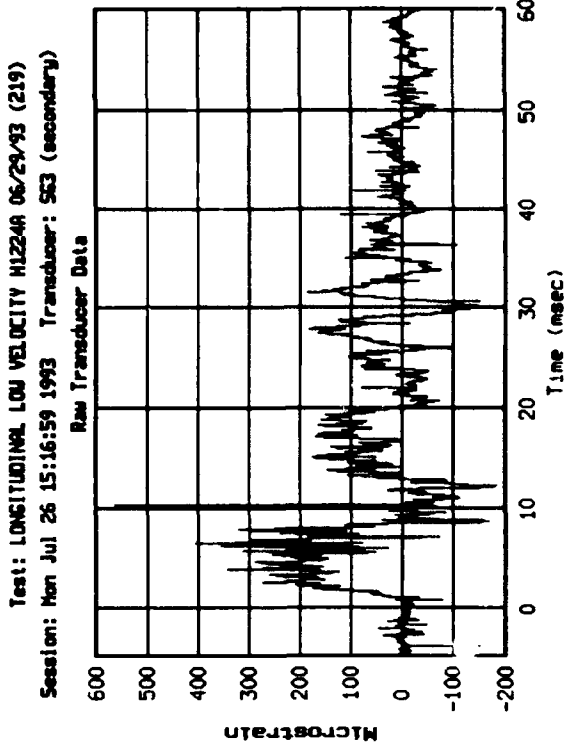
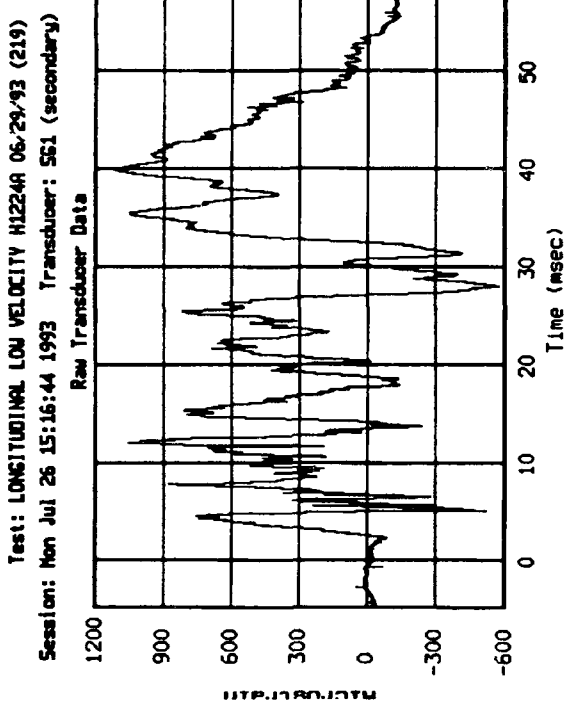
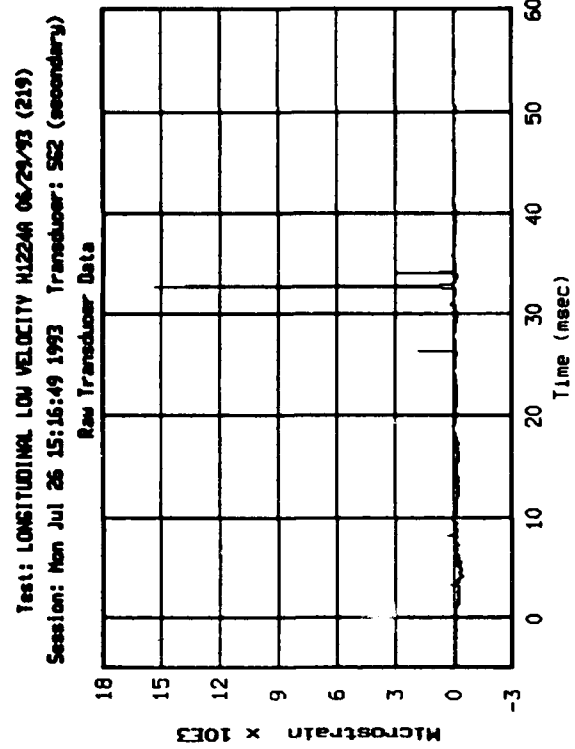
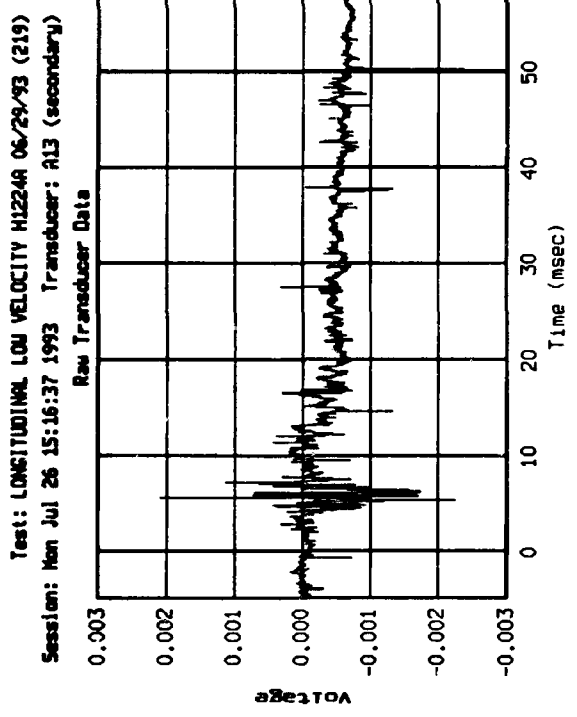
Appendix A. LLV Accelerometer and Strain Gage Data: Raw, Filtered, and Reduced

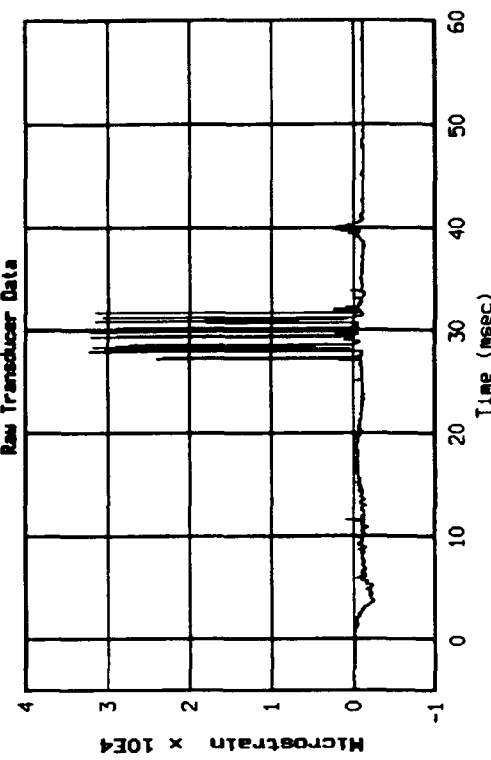
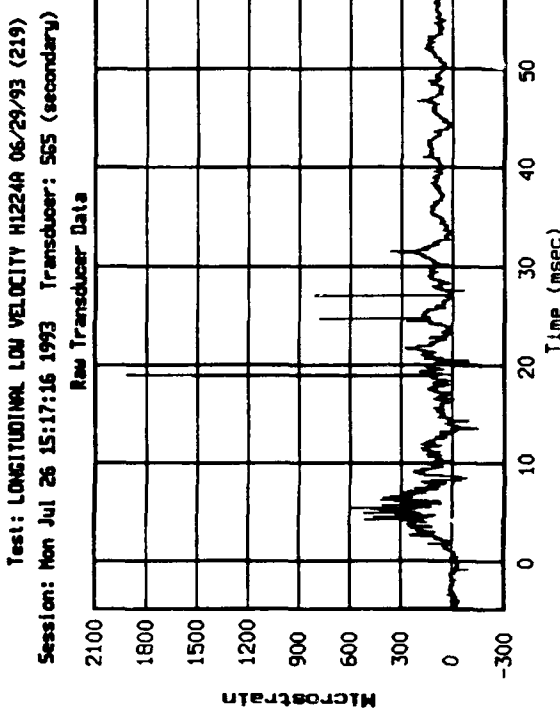
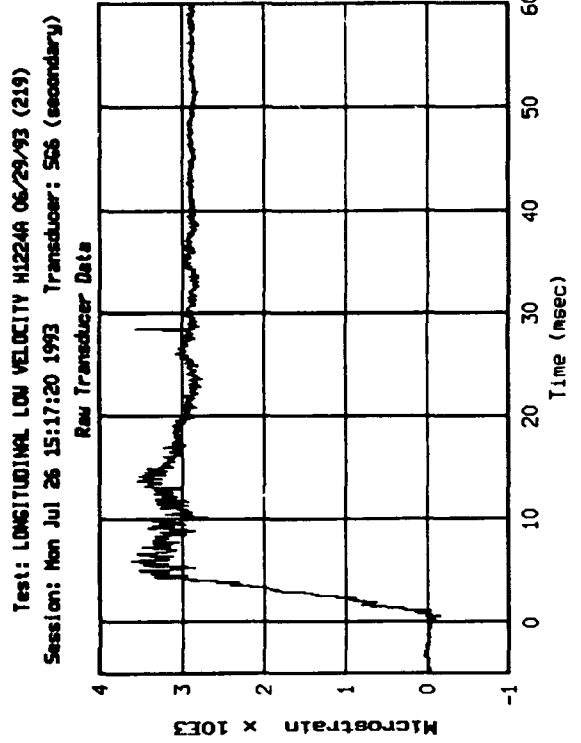
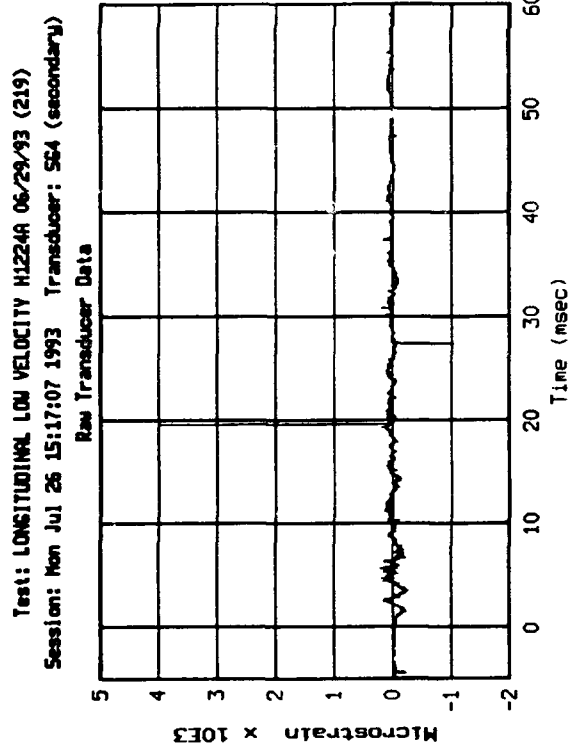
The following pages show raw (unfiltered) acceleration and strain gage data for the Longitudinal Low-Velocity (LLV) impact test. Following this raw data are plots of filtered data (using a low-pass Butterworth 6-stage filter) with cutoff frequencies of 250 Hz and 2,000 Hz. Integrated acceleration data, yielding velocity versus time plots, are presented to analyze kinetic energy values during the test. And finally, Fast Fourier Transforms (FFTs) for each raw data channel are included to analyze acceleration and strain amplitudes in the frequency domain.

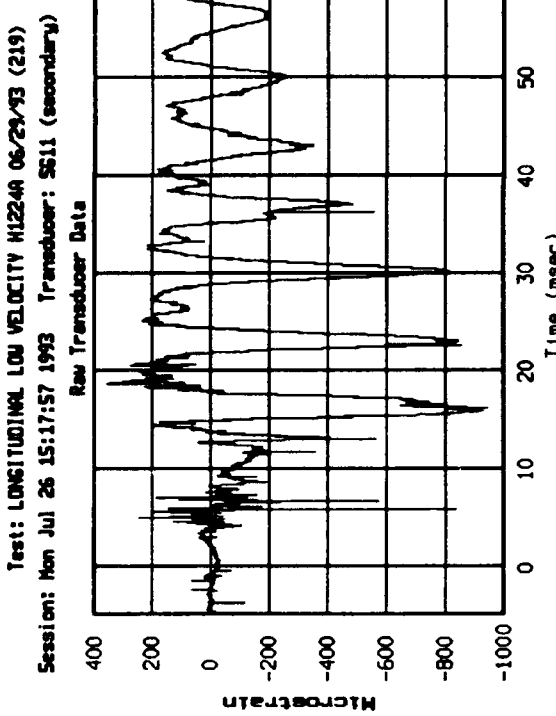
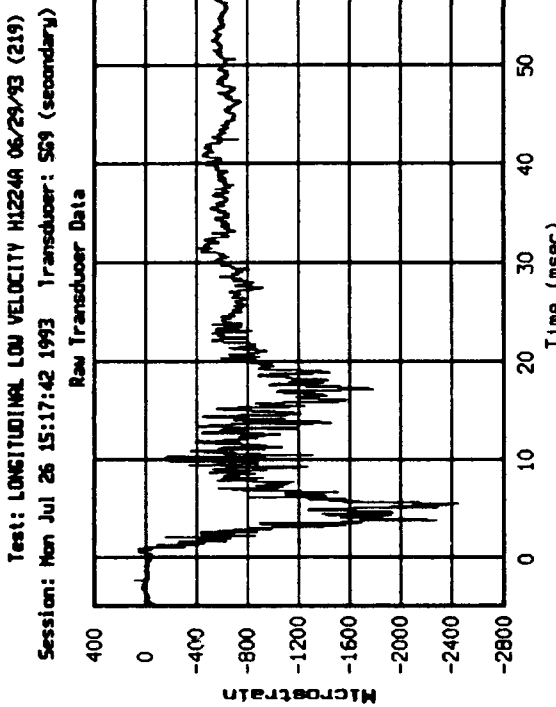
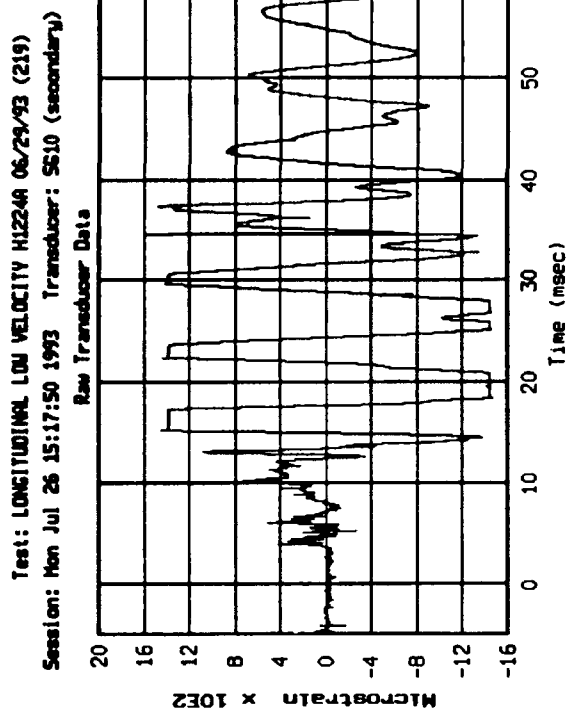
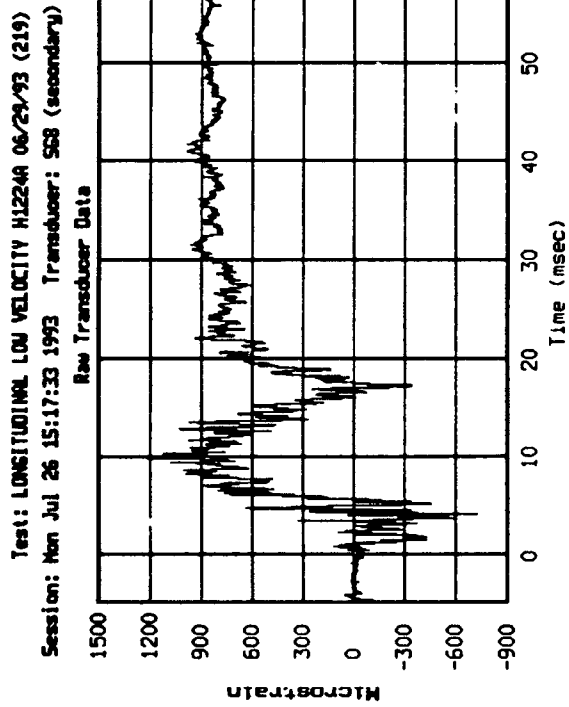




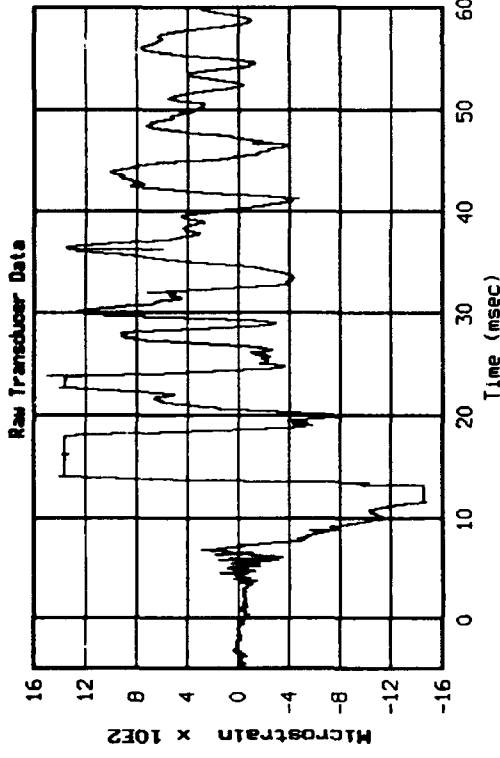




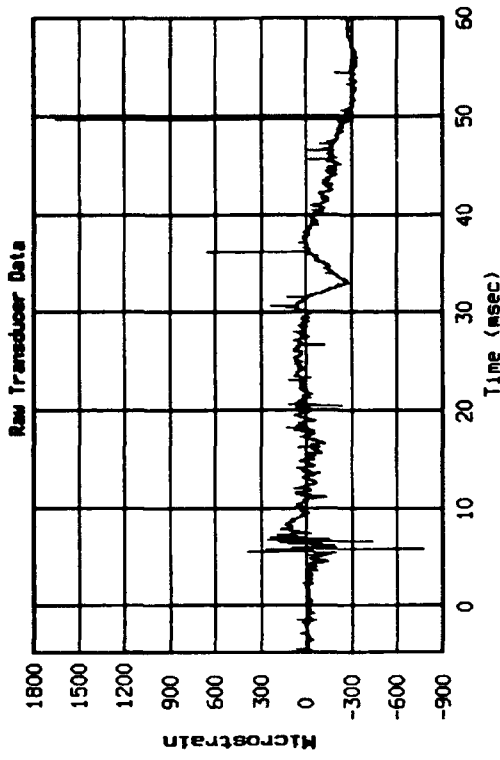




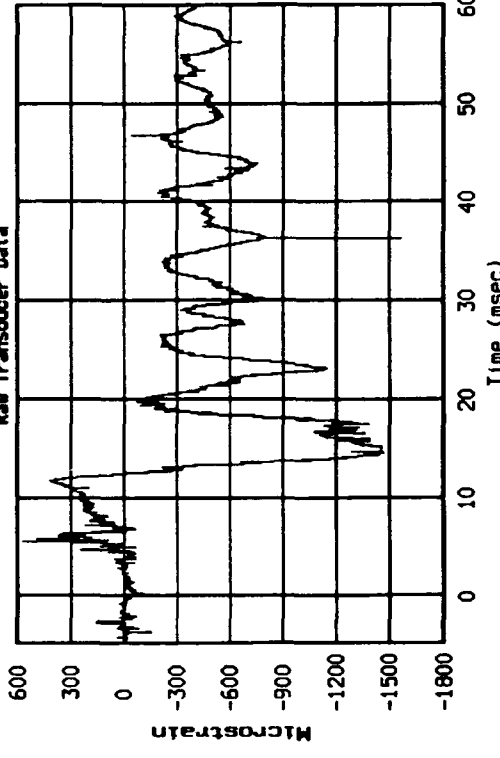
Test: LONGITUDINAL LOU VELOCITY H1224A 06/29/93 (219)
Session: Mon Jul 26 15:18:13 1993 Transducer: SG12 (secondary)



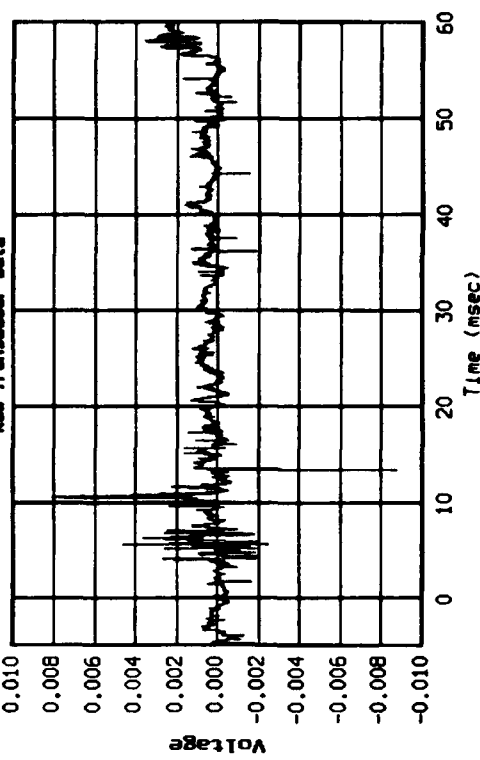
Test: LONGITUDINAL LOU VELOCITY H1224A 06/29/93 (219)
Session: Mon Jul 26 15:18:03 1993 Transducer: SG14 (secondary)



Test: LONGITUDINAL LOU VELOCITY H1224A 06/29/93 (219)
Session: Mon Jul 26 15:18:20 1993 Transducer: SG13 (secondary)

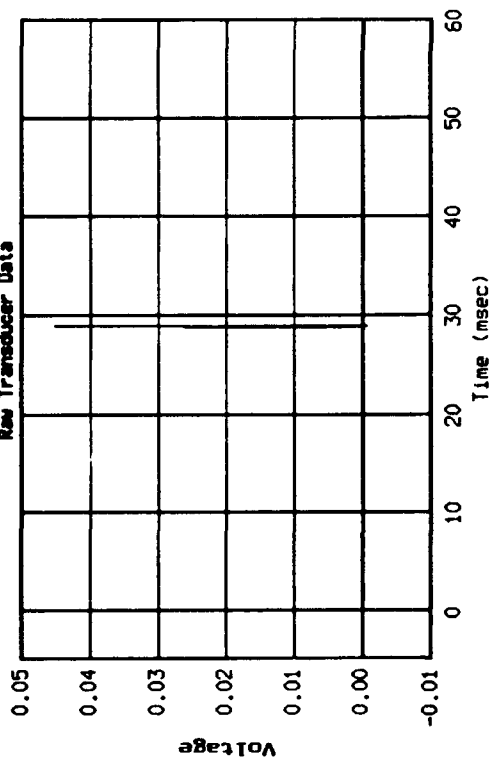


Test: LONGITUDINAL LOU VELOCITY H1224A 06/29/93 (219)
Session: Mon Jul 26 15:18:31 1993 Transducer: SG15 (secondary)



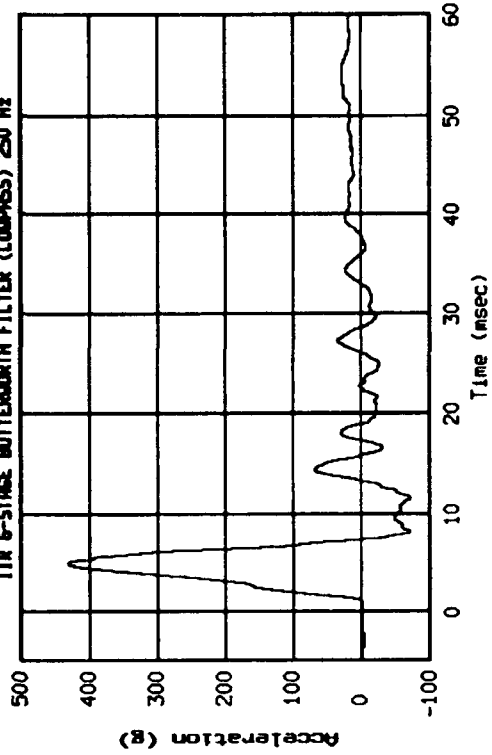
Test: LONGITUDINAL LOW VELOCITY H1224A 06/29/93 (219)
Session: Mon Jul 26 15:18:36 1993 Transducer: S16 (secondary)

Raw Transducer Data



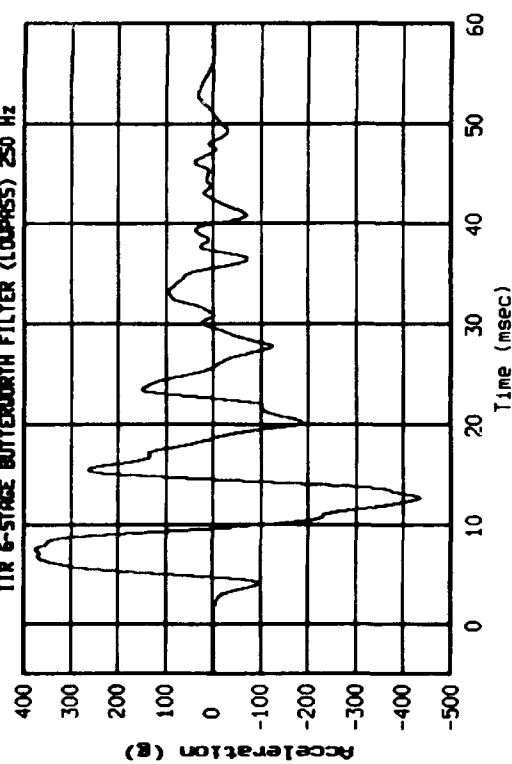
Test: LONGITUDINAL LOW VELOCITY H1224A 06/29/93 (219)
Session: Tue Jul 27 10:38:59 1993 Transducer: A2 (secondary)

IIR 6-STAGE BUTTERWORTH FILTER (LOPSS) 250 Hz



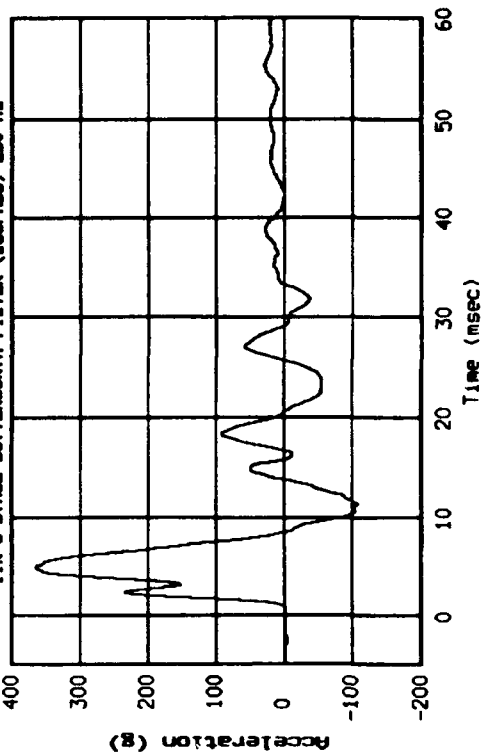
Test: LONGITUDINAL LOW VELOCITY H1224A 06/29/93 (219)
Session: Tue Jul 27 10:38:57 1993 Transducer: A1 (secondary)

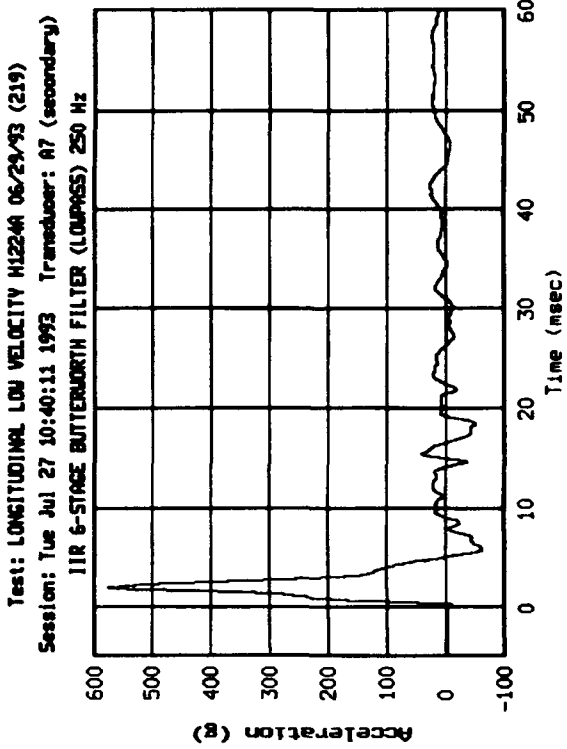
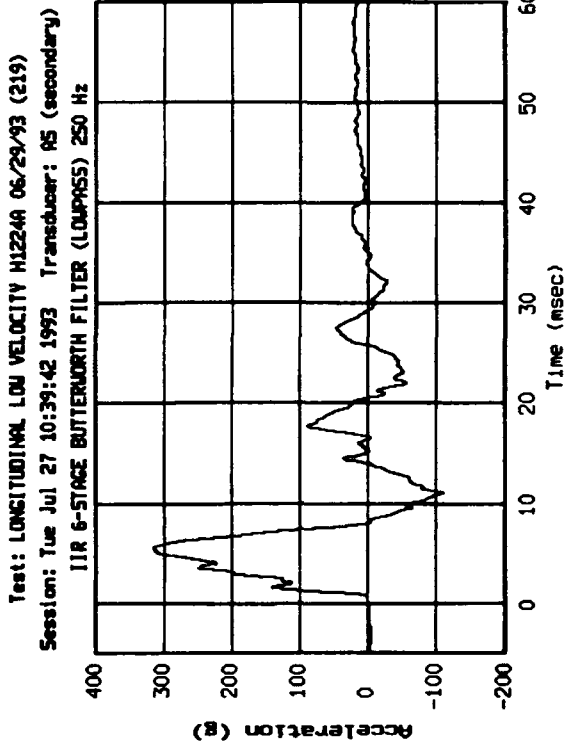
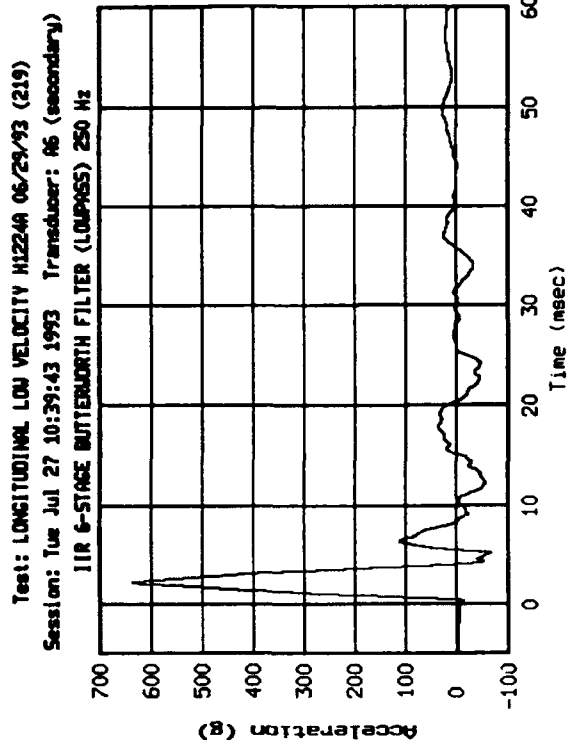
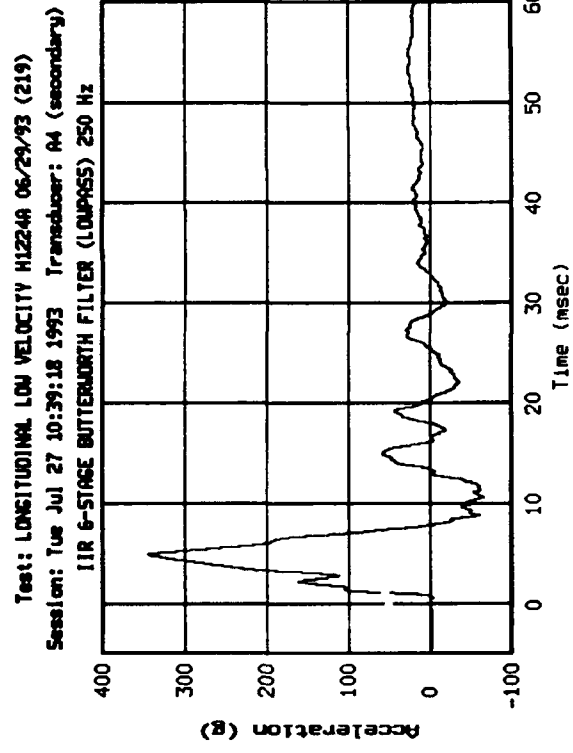
IIR 6-STAGE BUTTERWORTH FILTER (LOPSS) 250 Hz

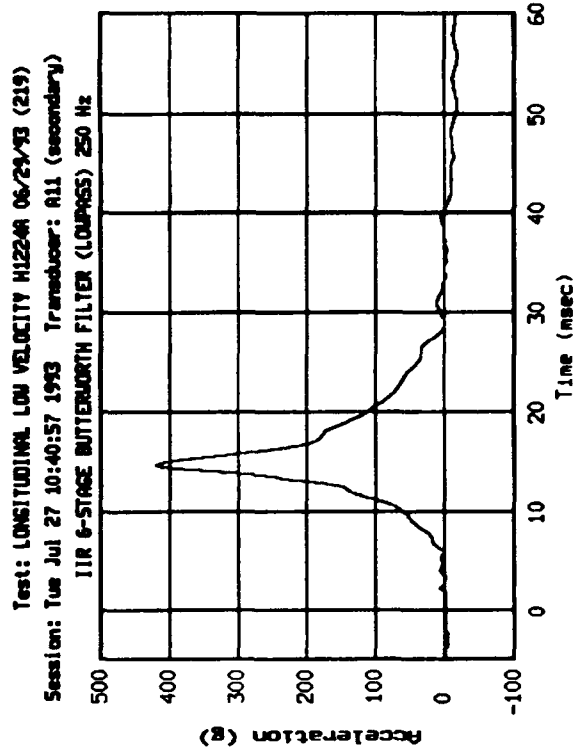
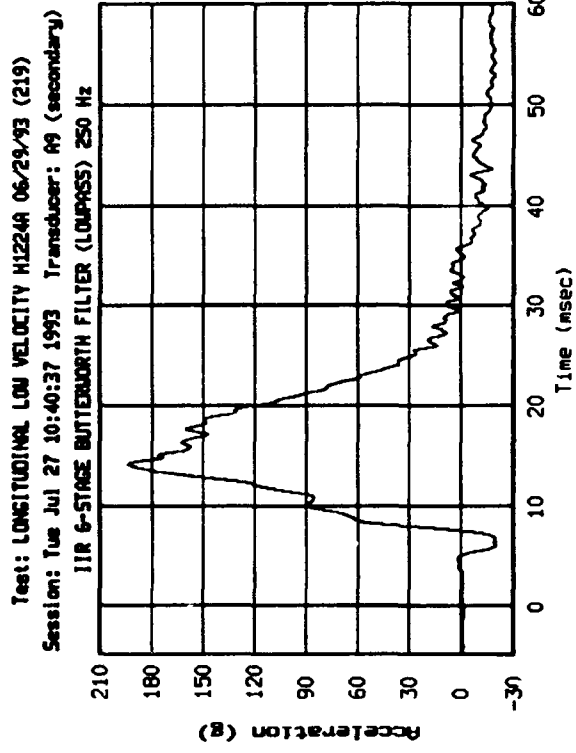
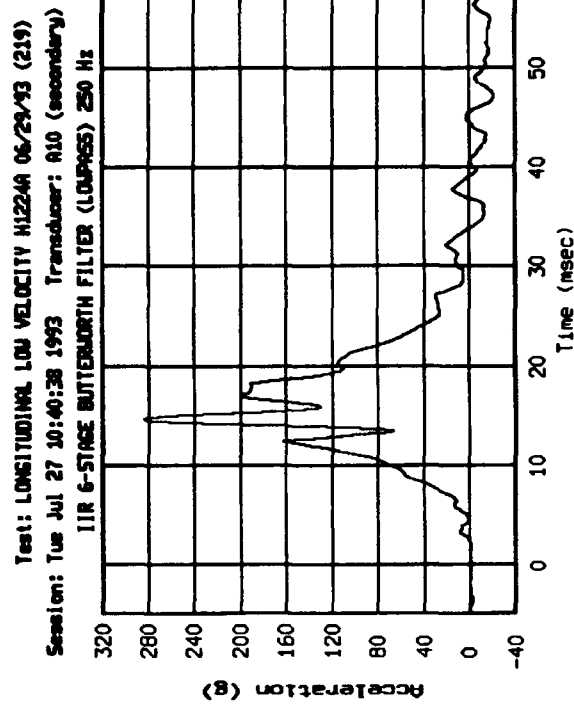
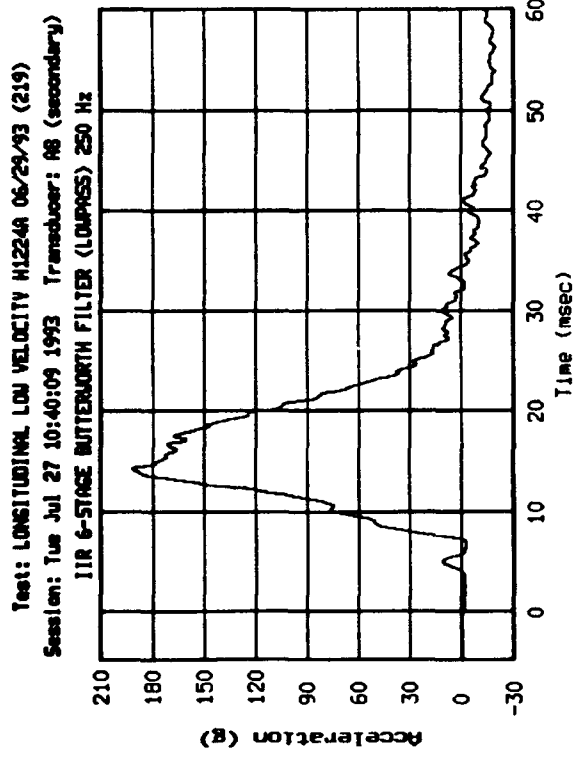


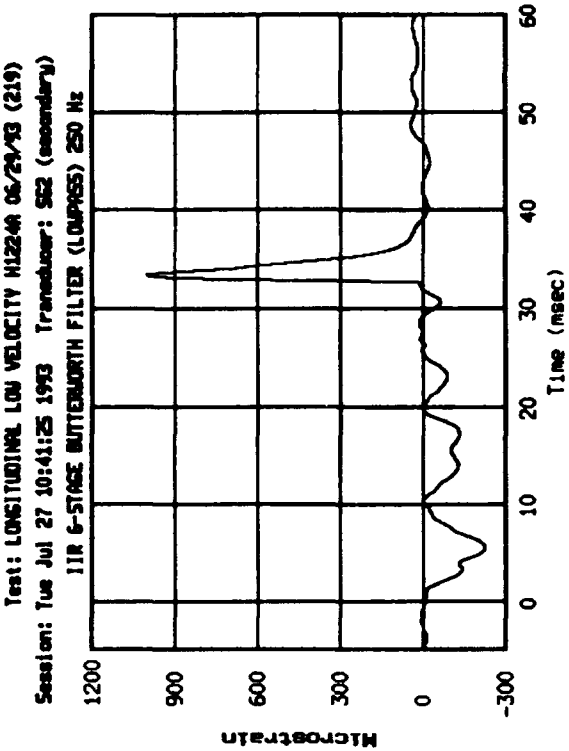
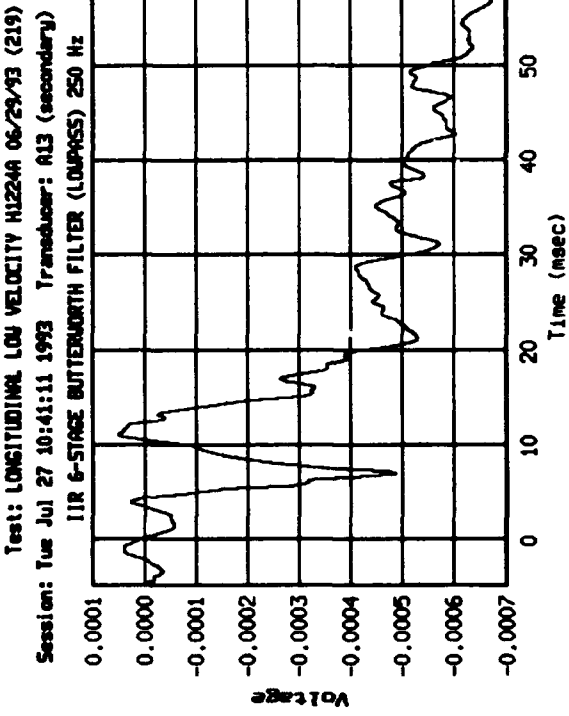
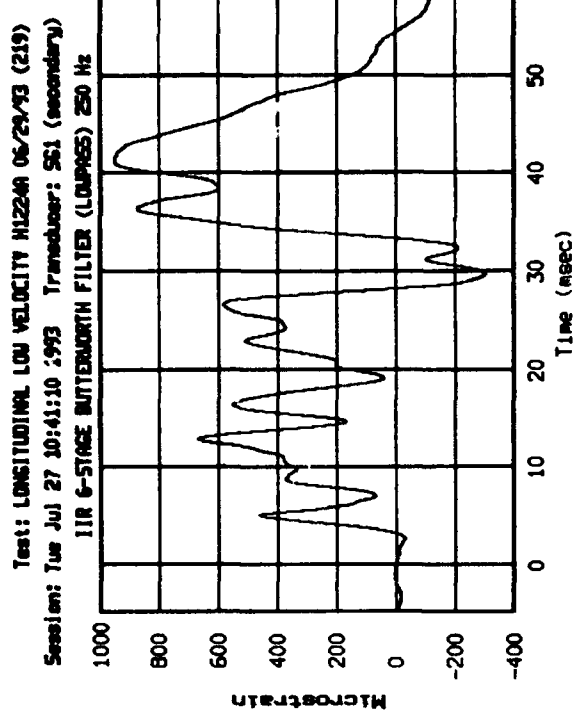
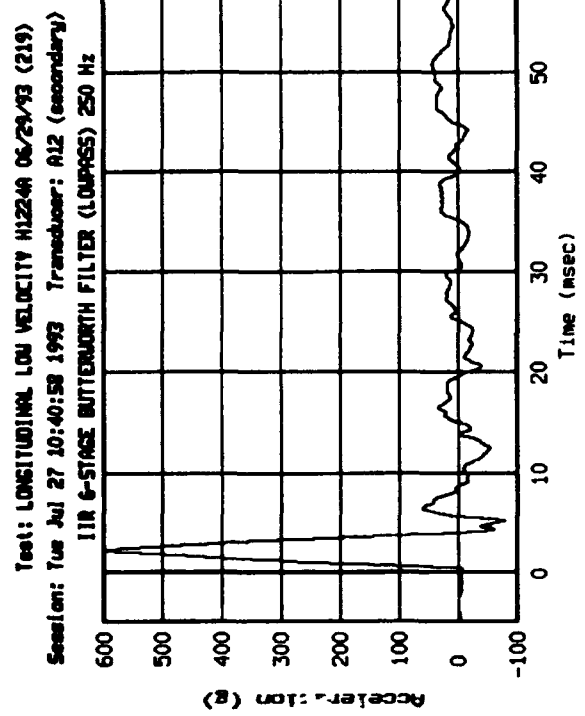
Test: LONGITUDINAL LOW VELOCITY H1224A 06/29/93 (219)
Session: Tue Jul 27 10:39:15 1993 Transducer: A3 (secondary)

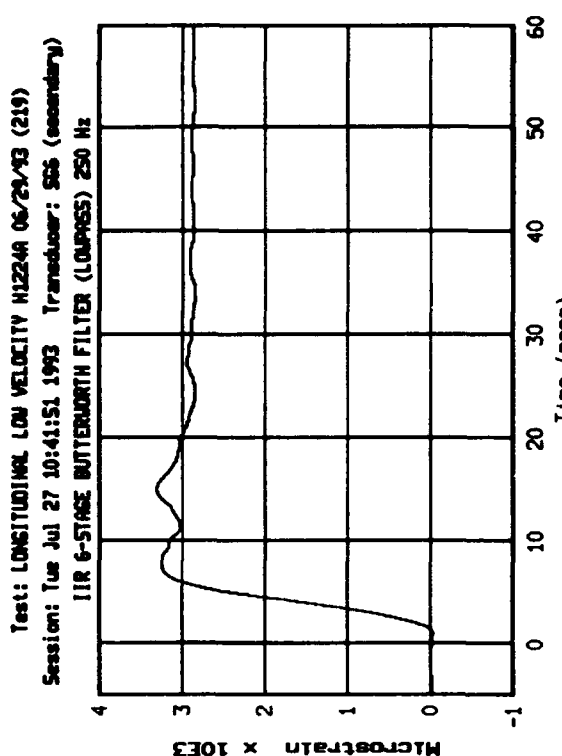
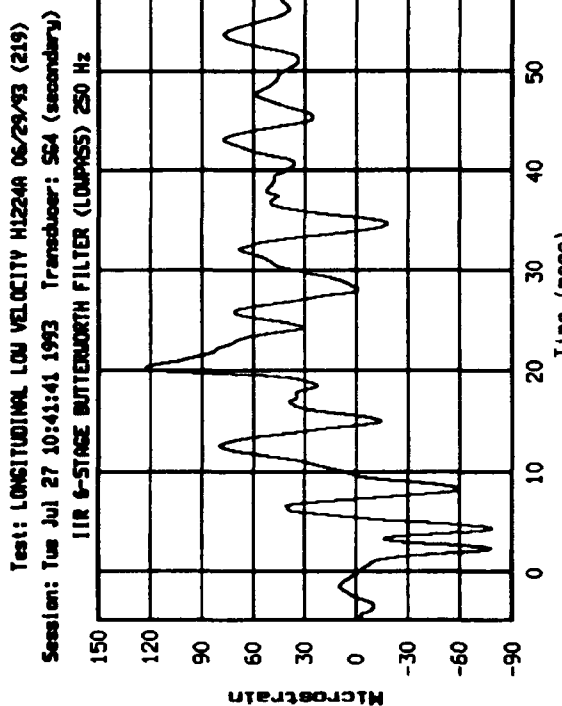
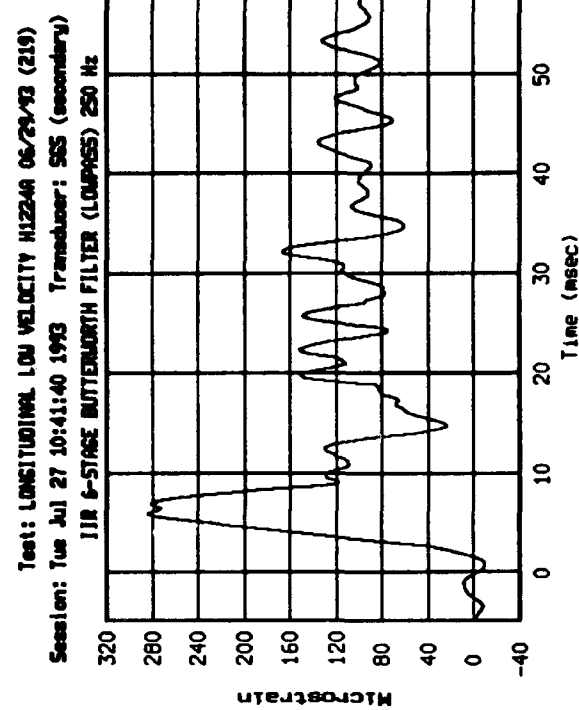
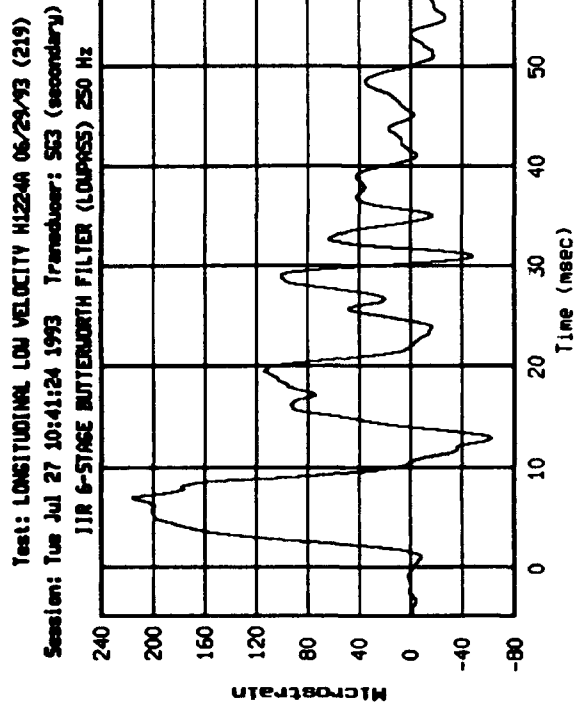
IIR 6-STAGE BUTTERWORTH FILTER (LOPSS) 250 Hz

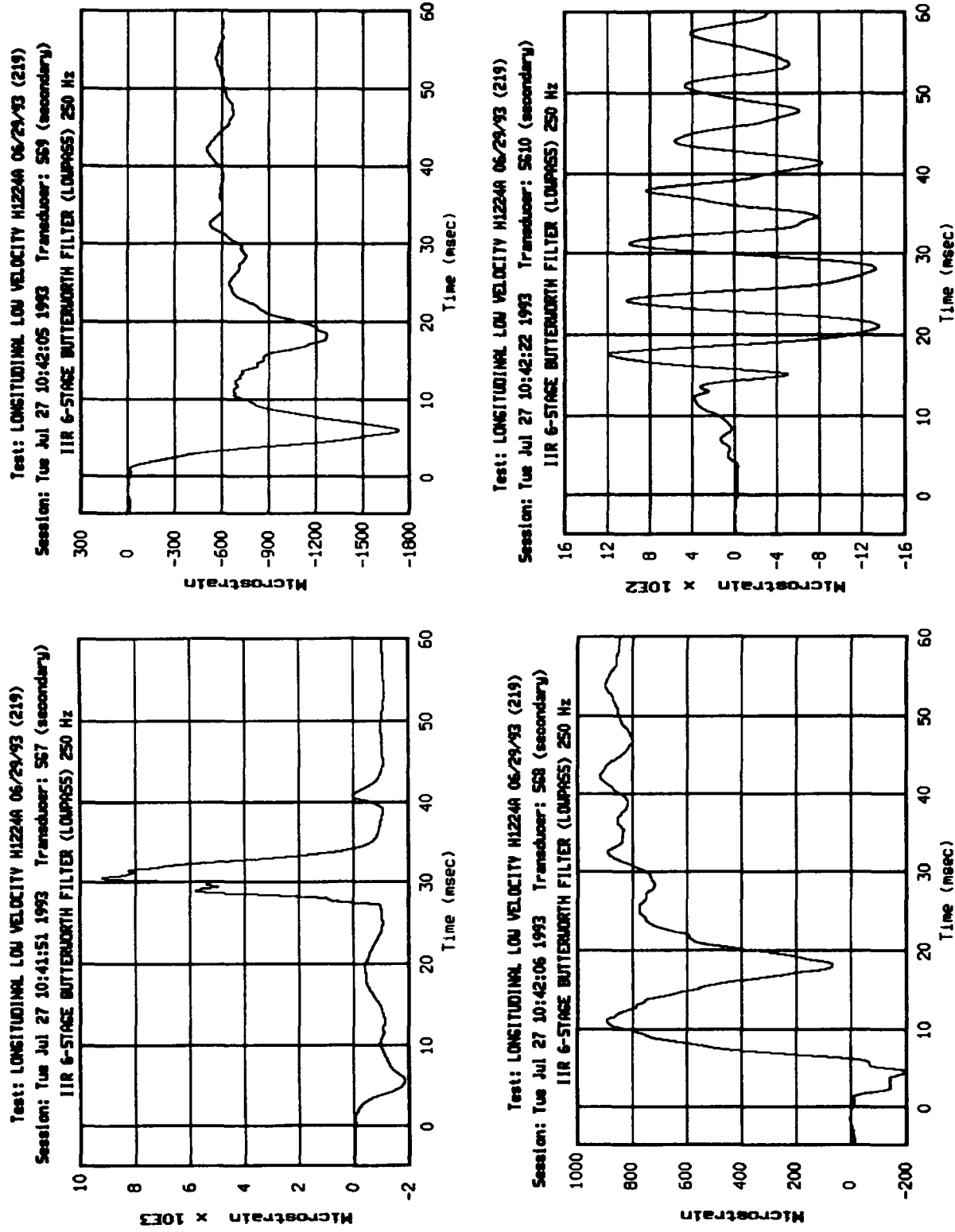




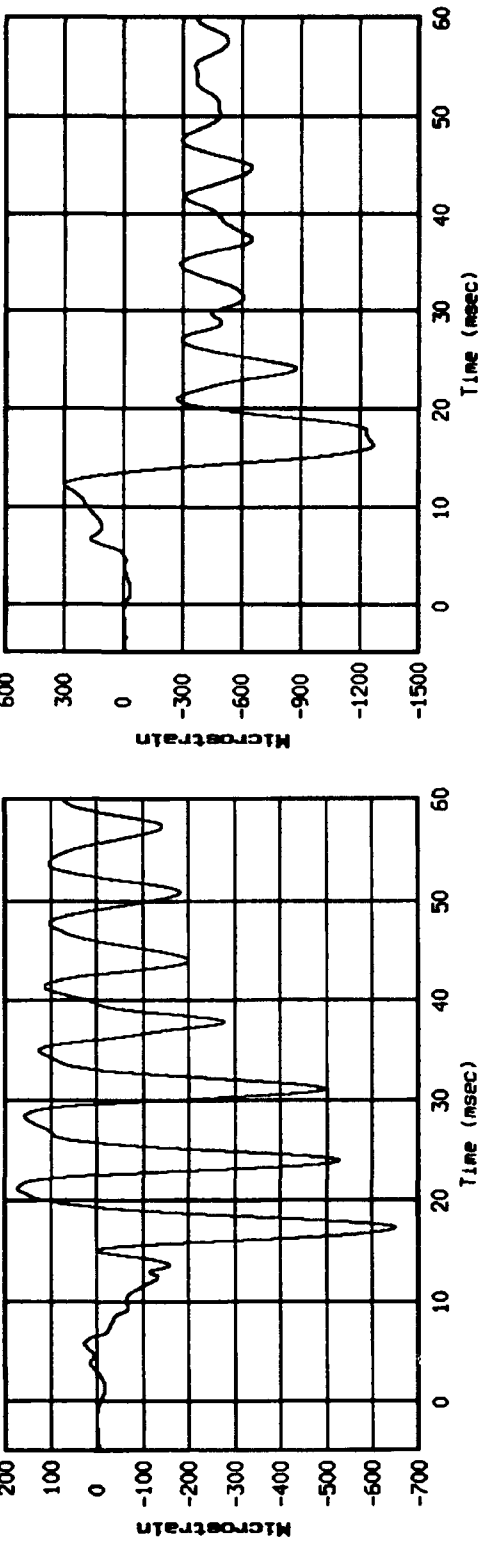




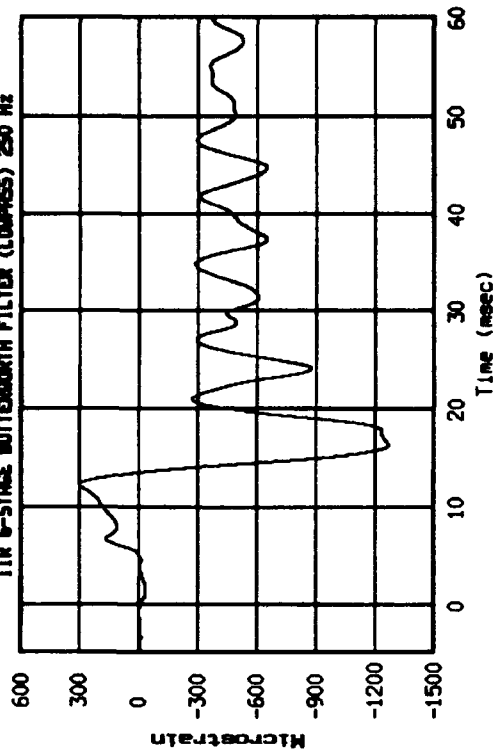




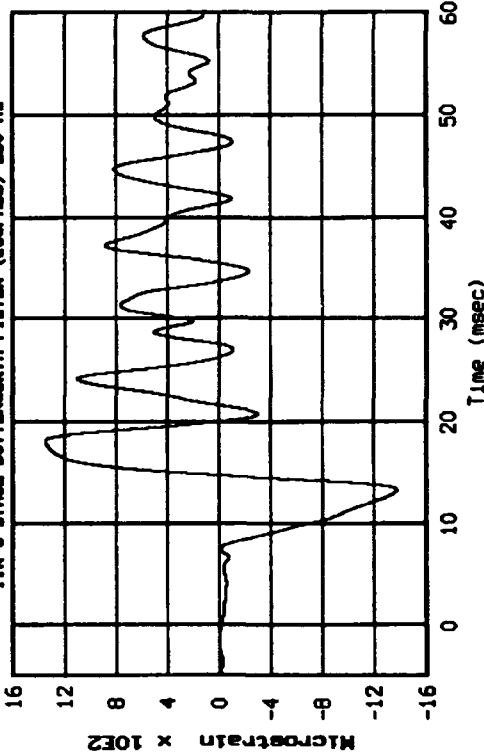
Test: LONGITUDINAL LOU VELOCITY H1224A 06/29/93 (219)
Session: Tue Jul 27 10:42:22 1993 Transducer: SE11 (secondary)
IIR 6-STAGE BUTTERWORTH FILTER (LOPASS) 250 Hz



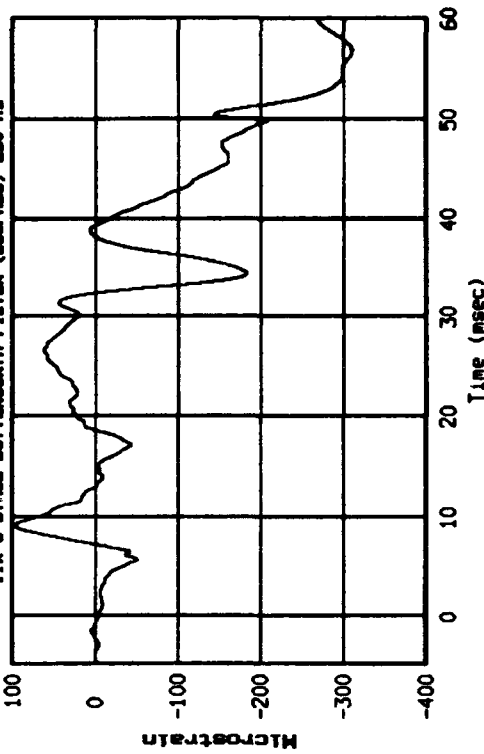
Test: LONGITUDINAL LOU VELOCITY H1224A 06/29/93 (219)
Session: Tue Jul 27 10:42:46 1993 Transducer: SE13 (secondary)
IIR 6-STAGE BUTTERWORTH FILTER (LOPASS) 250 Hz

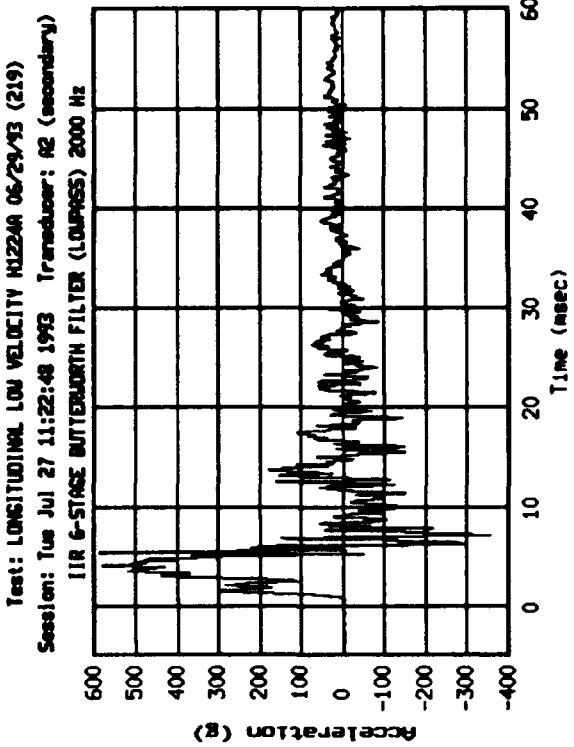
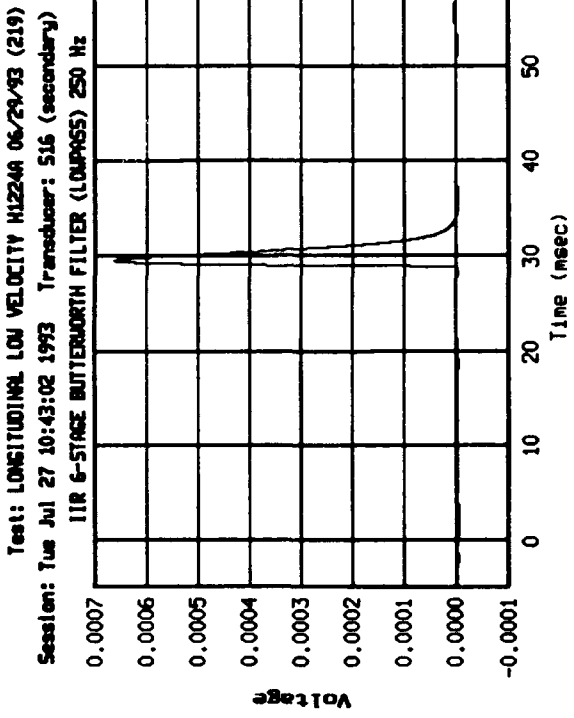
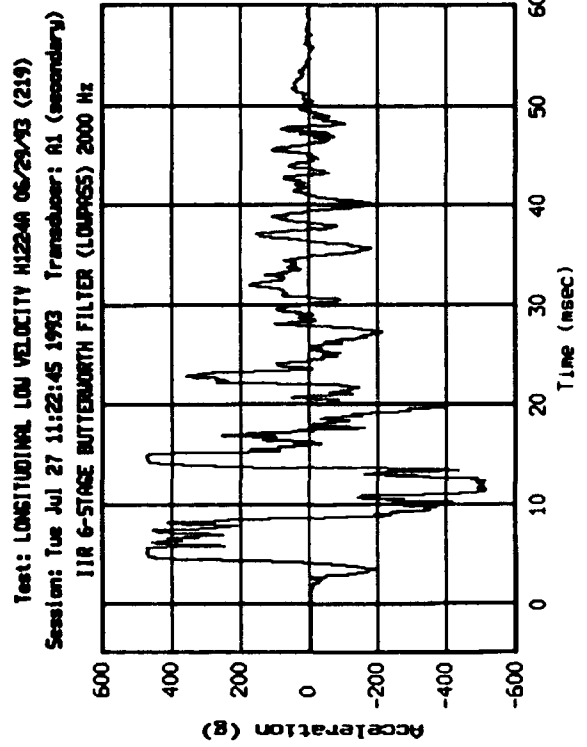
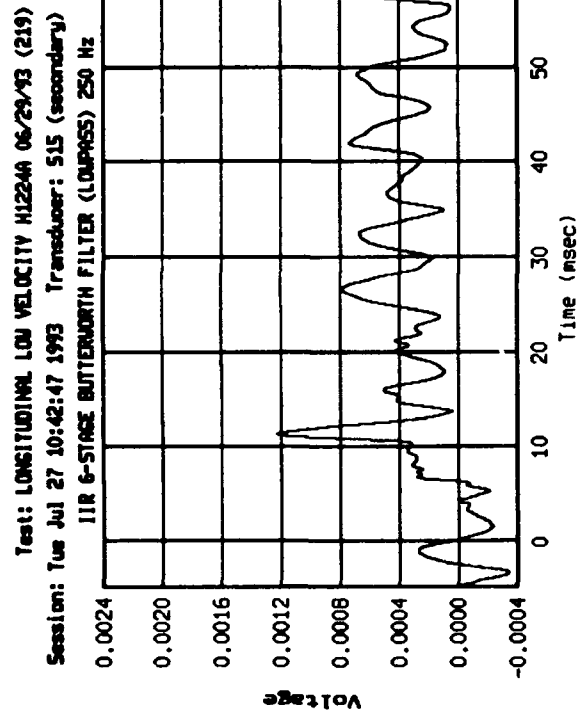


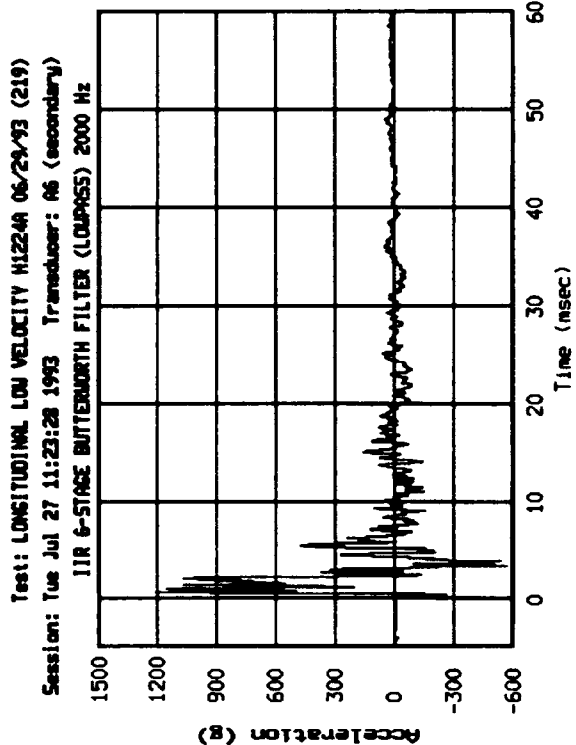
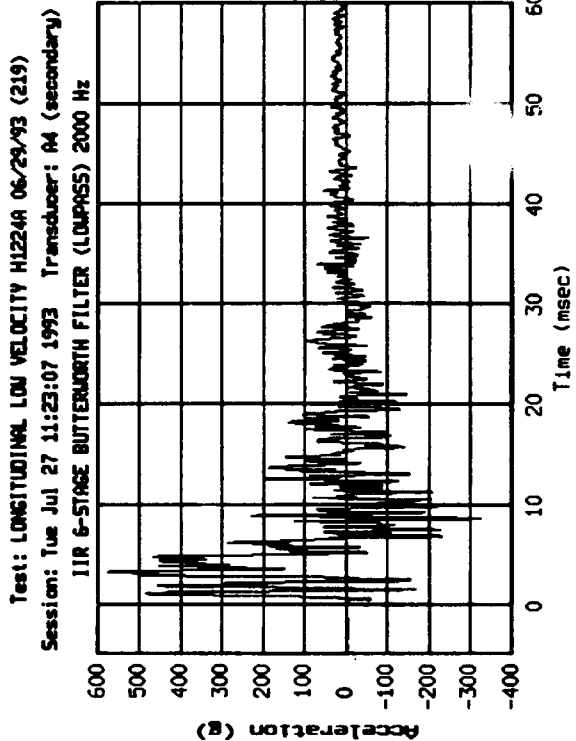
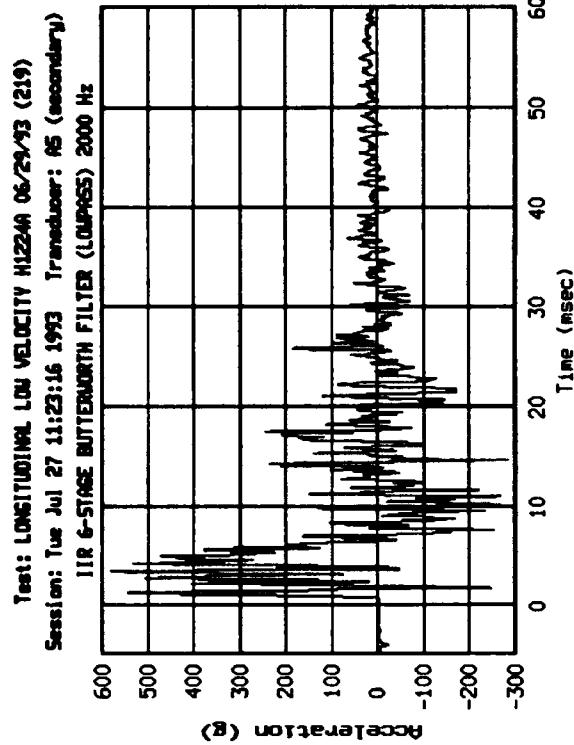
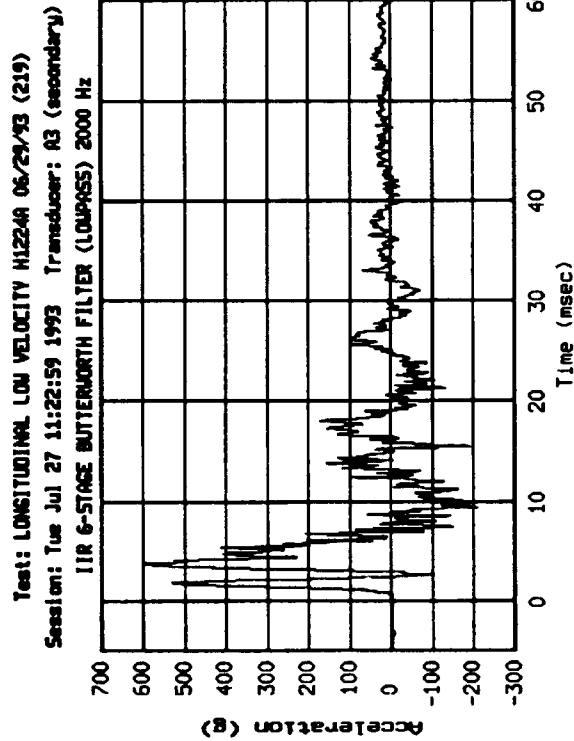
Test: LONGITUDINAL LOU VELOCITY H1224A 06/29/93 (219)
Session: Tue Jul 27 10:42:33 1993 Transducer: SE12 (secondary)
IIR 6-STAGE BUTTERWORTH FILTER (LOPASS) 250 Hz

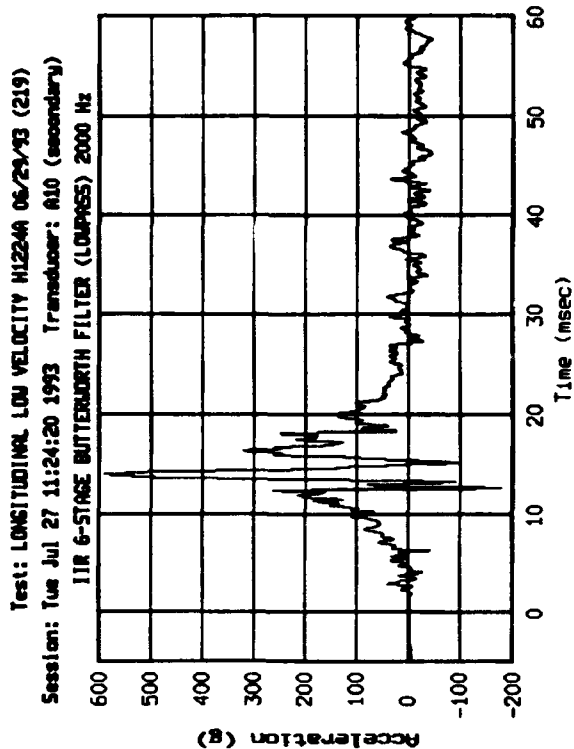
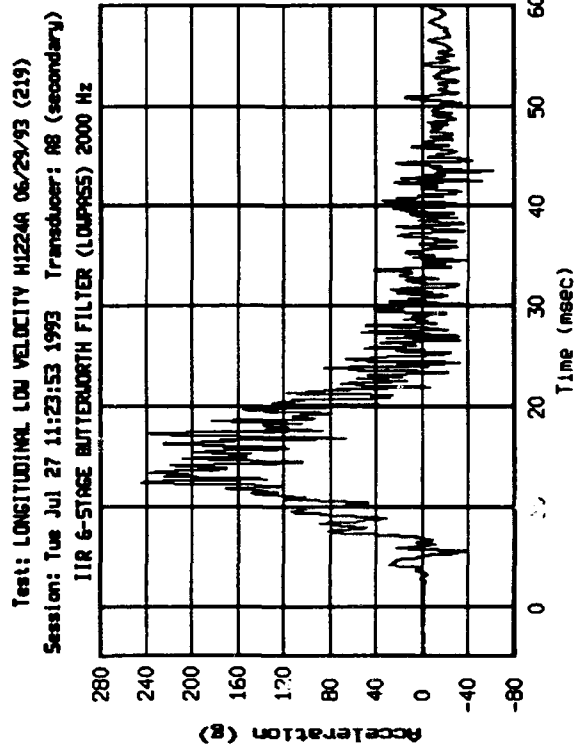
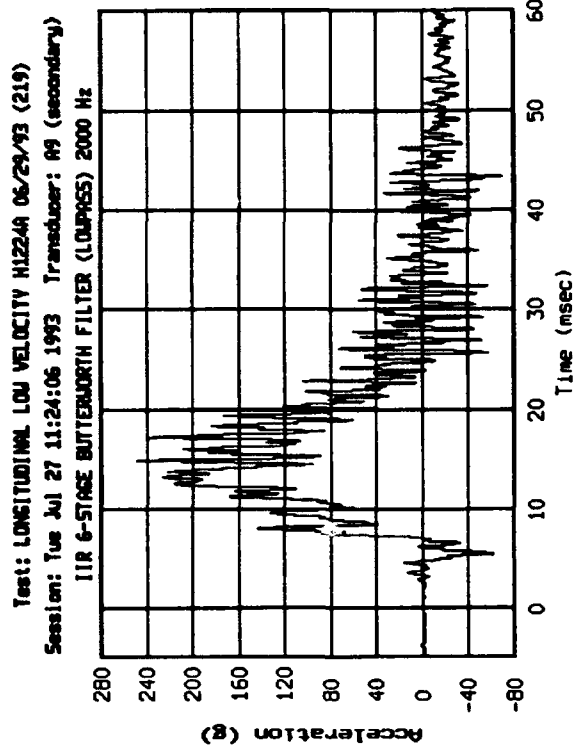
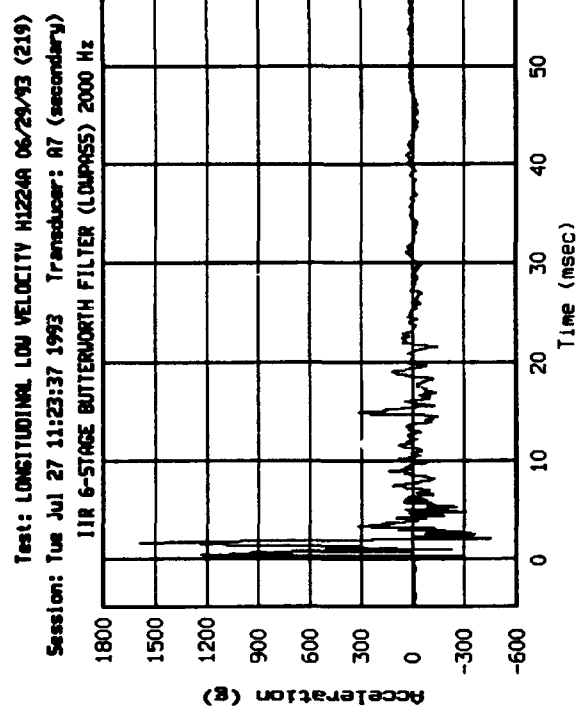


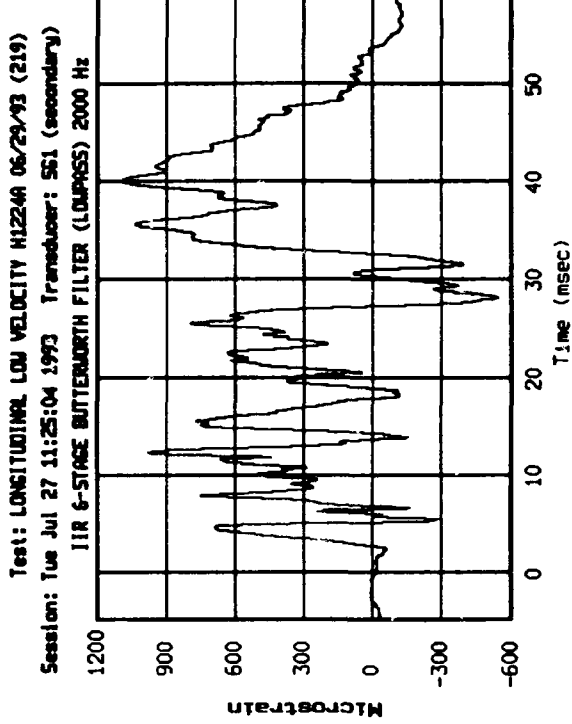
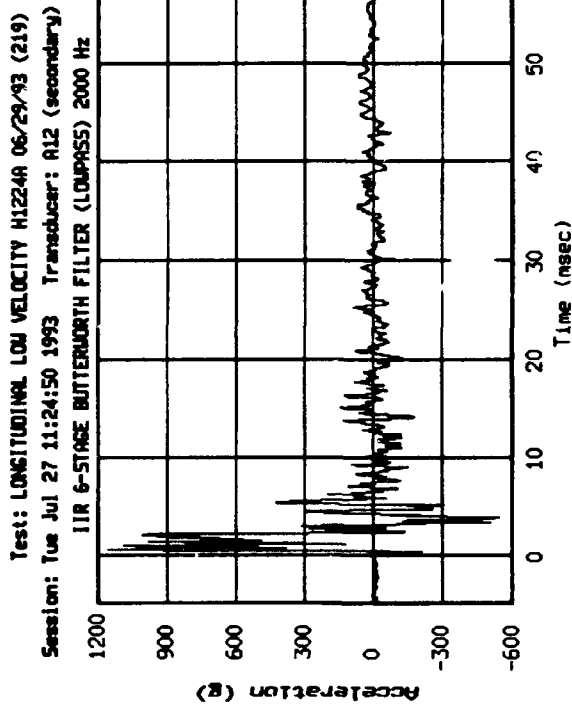
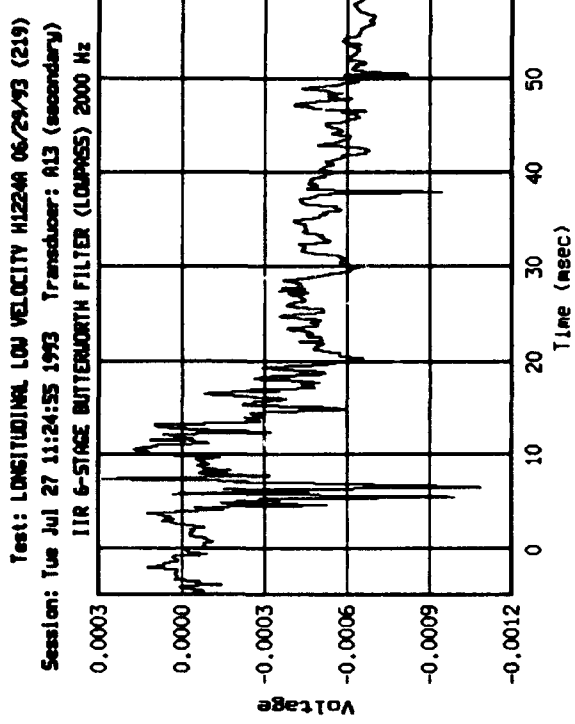
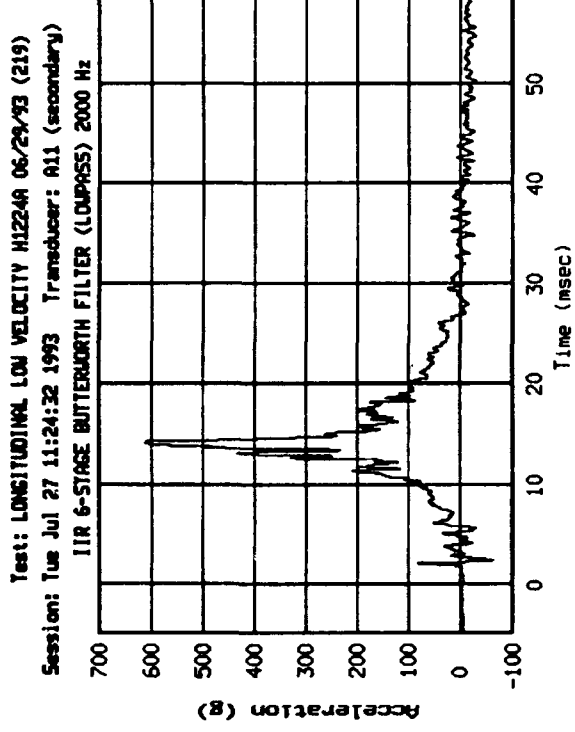
Test: LONGITUDINAL LOU VELOCITY H1224A 06/29/93 (219)
Session: Tue Jul 27 10:42:32 1993 Transducer: SE14 (secondary)
IIR 6-STAGE BUTTERWORTH FILTER (LOPASS) 250 Hz

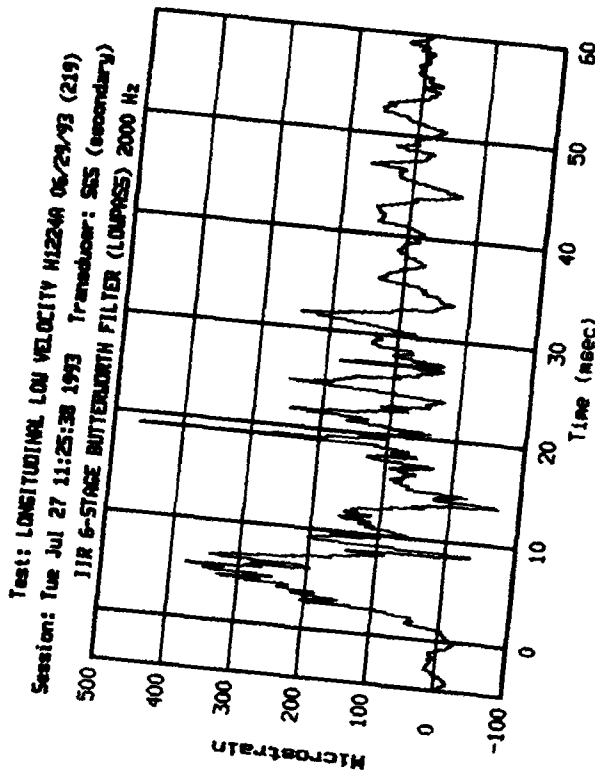
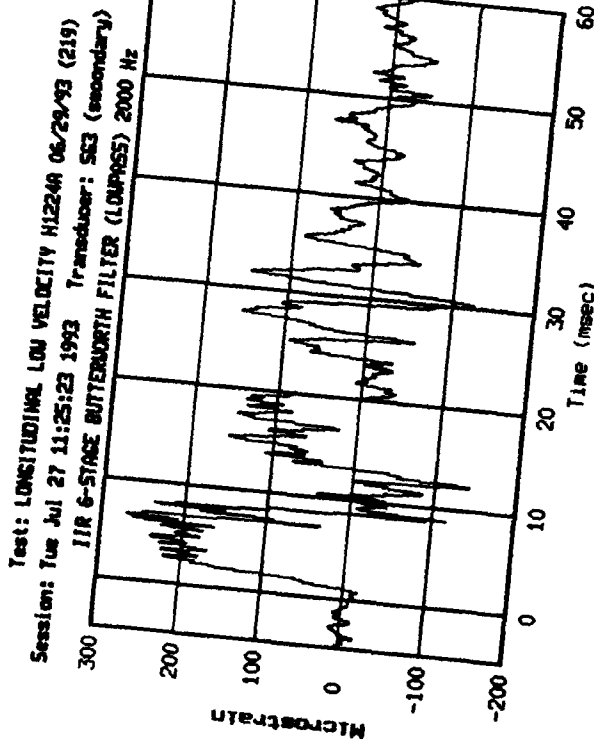
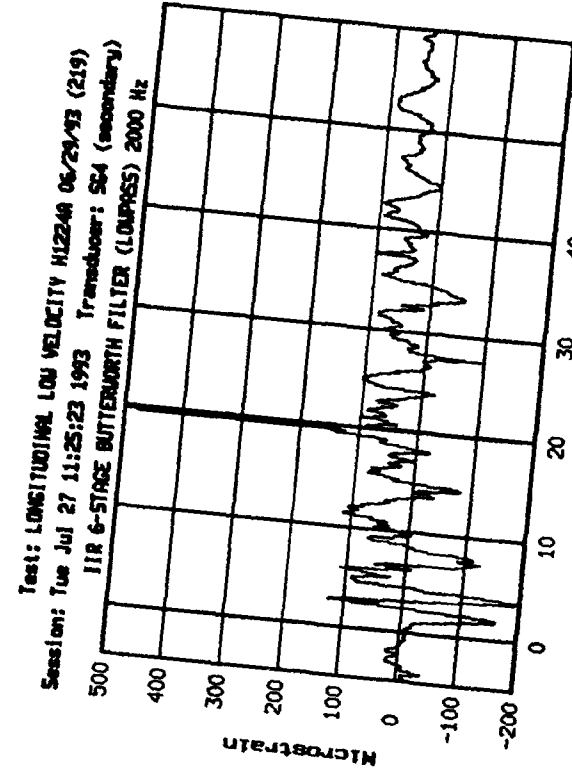
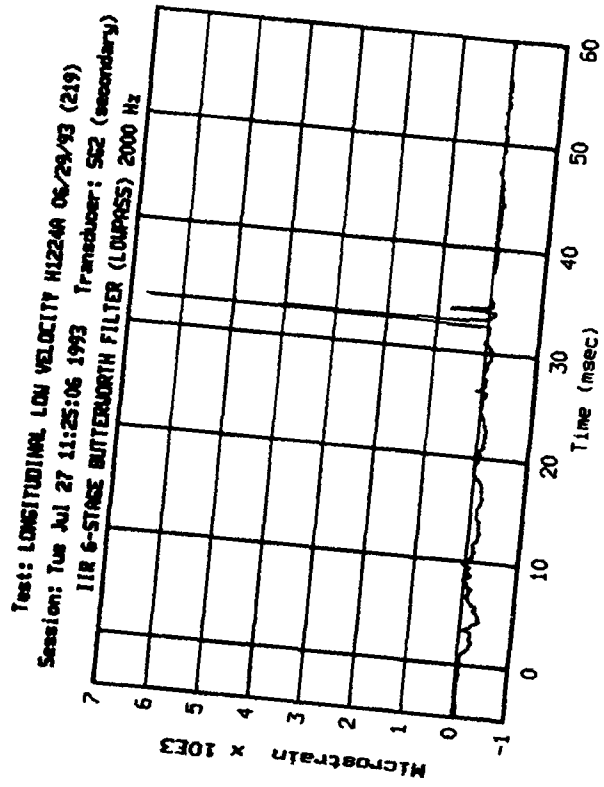


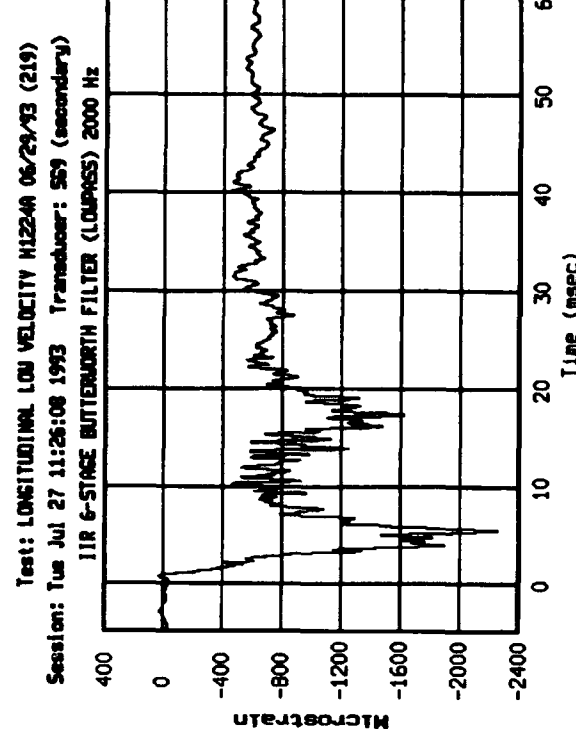
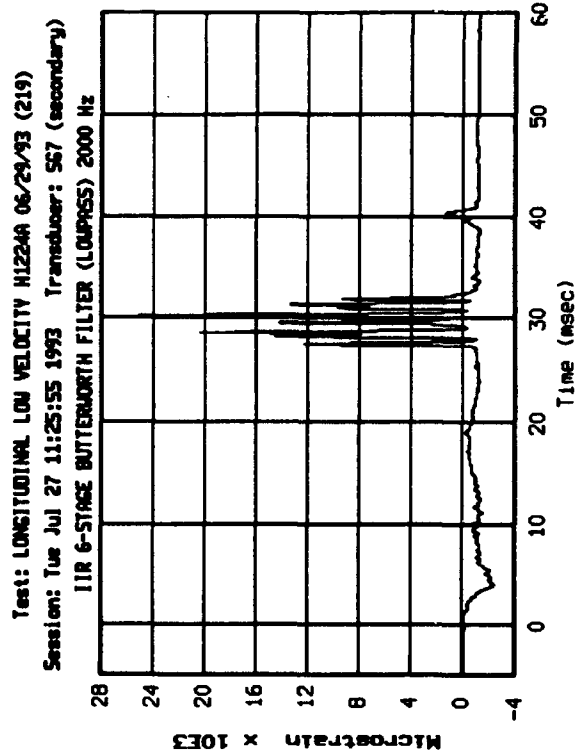
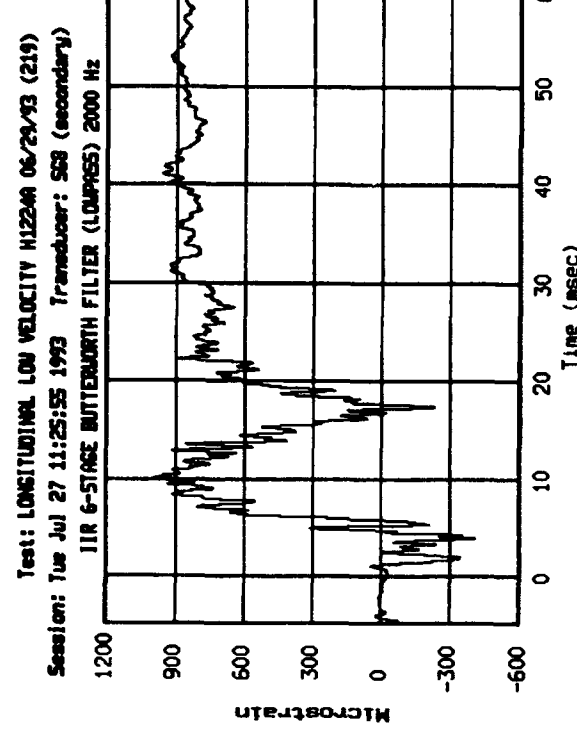
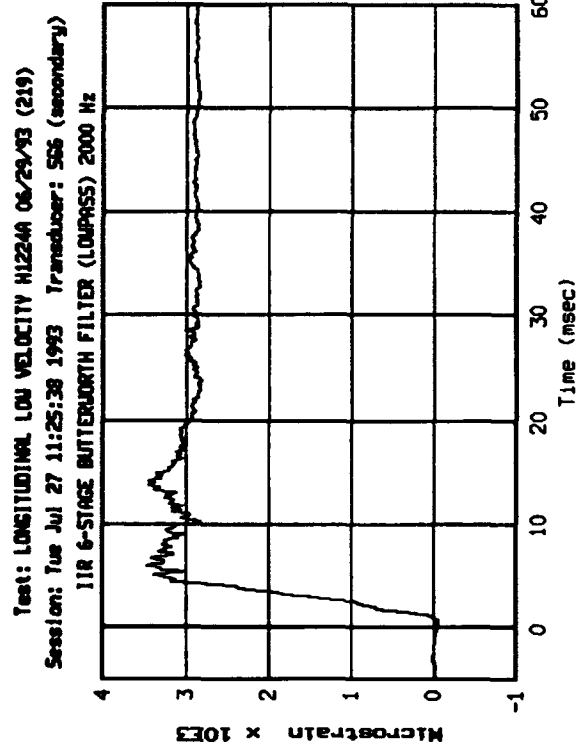


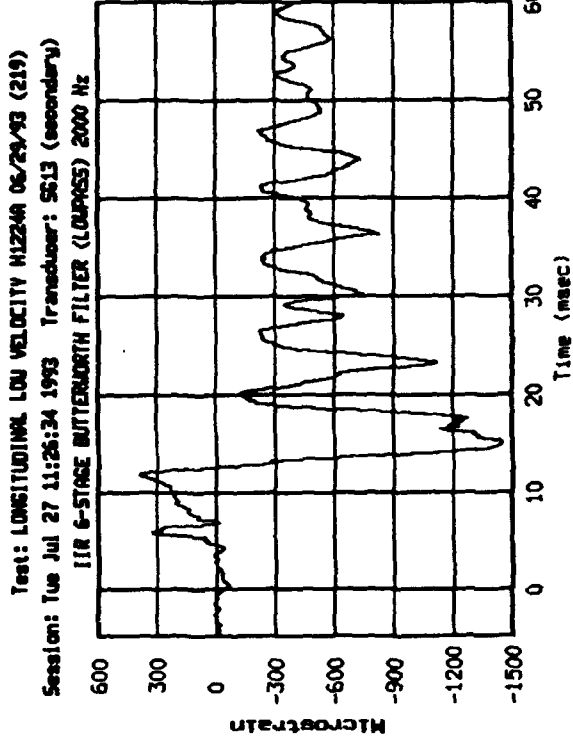
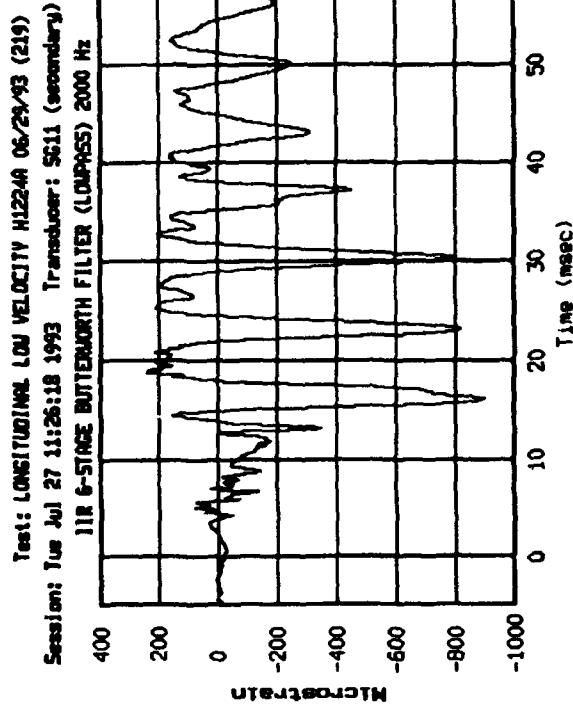
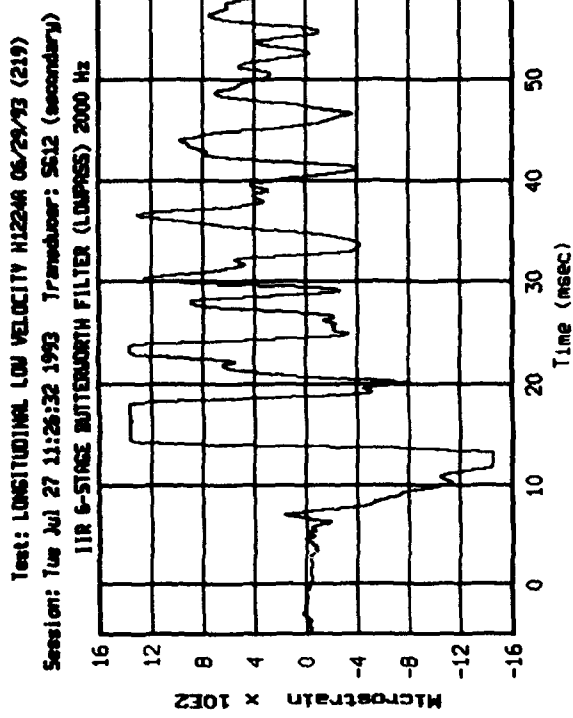
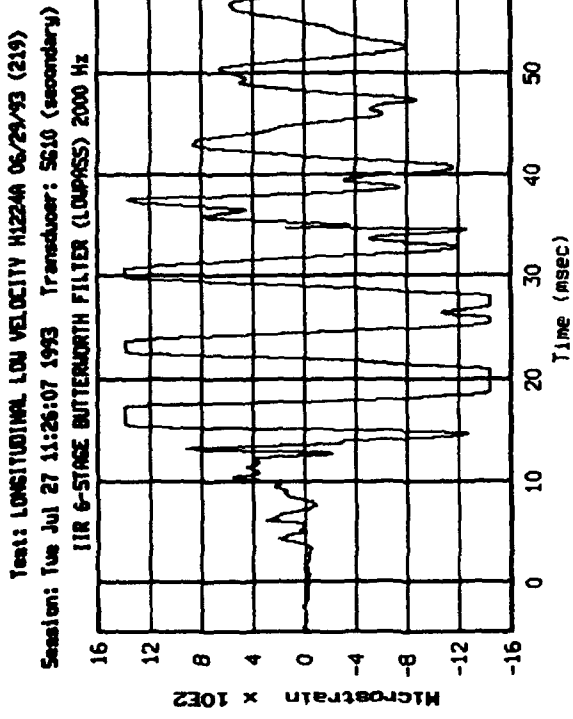


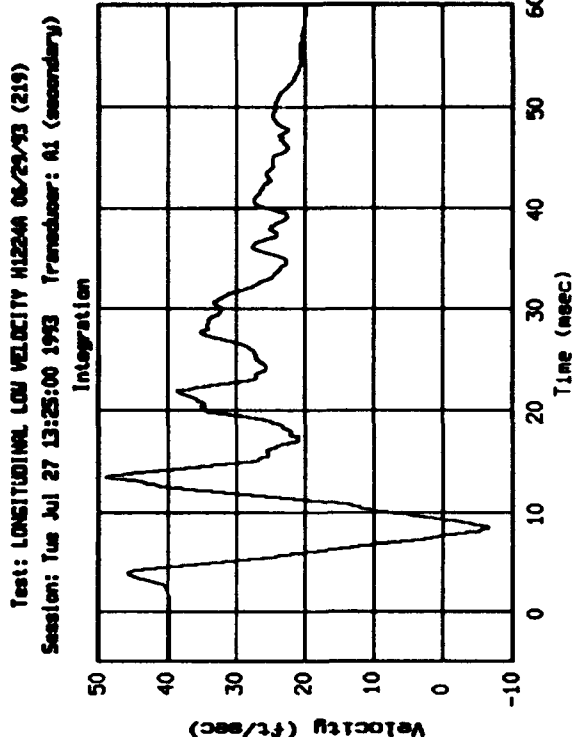
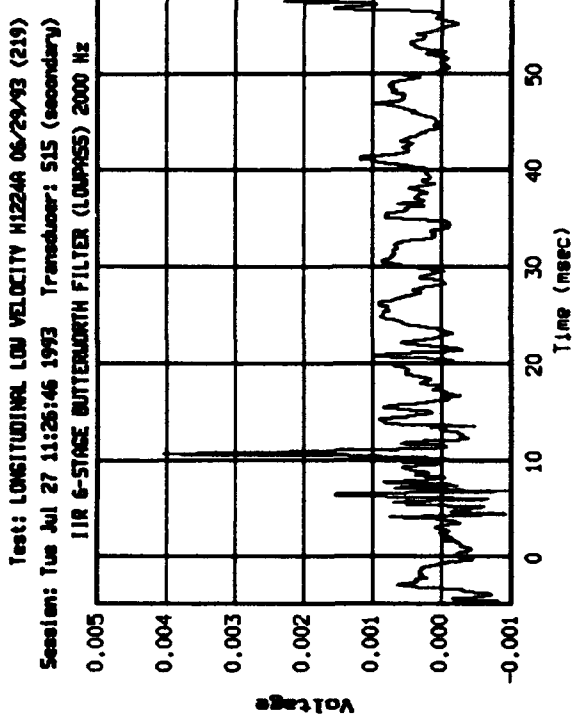
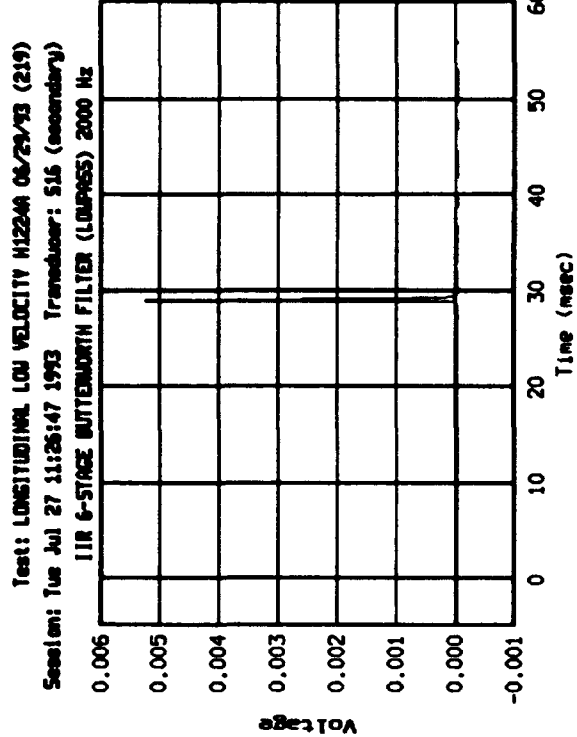
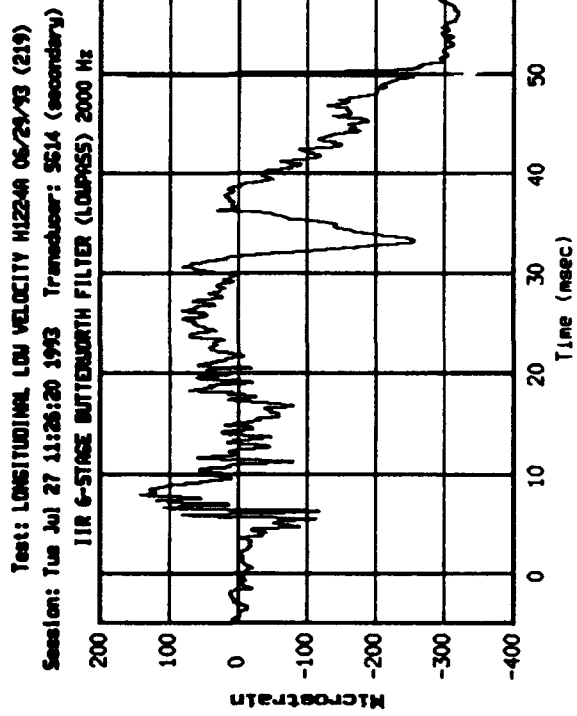


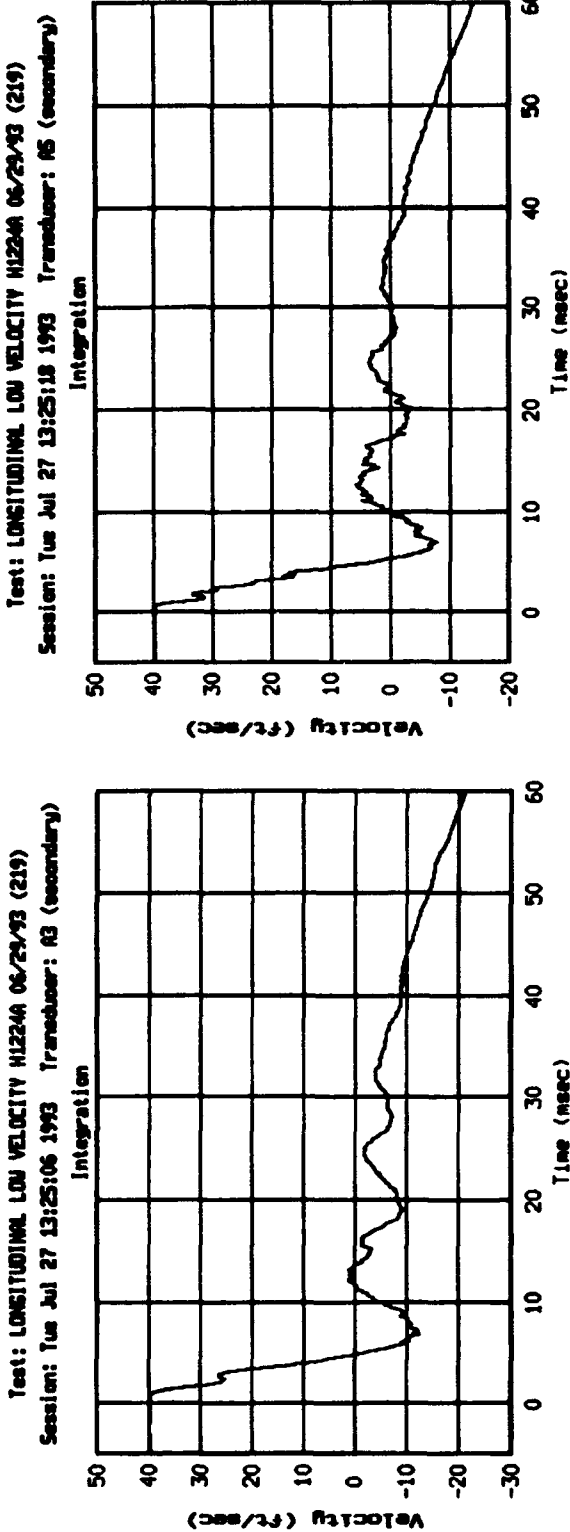
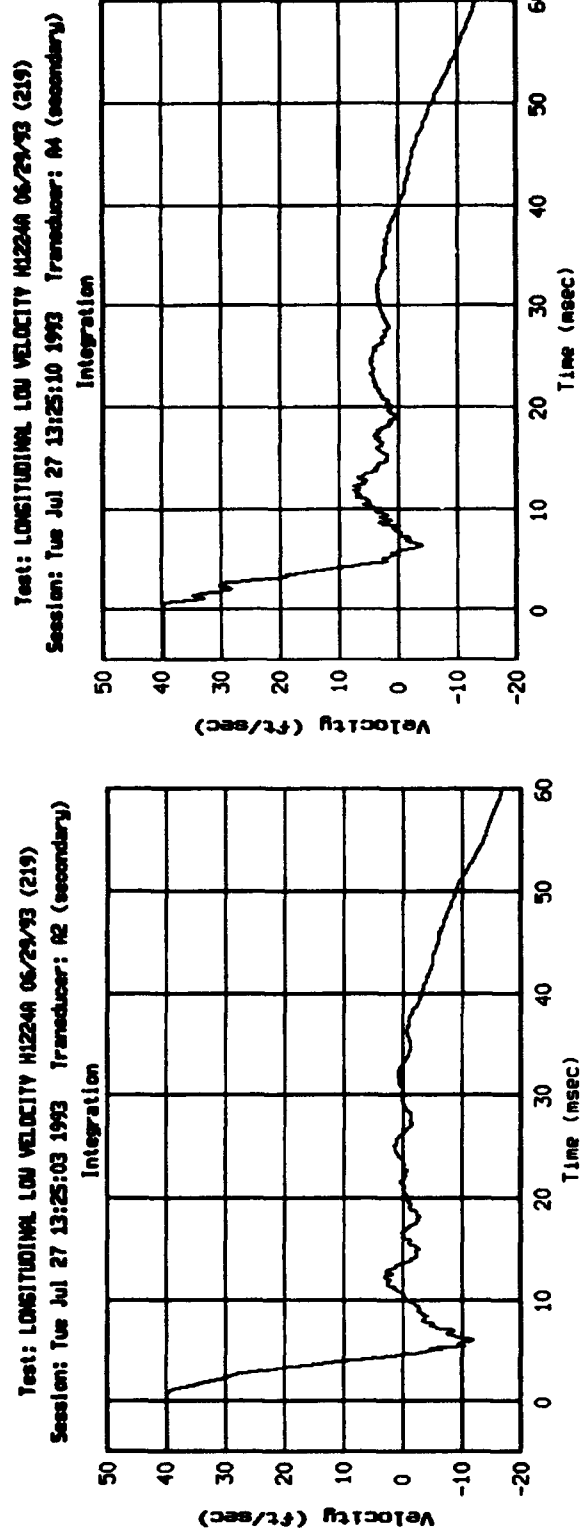


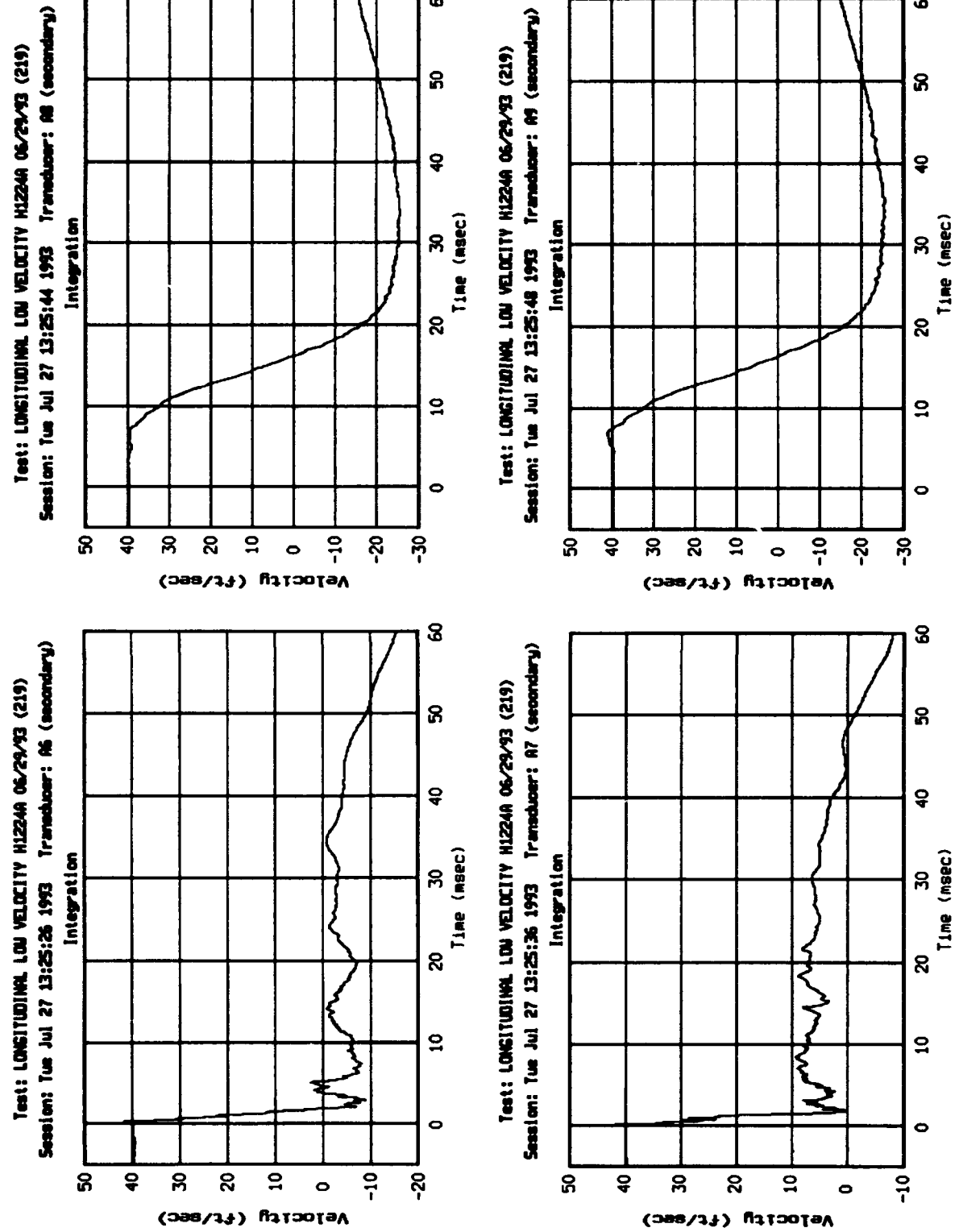


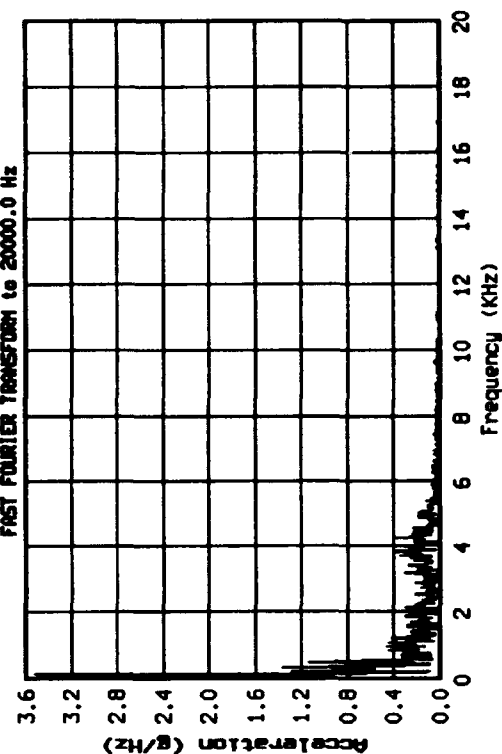
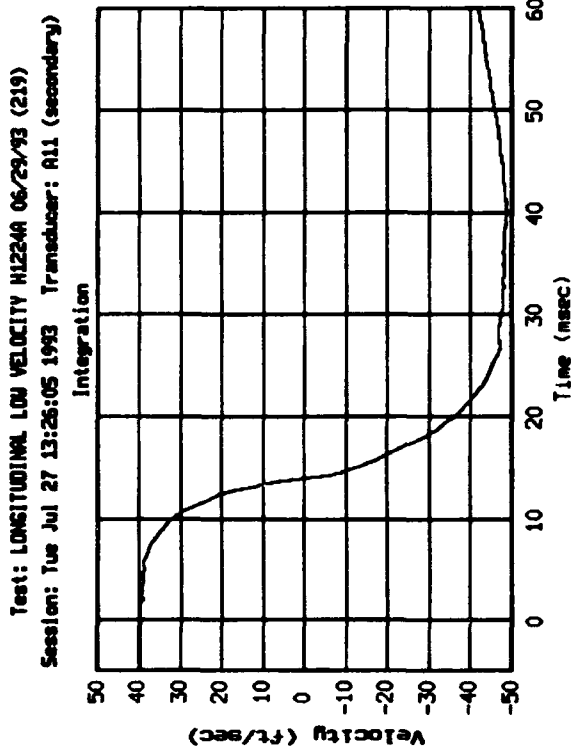
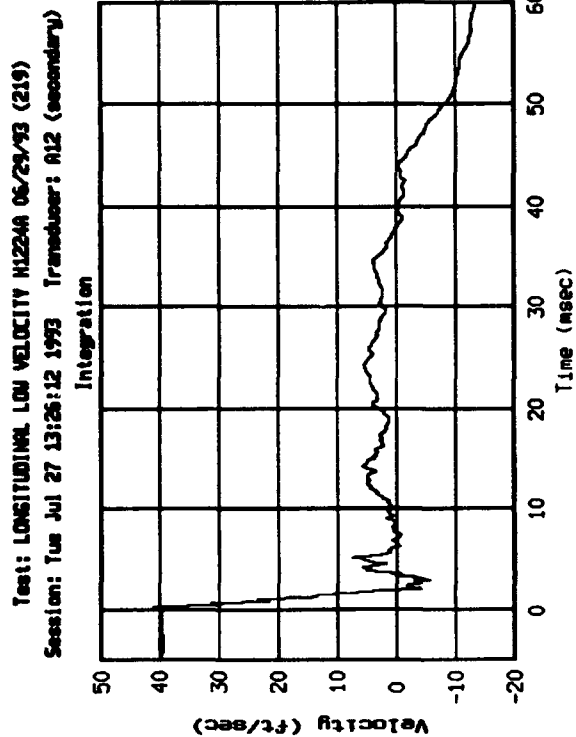
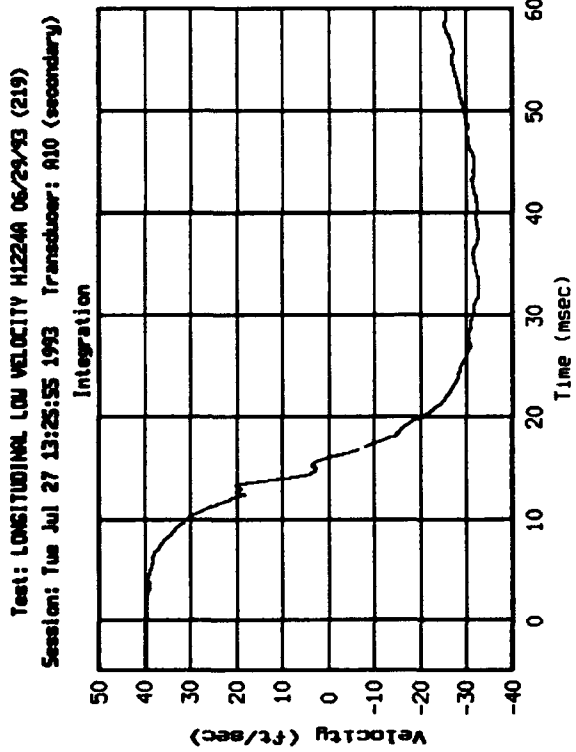


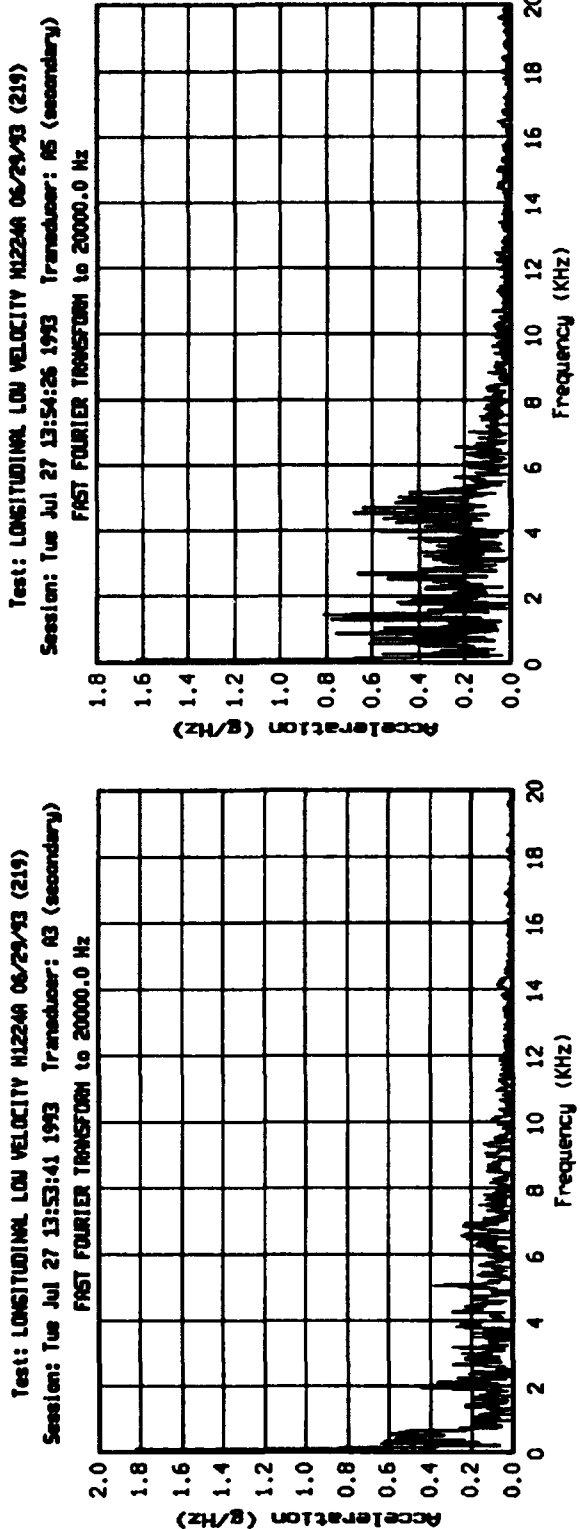
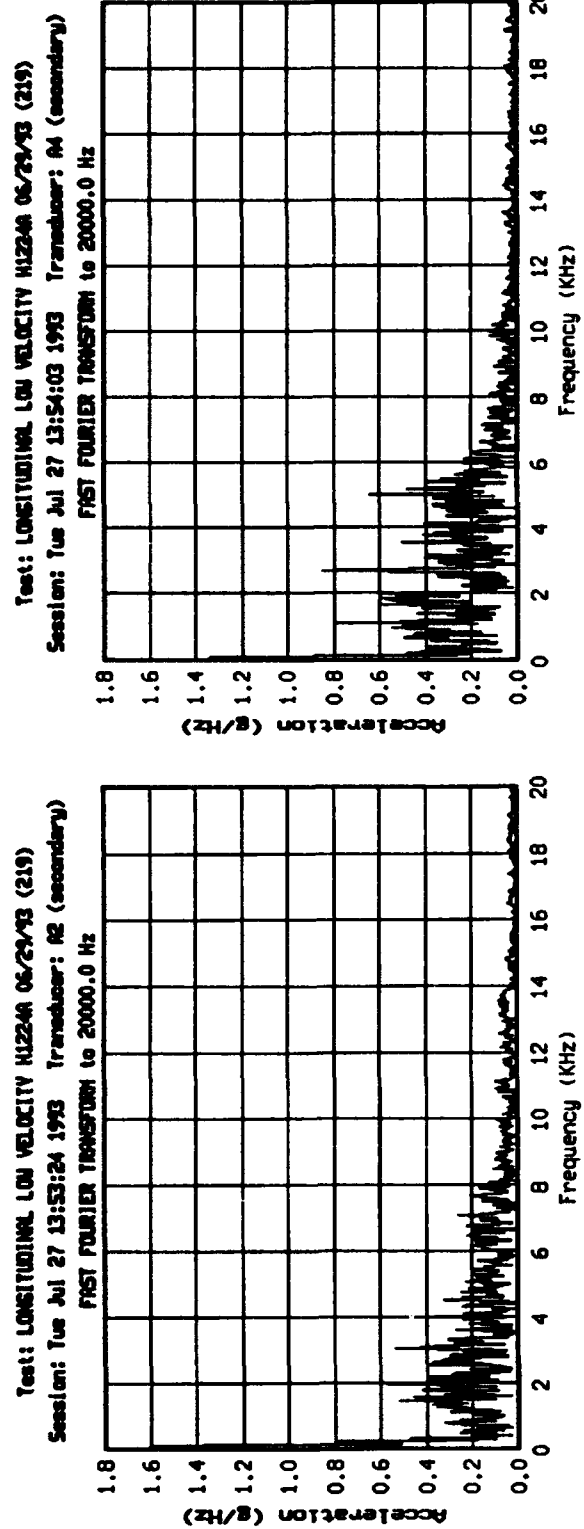


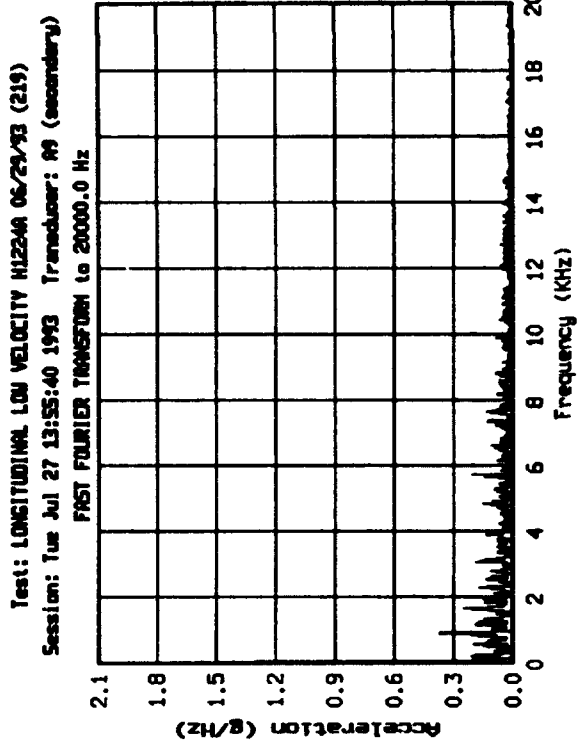
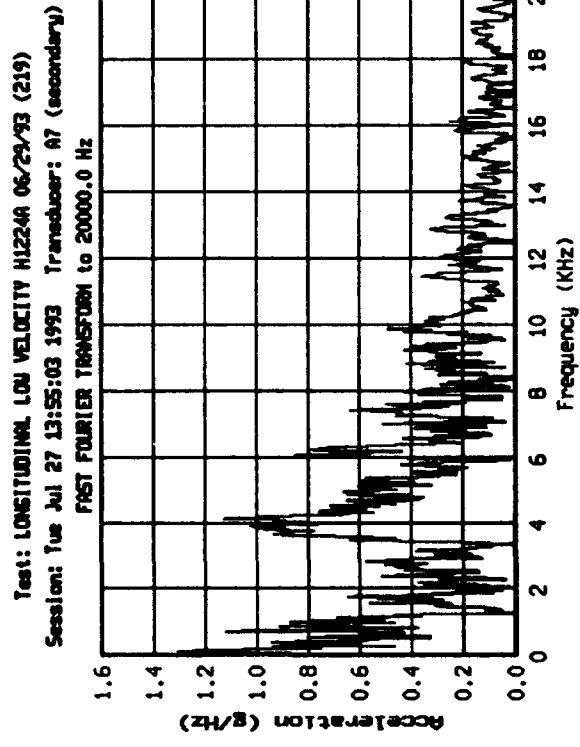
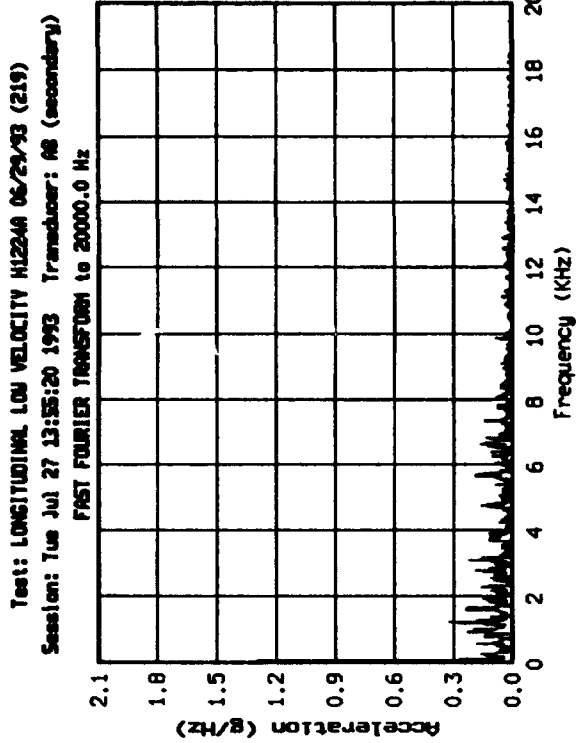
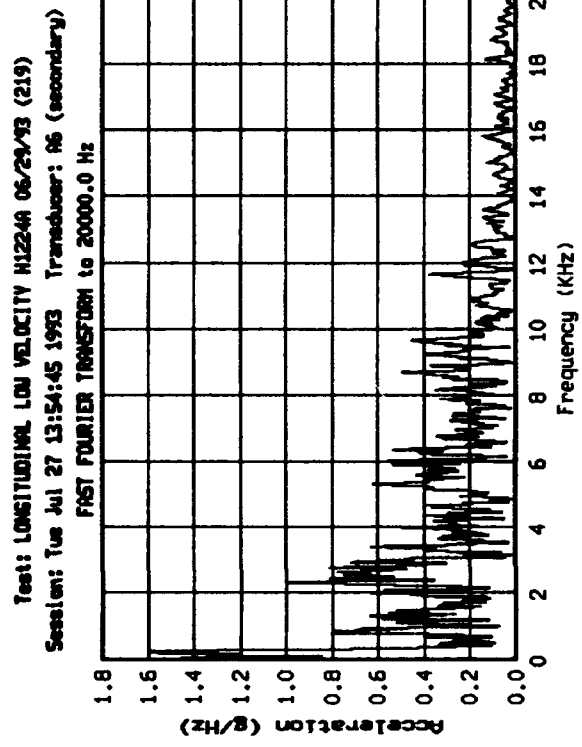


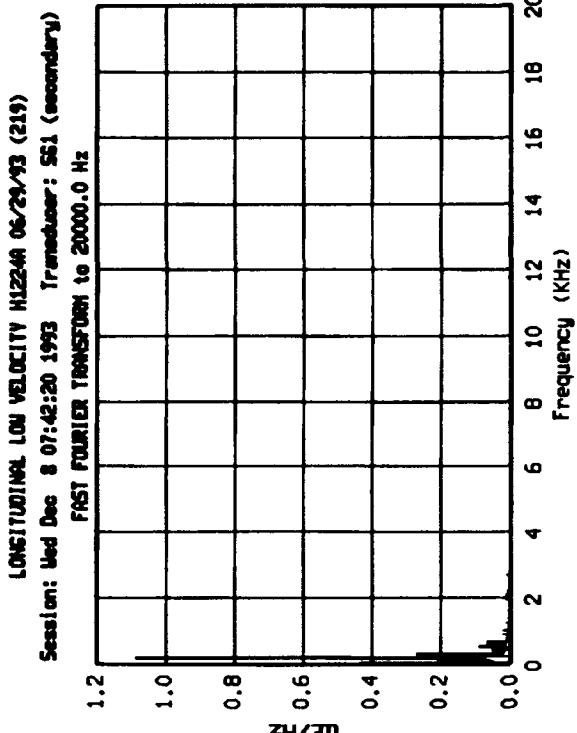
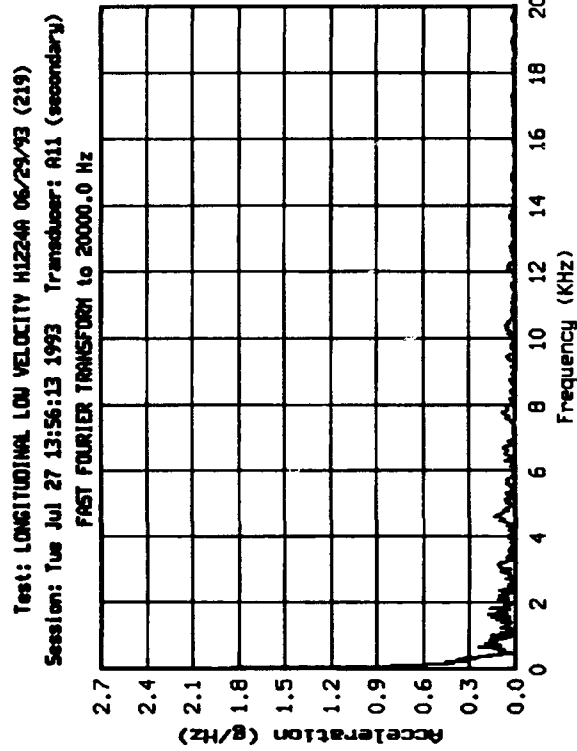
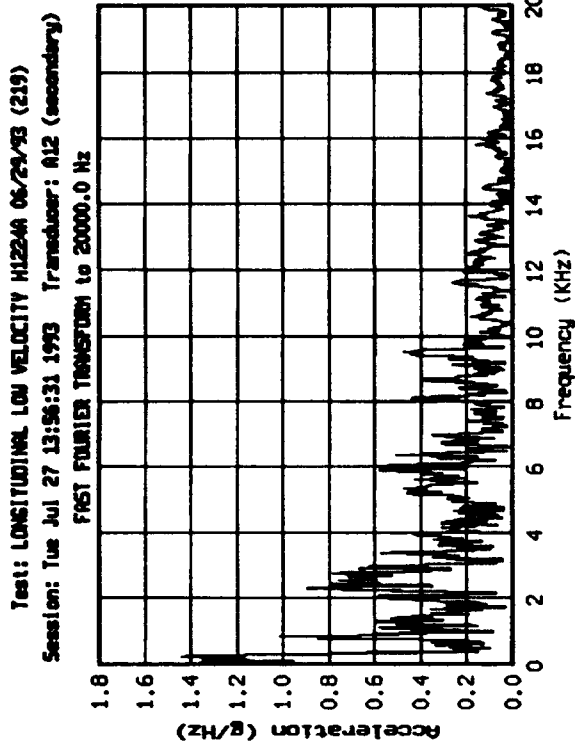
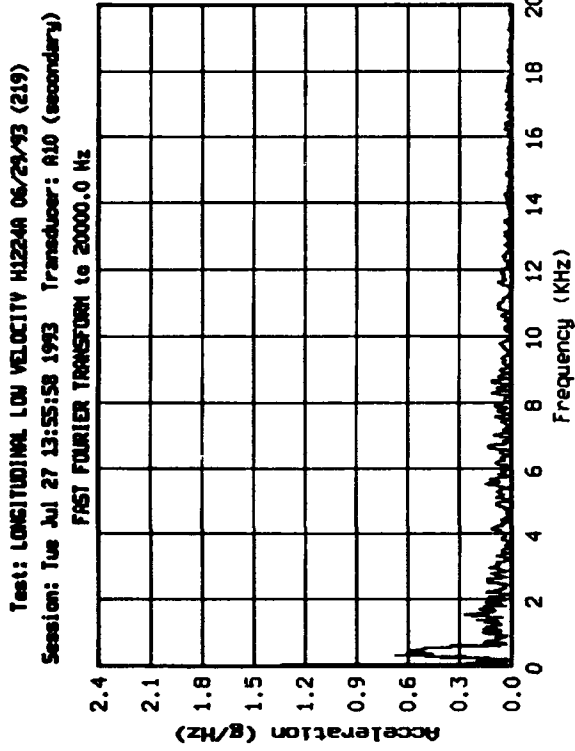


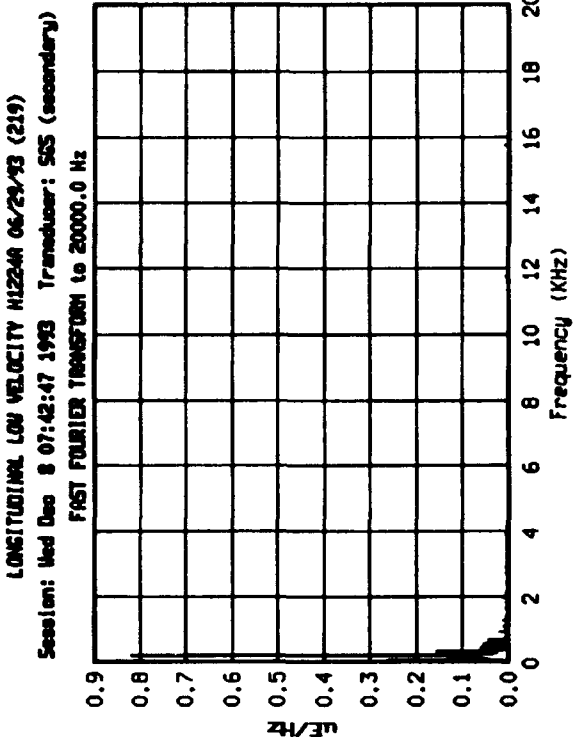
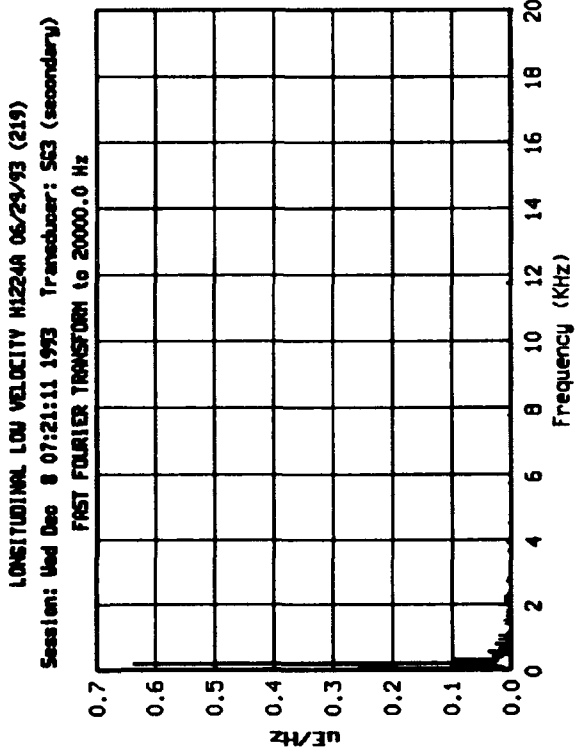
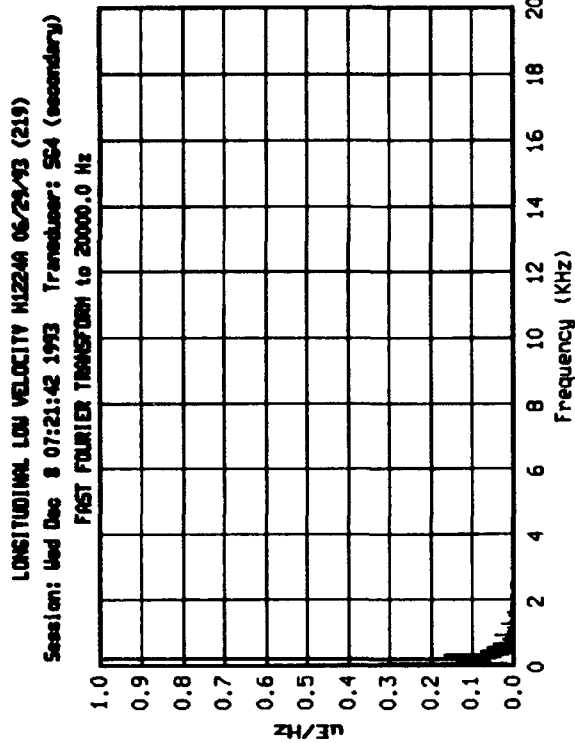
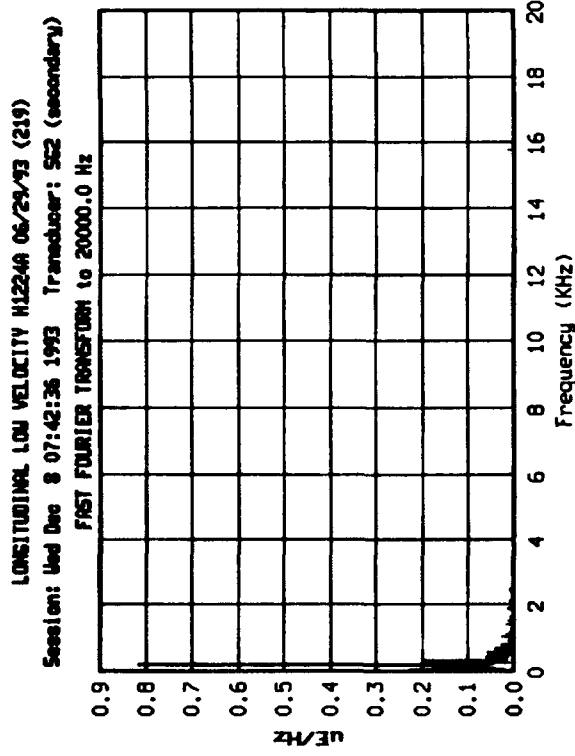


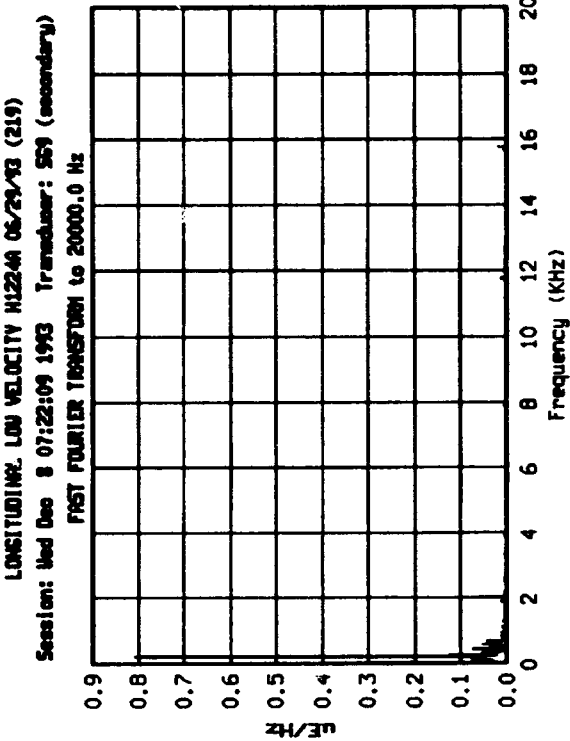
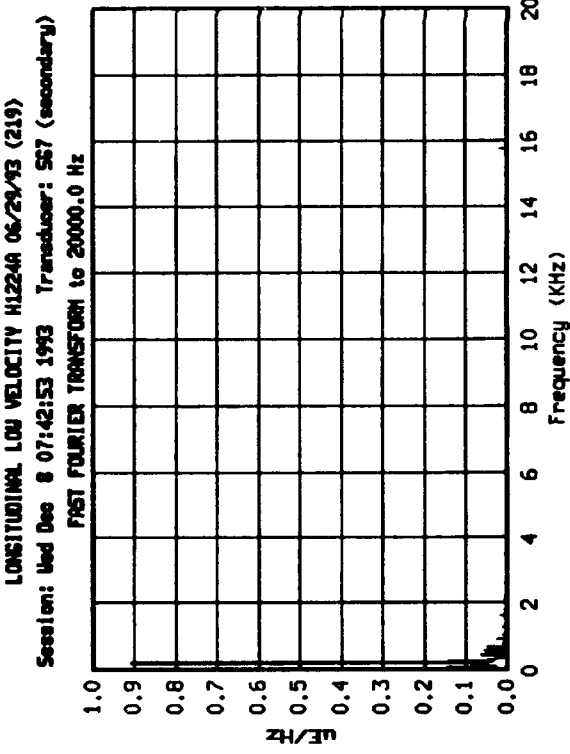
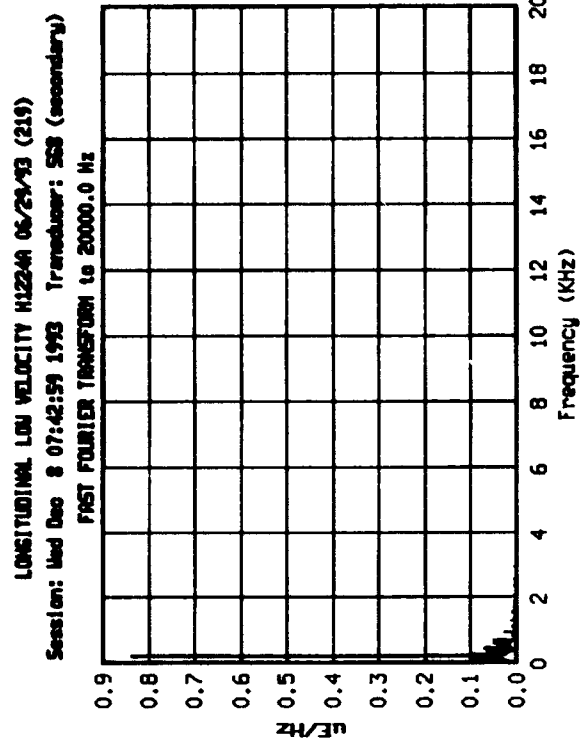
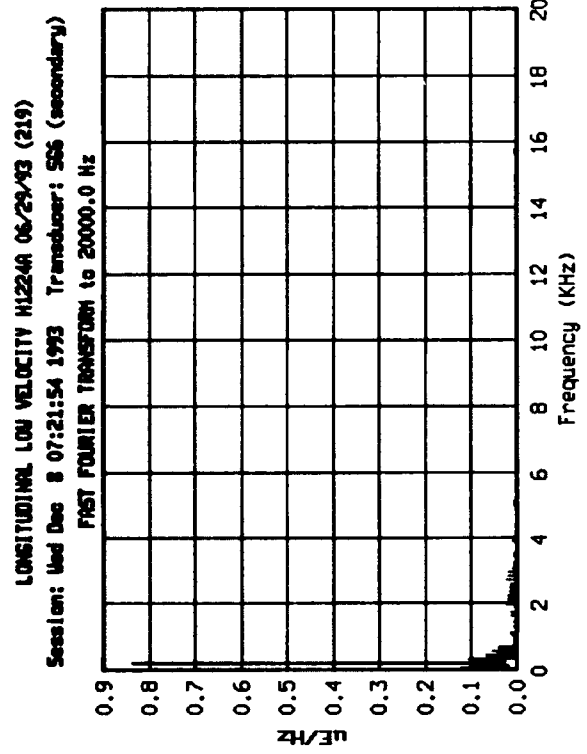


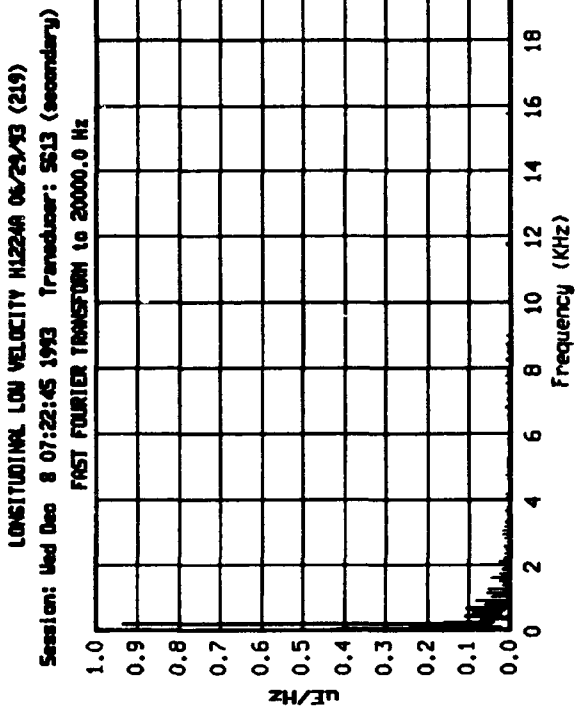
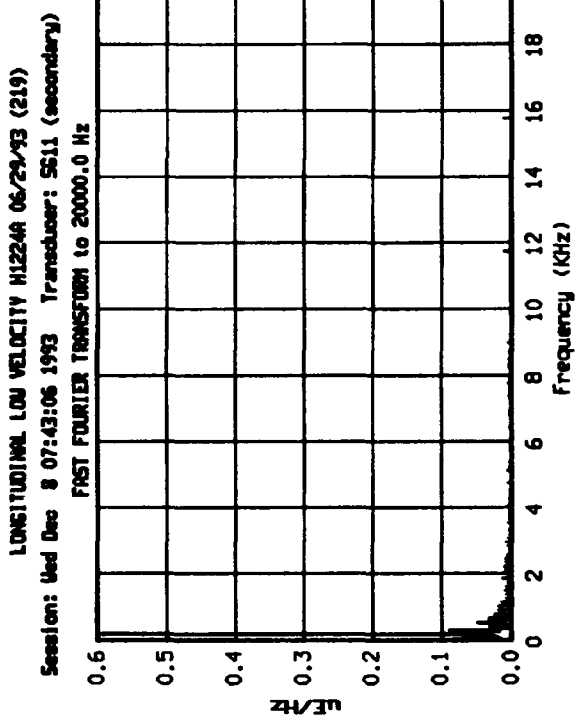
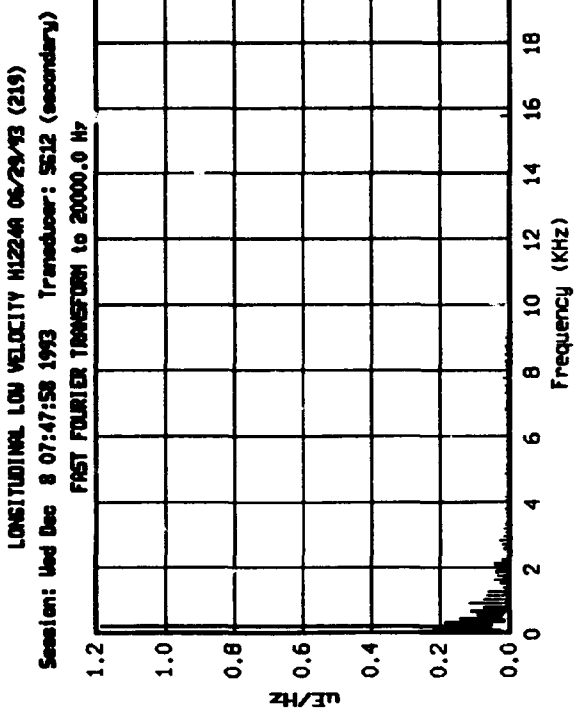
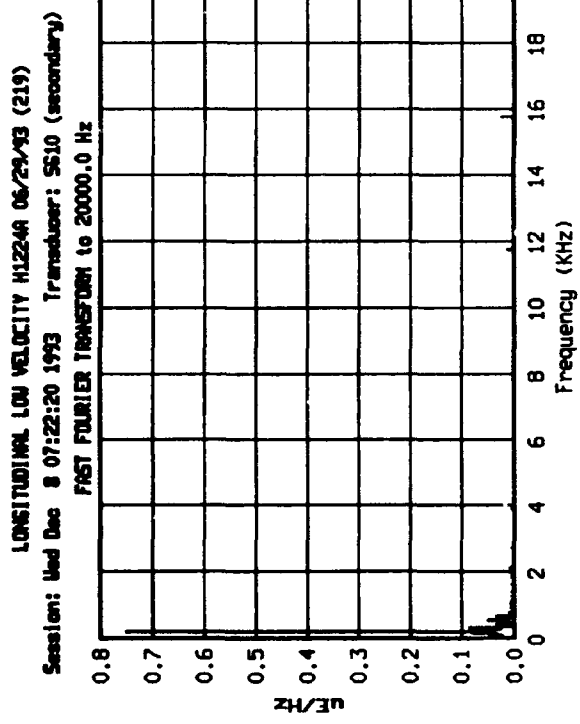


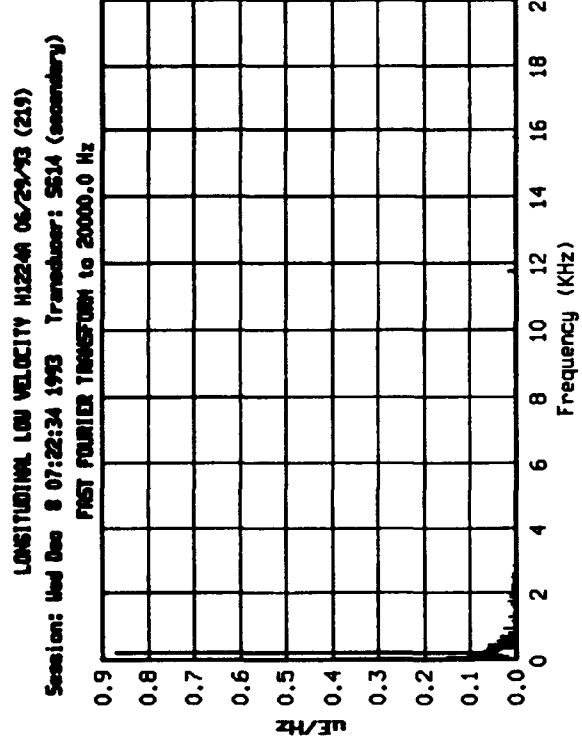






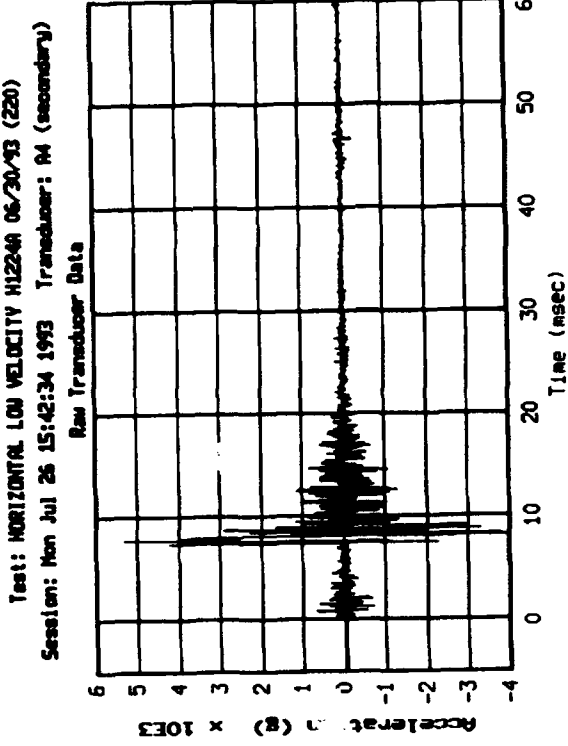
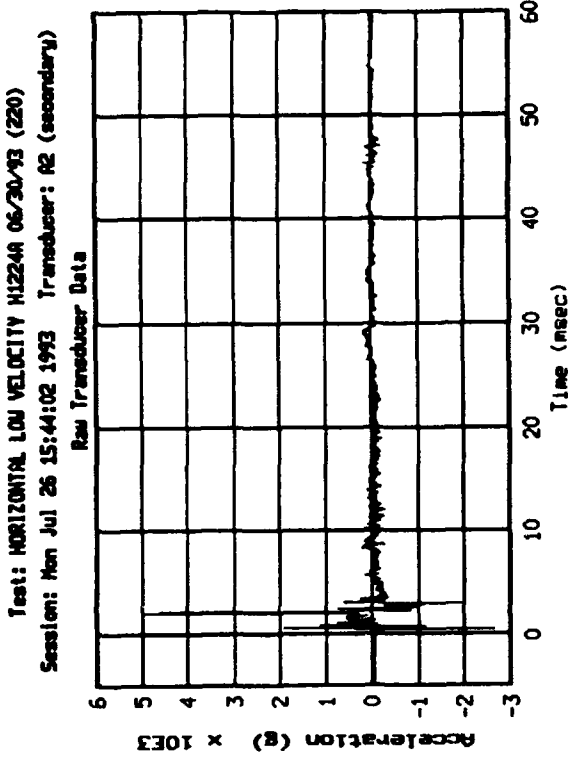
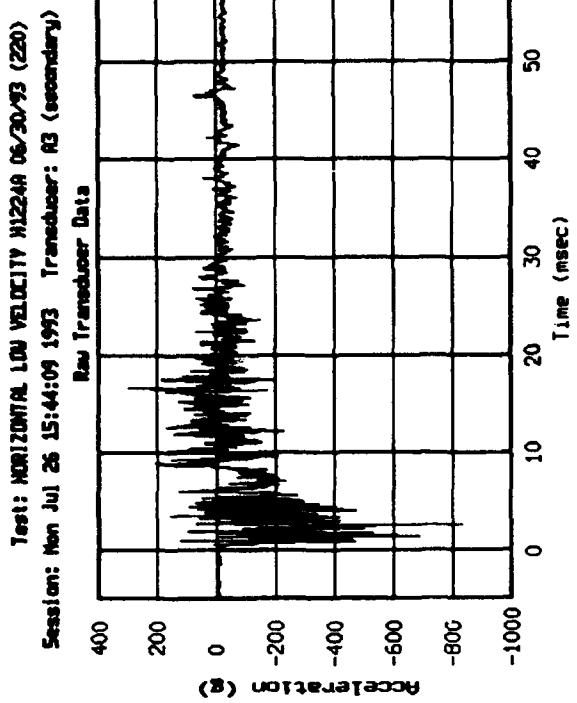
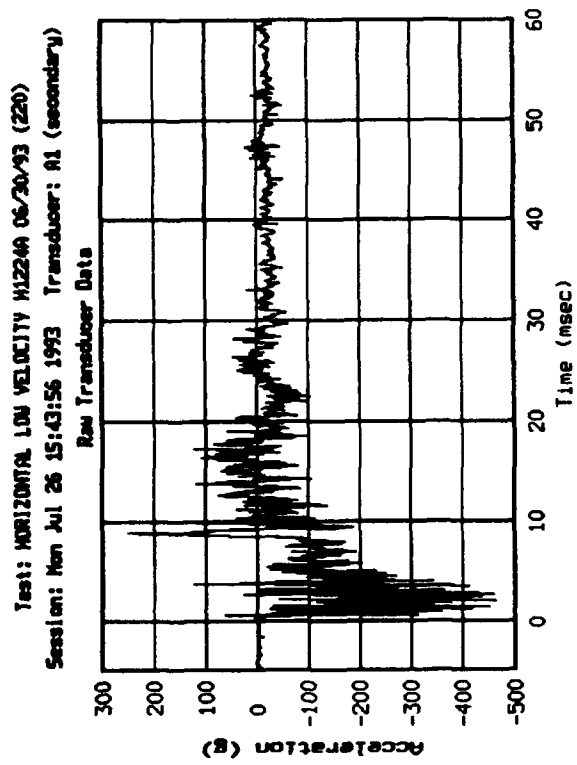


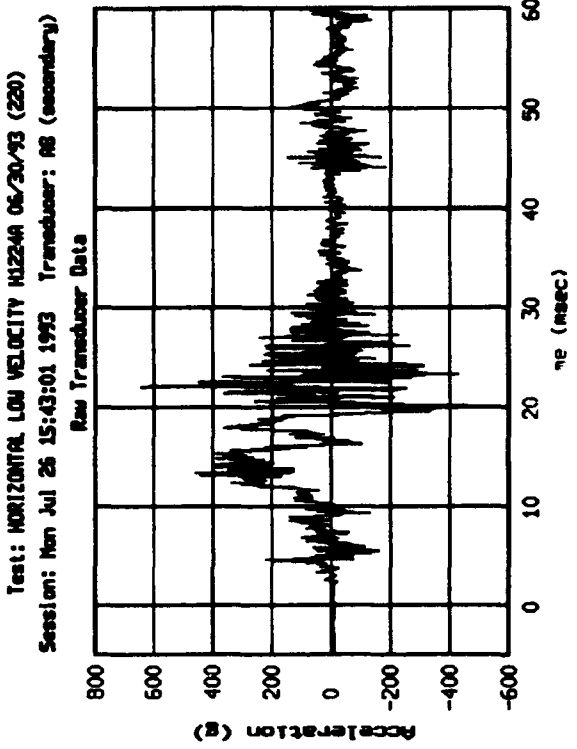
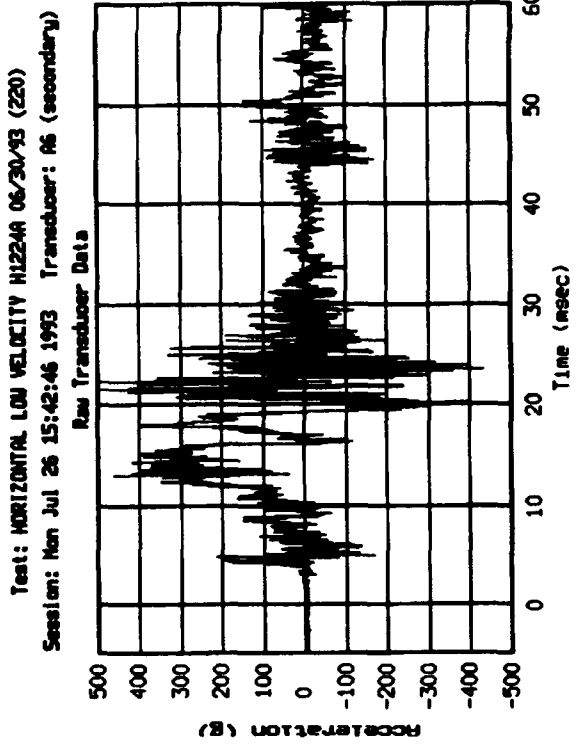
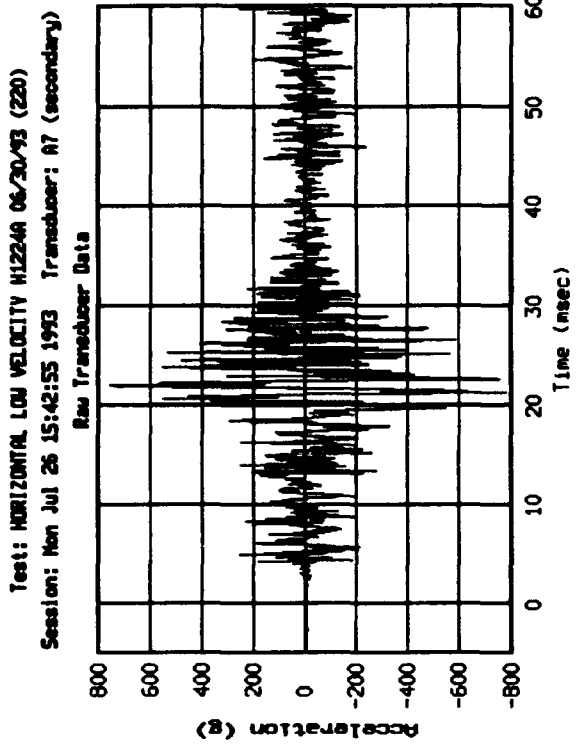
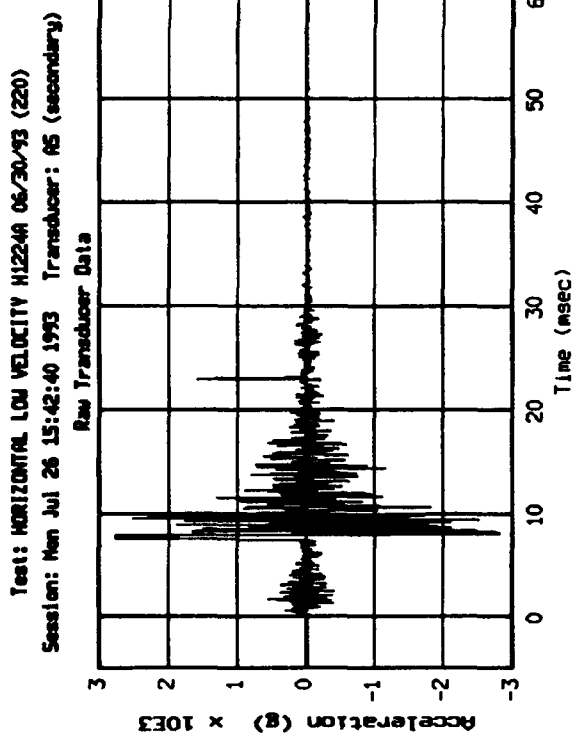




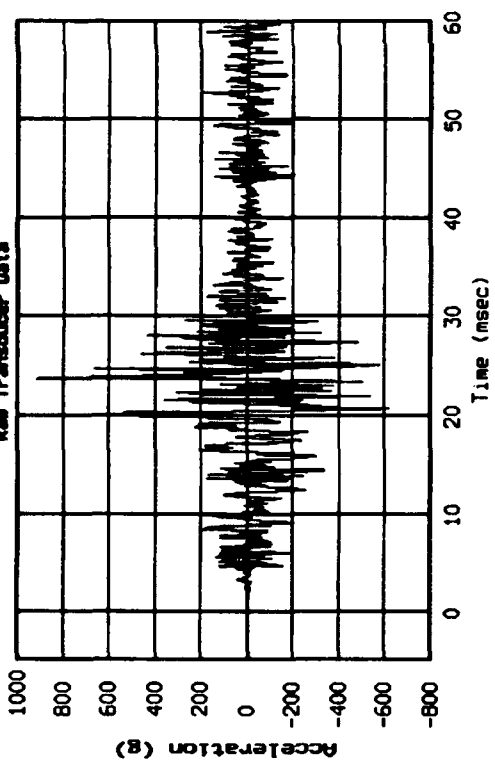
Appendix B. HLV Accelerometer and Strain Gage Data: Raw, Filtered, and Reduced

The following pages show raw (unfiltered) acceleration and strain gage data for the Horizontal Low-Velocity (HLV) impact test. Following this raw data are plots of filtered data (using a low-pass Butterworth 6-stage filter) with cutoff frequencies of 250 Hz and 2,000 Hz. Integrated acceleration data, yielding velocity versus time plots, are presented to analyze kinetic energy values during the test. And finally, Fast Fourier Transforms (FFTs) for each raw data channel are included to analyze acceleration and strain amplitudes in the frequency domain.

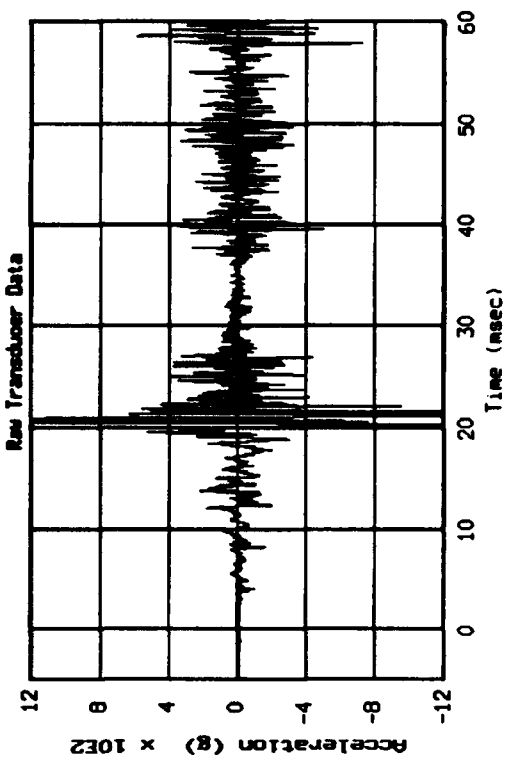




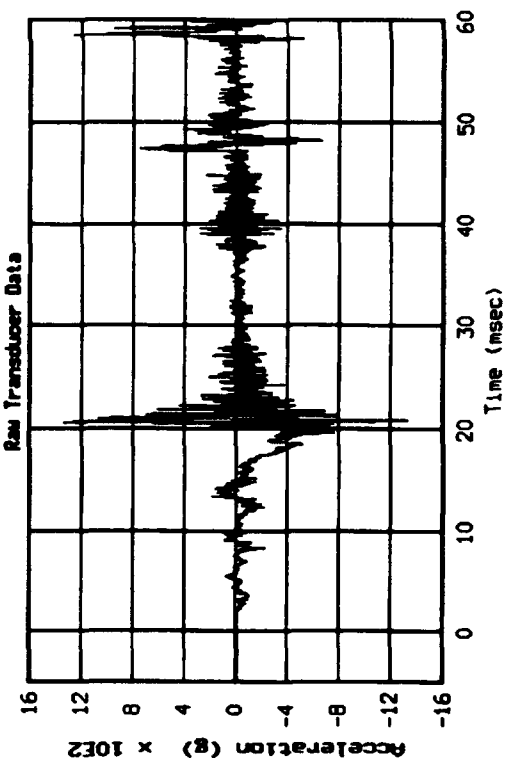
Test: HORIZONTAL LOU VELOCITY HI224A 06/30/93 (220)
Session: Mon Jul 26 15:43:09 1993 Transducer: A9 (secondary)



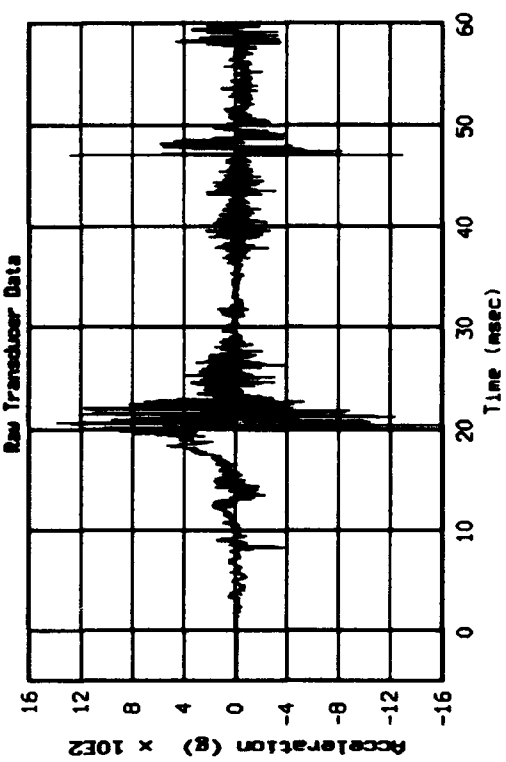
Test: HORIZONTAL LOU VELOCITY HI224A 06/30/93 (220)
Session: Mon Jul 26 15:43:24 1993 Transducer: A11 (secondary)

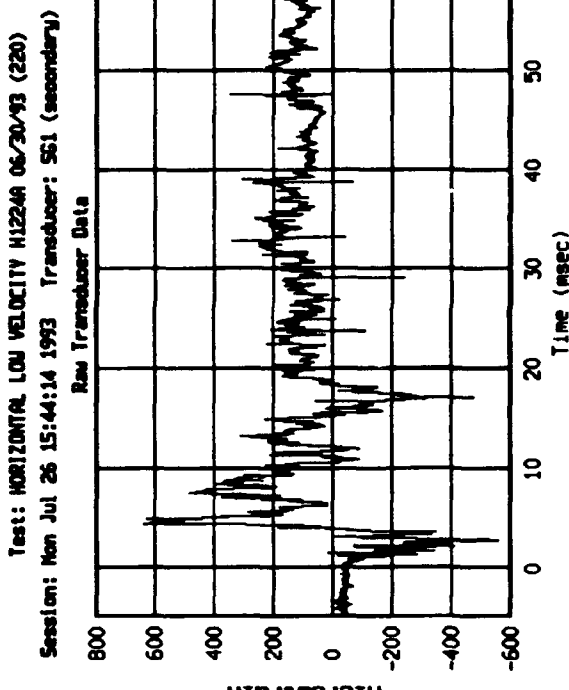
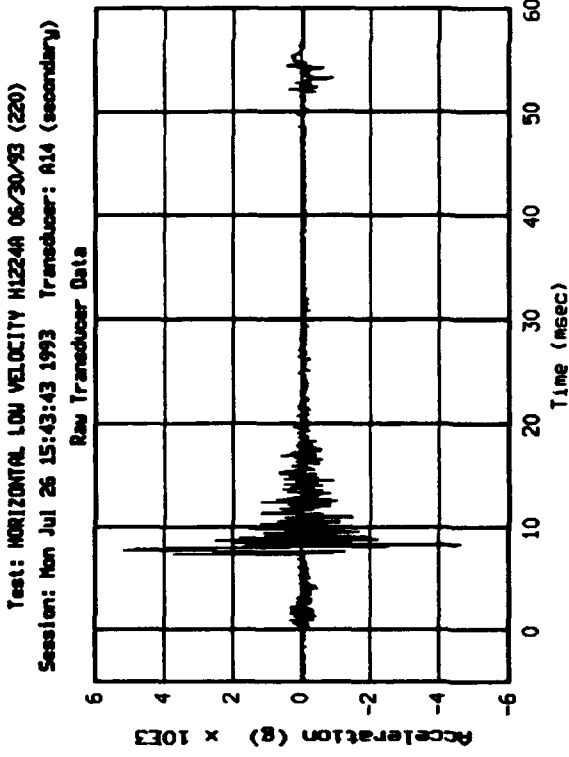
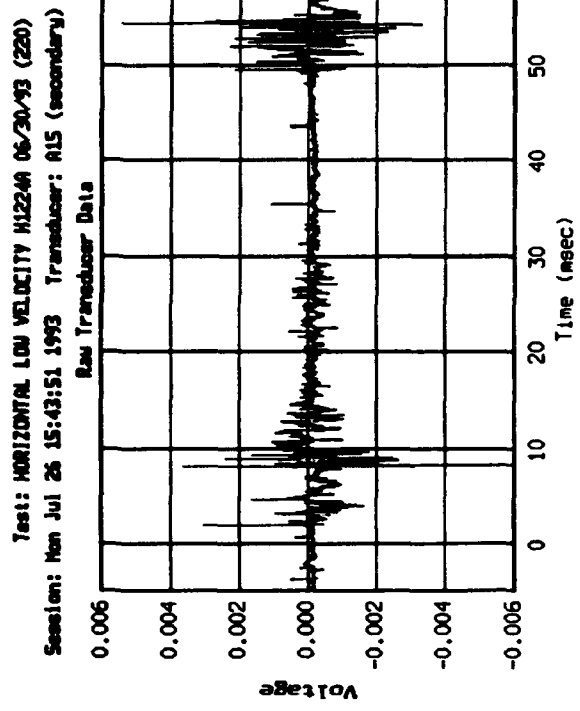
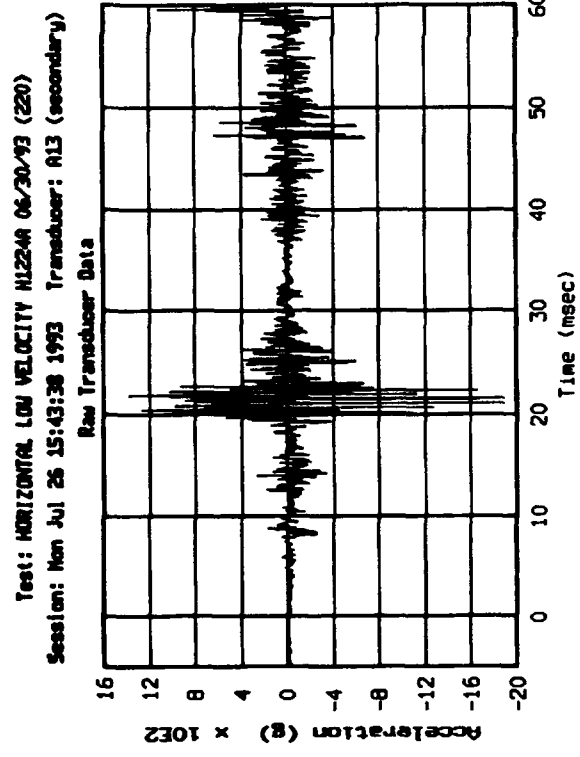


Test: HORIZONTAL LOU VELOCITY HI224A 06/30/93 (220)
Session: Mon Jul 26 15:43:16 1993 Transducer: A10 (secondary)

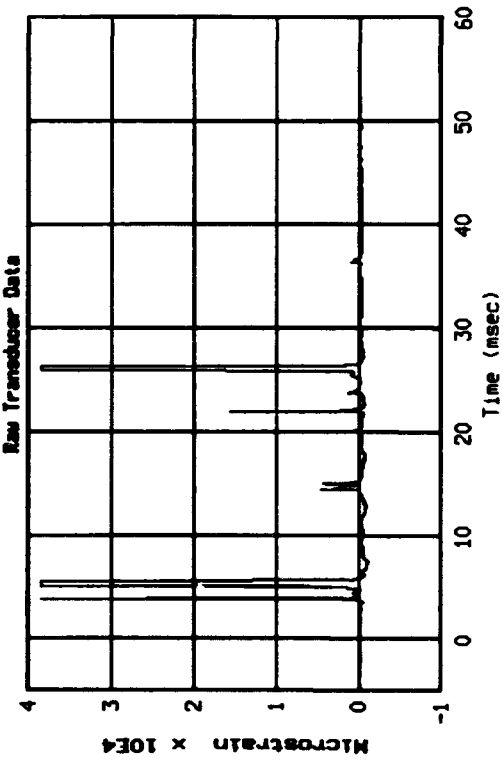


Test: HORIZONTAL LOU VELOCITY HI224A 06/30/93 (220)
Session: Mon Jul 26 15:43:24 1993 Transducer: A12 (secondary)

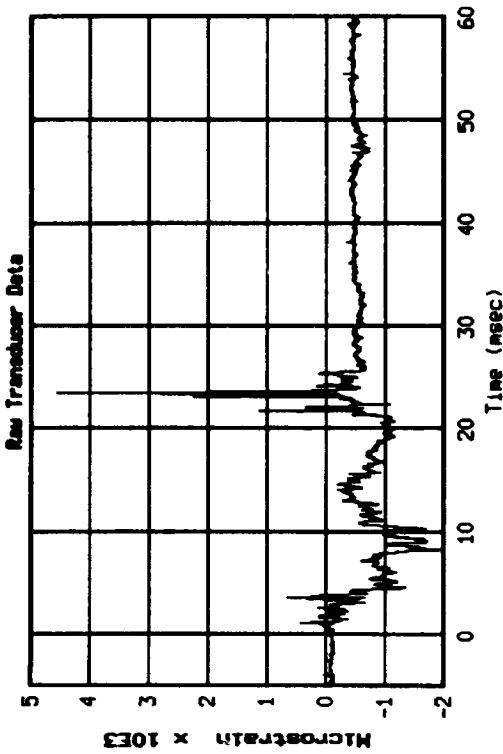




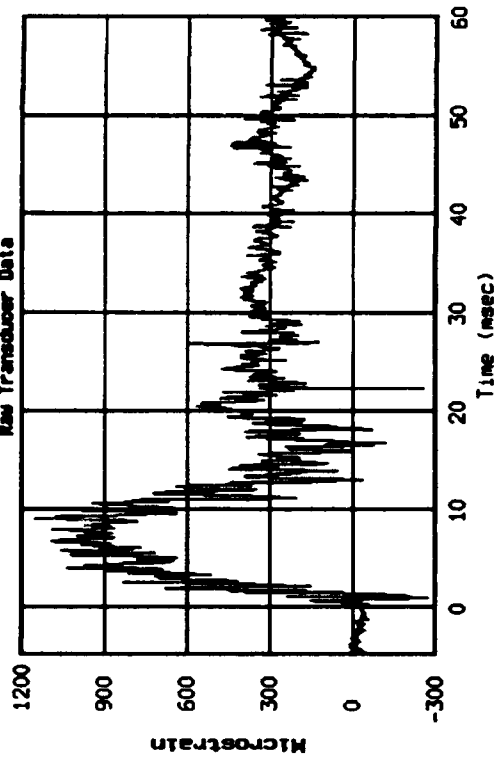
Test: HORIZONTAL LOU VELCITY H12244 06/30/93 (220)
Session: Mon Jul 26 15:44:21 1993 Transducer: SS2 (secondary)



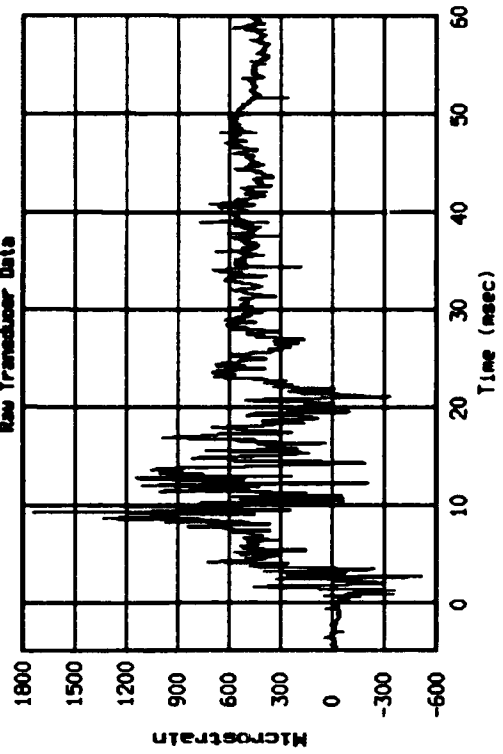
Test: HORIZONTAL LOU VELCITY H12244 06/30/93 (220)
Session: Mon Jul 26 15:44:35 1993 Transducer: SS4 (secondary)

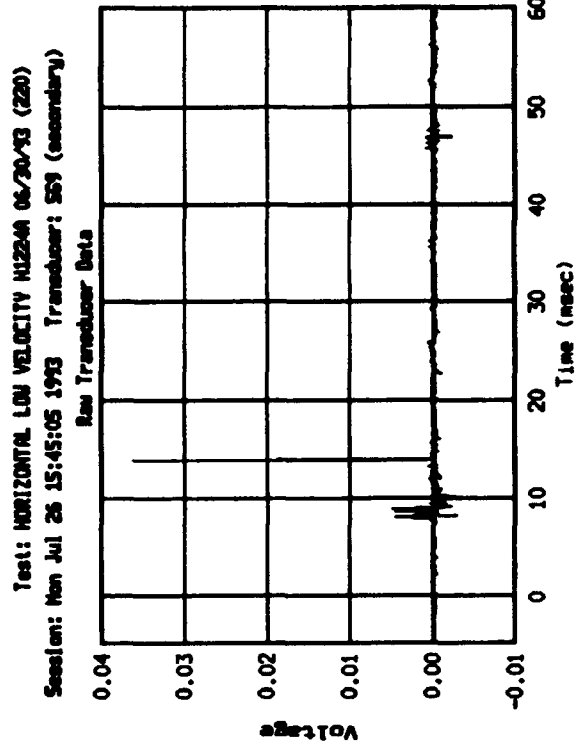
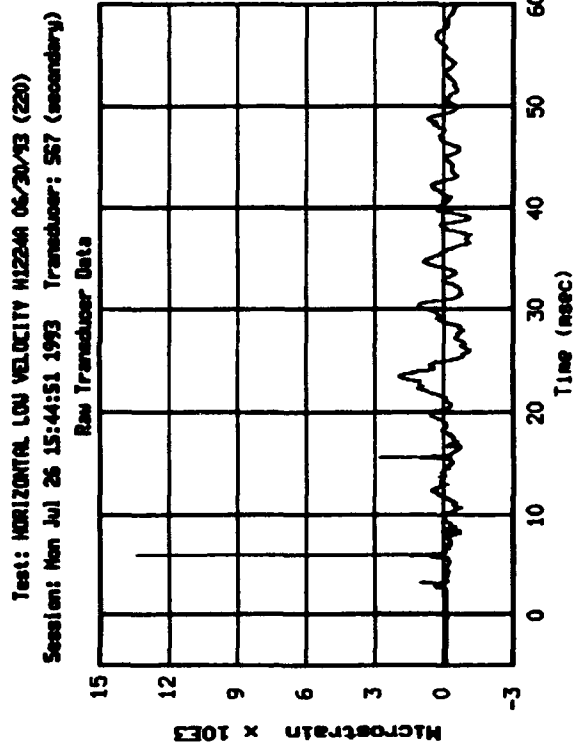
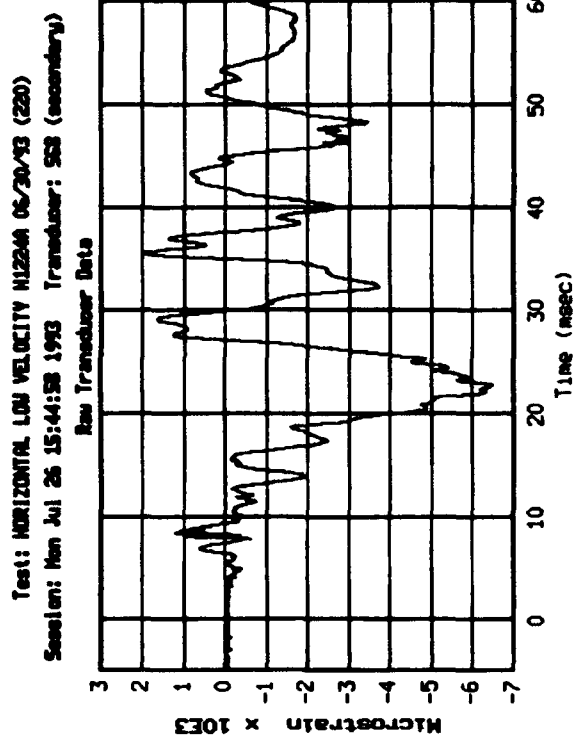
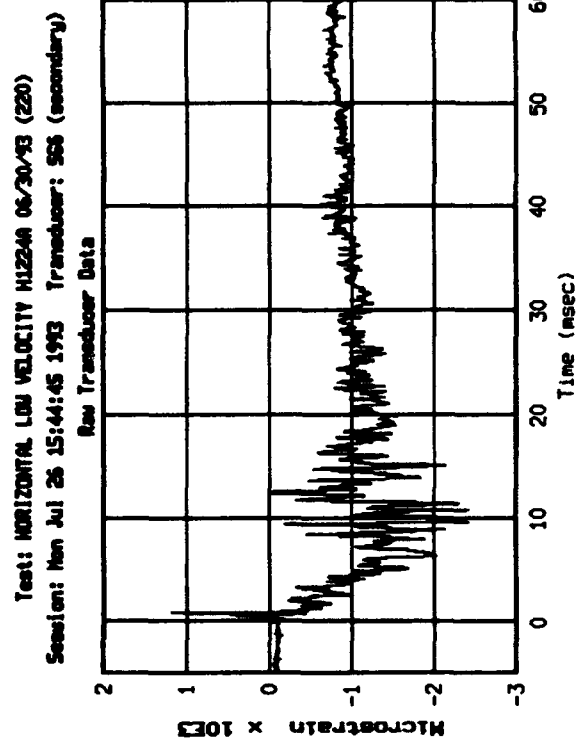


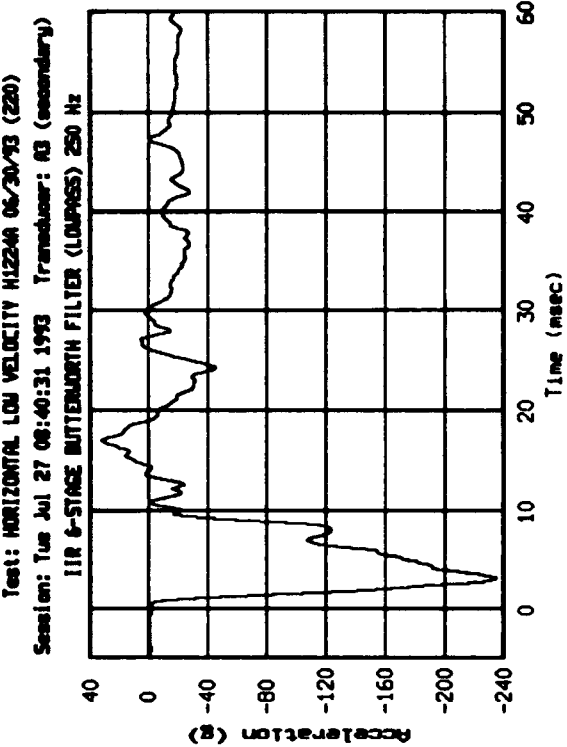
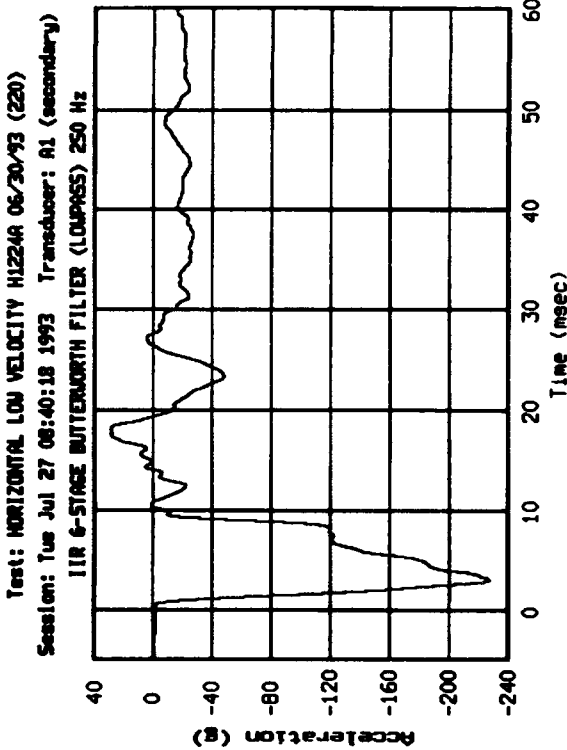
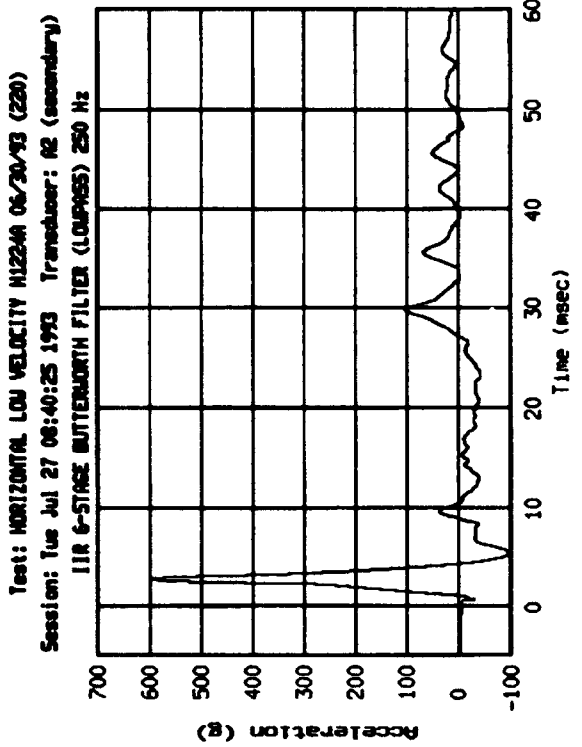
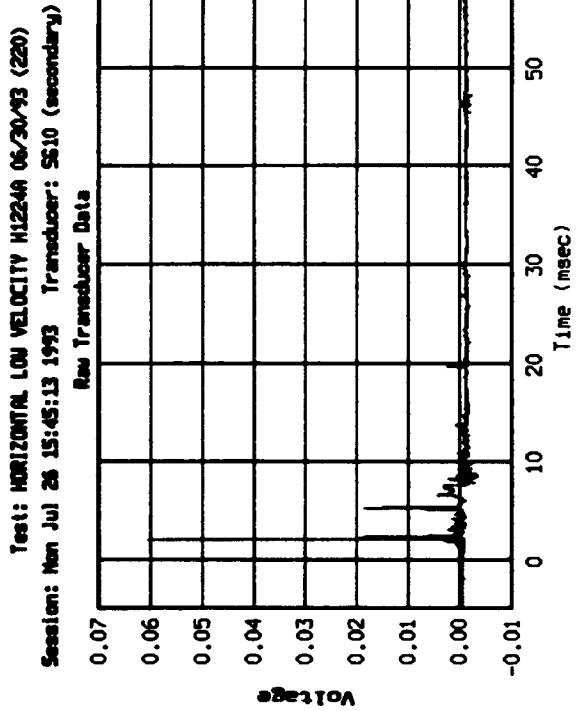
Test: HORIZONTAL LOU VELCITY H12244 06/30/93 (220)
Session: Mon Jul 26 15:44:28 1993 Transducer: SS3 (secondary)

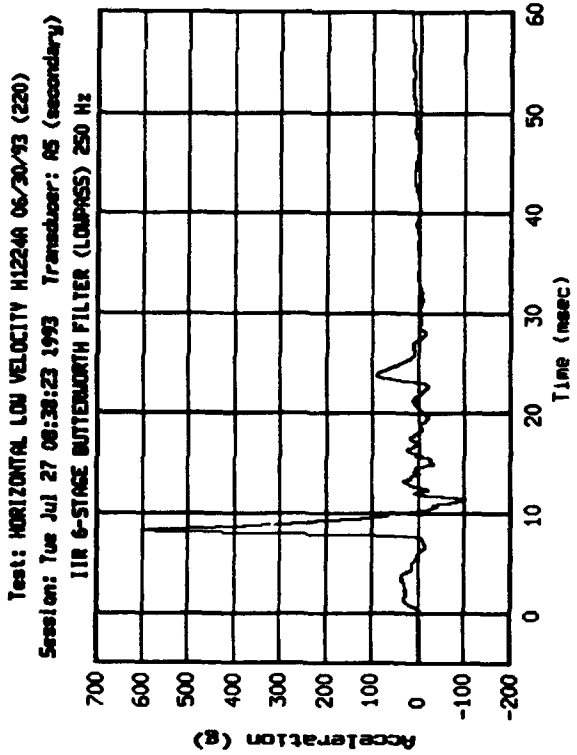
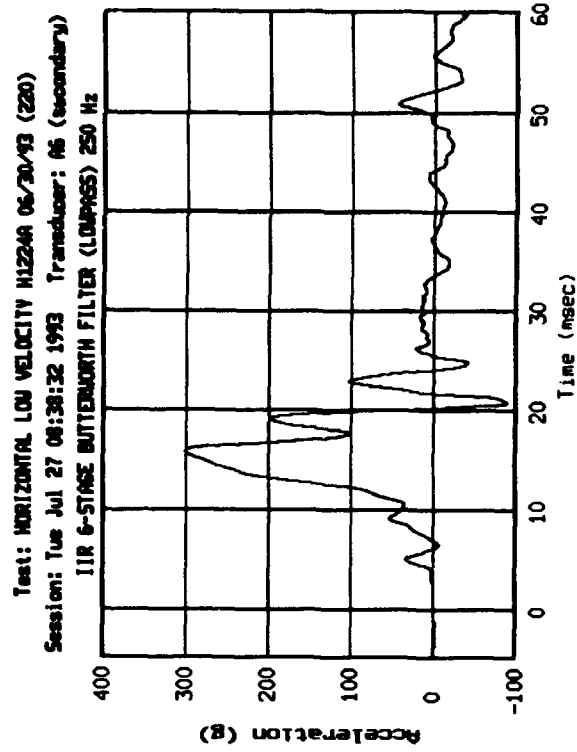
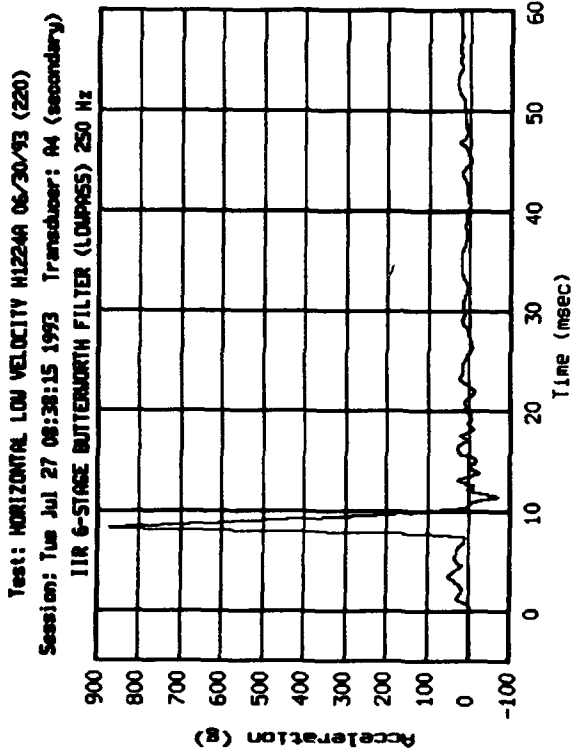


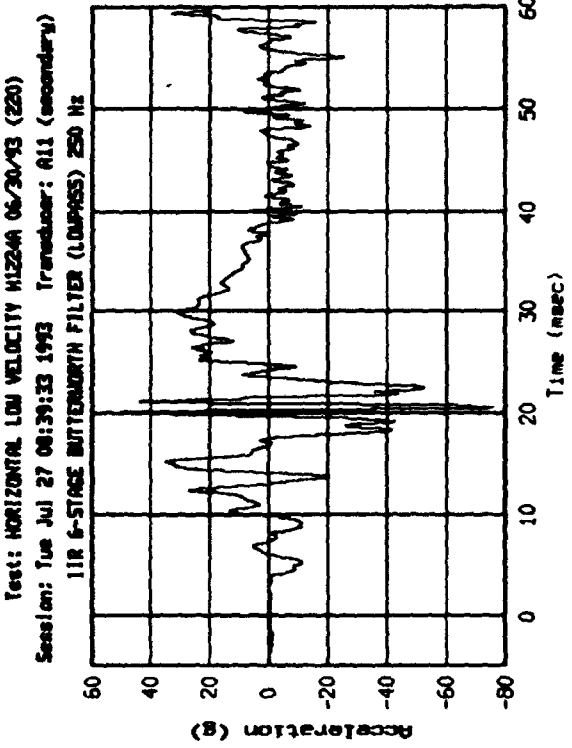
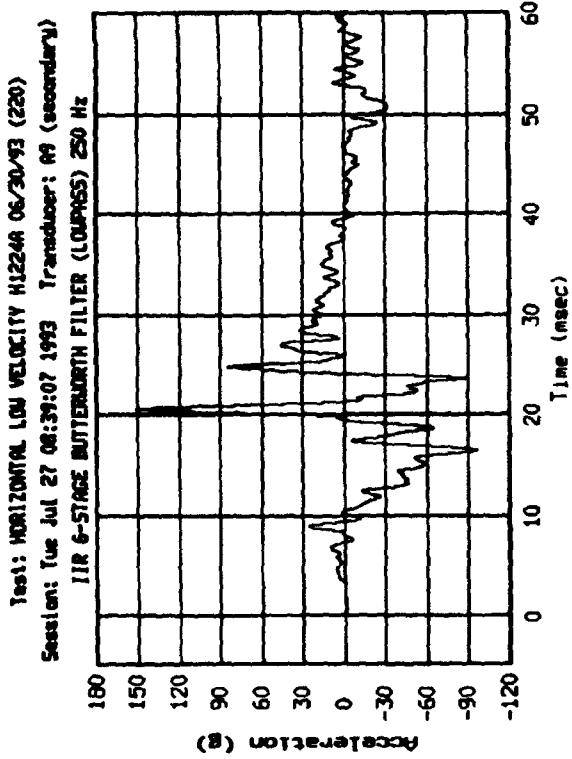
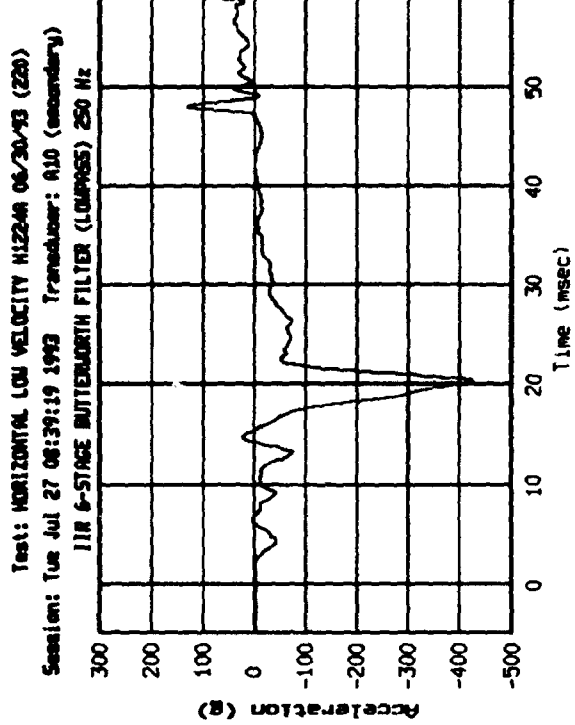
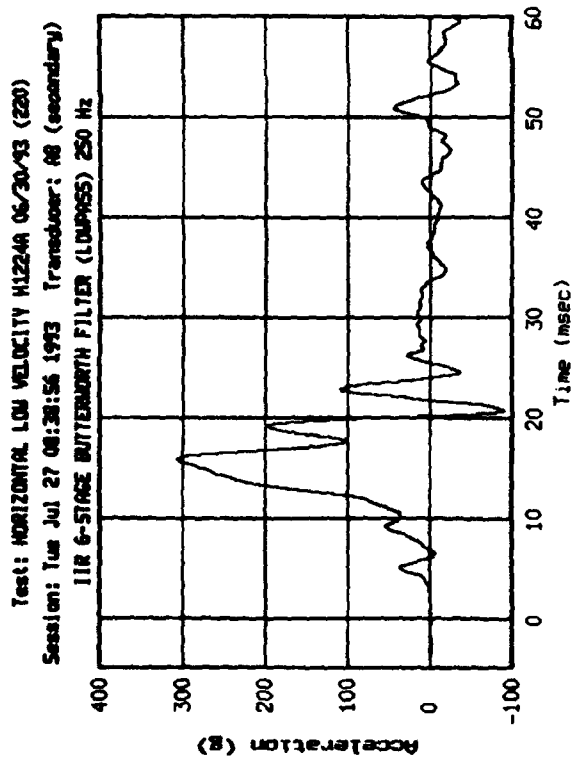
Test: HORIZONTAL LOU VELCITY H12244 06/30/93 (220)
Session: Mon Jul 26 15:44:40 1993 Transducer: SS5 (secondary)

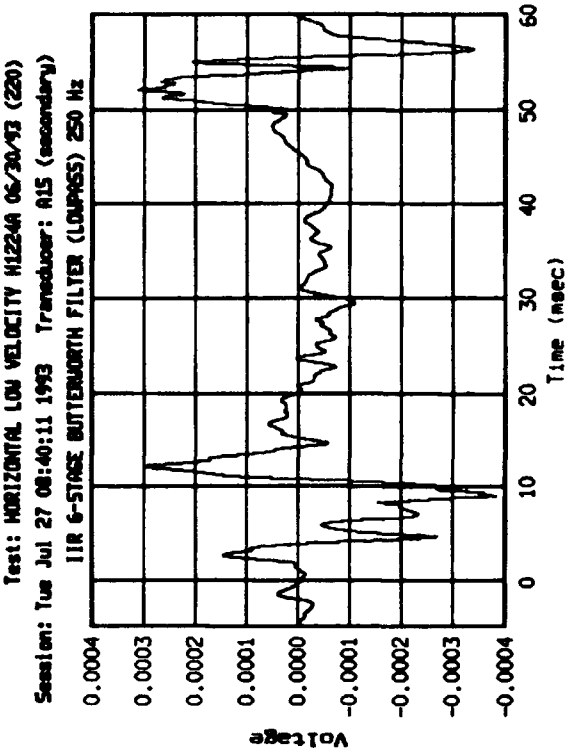
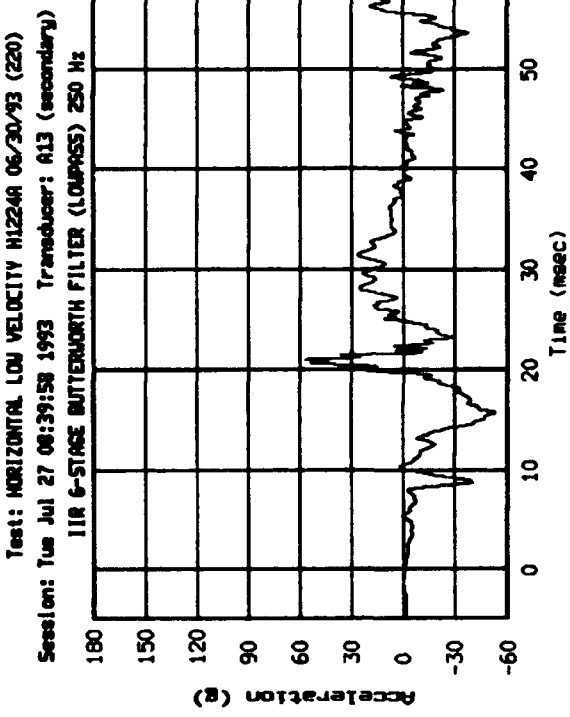
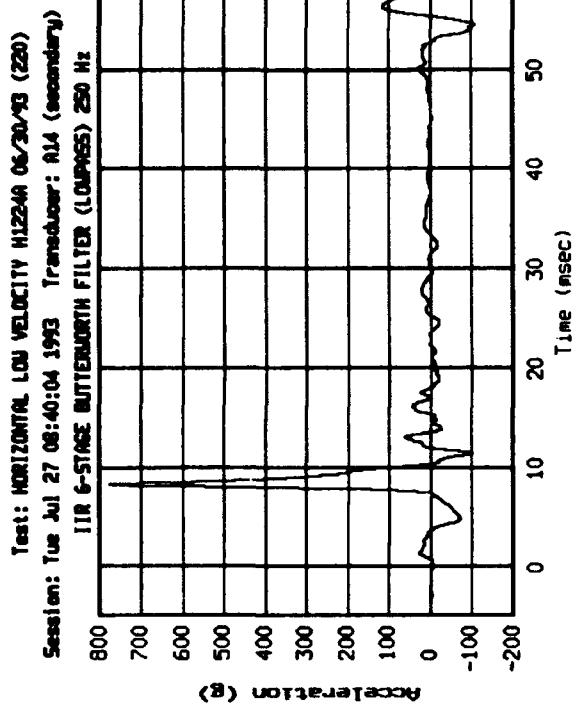
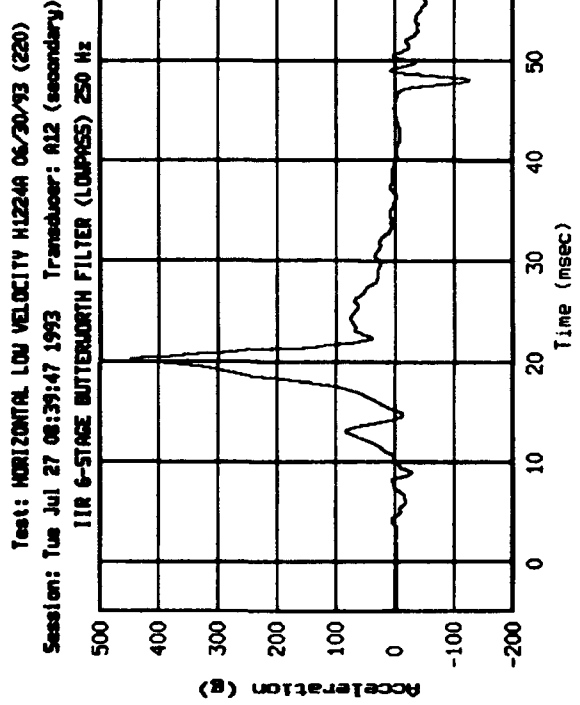


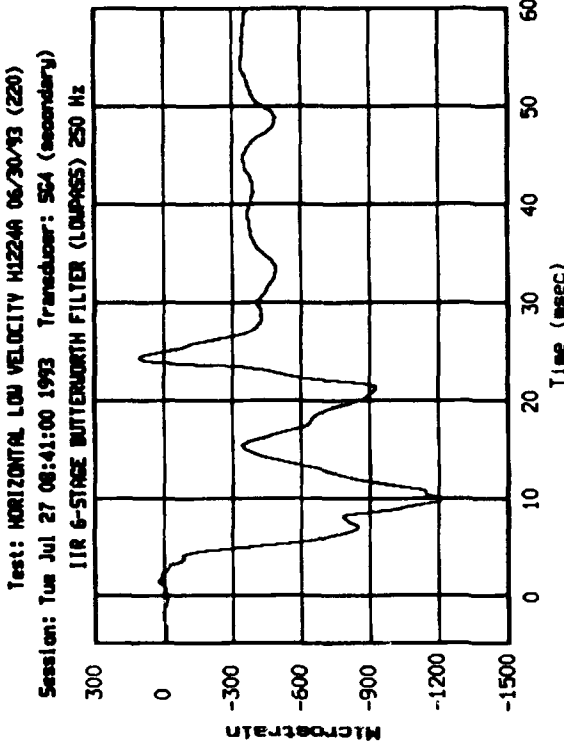
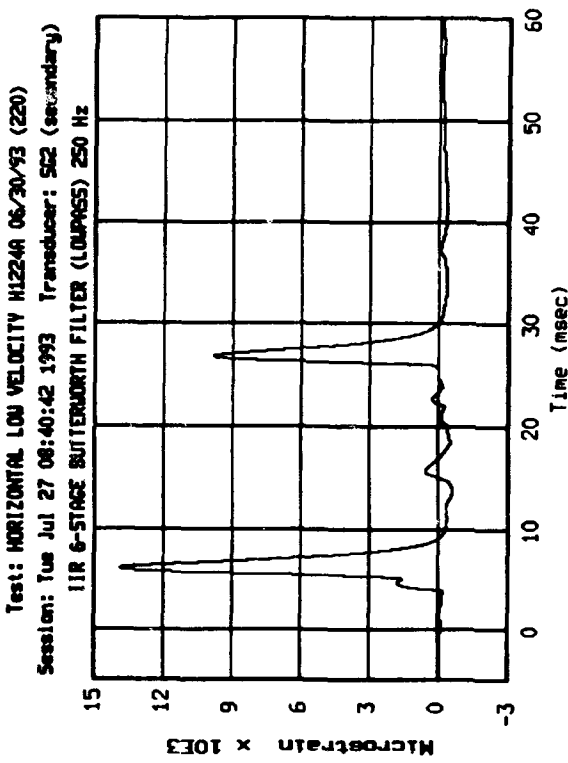
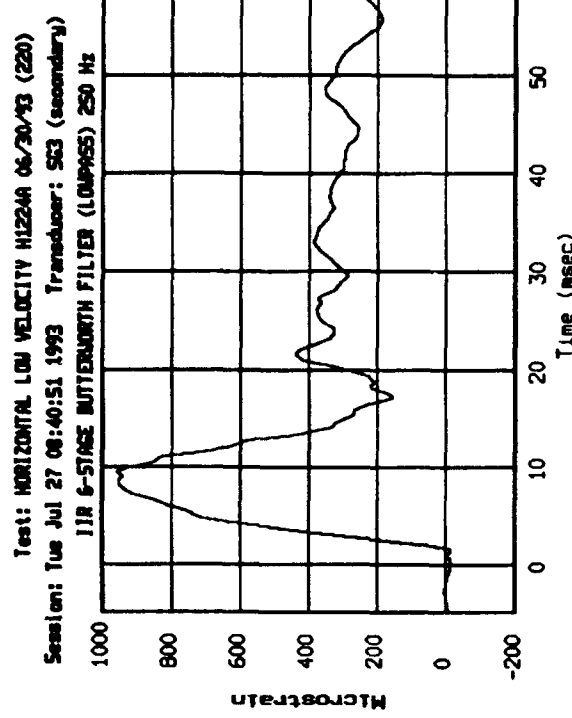
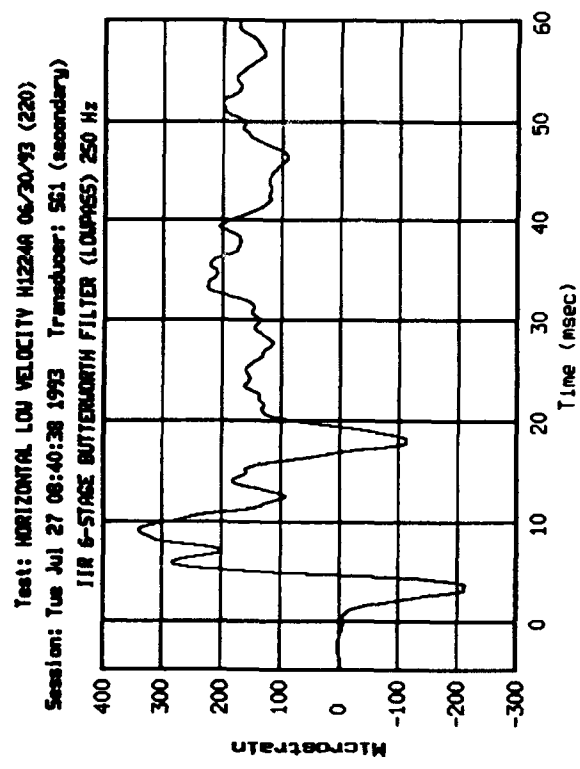


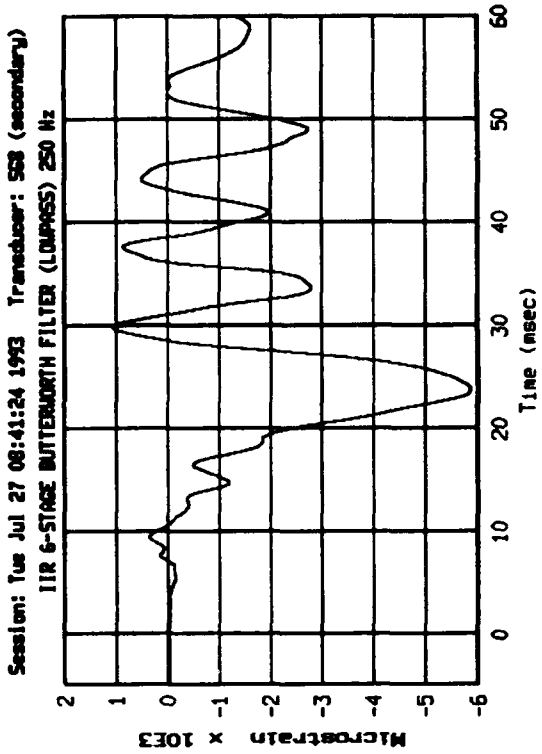
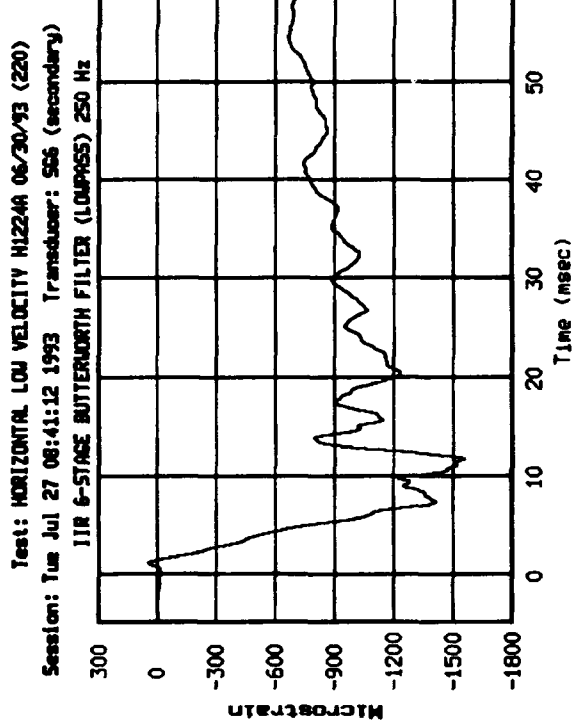
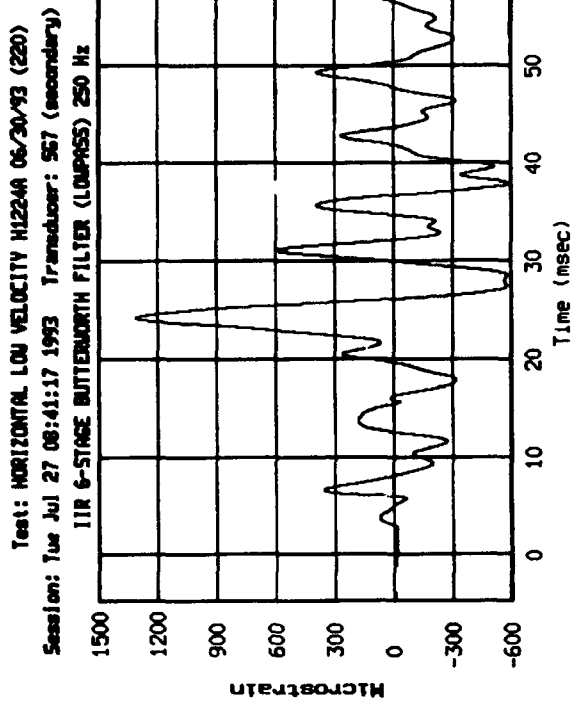
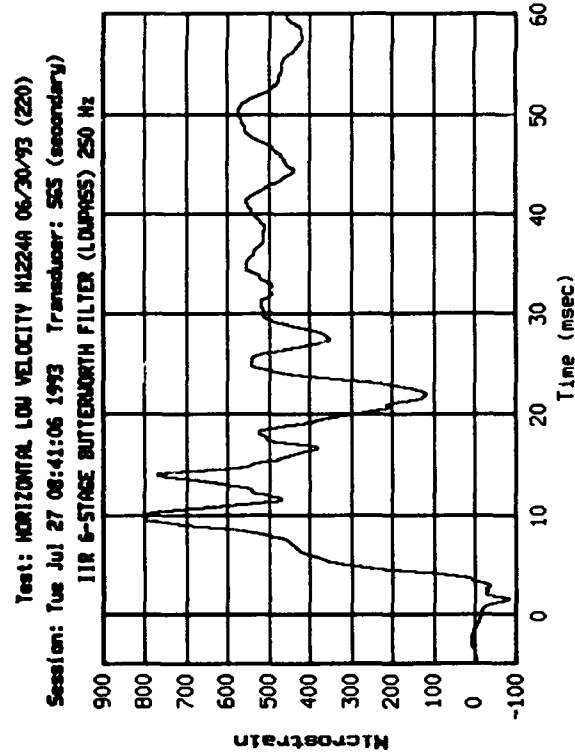


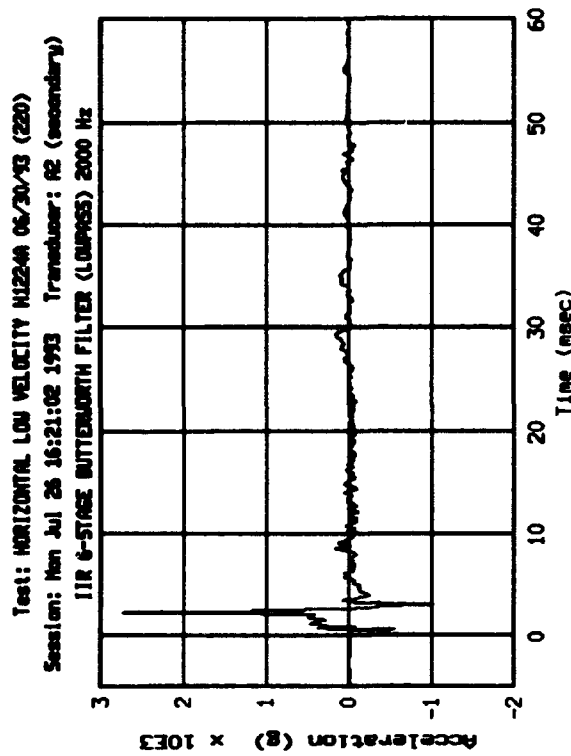
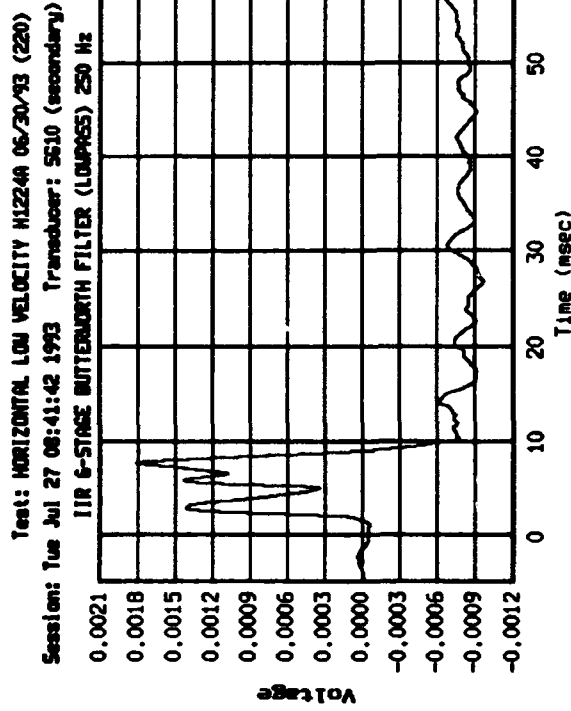
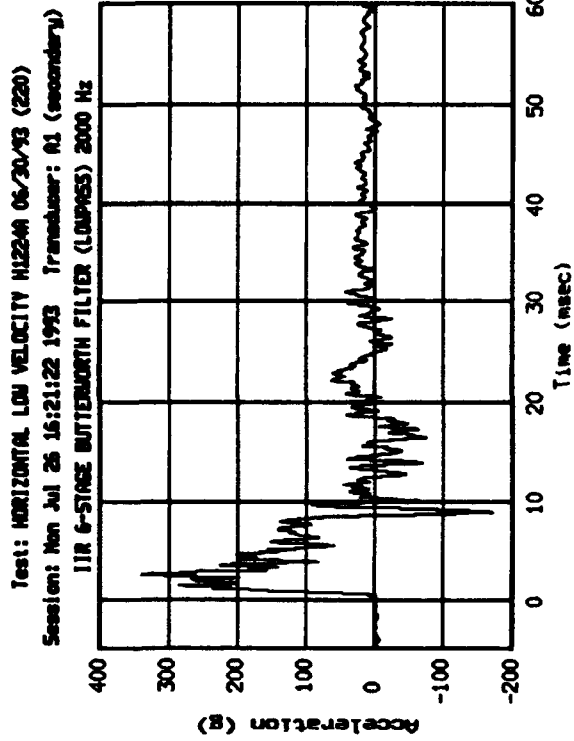
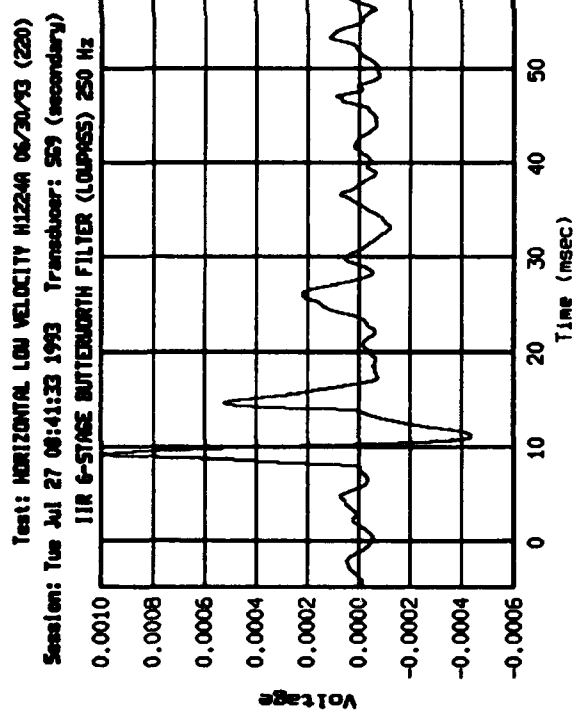


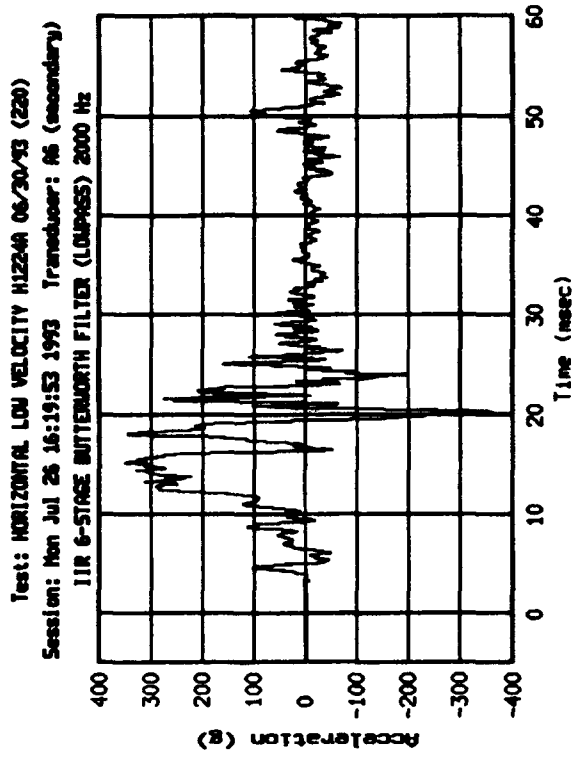
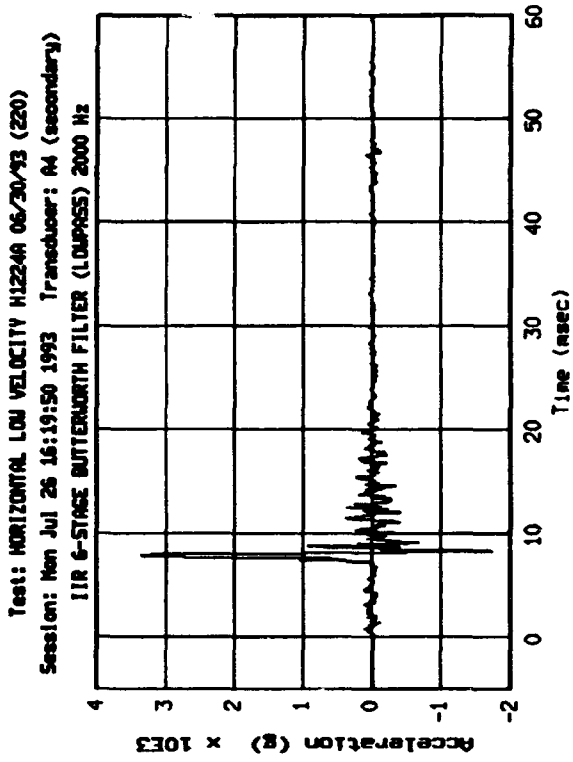
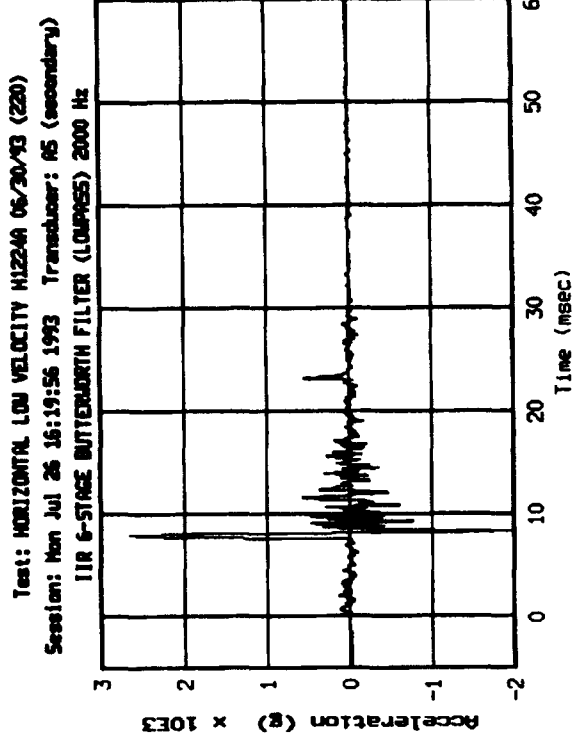
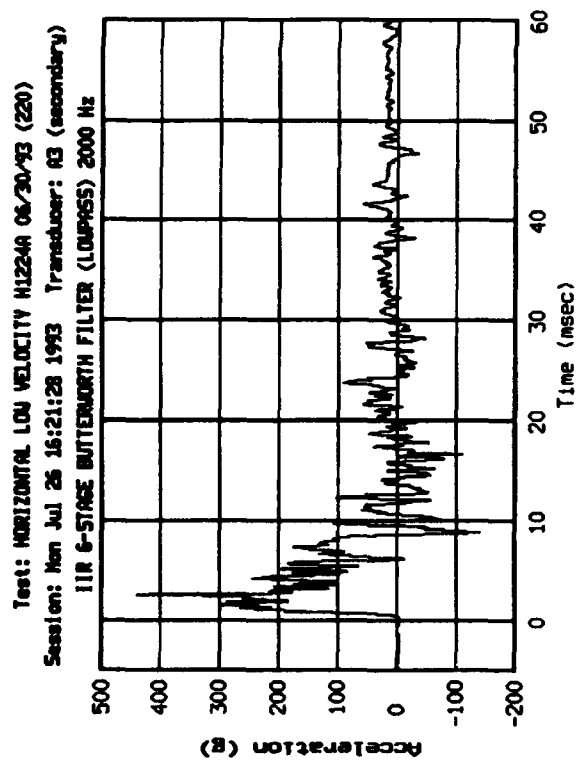


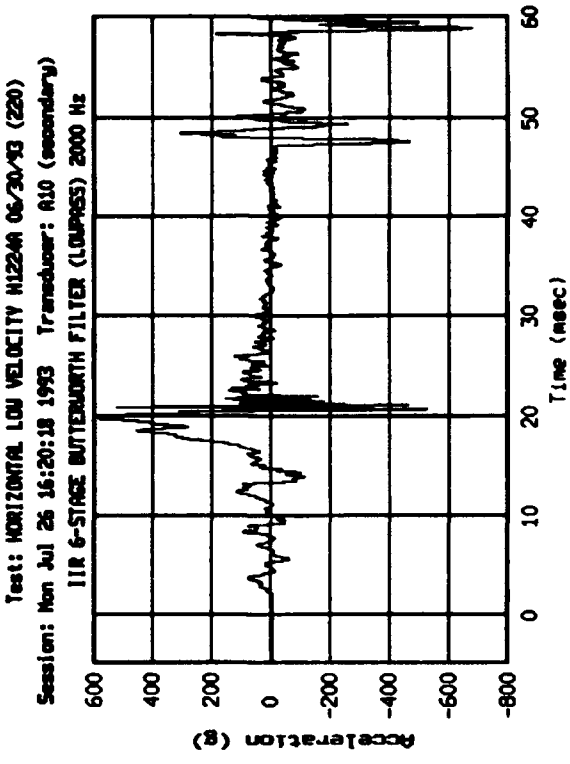
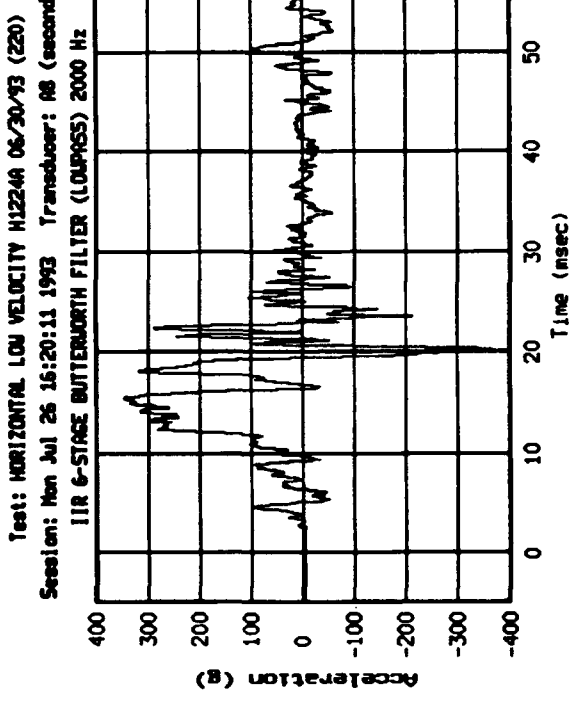
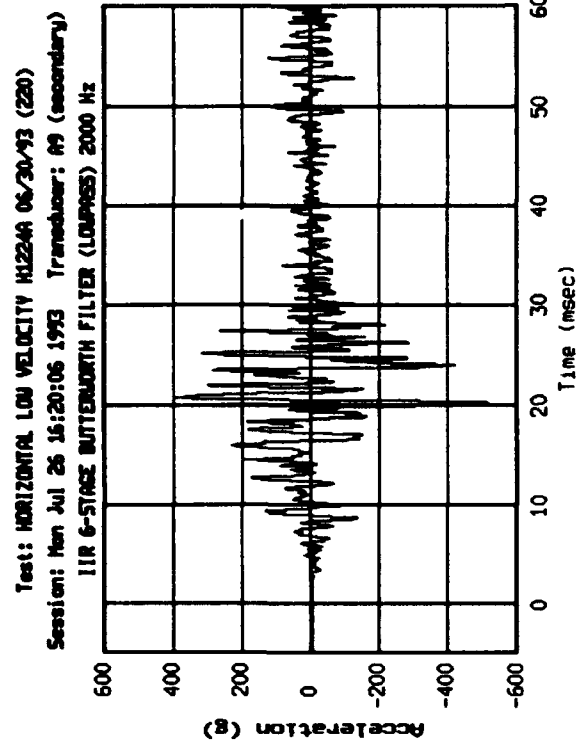
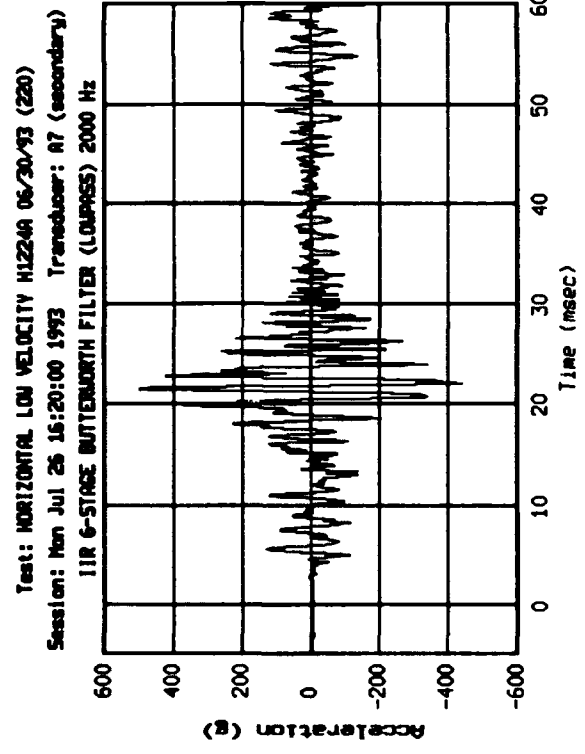


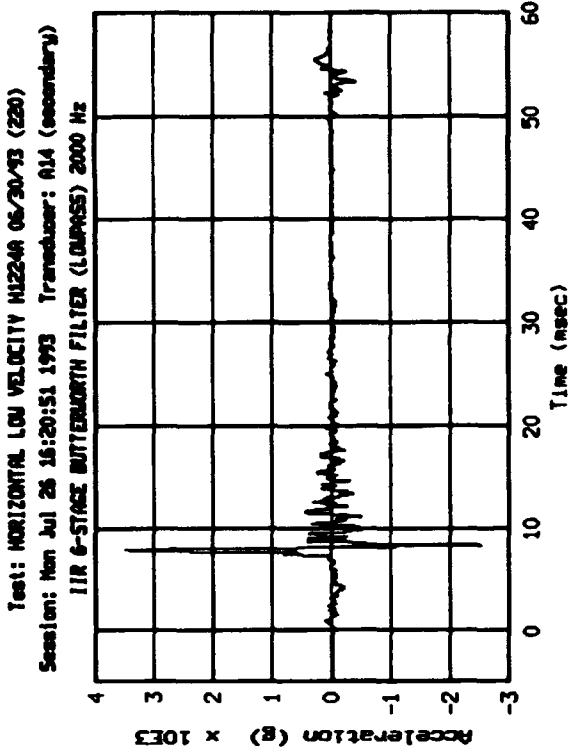
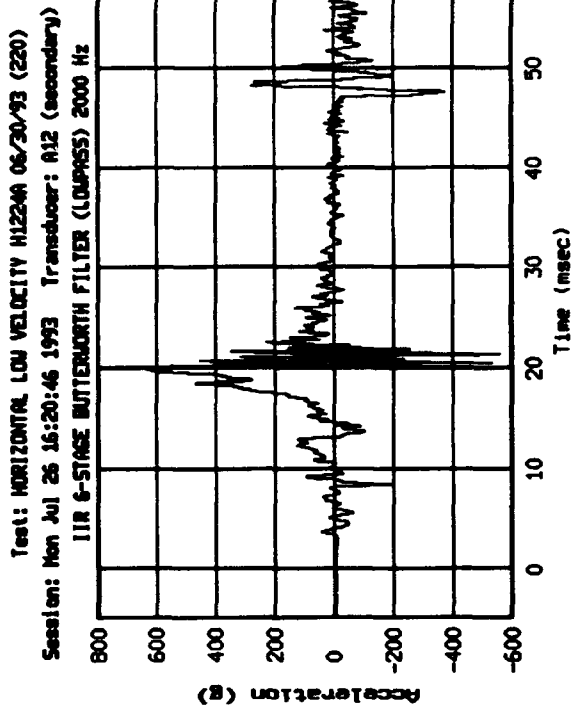
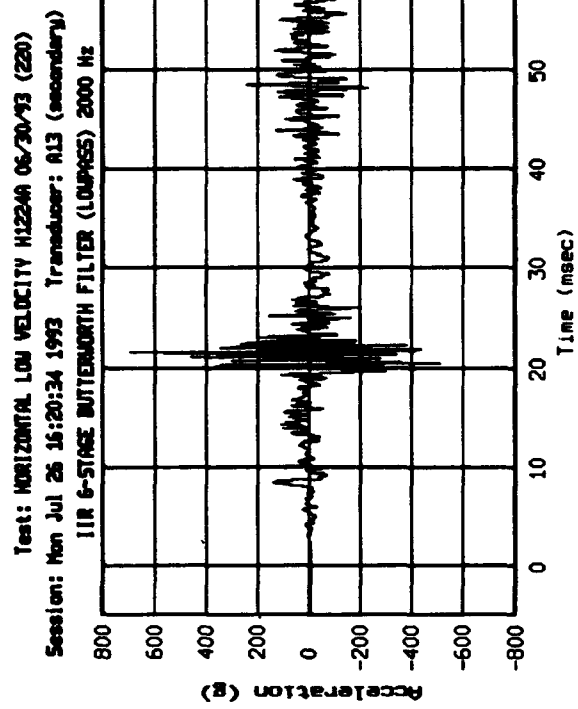
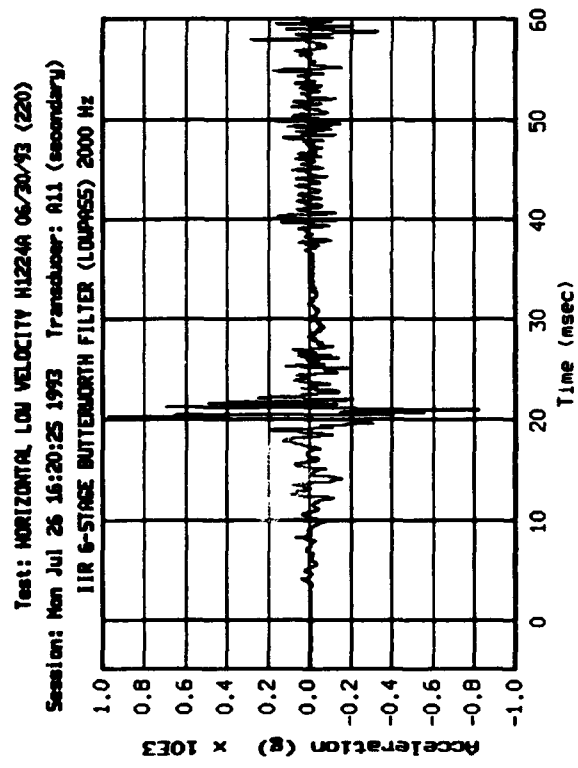


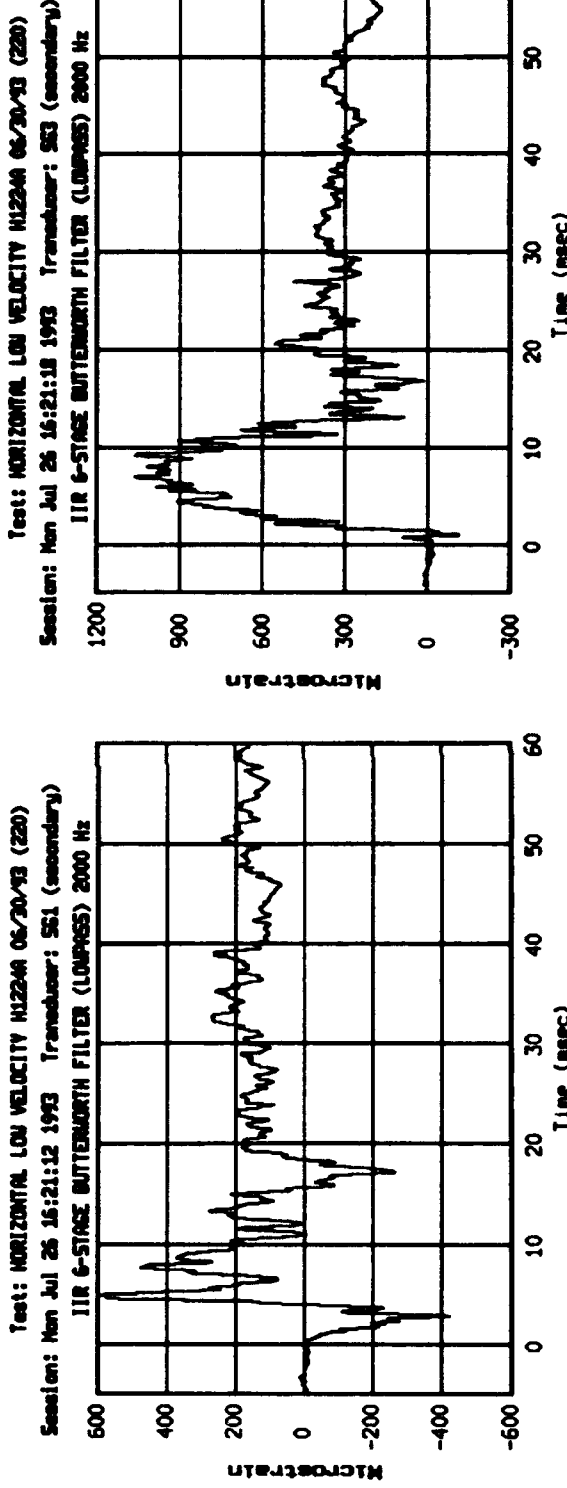
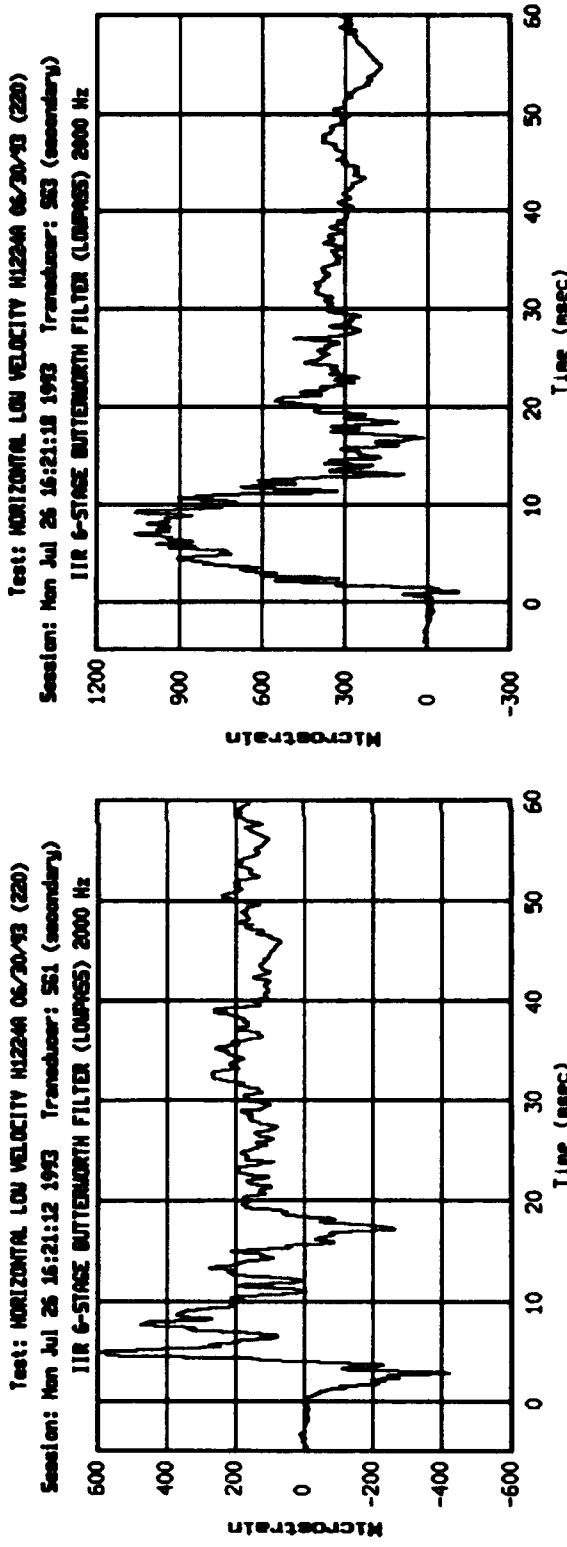
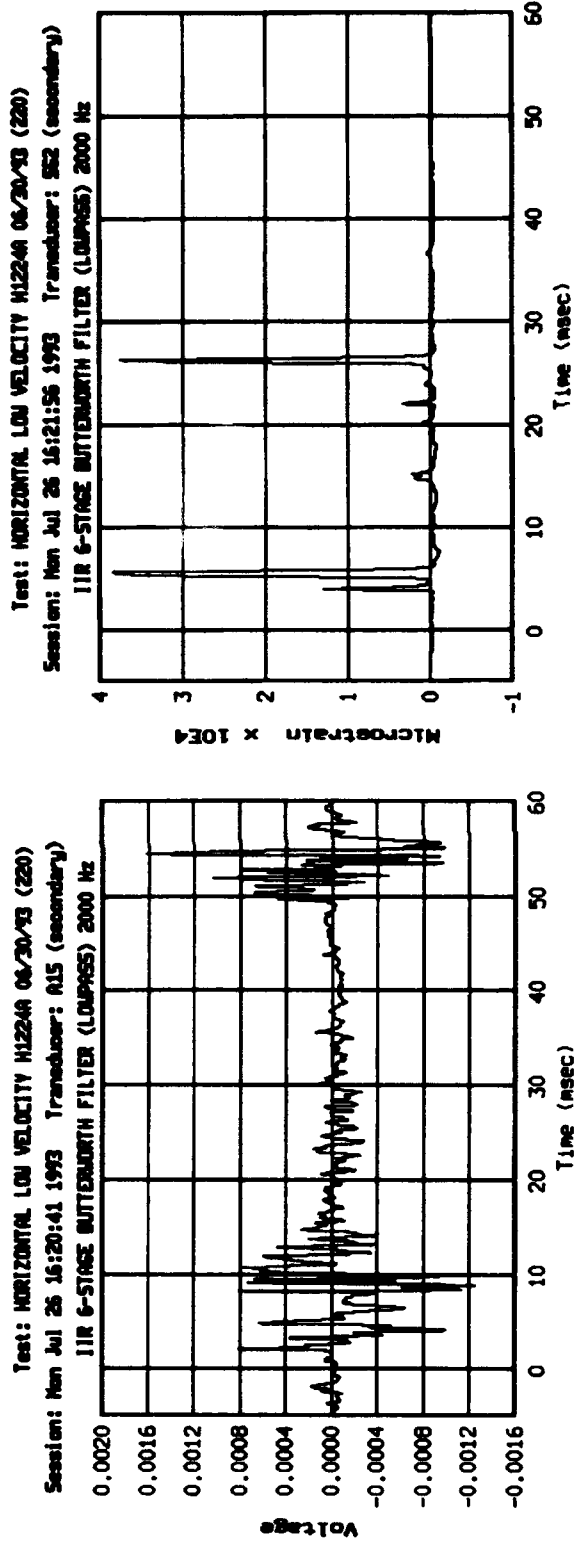


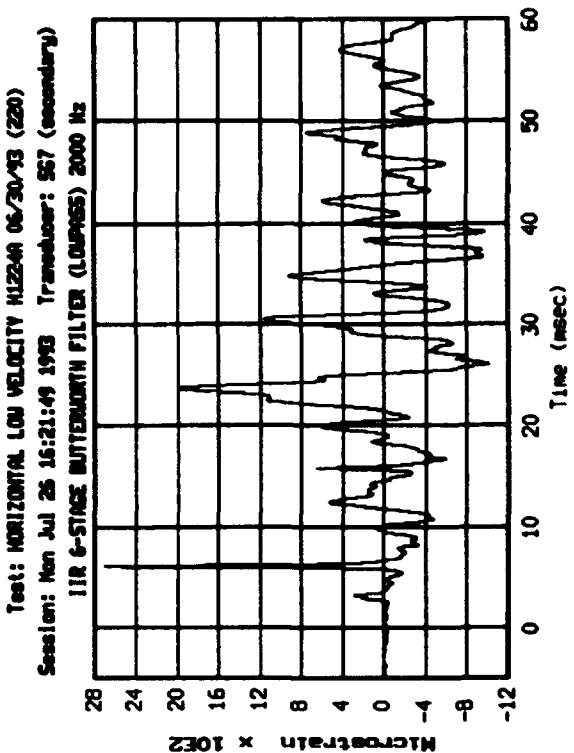
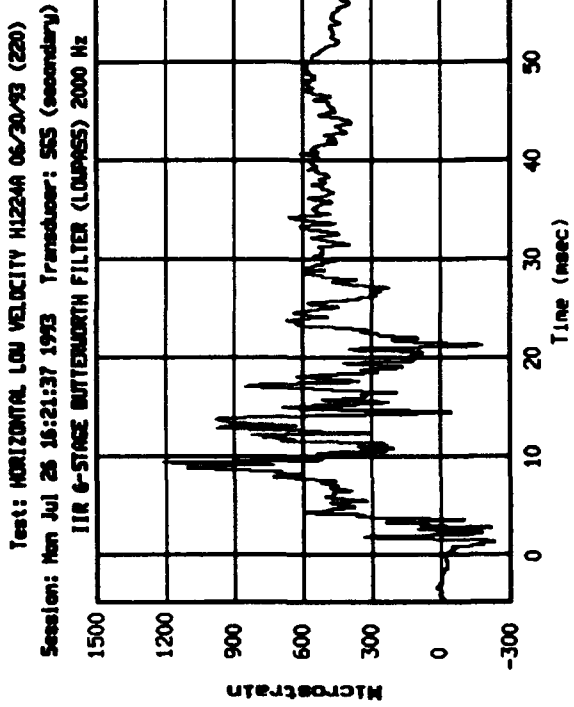
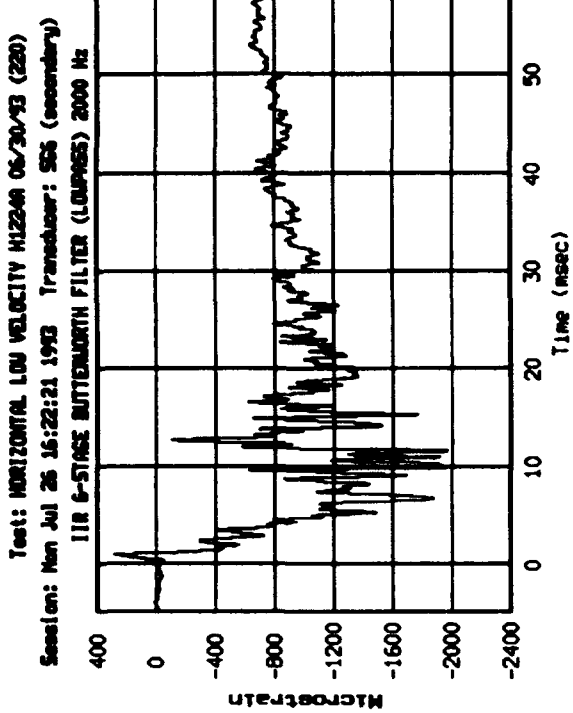
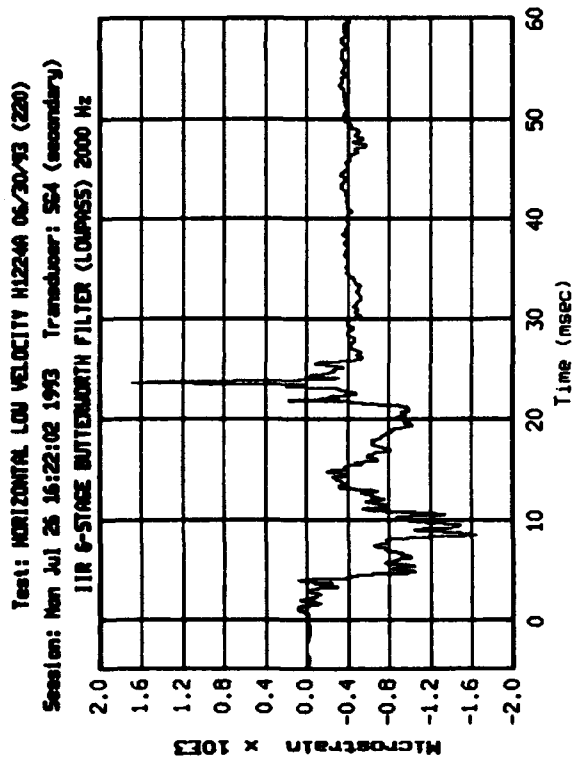


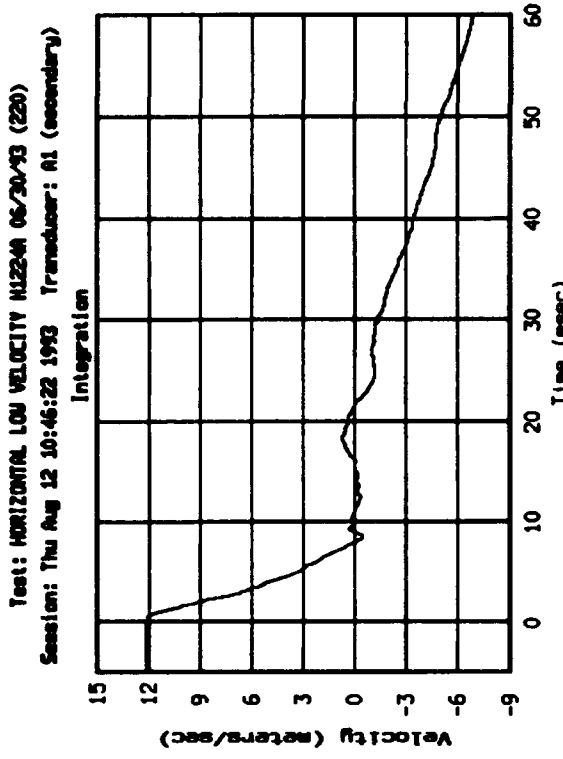
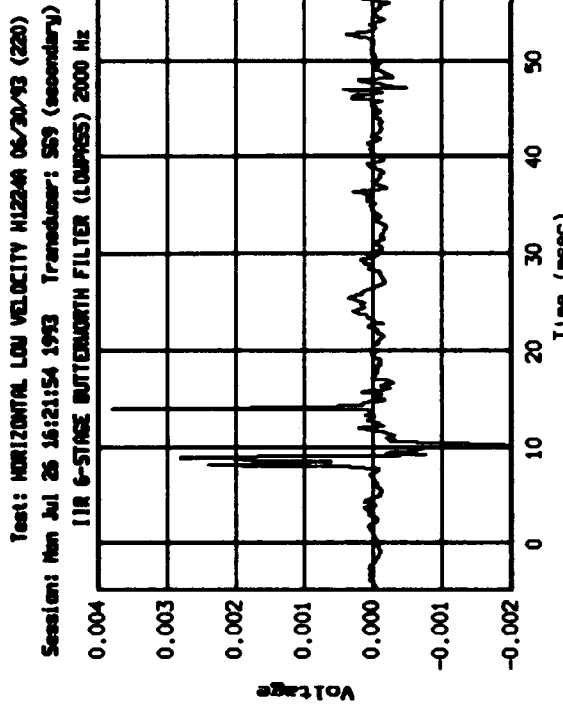
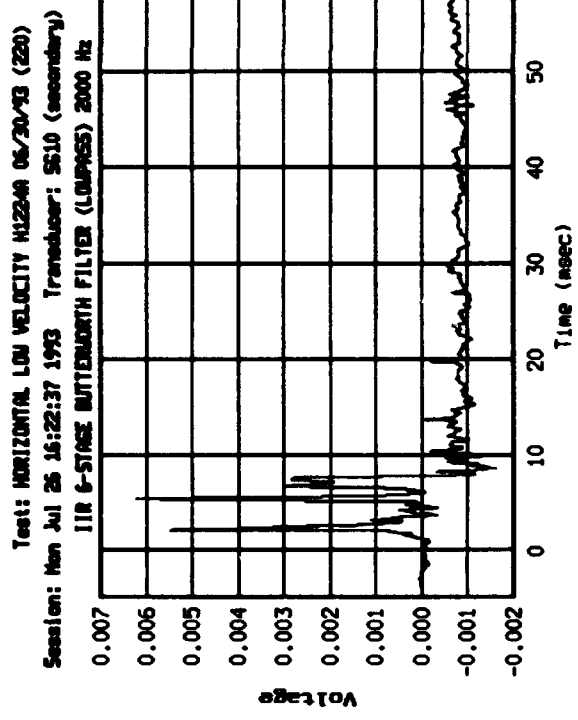
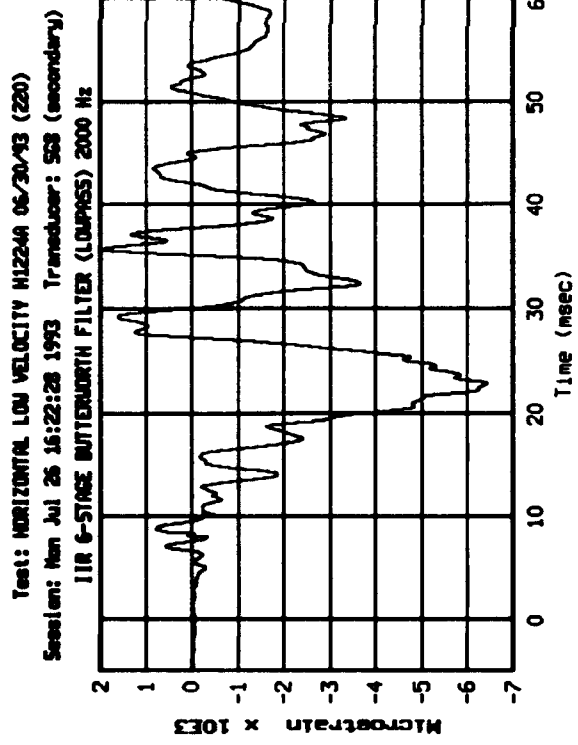


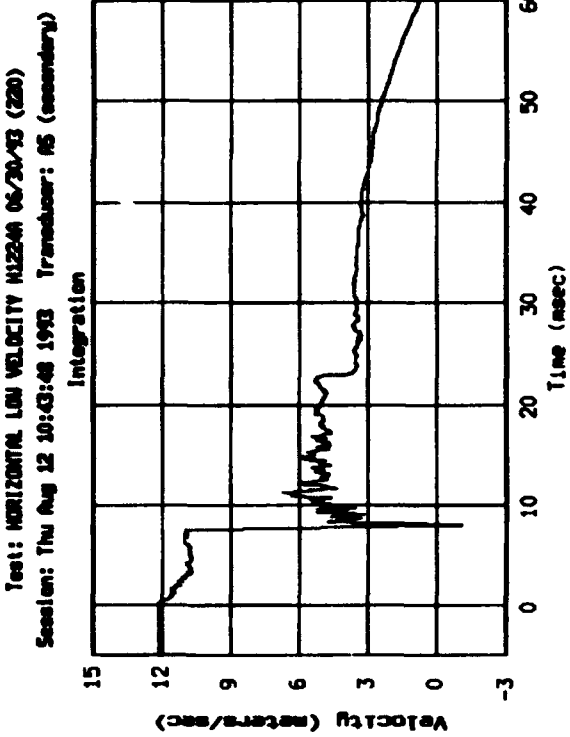
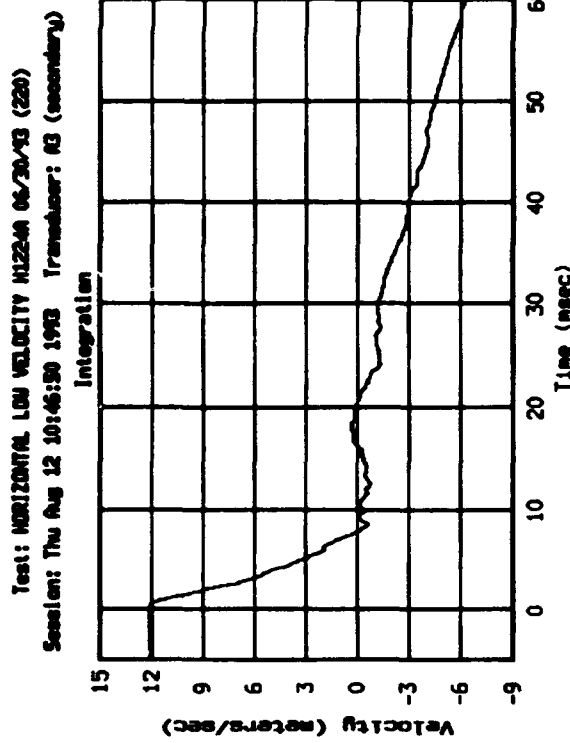
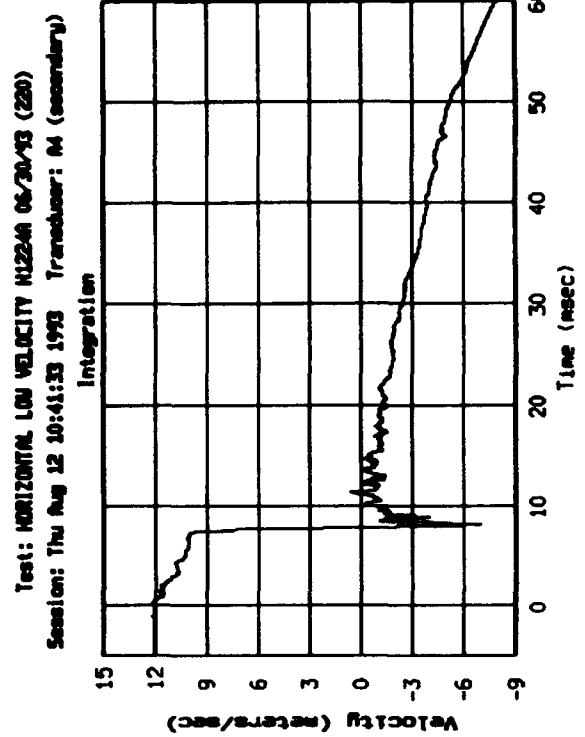
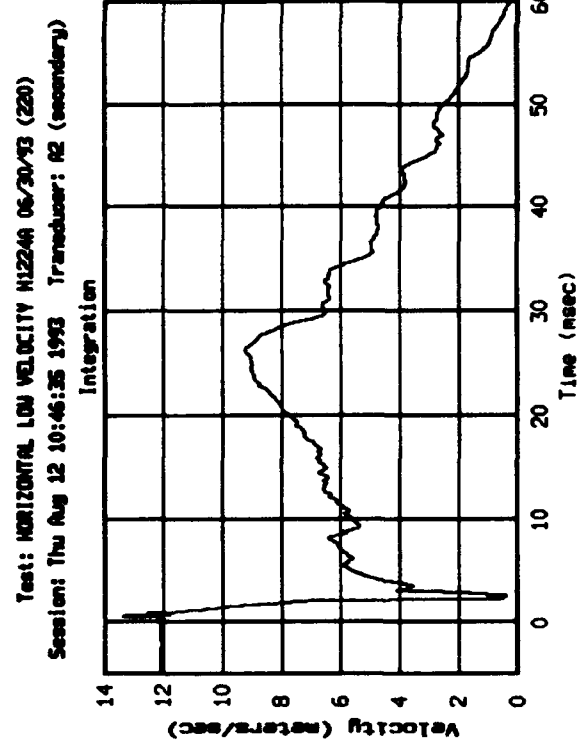


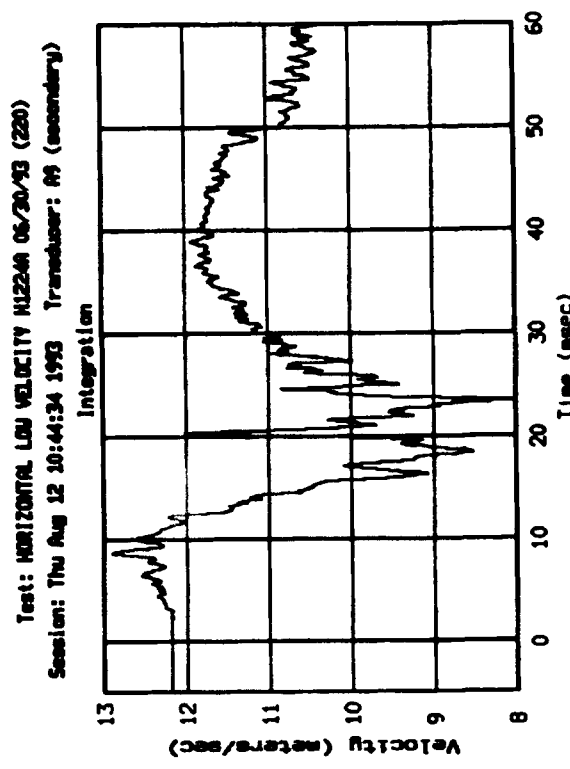
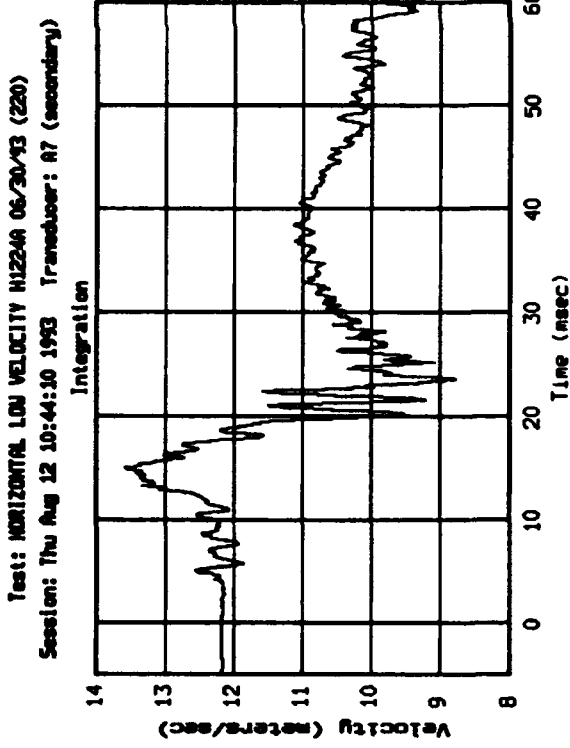
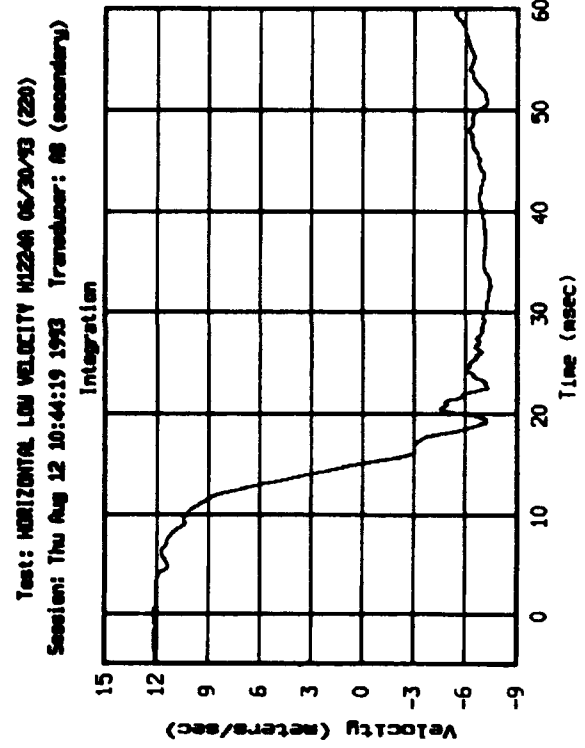
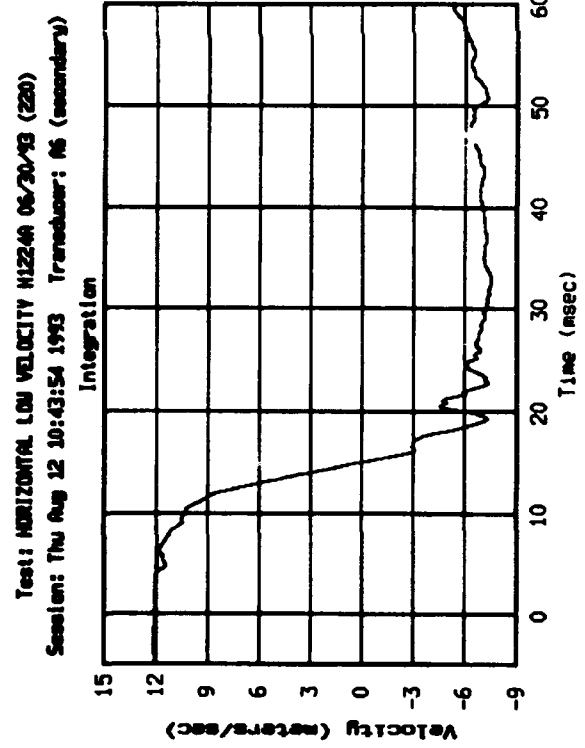


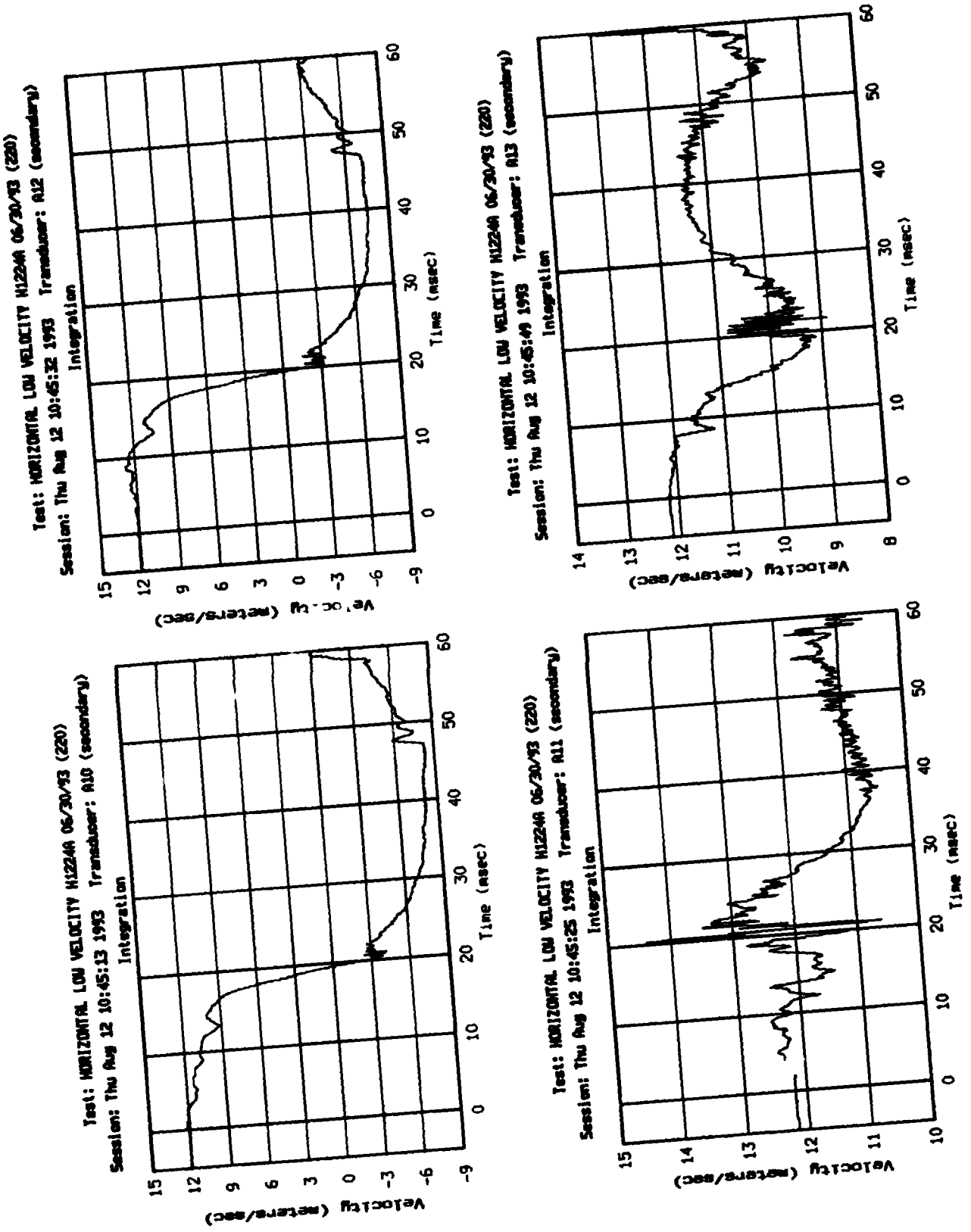


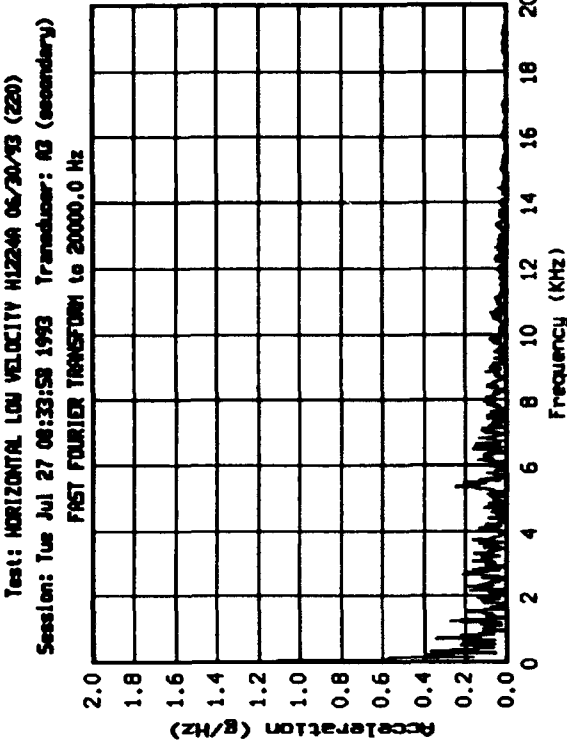
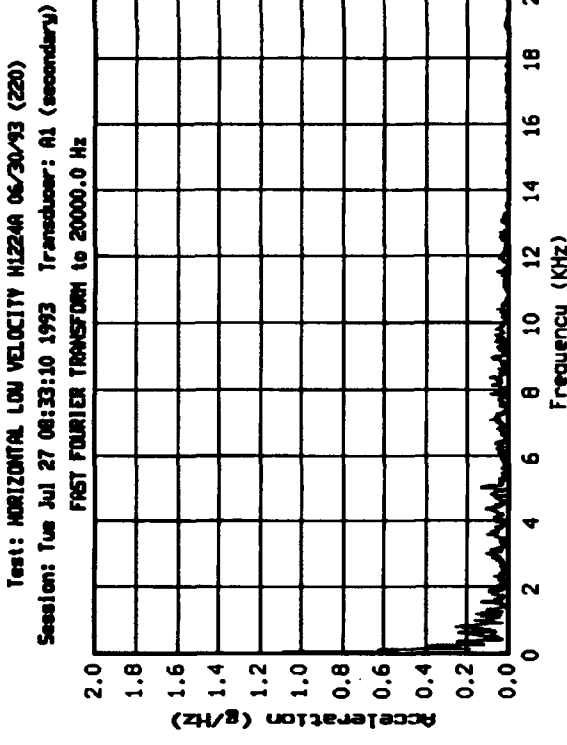
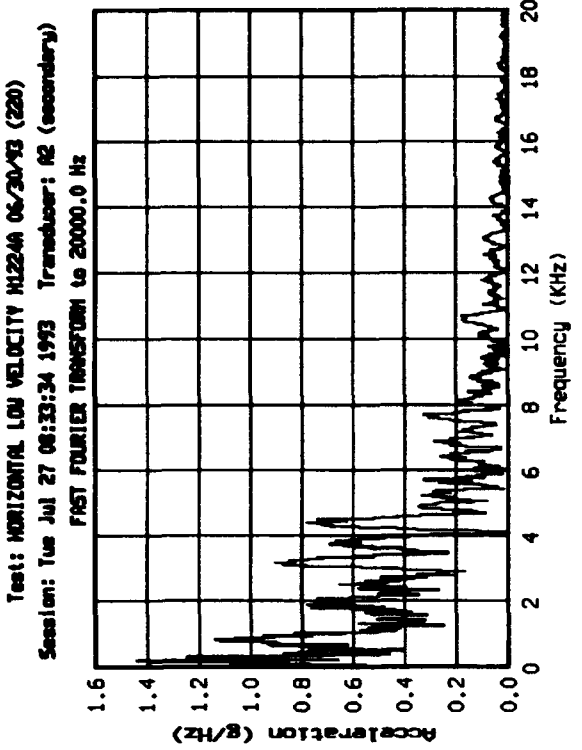
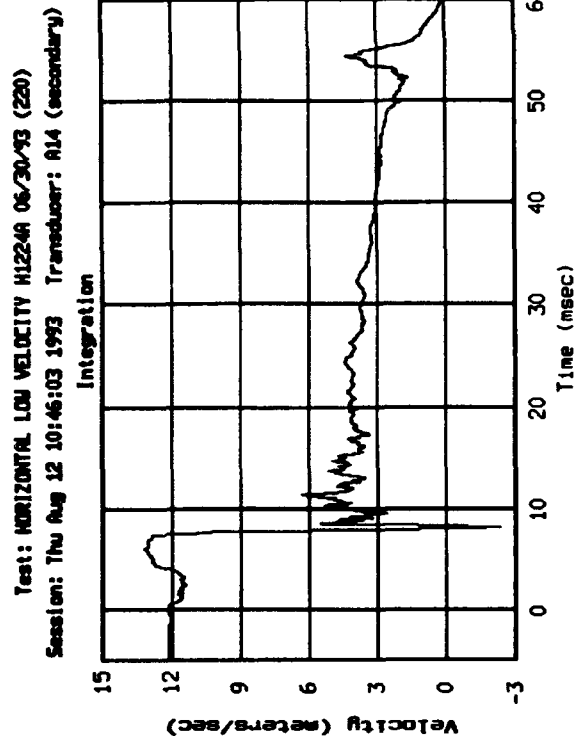


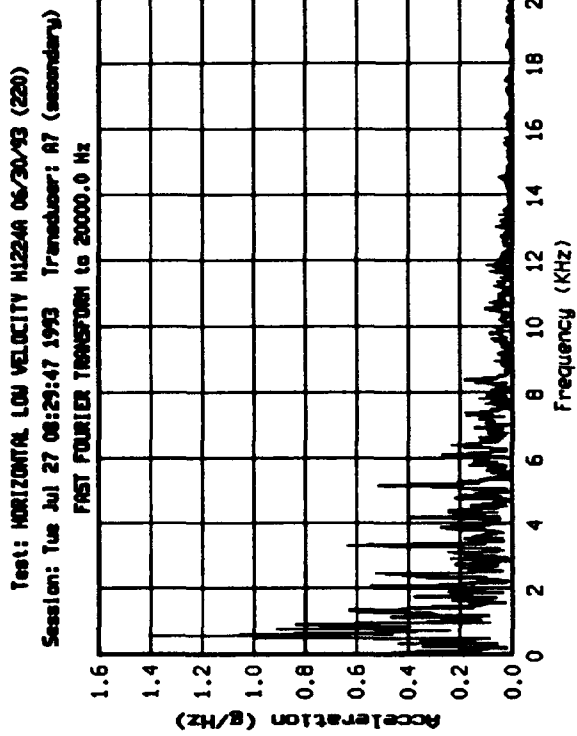
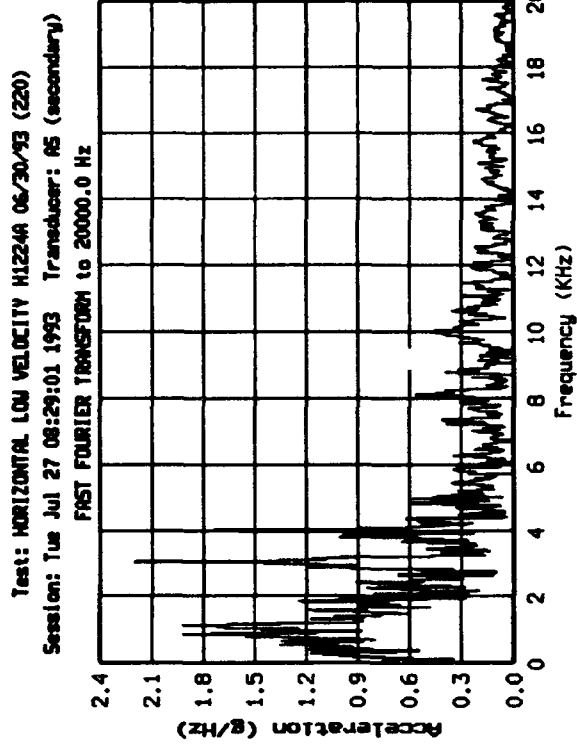
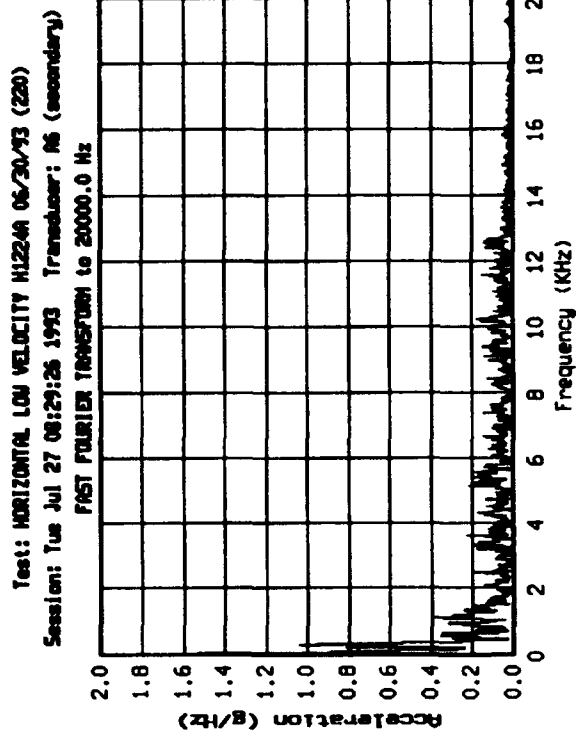
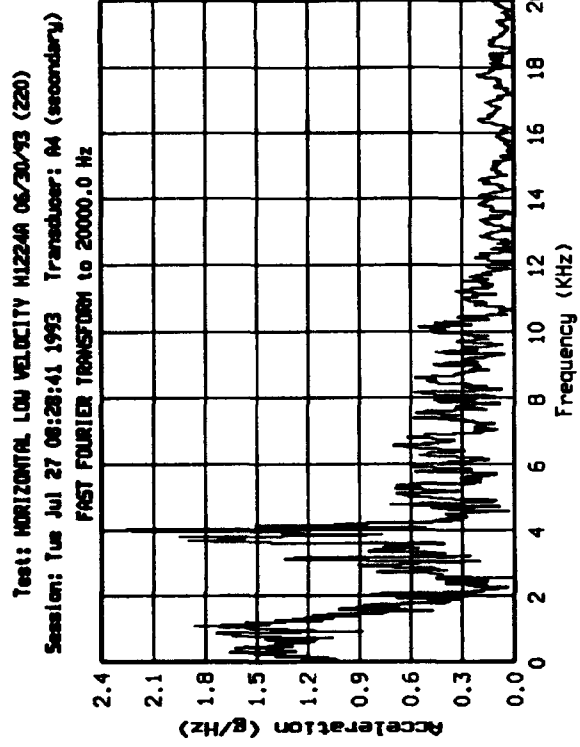


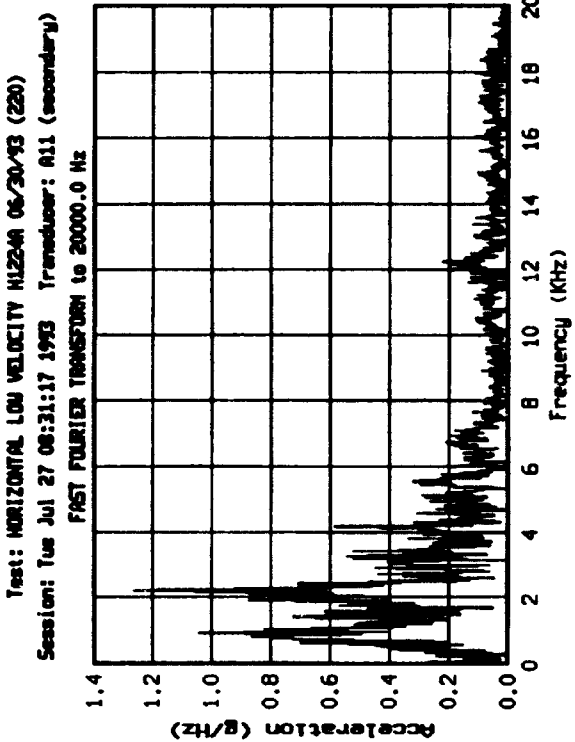
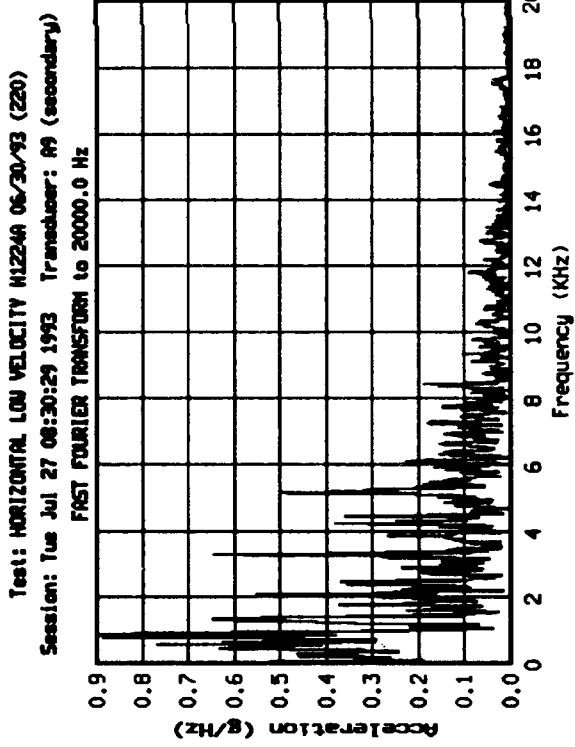
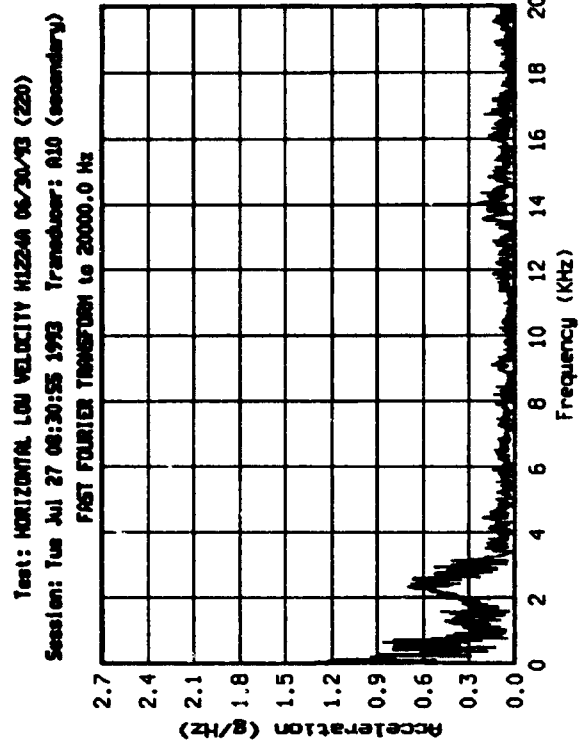
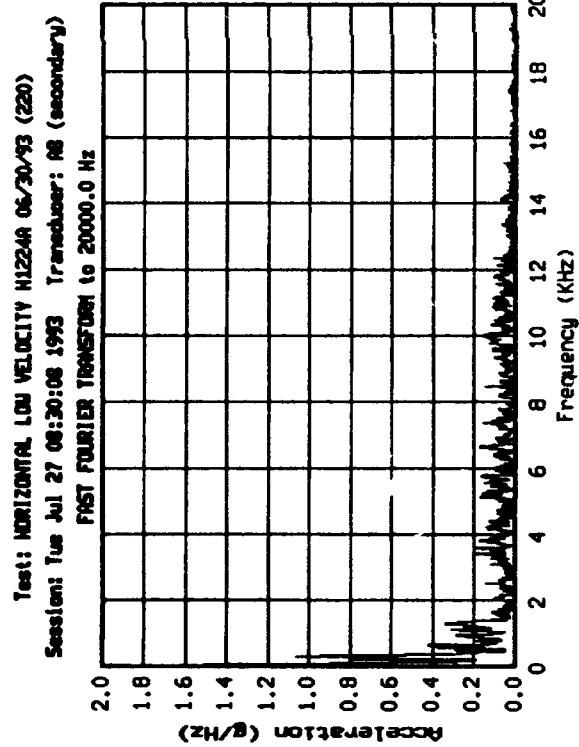


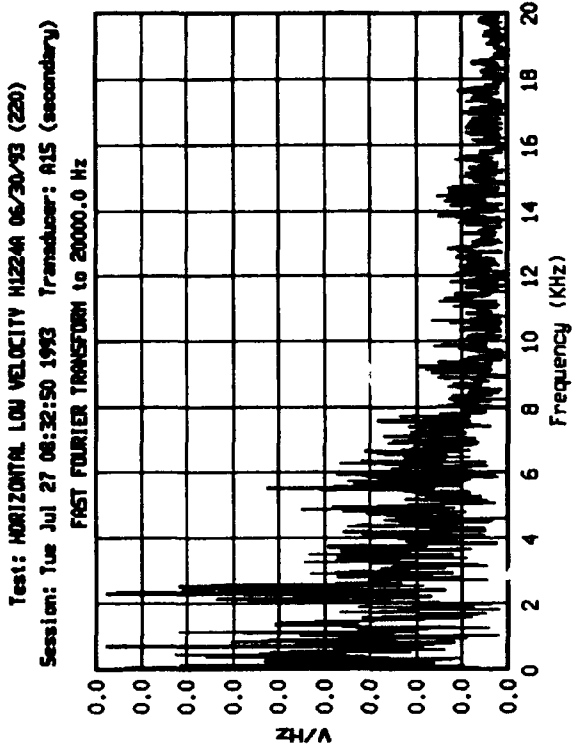
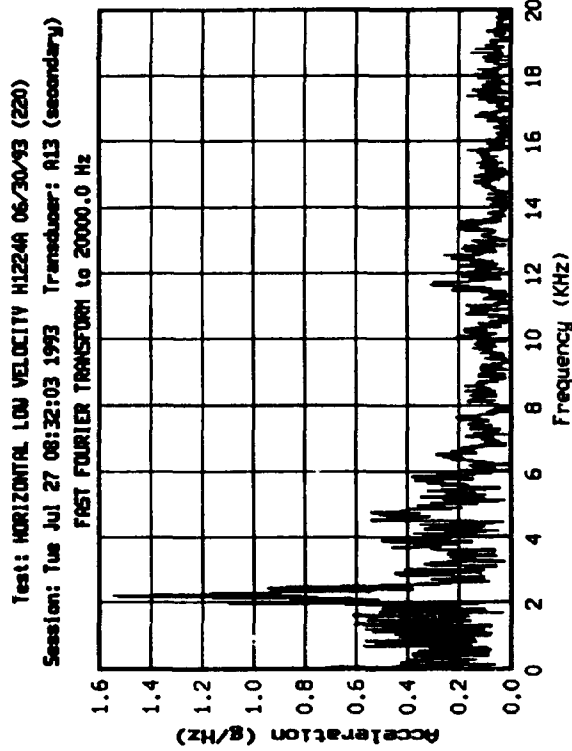
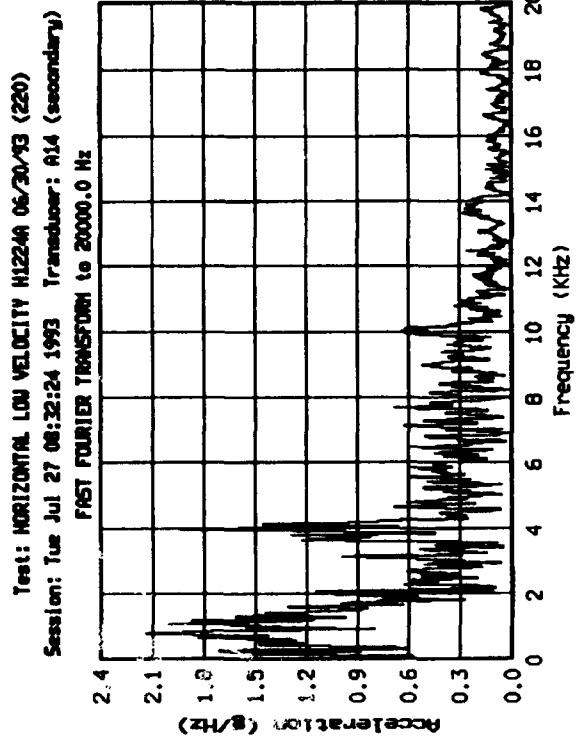
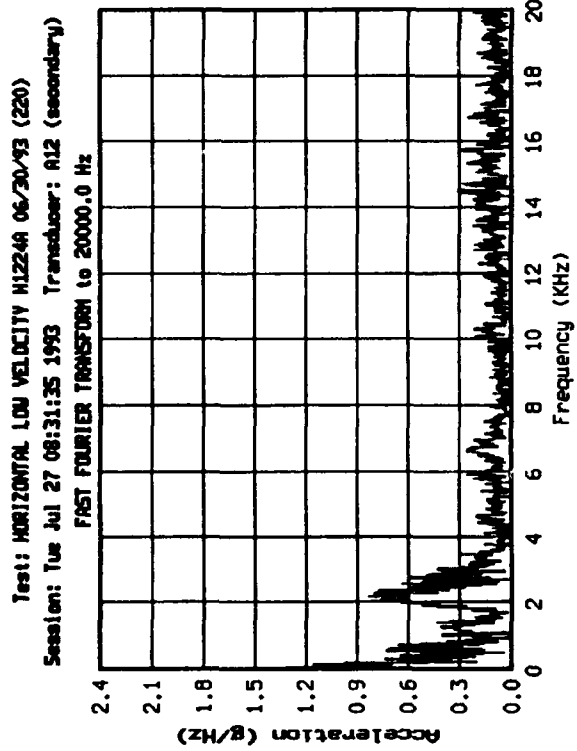


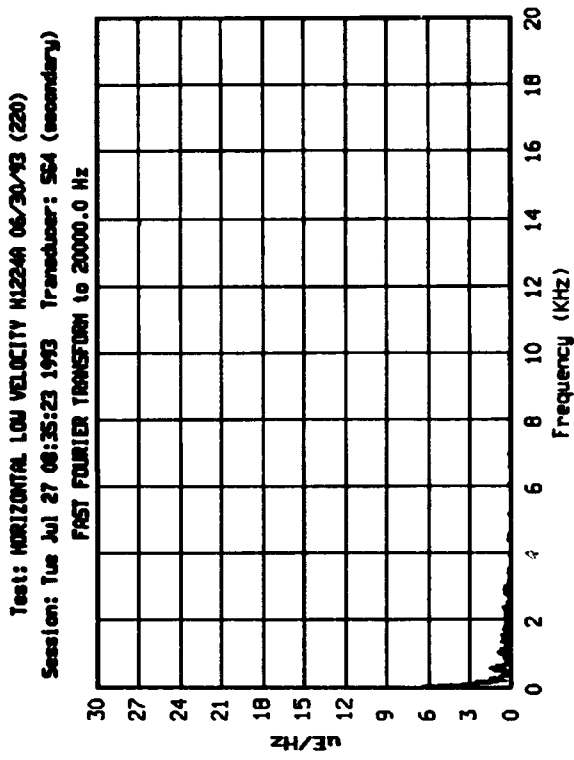
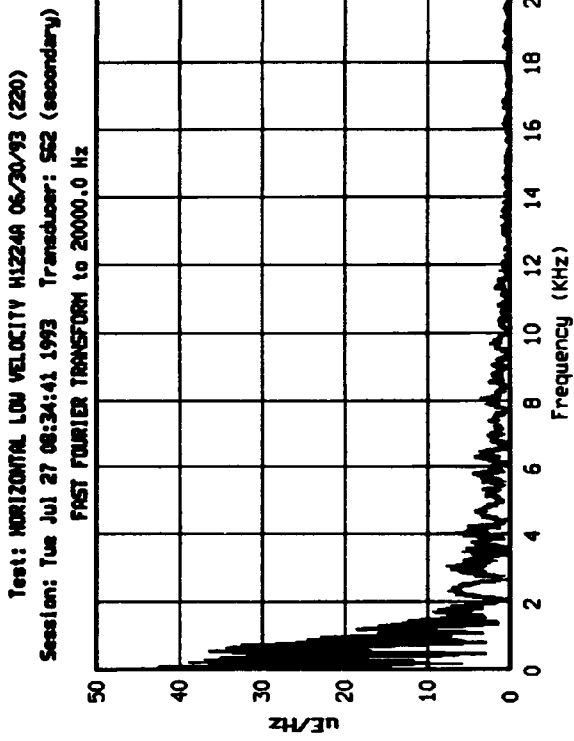
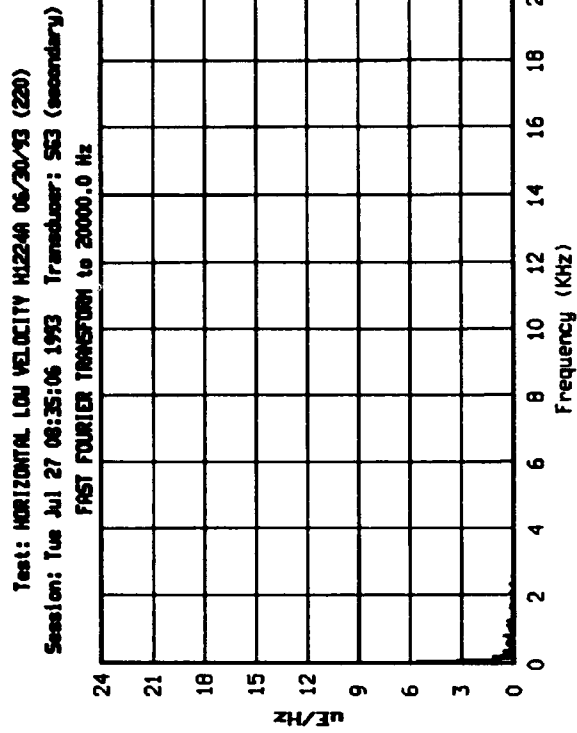
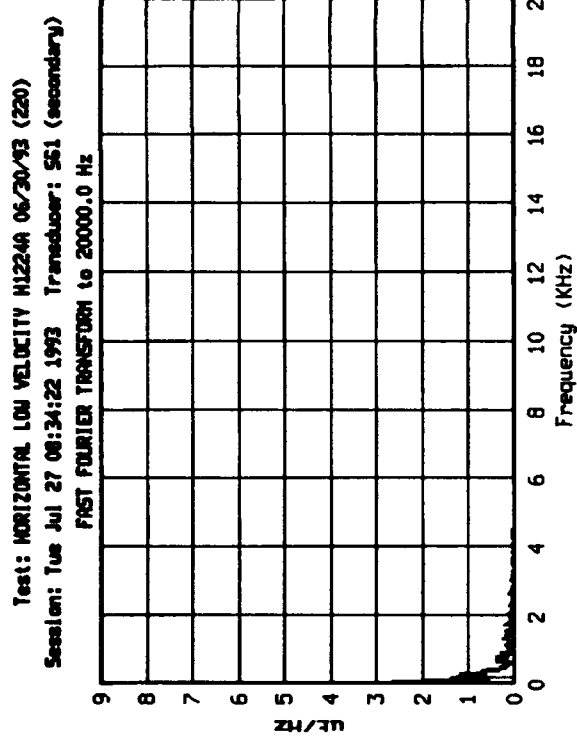


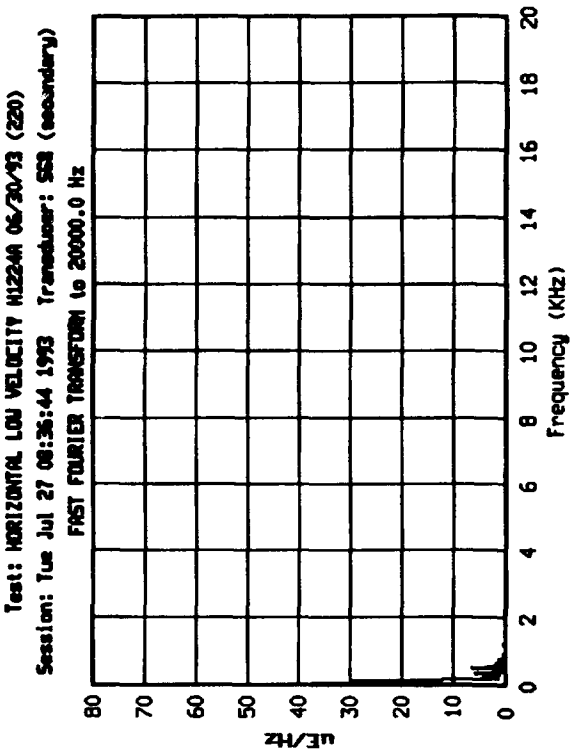
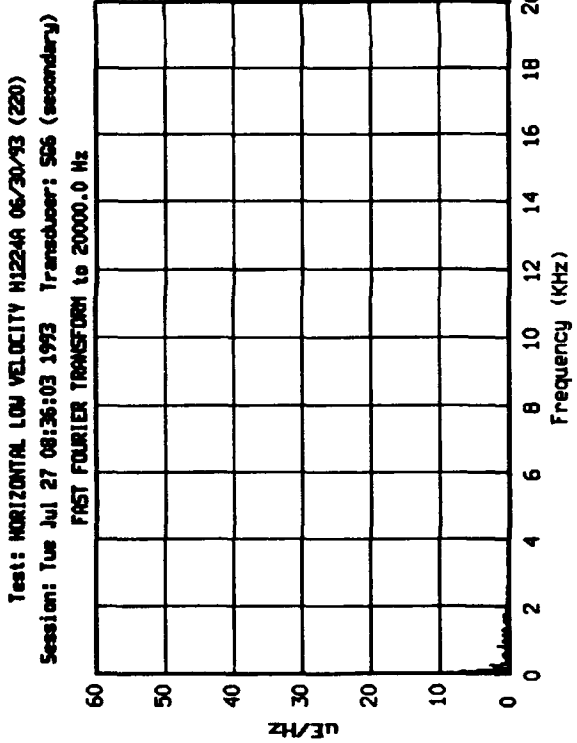
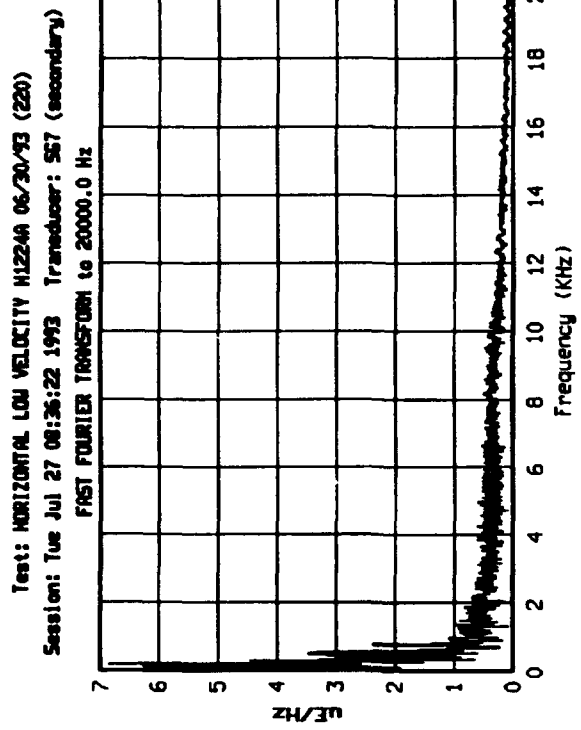
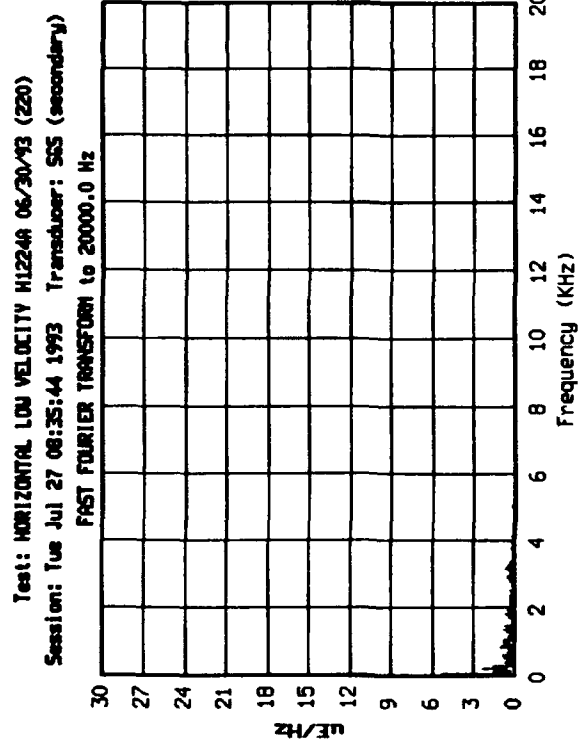


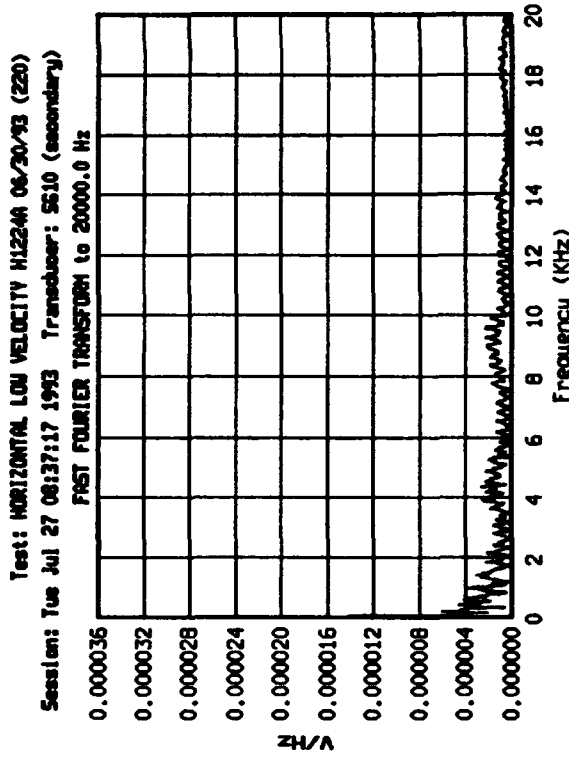
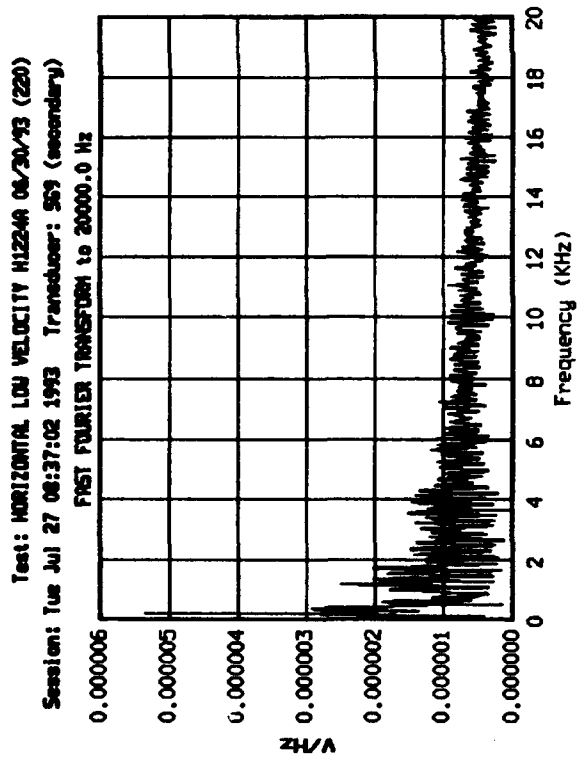






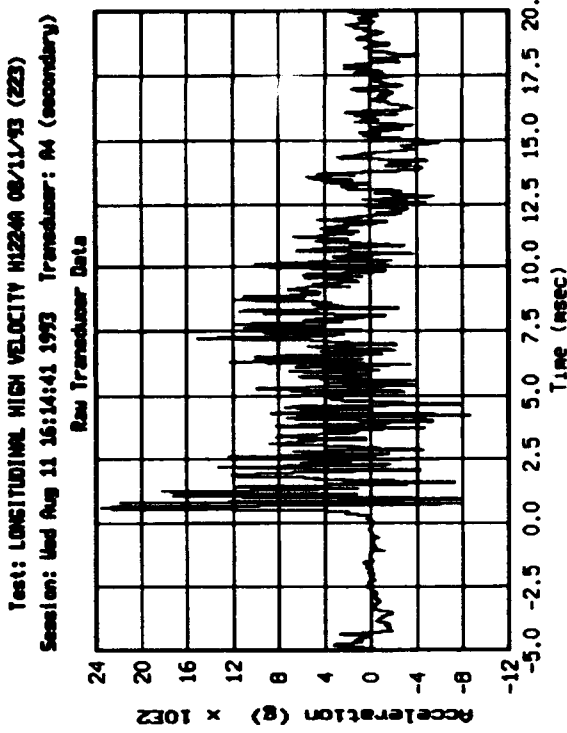
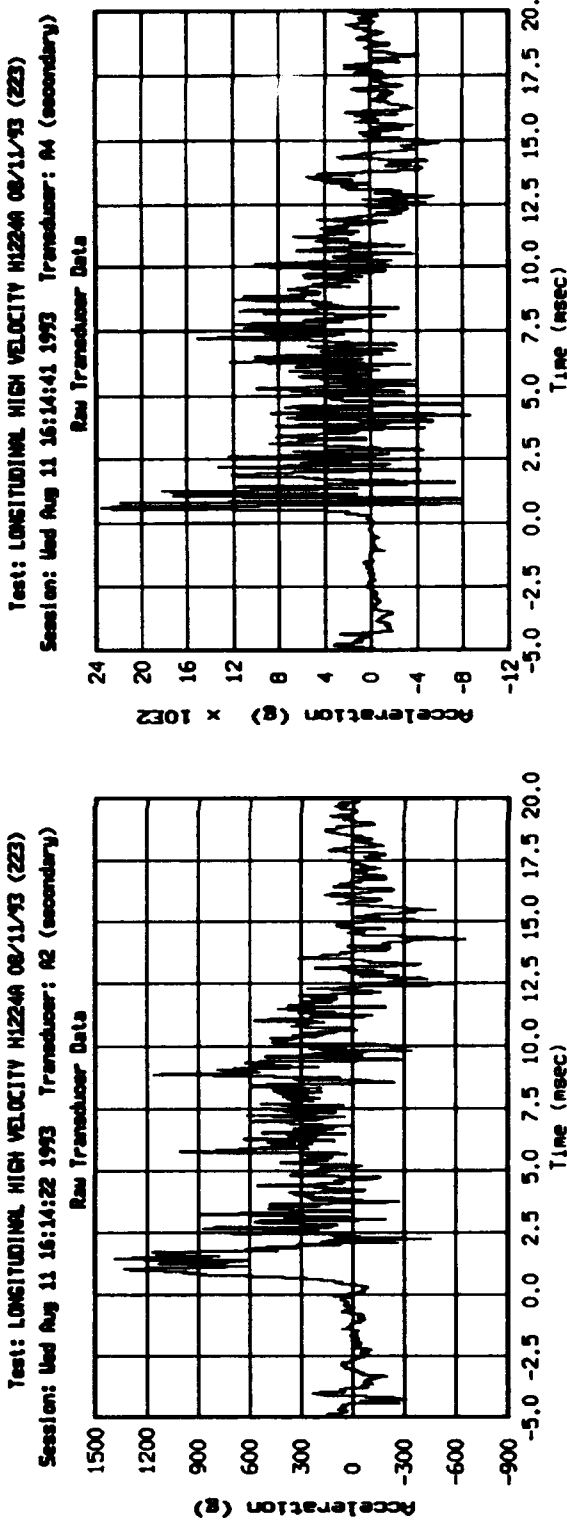
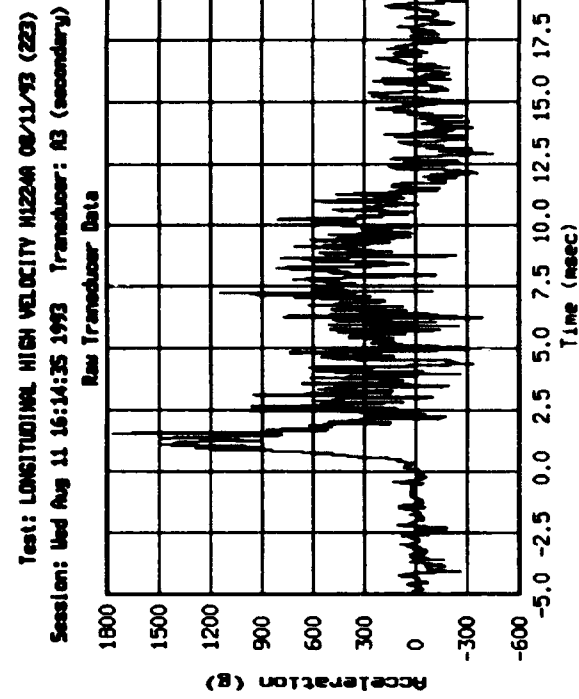
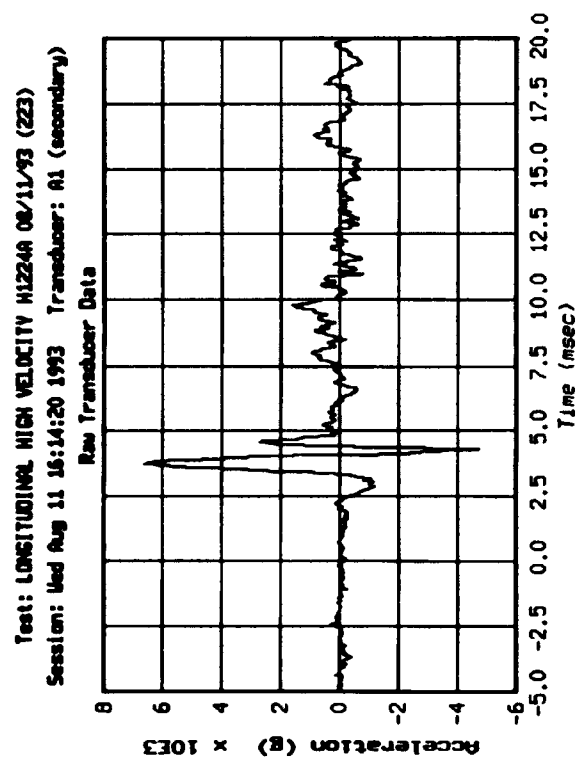


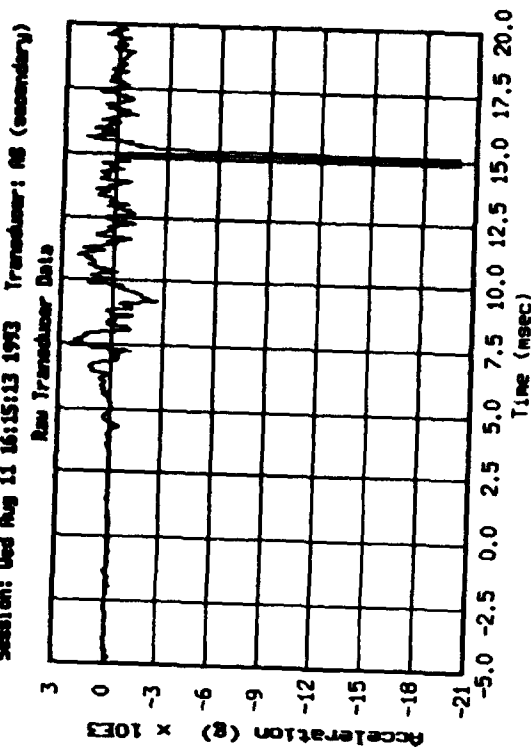
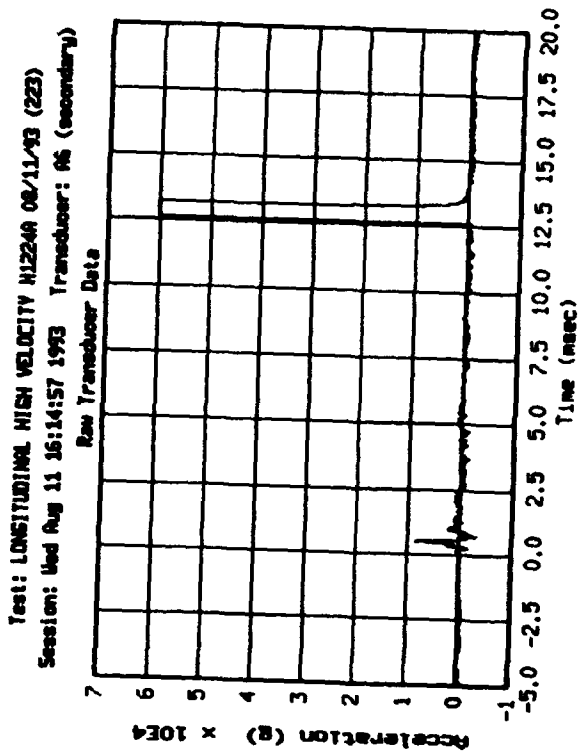
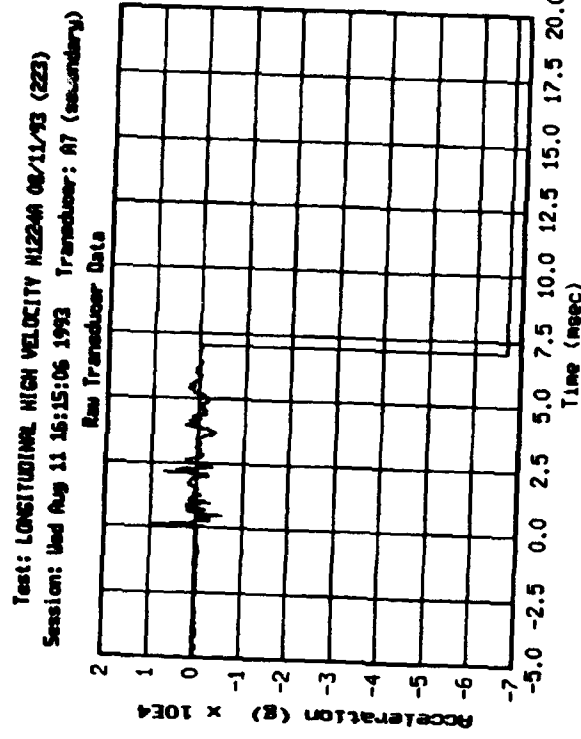
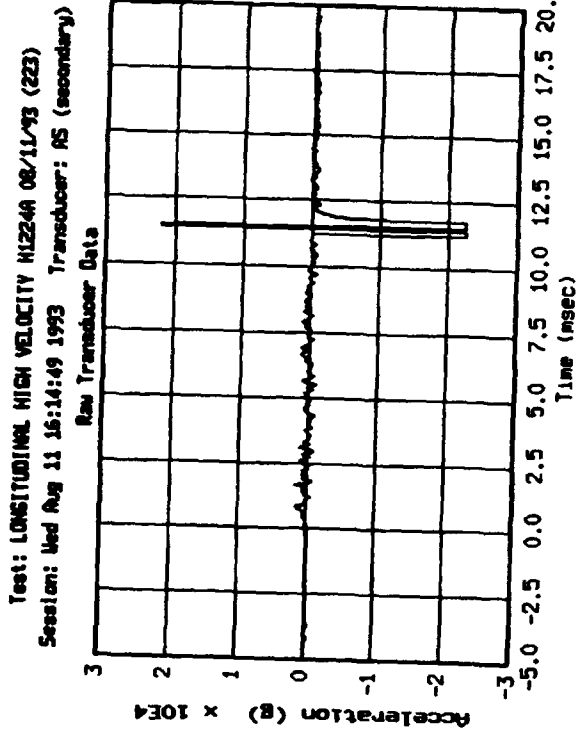


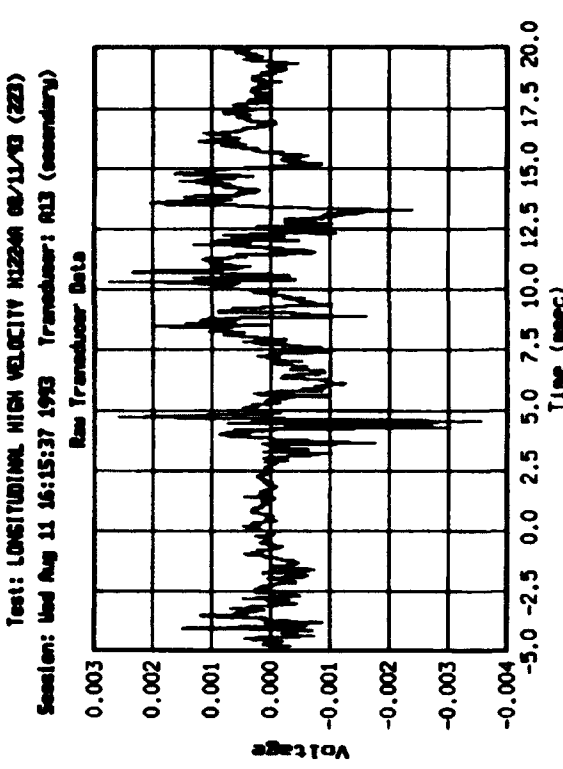
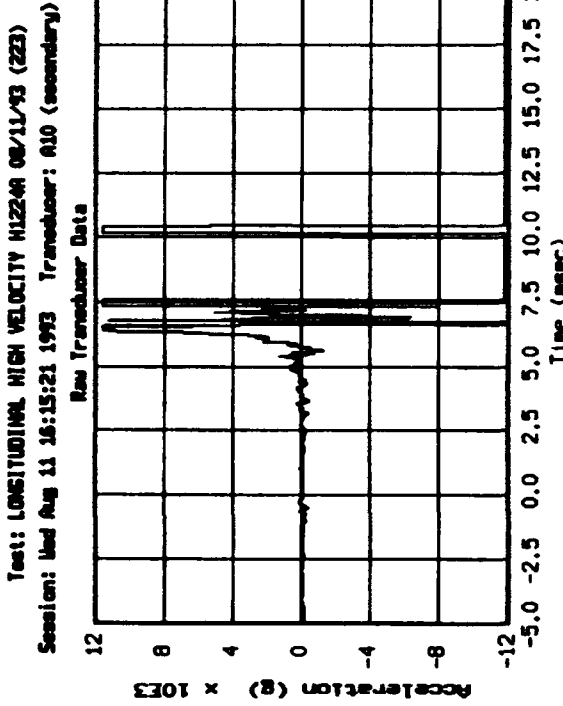
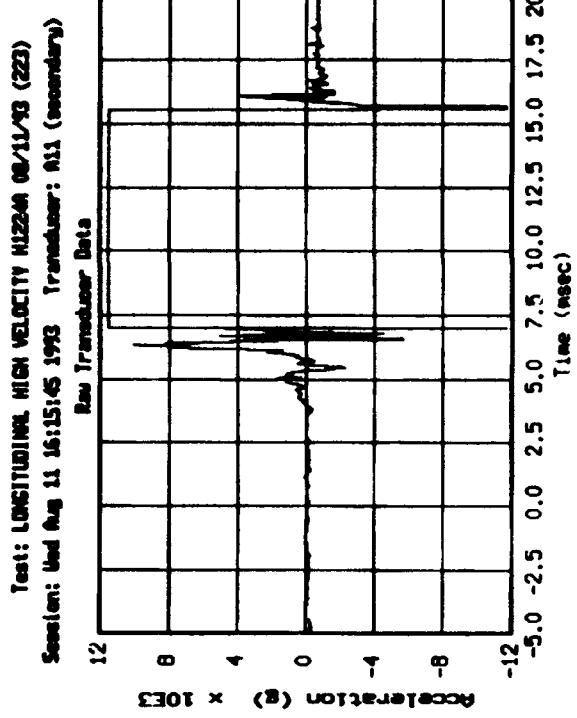
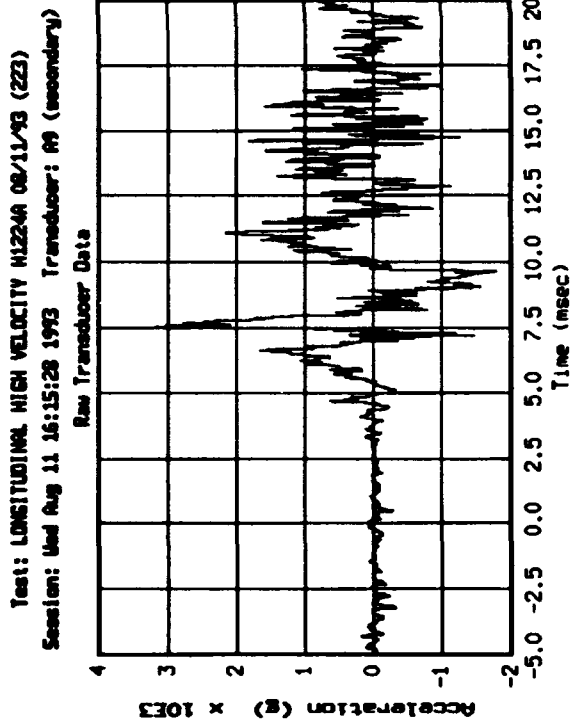


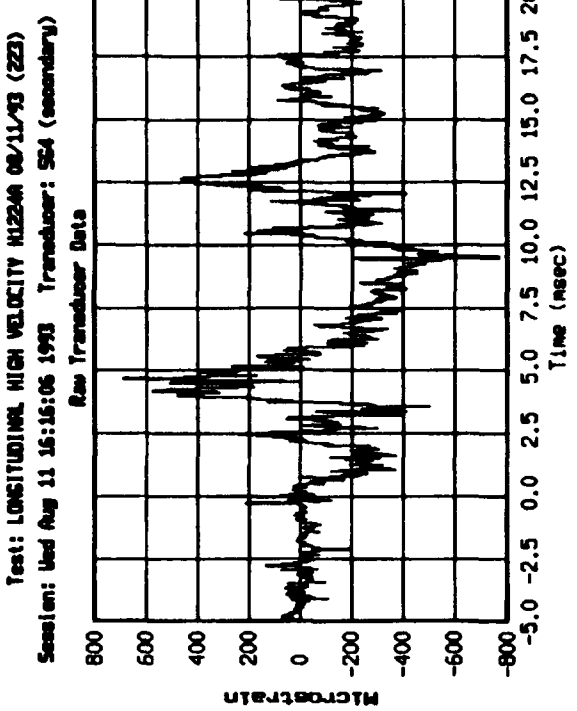
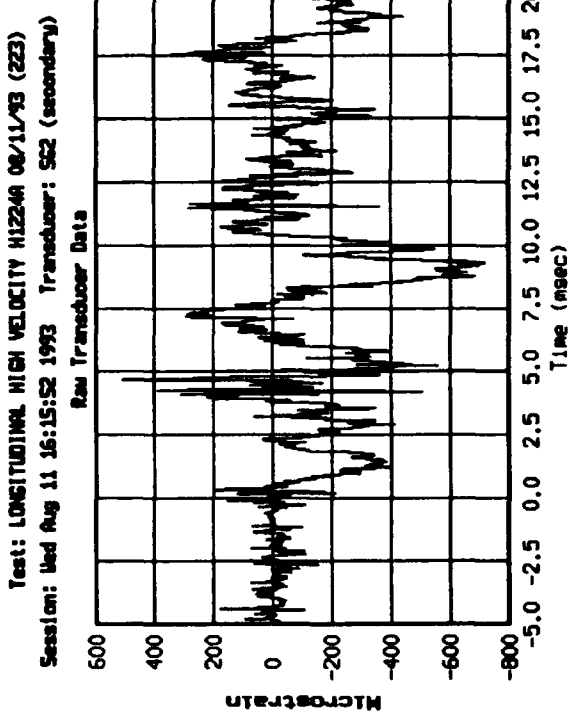
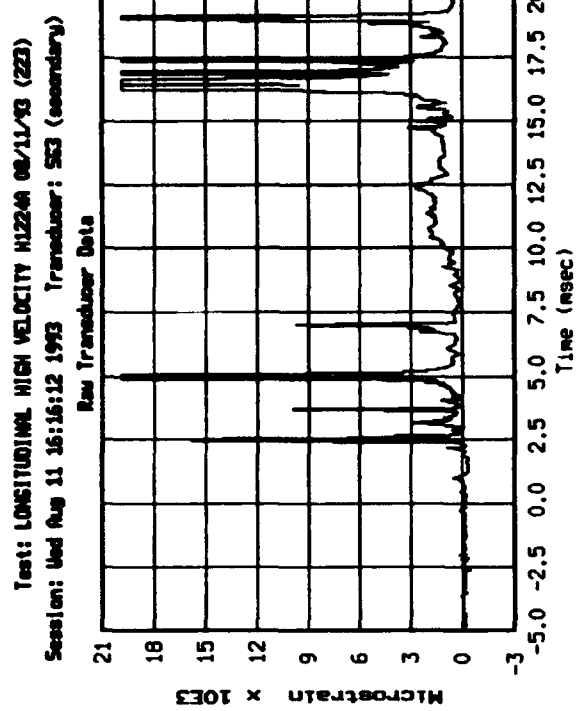
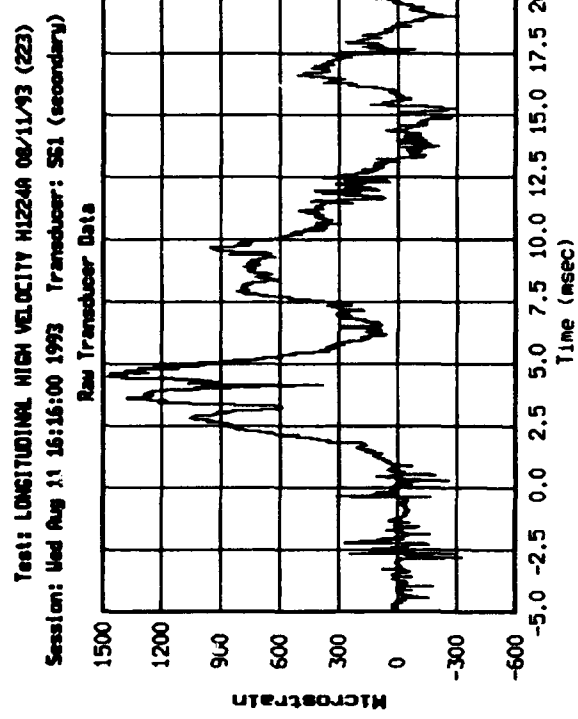
Appendix C. LHV Accelerometer and Strain Gage Data: Raw, Filtered, and Reduced

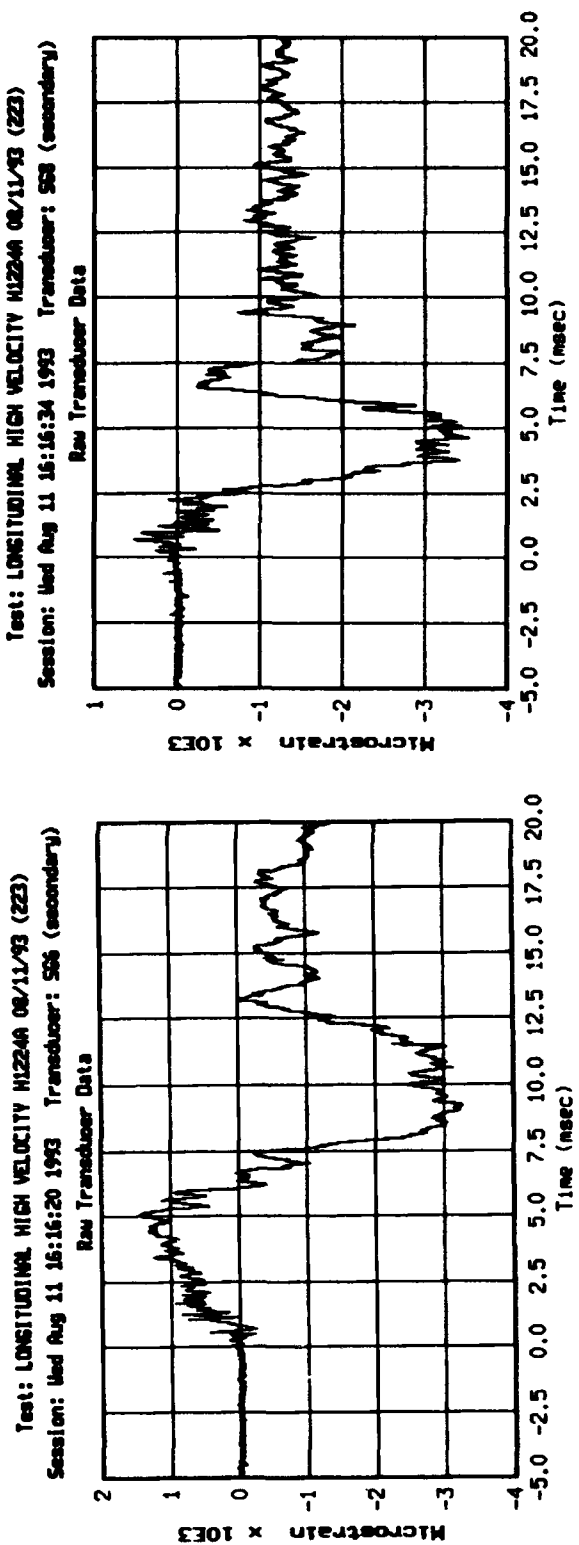
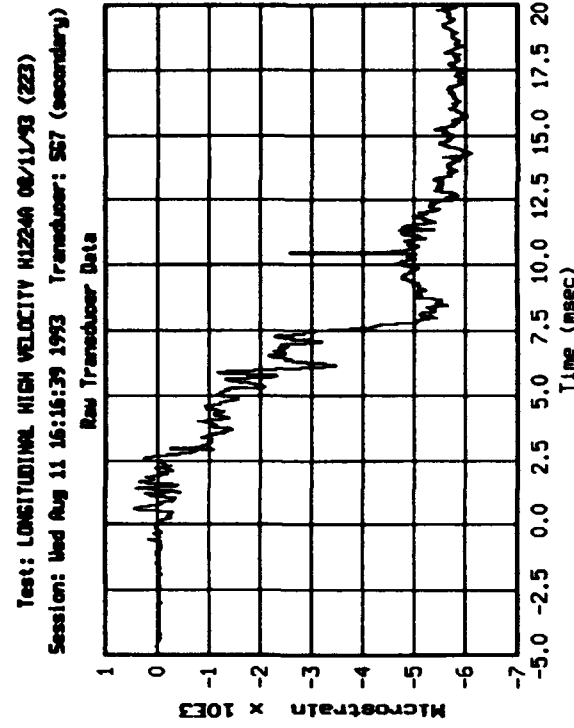
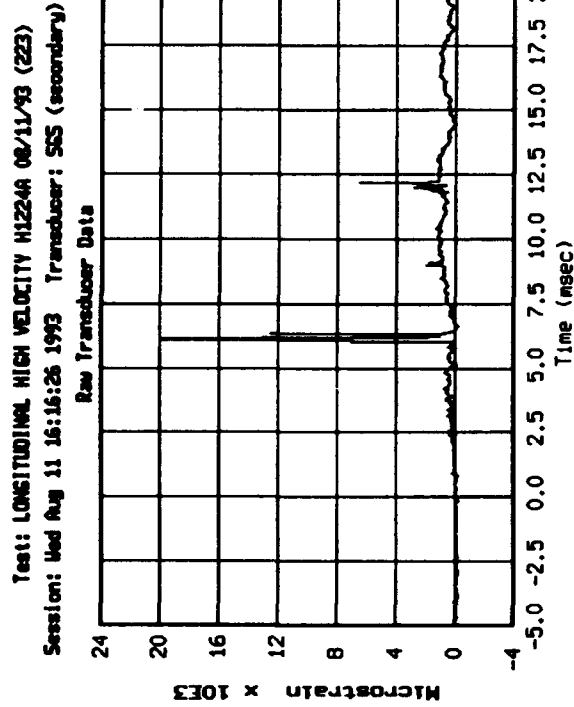
The following pages show raw (unfiltered) acceleration and strain gage data for the Longitudinal High-Velocity (LHV) impact test. Following this raw data are plots of filtered data (using a low-pass Butterworth 6-stage filter) with cutoff frequencies of 250 Hz and 2,000 Hz. Integrated acceleration data, yielding velocity versus time plots, are presented to analyze kinetic energy values during the test. And finally, Fast Fourier Transforms (FFTs) for each raw data channel are included to analyze acceleration and strain amplitudes in the frequency domain.

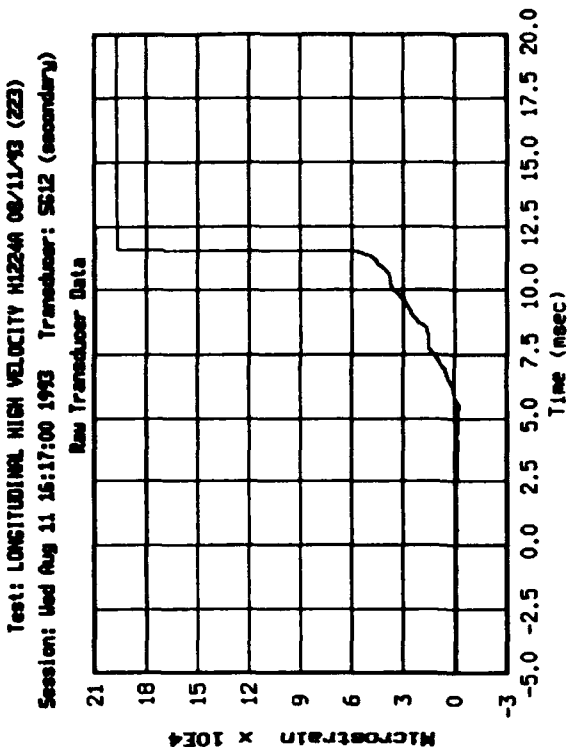
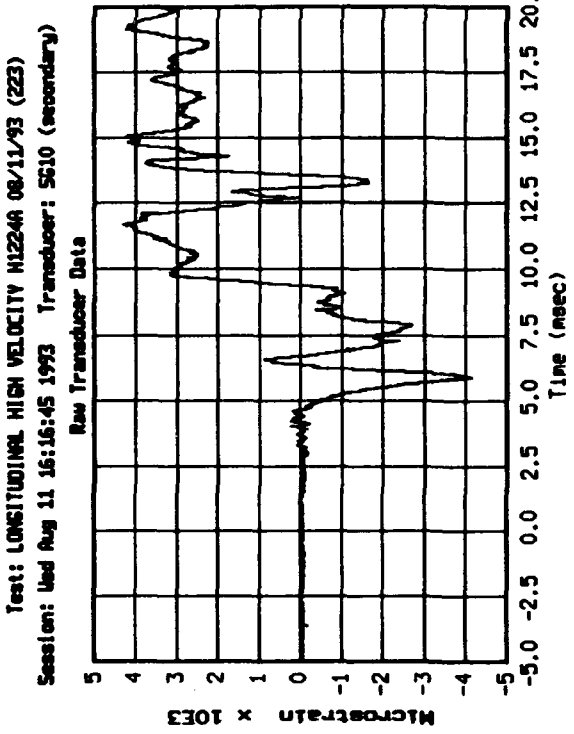
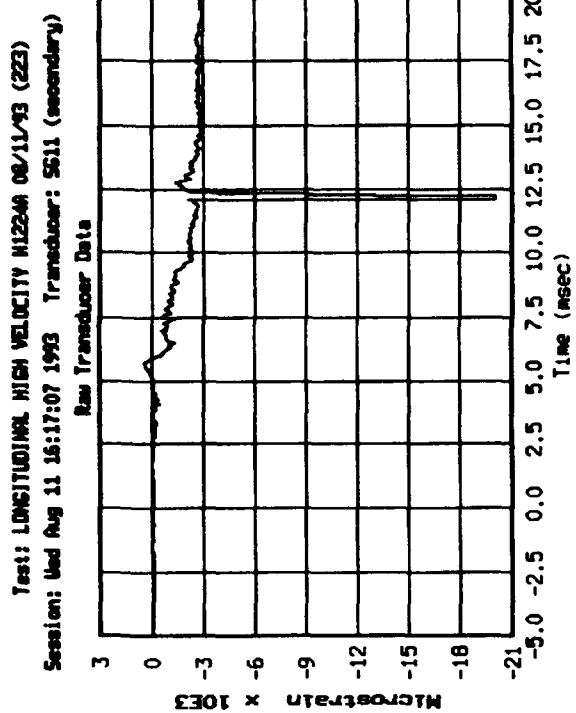
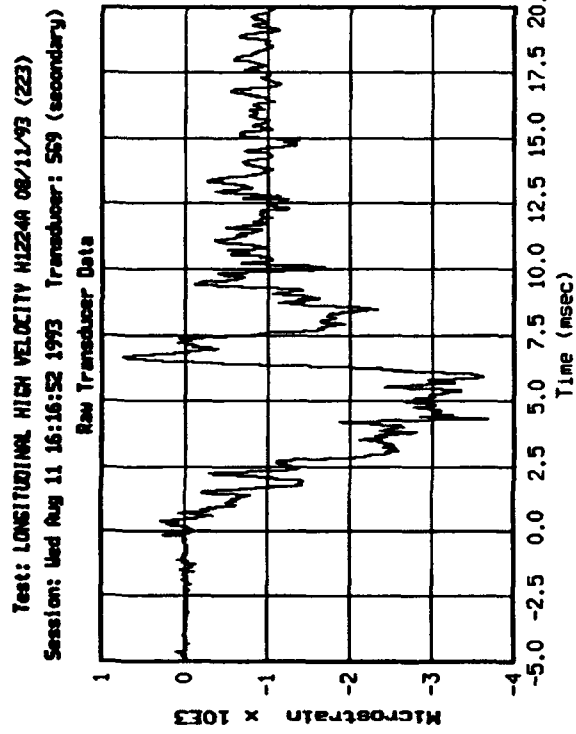


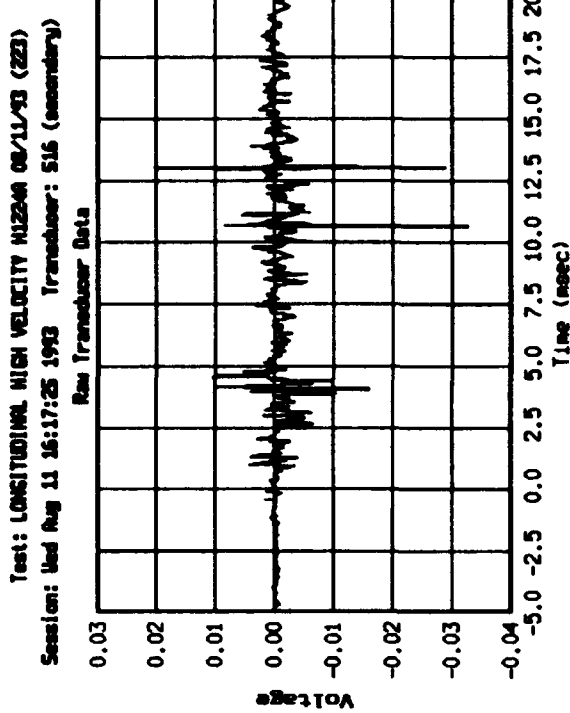
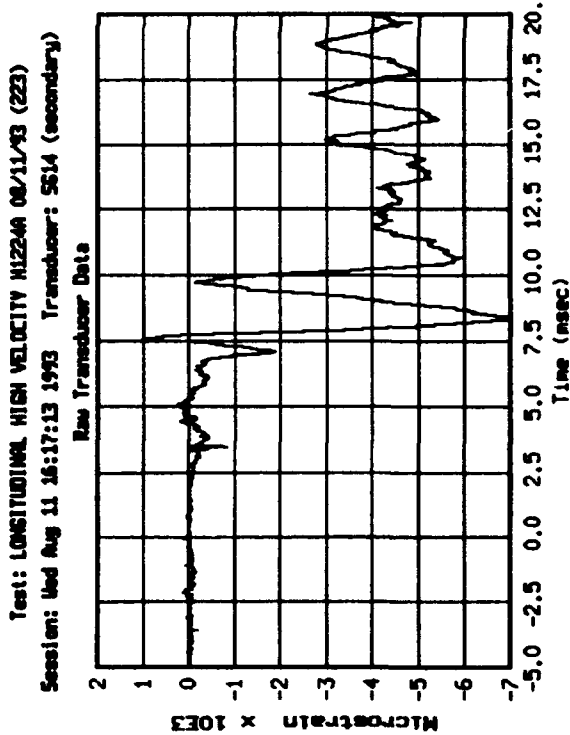
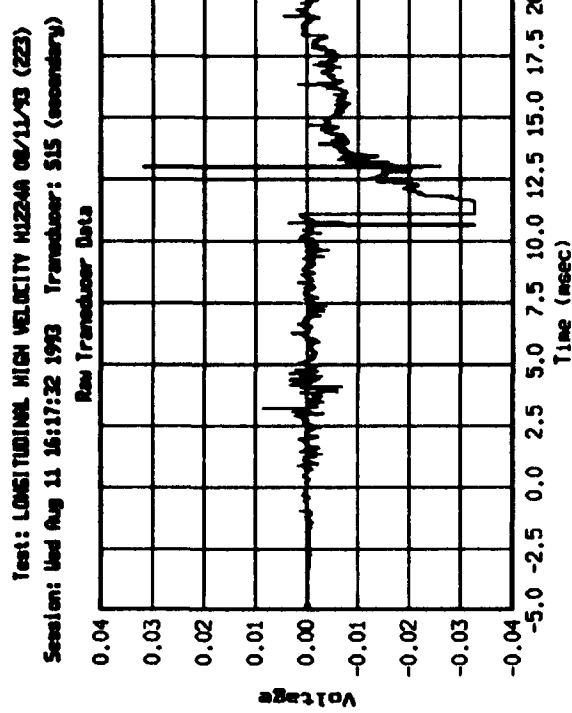
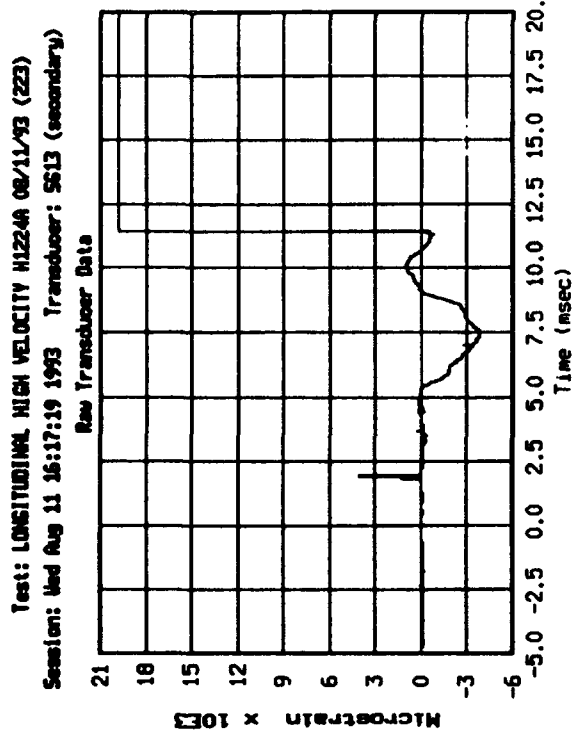


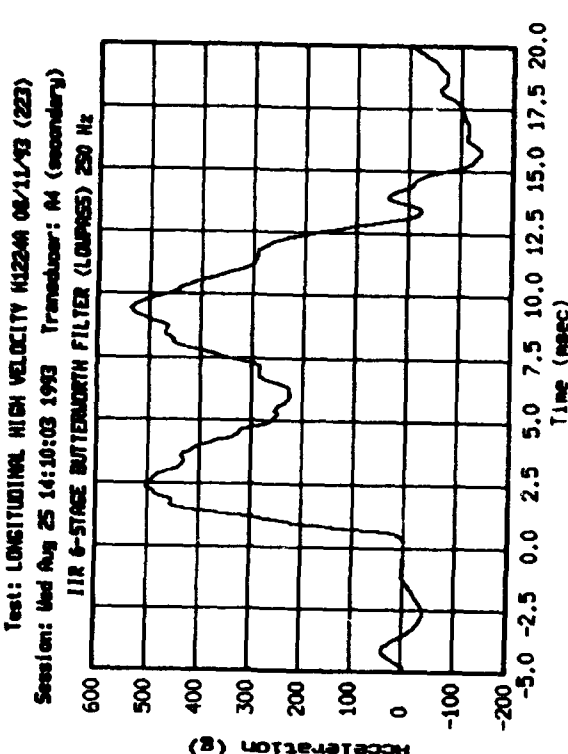
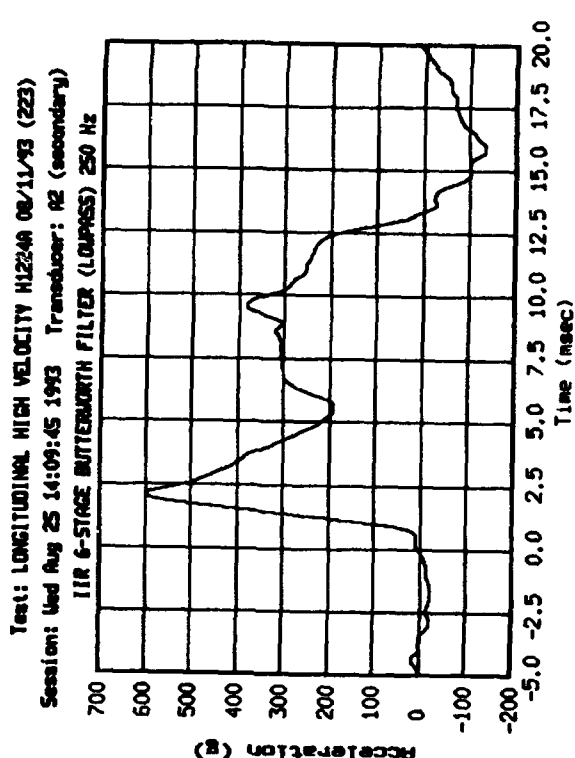
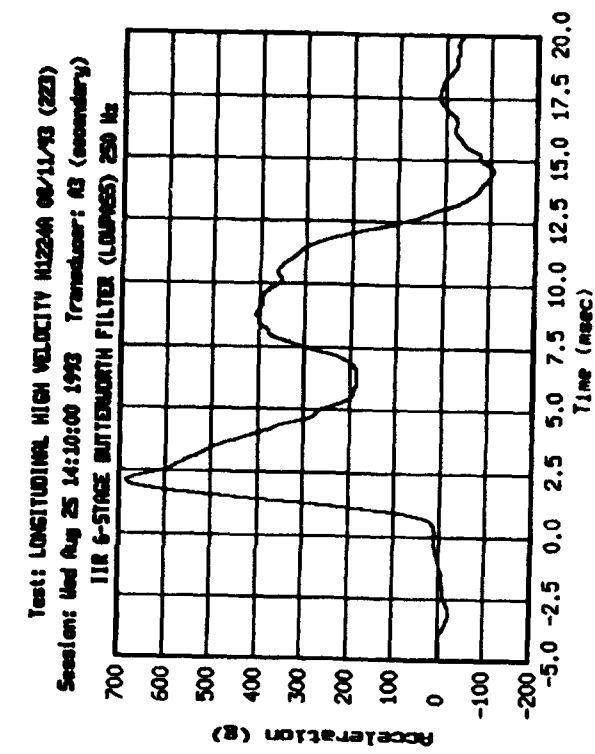
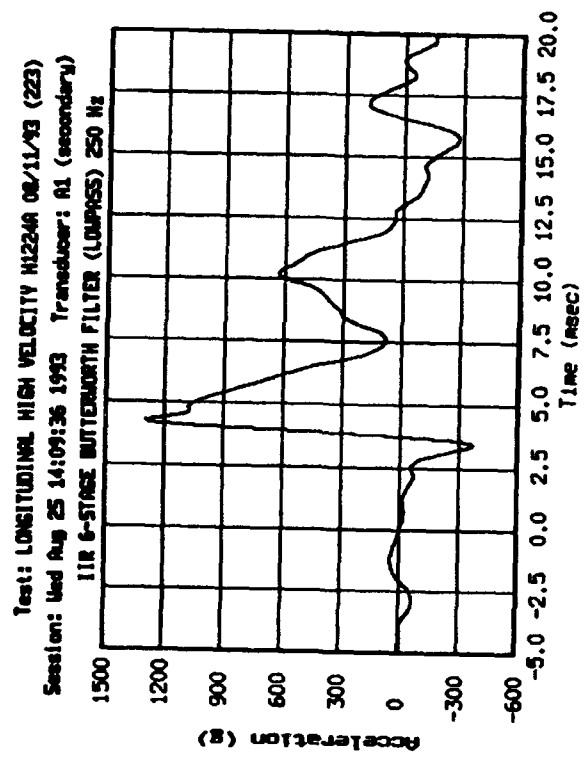


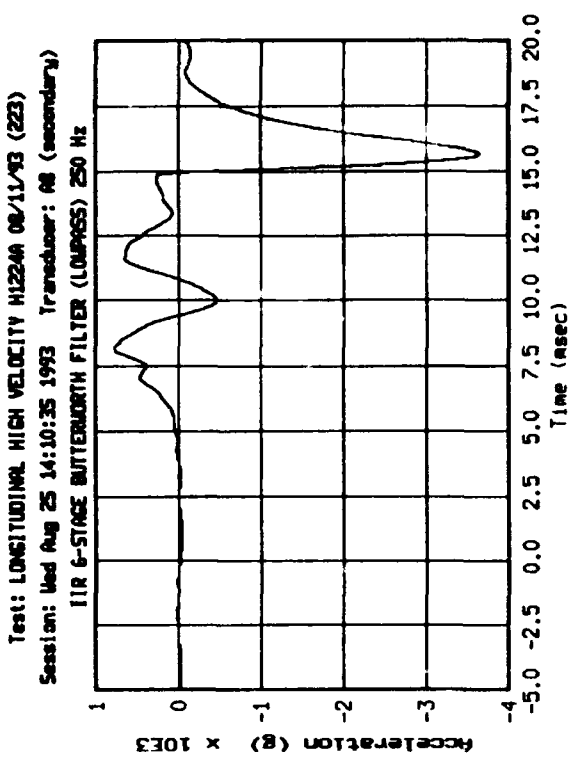
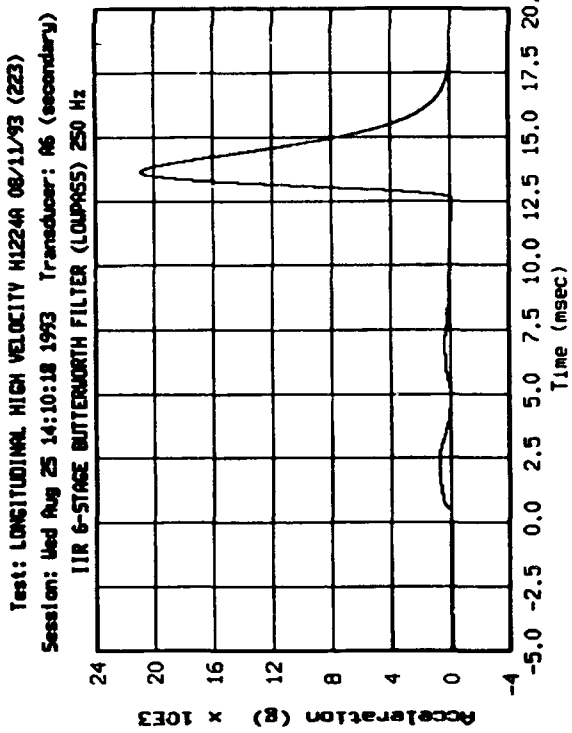
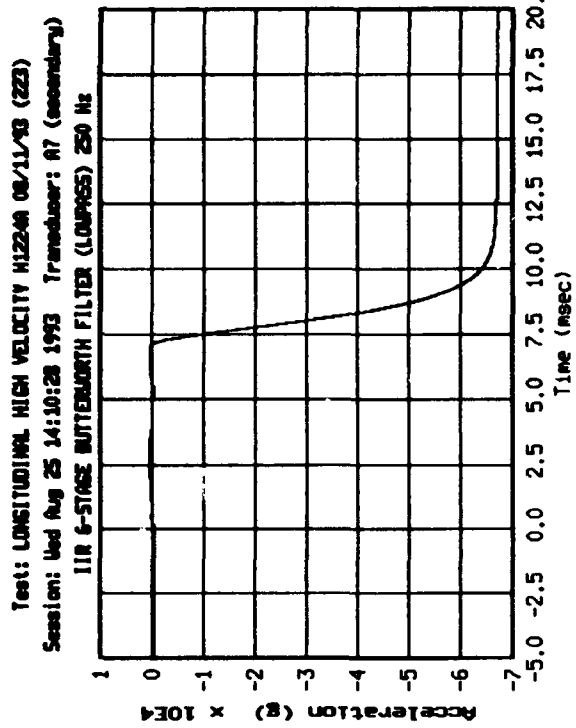
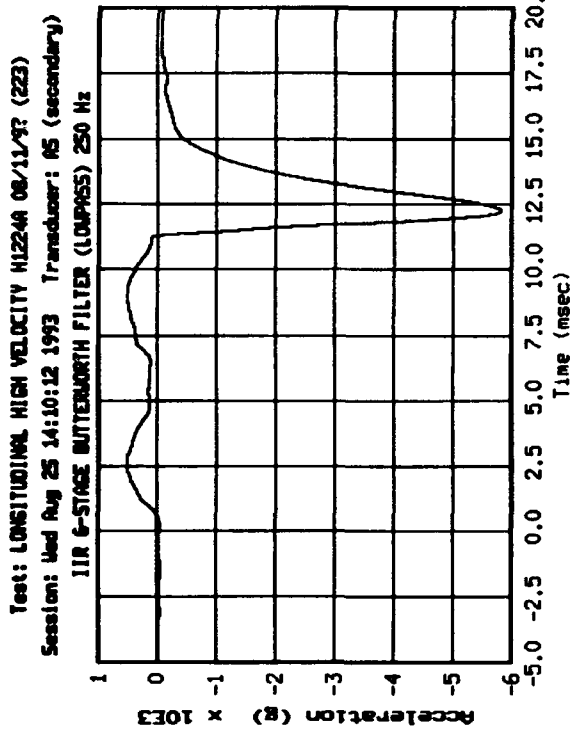


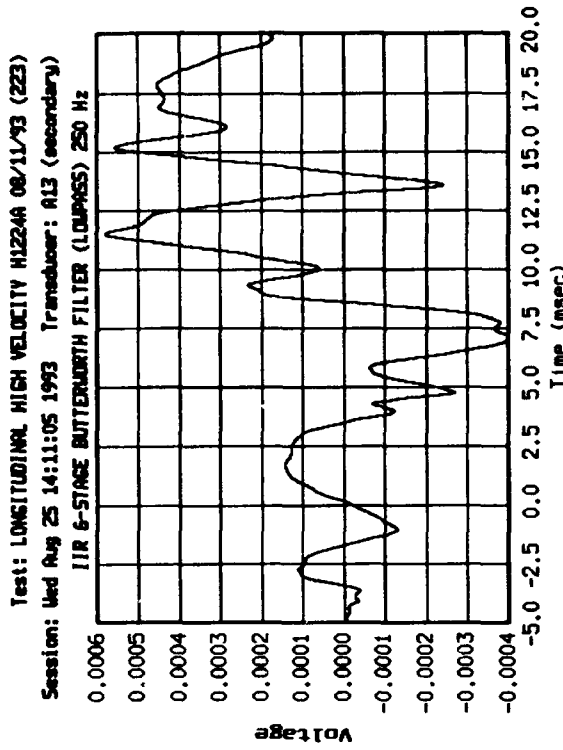
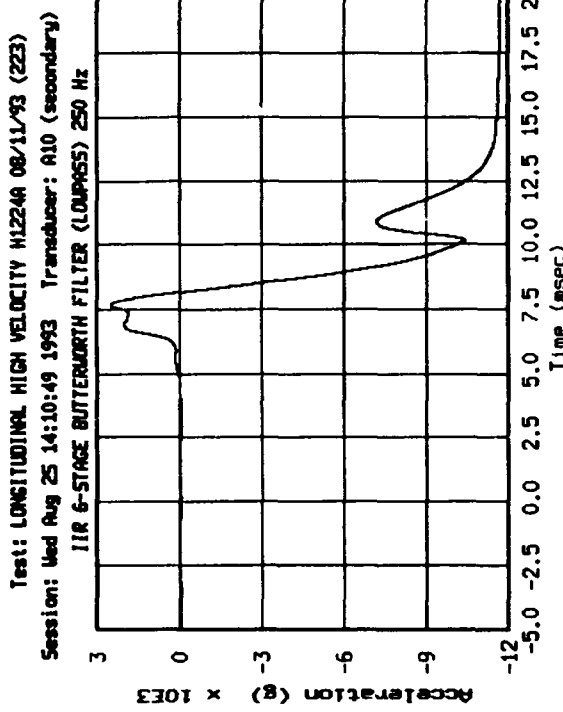
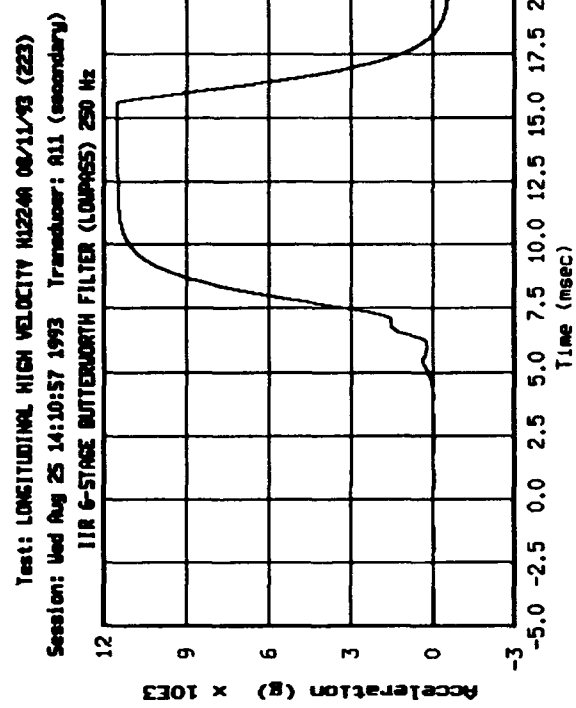
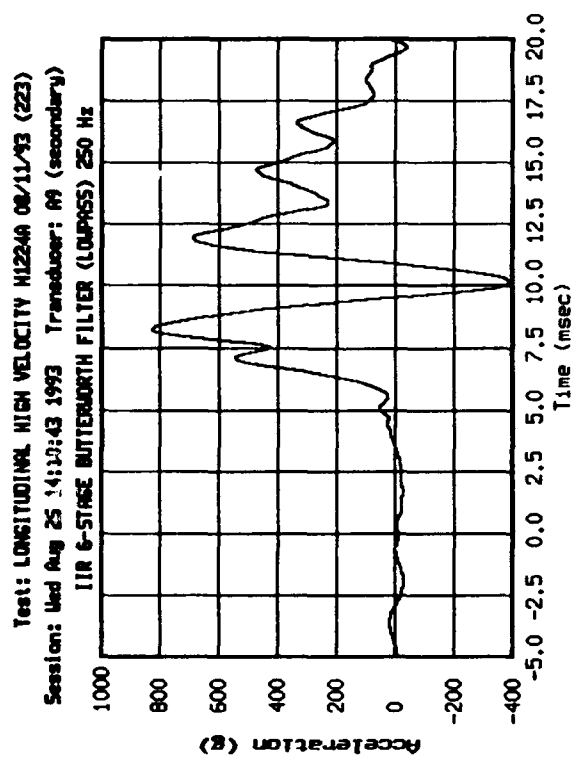


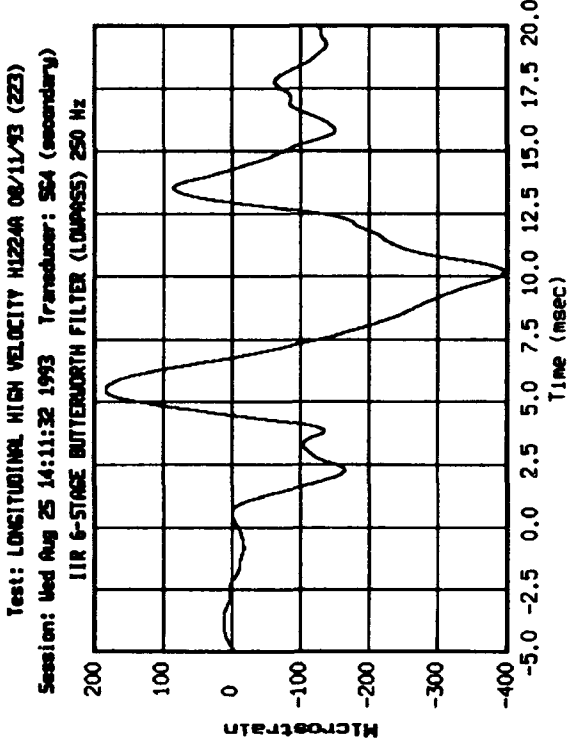
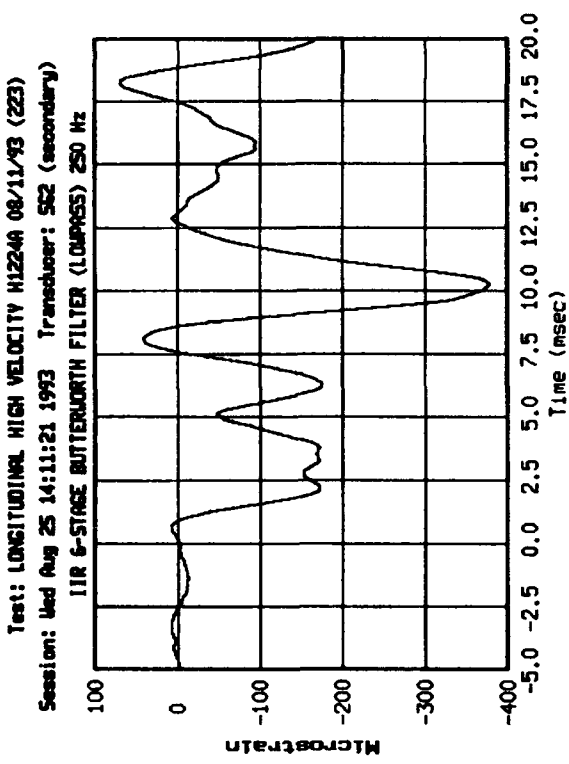
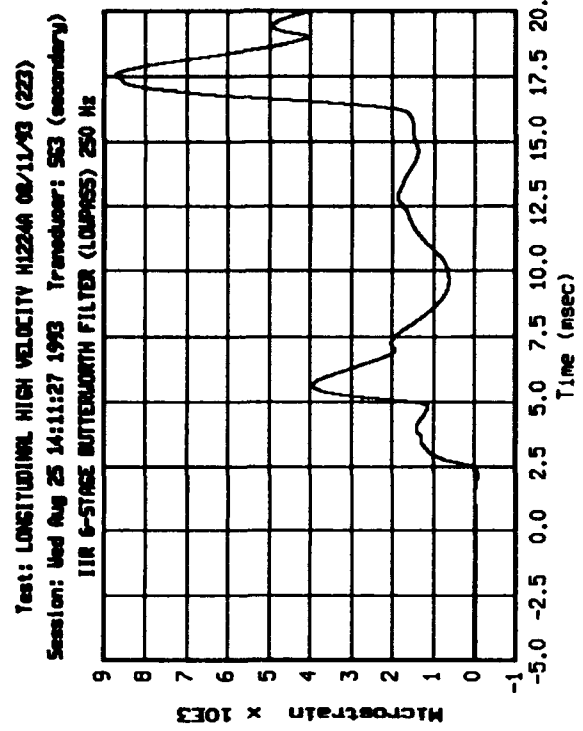
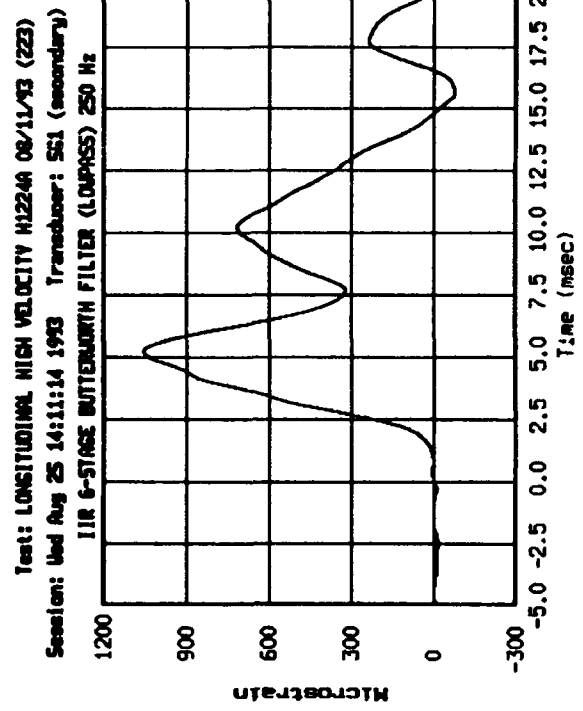


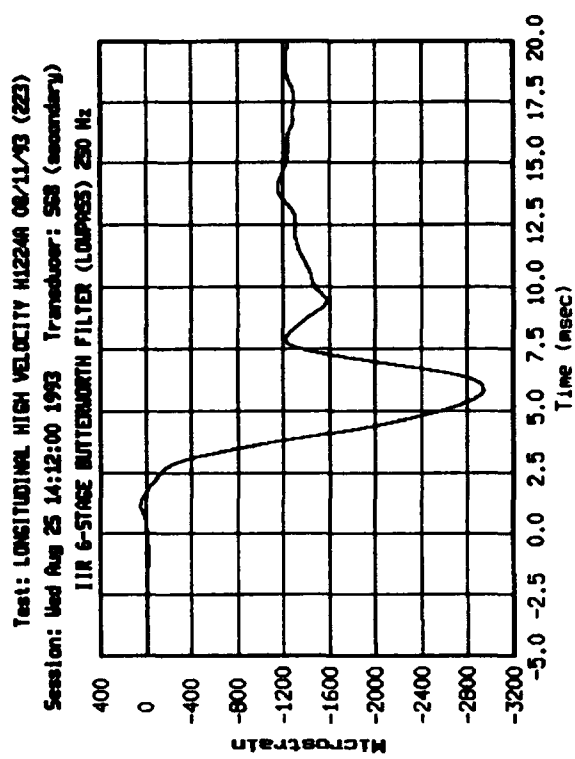
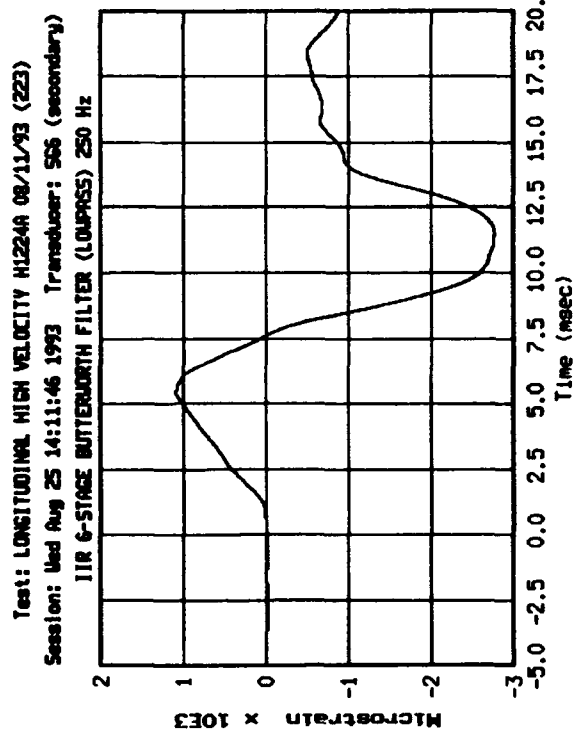
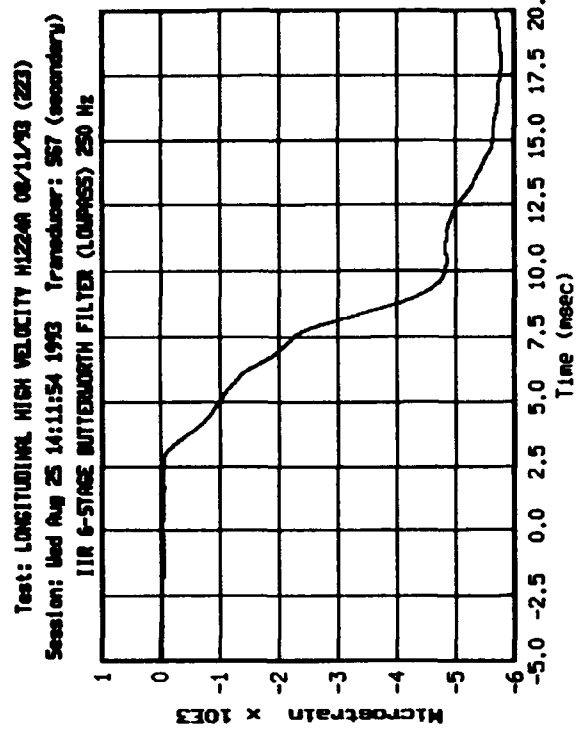
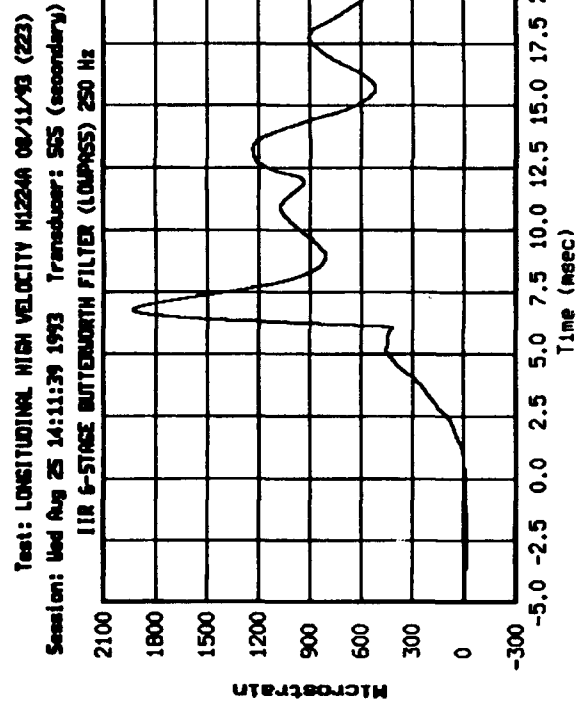


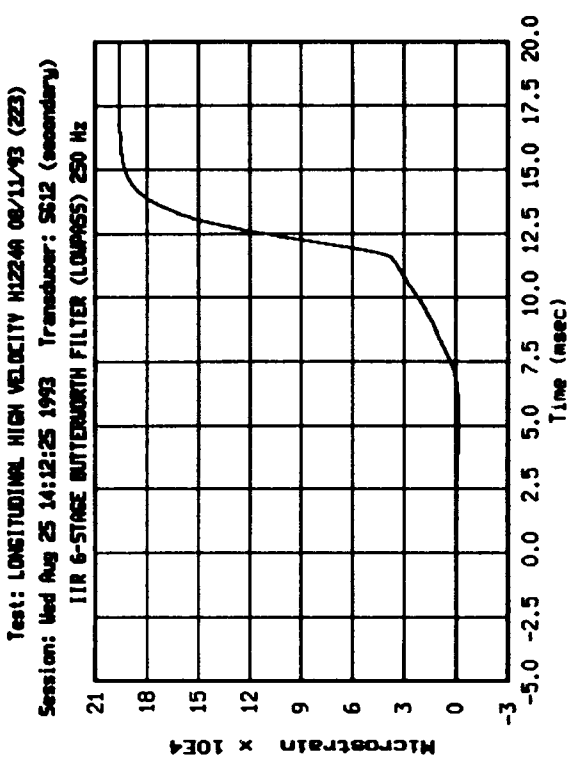
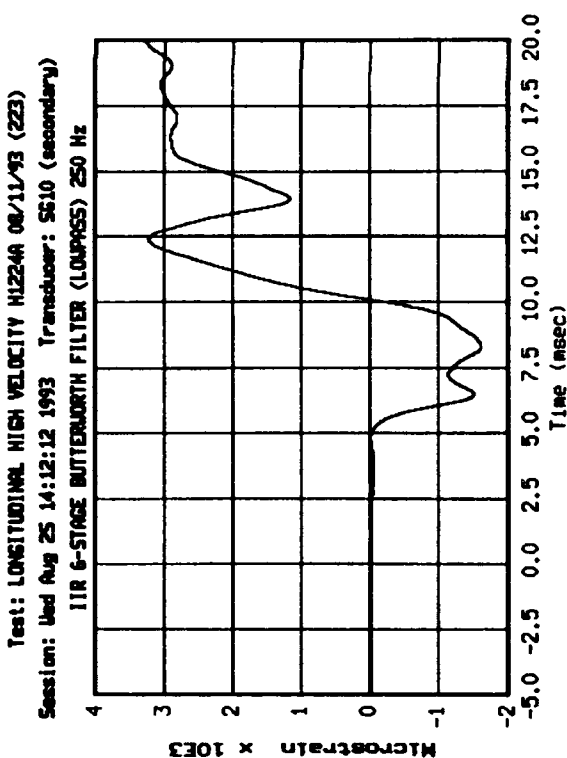
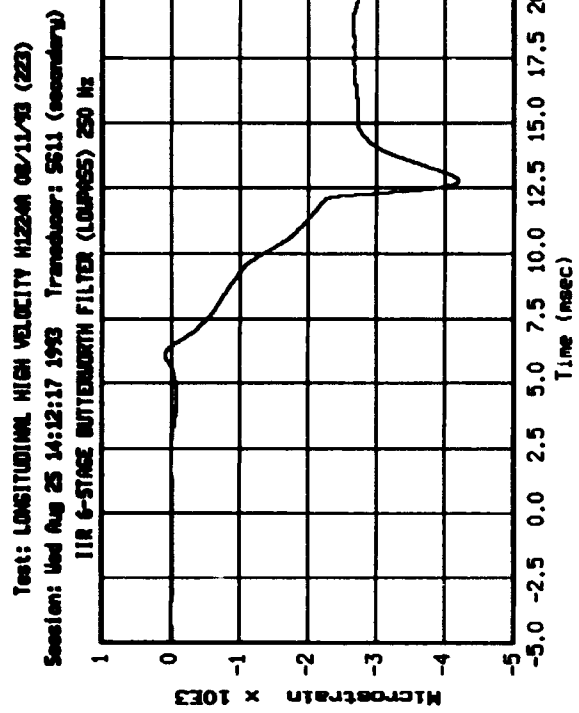
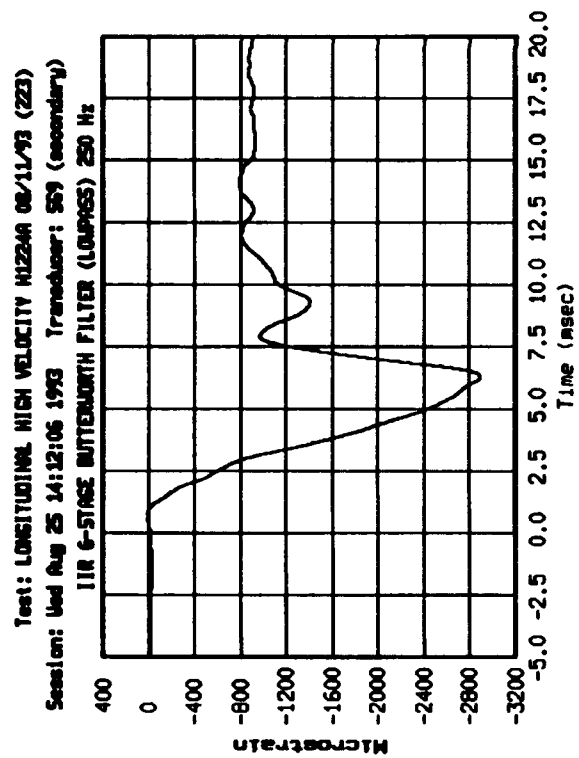


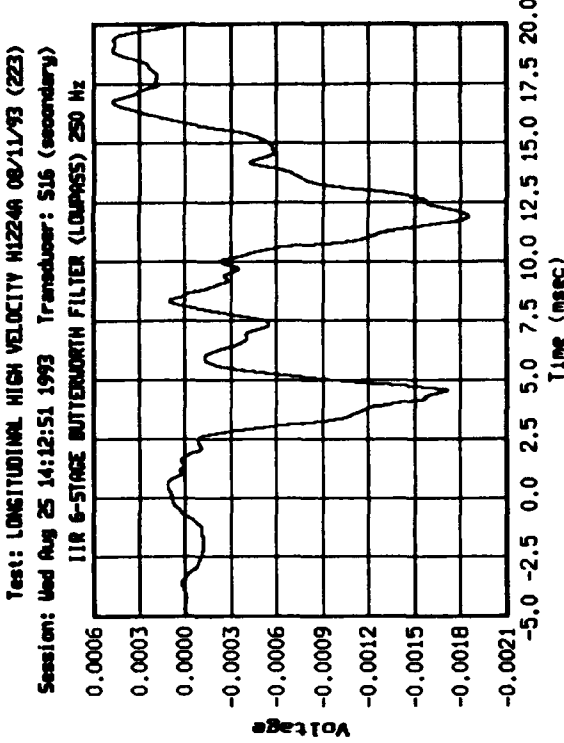
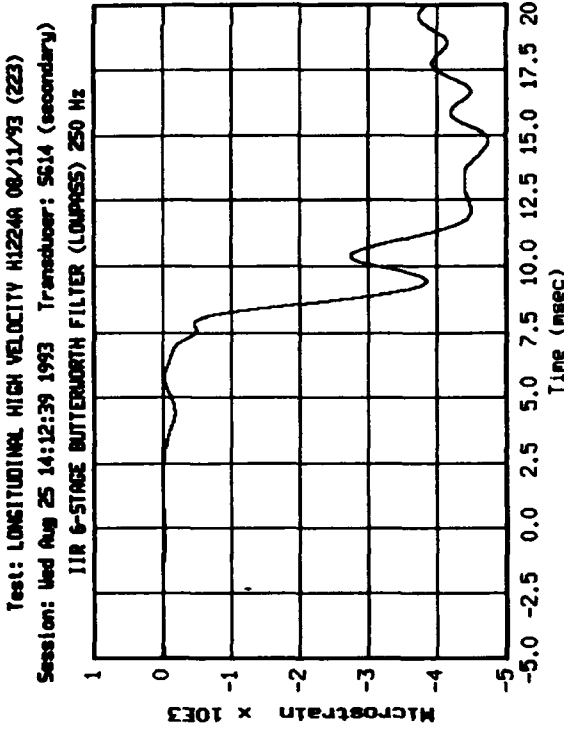
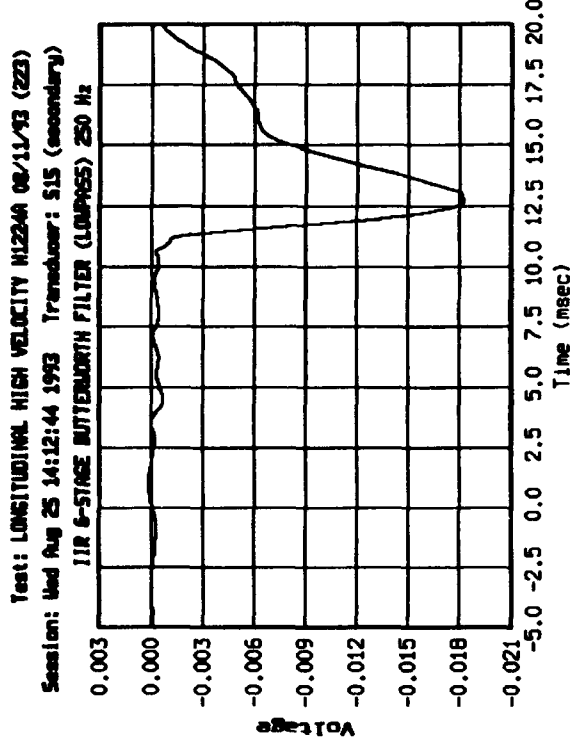
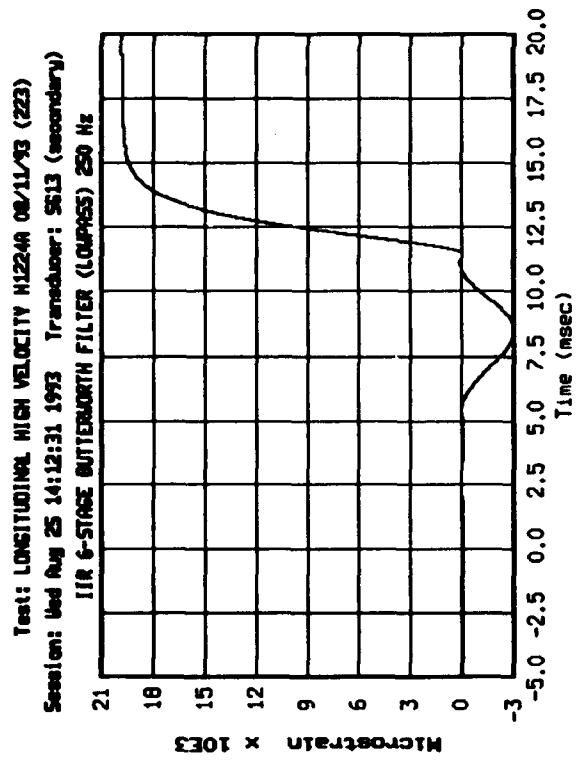


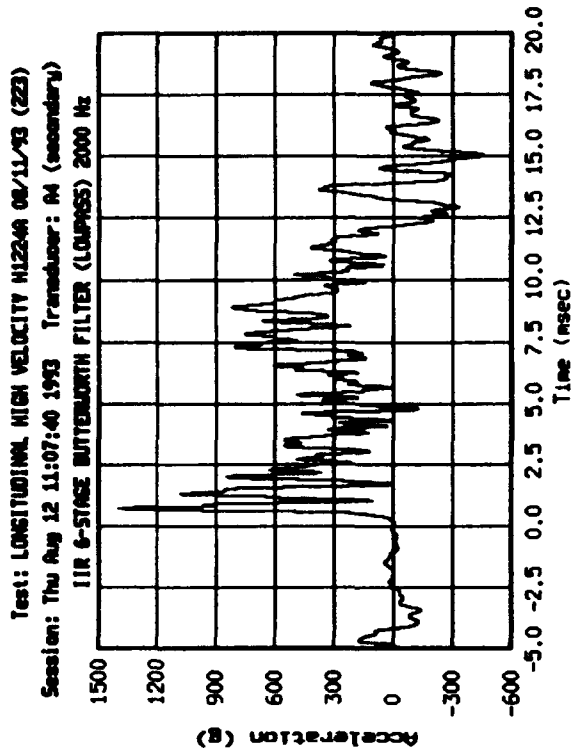
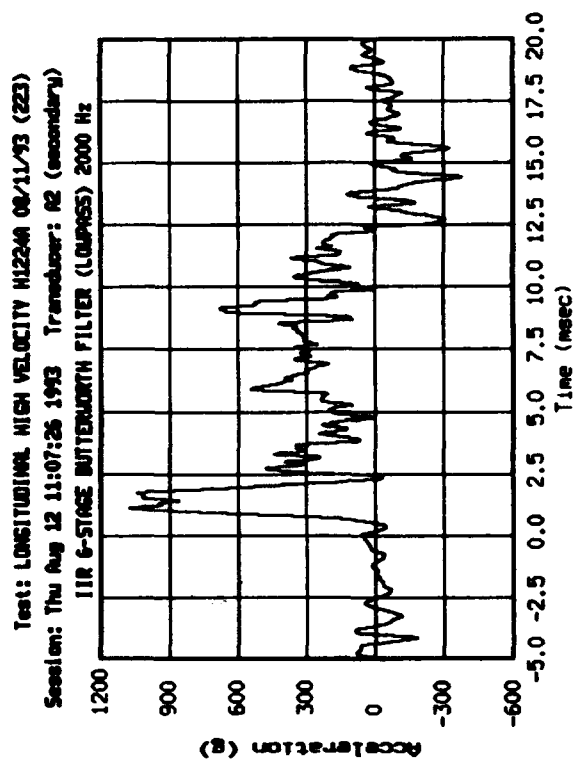
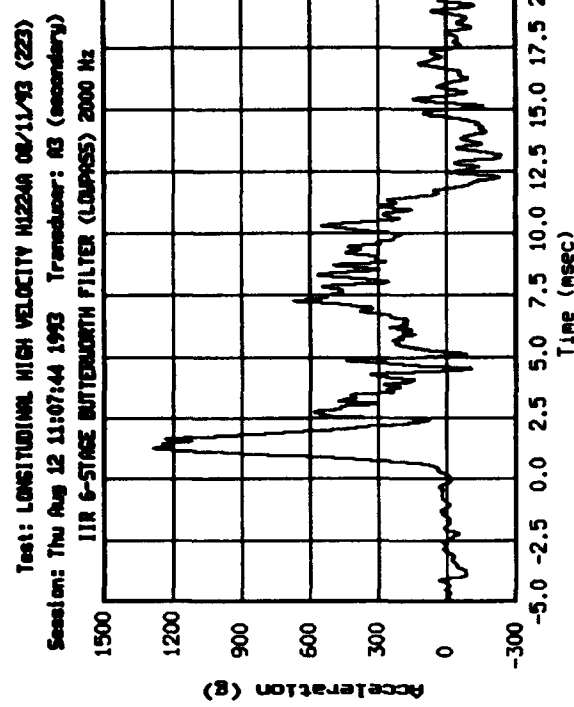
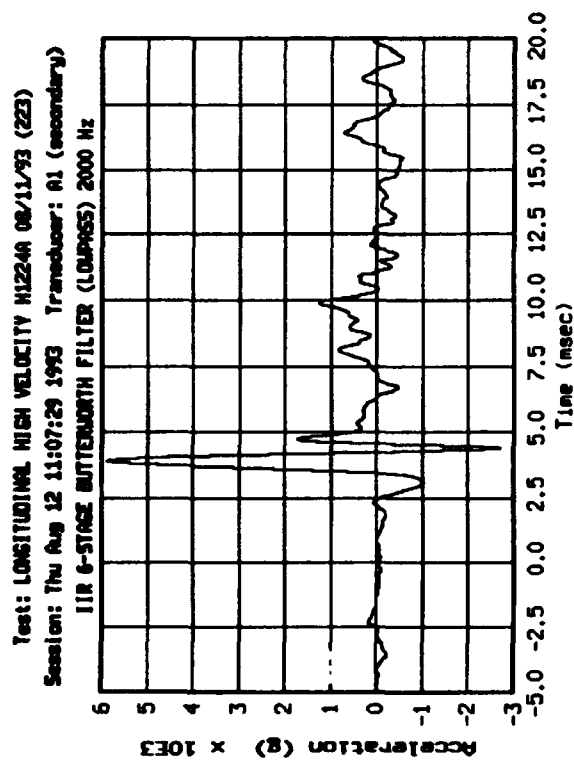


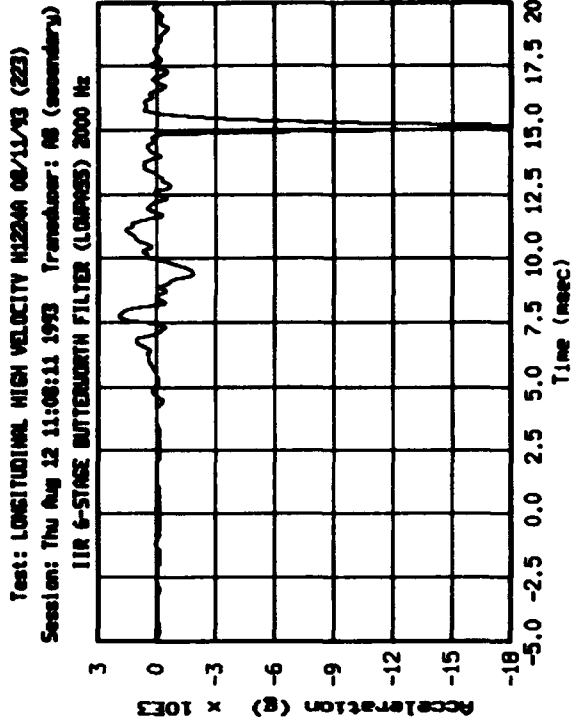
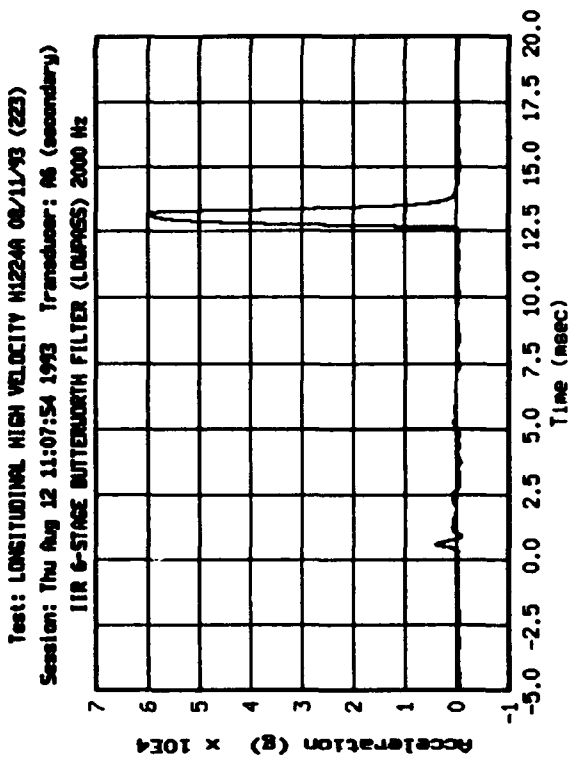
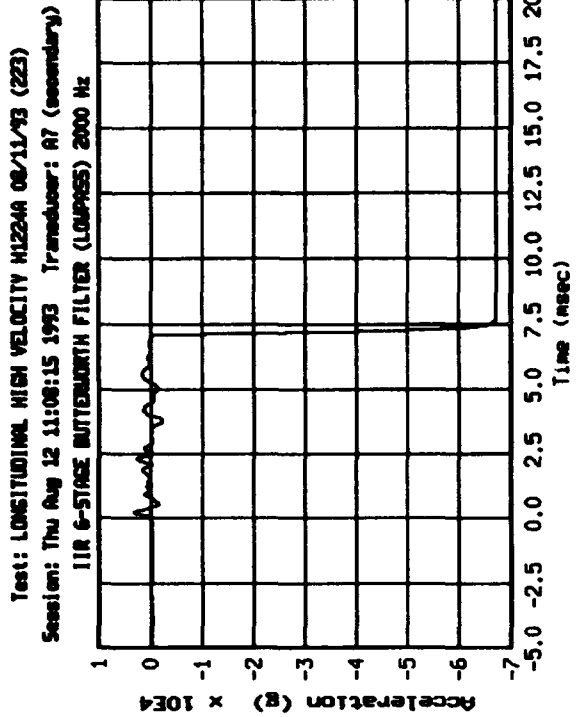
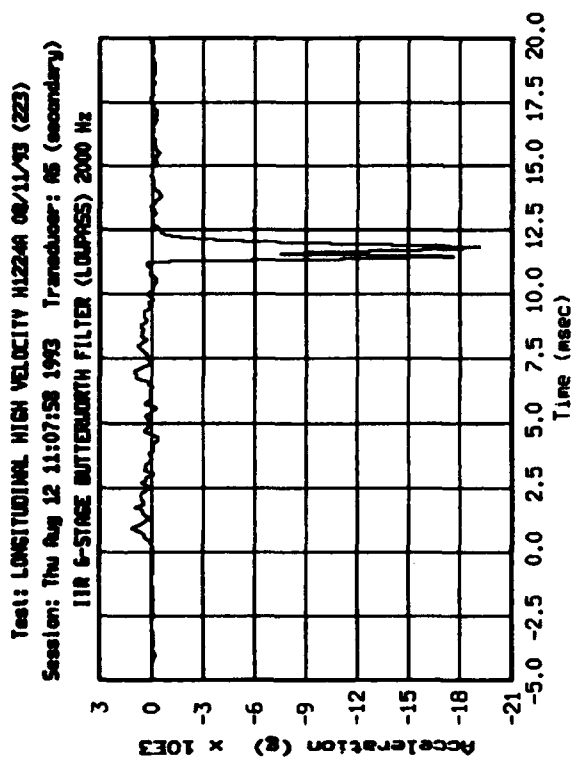


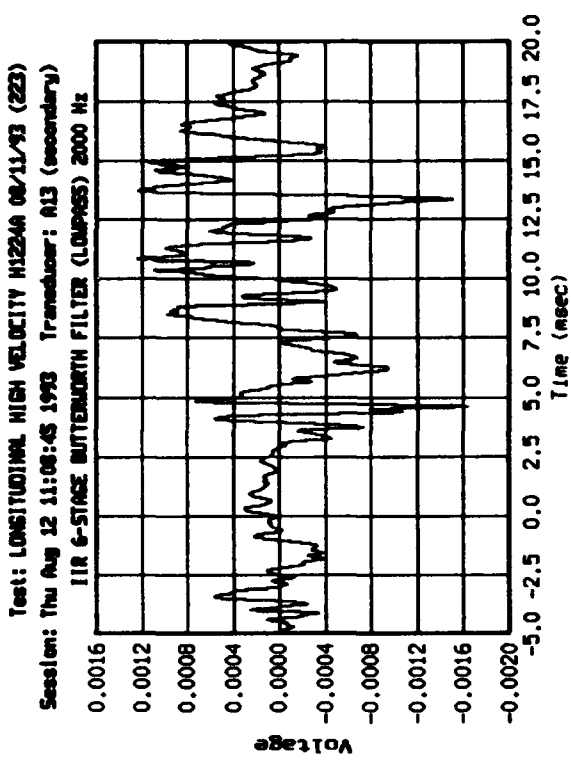
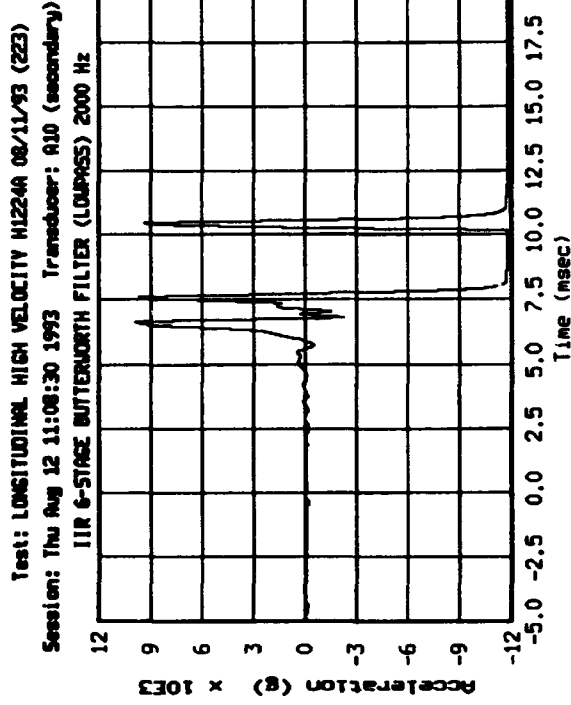
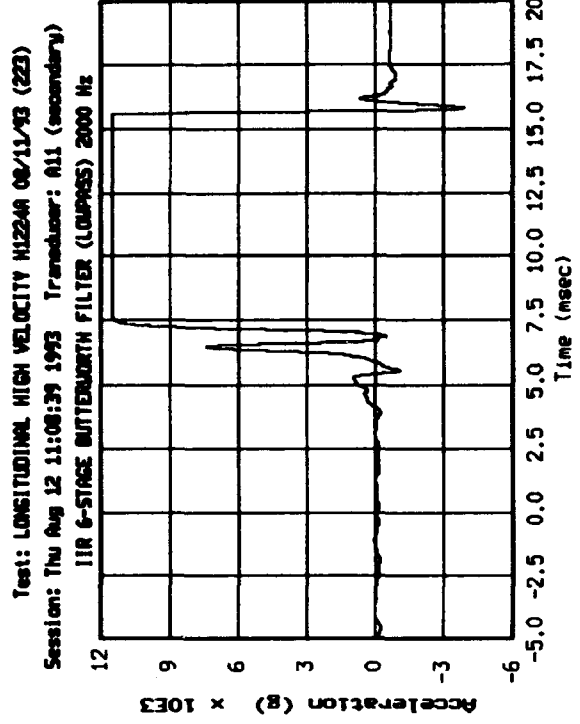
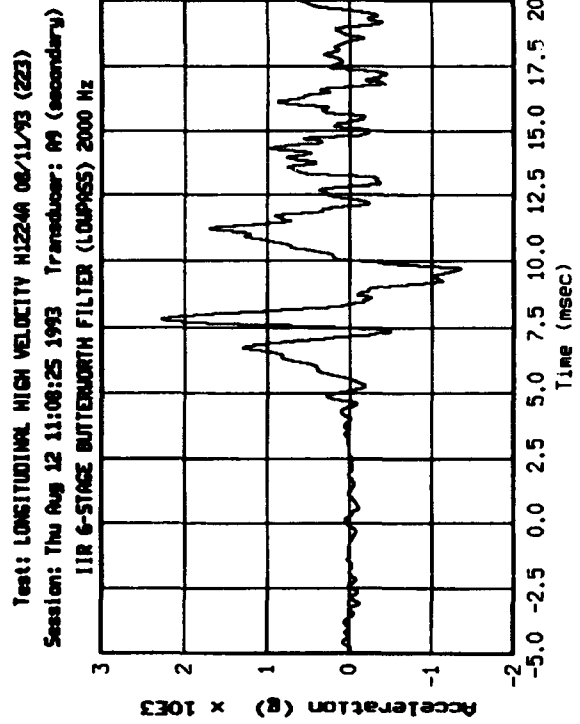


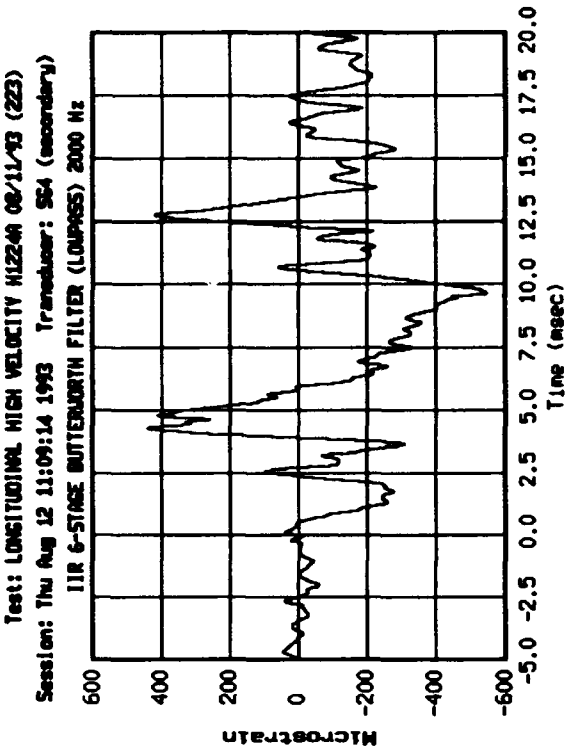
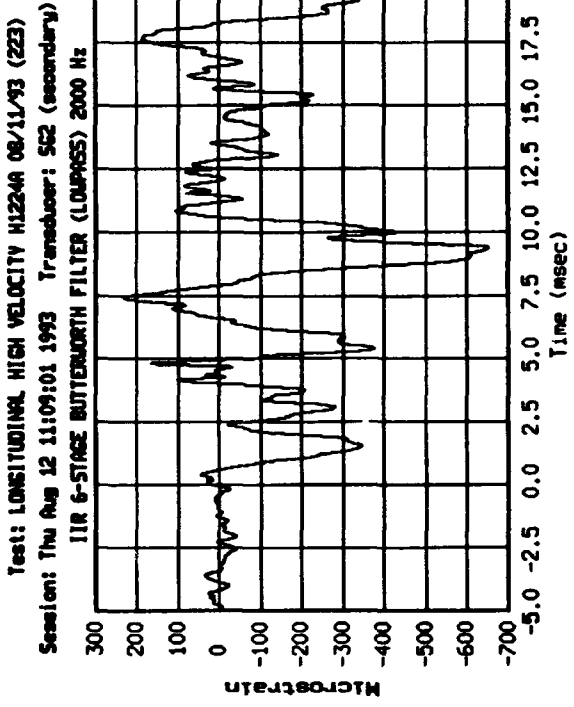
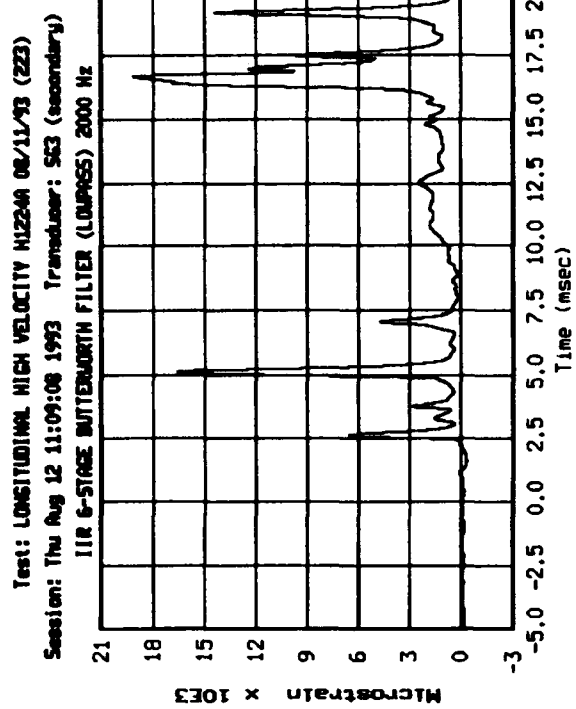
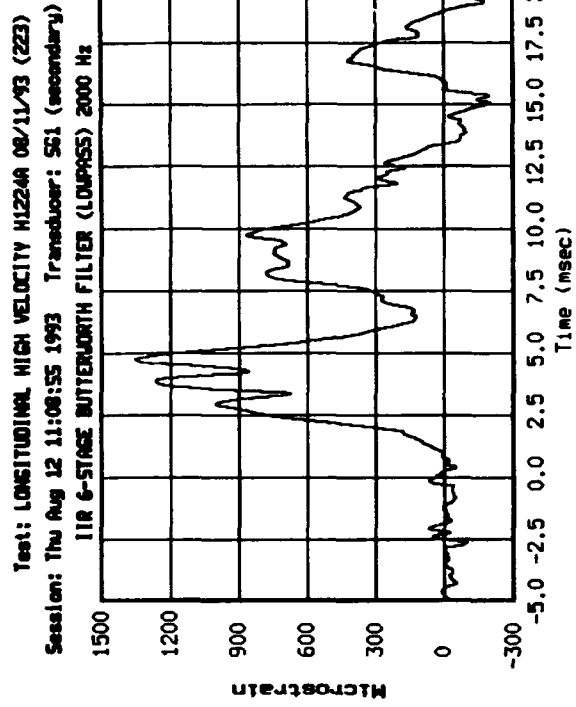


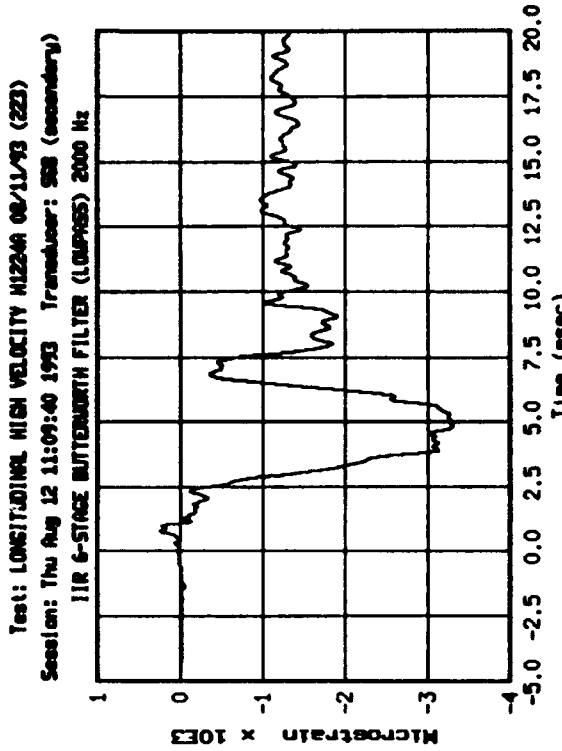
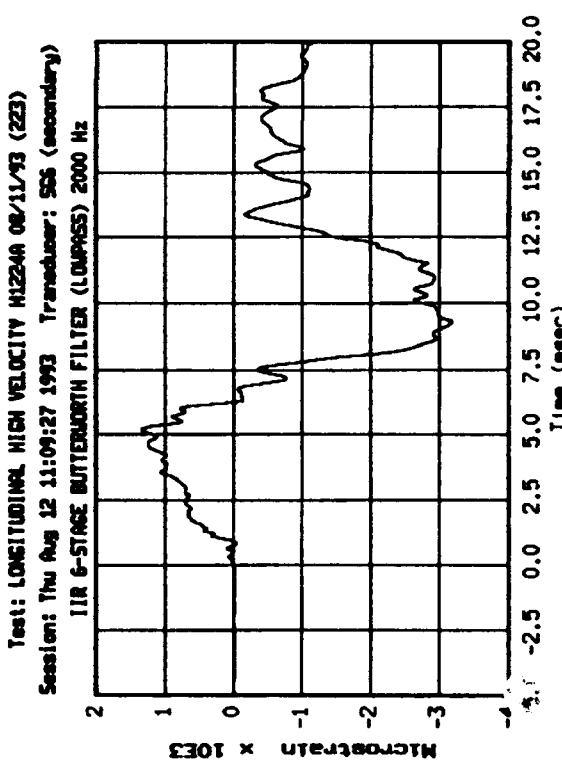
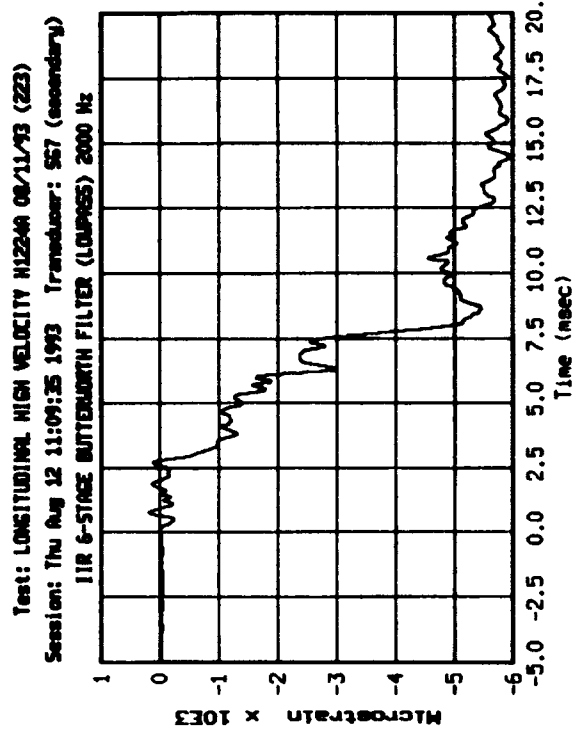
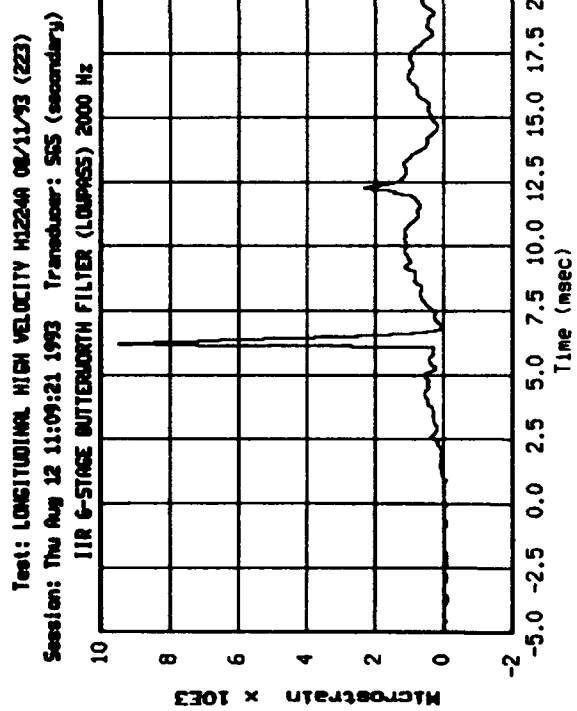


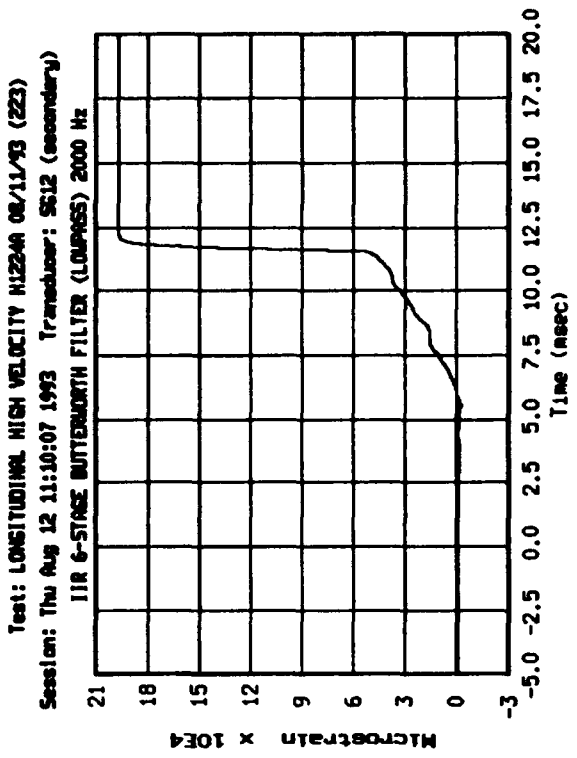
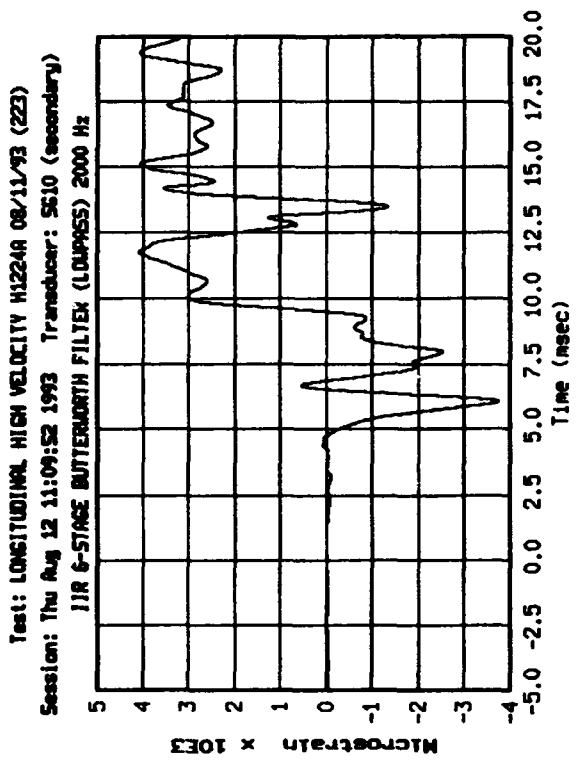
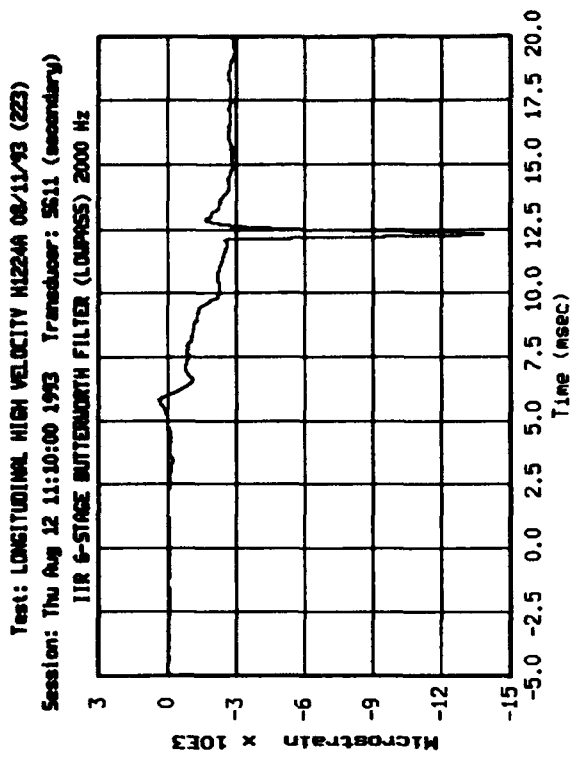
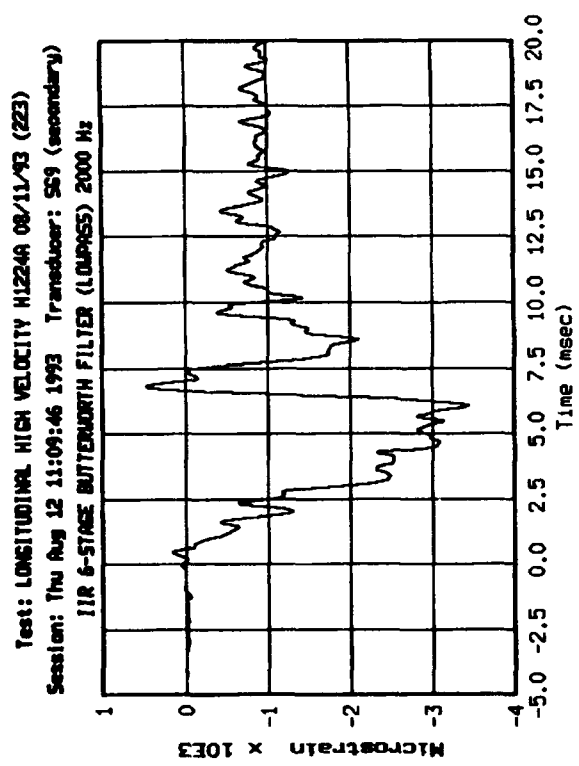


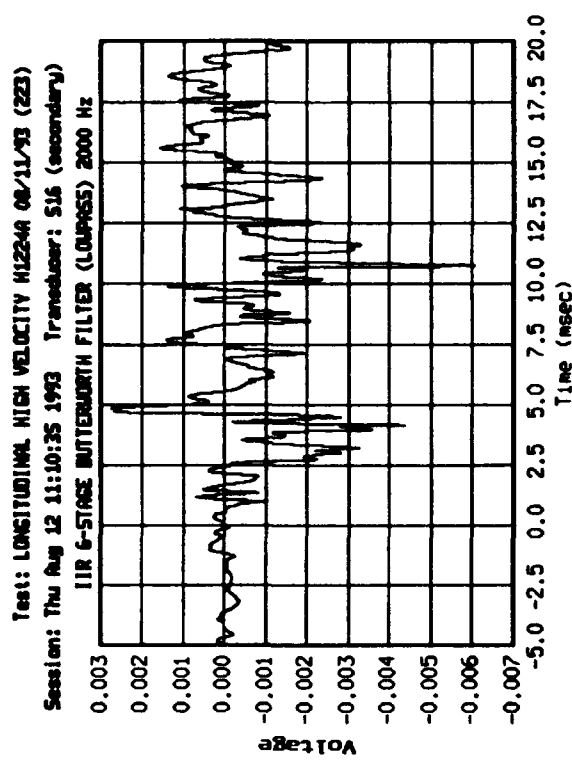
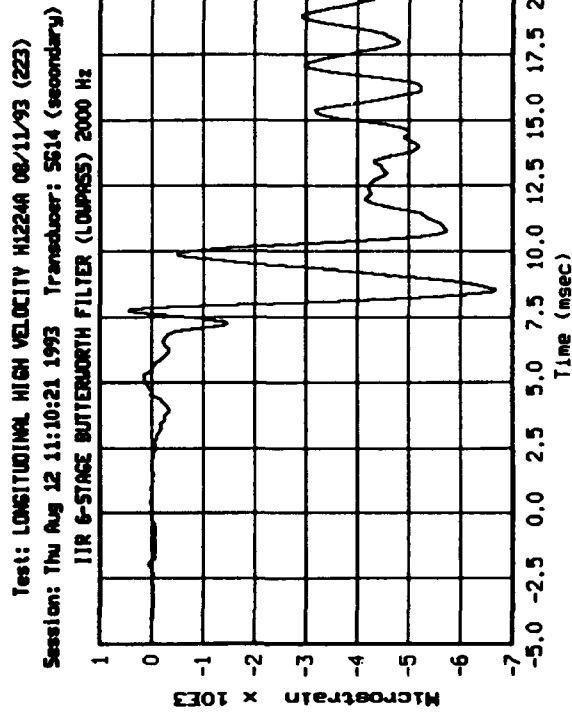
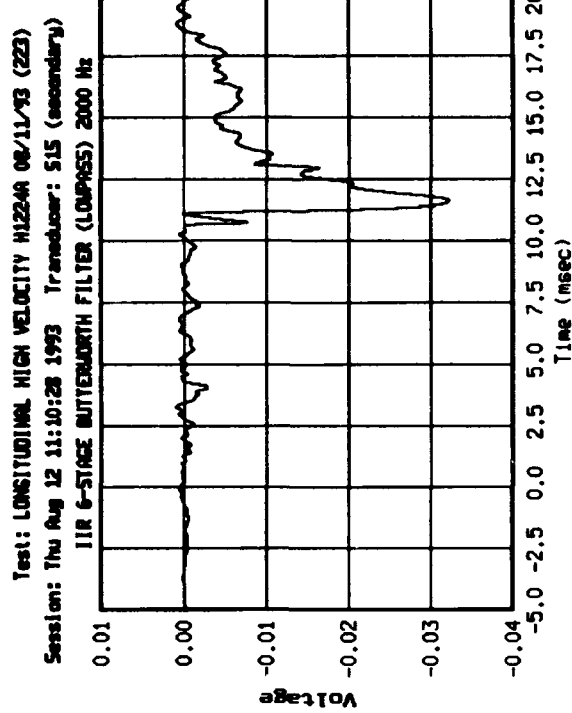
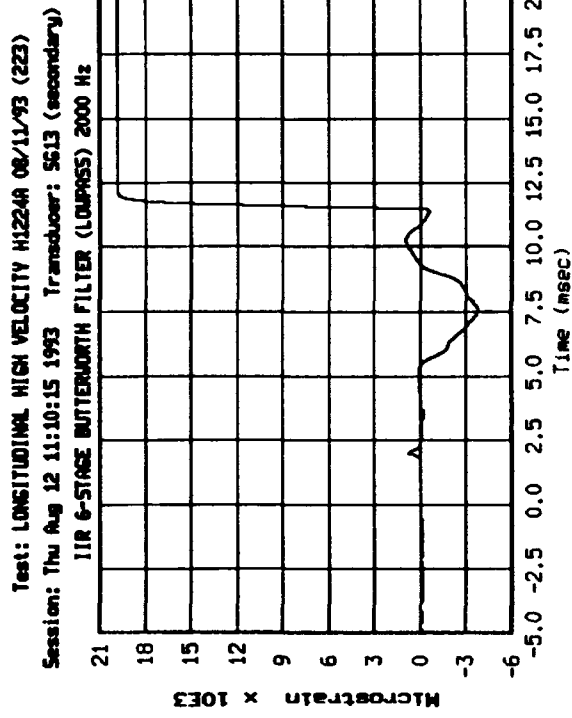


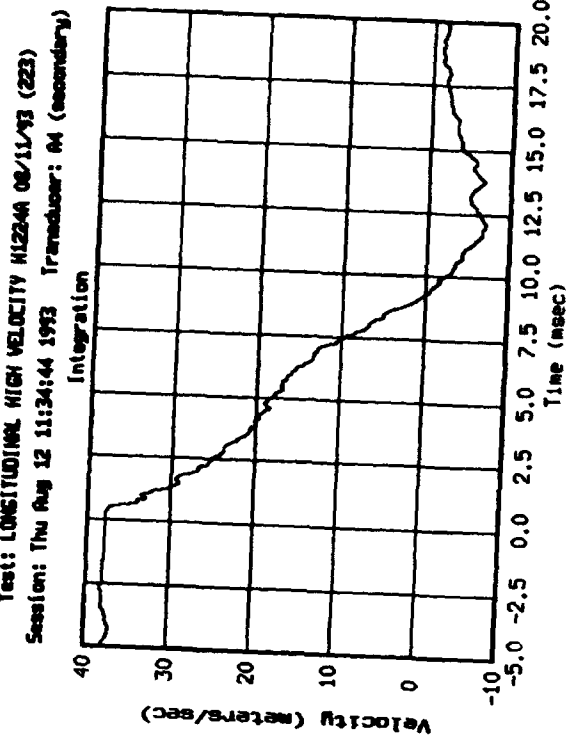
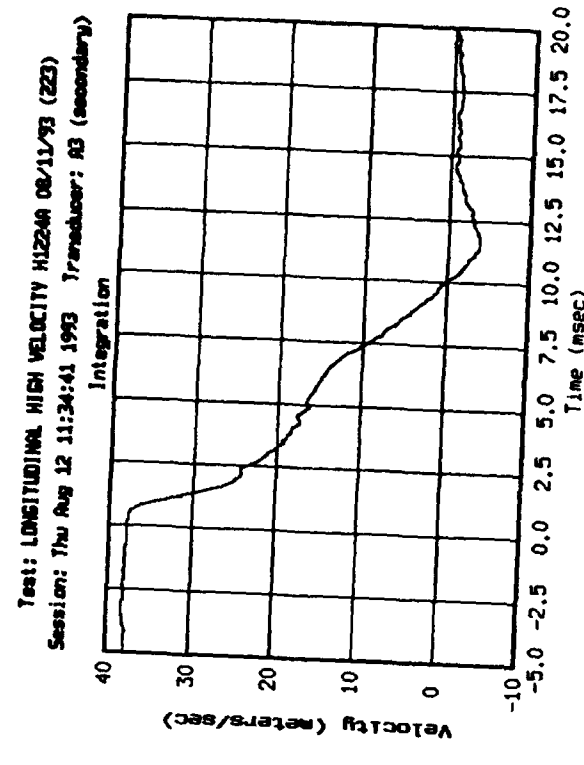
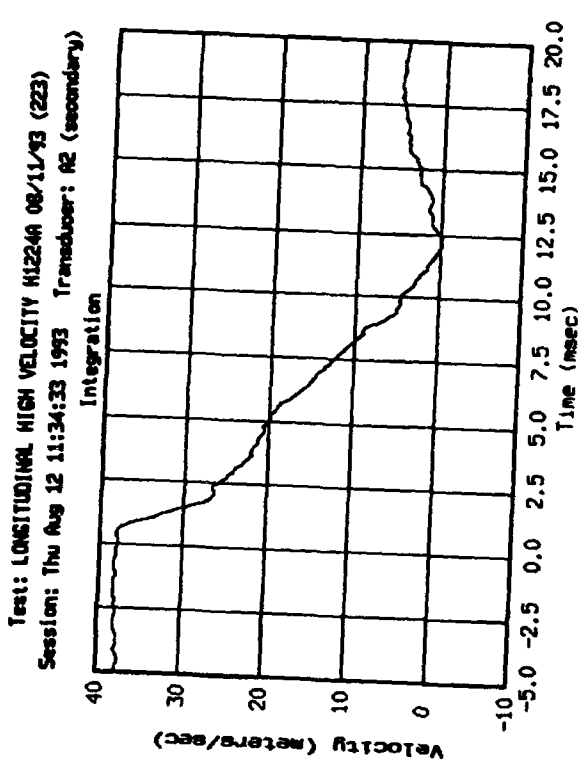
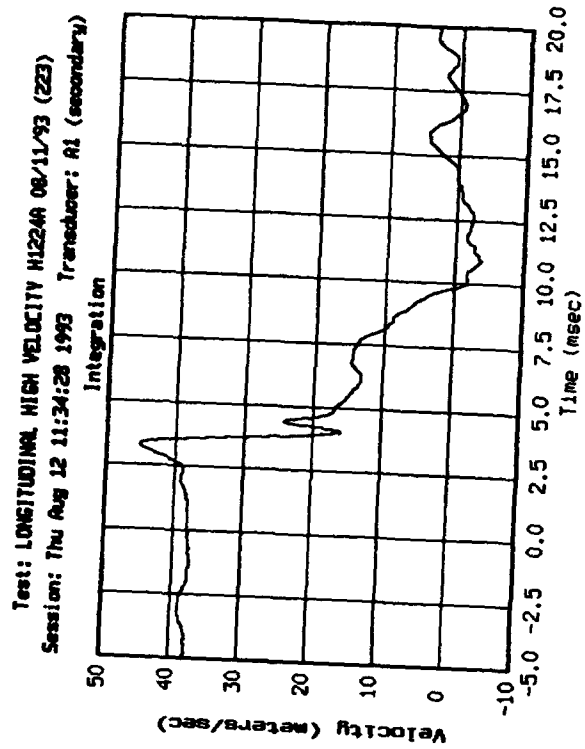


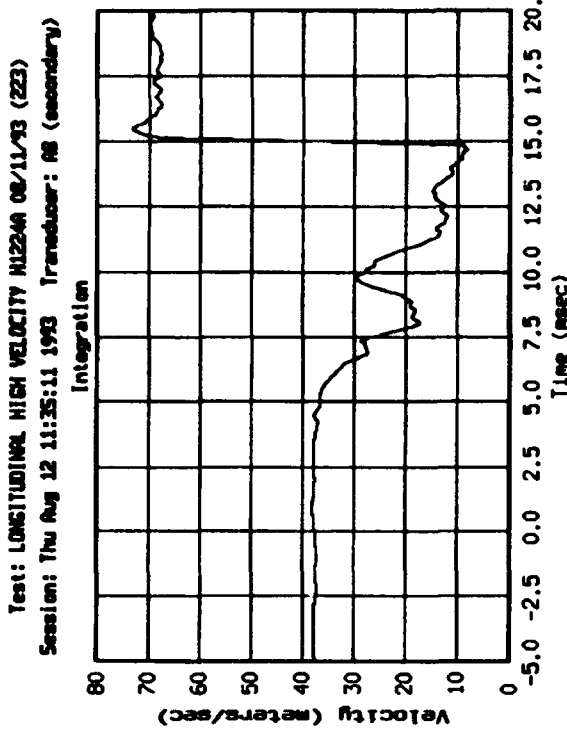
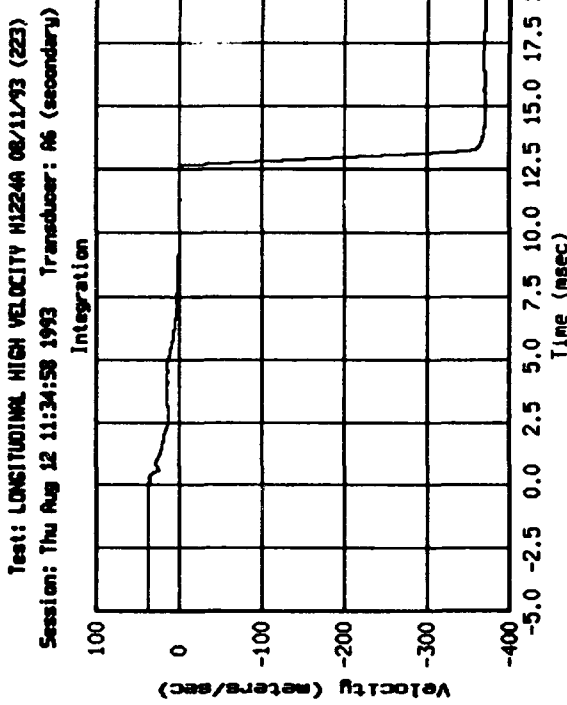
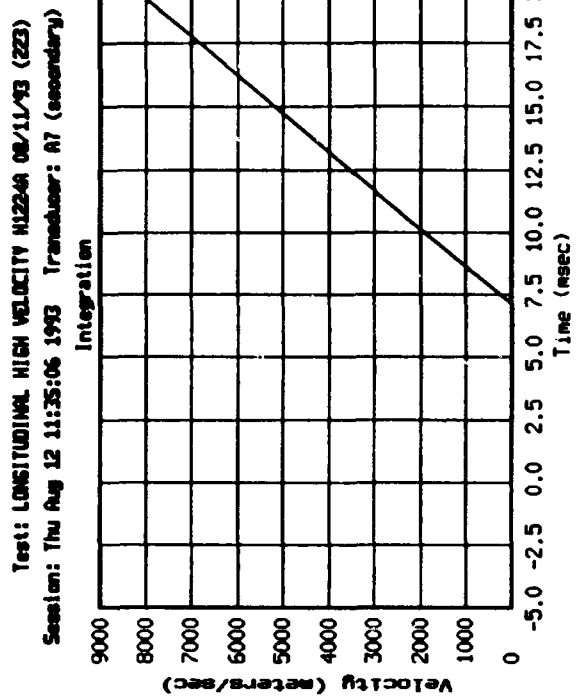
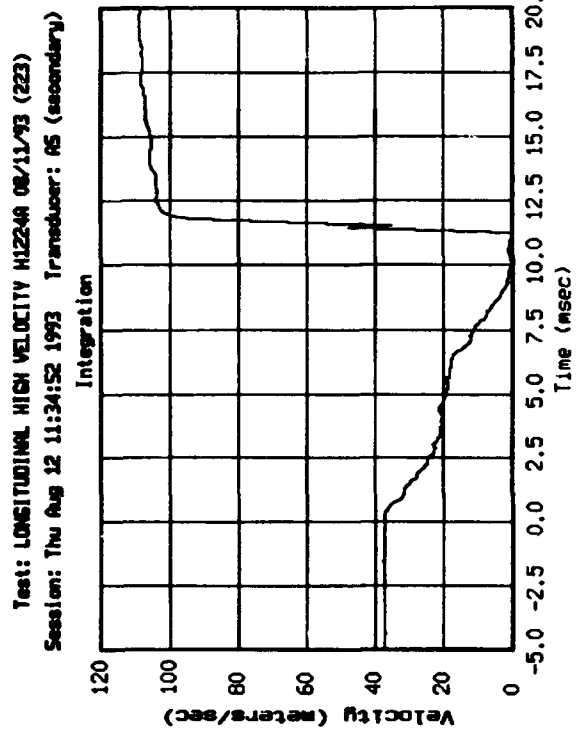


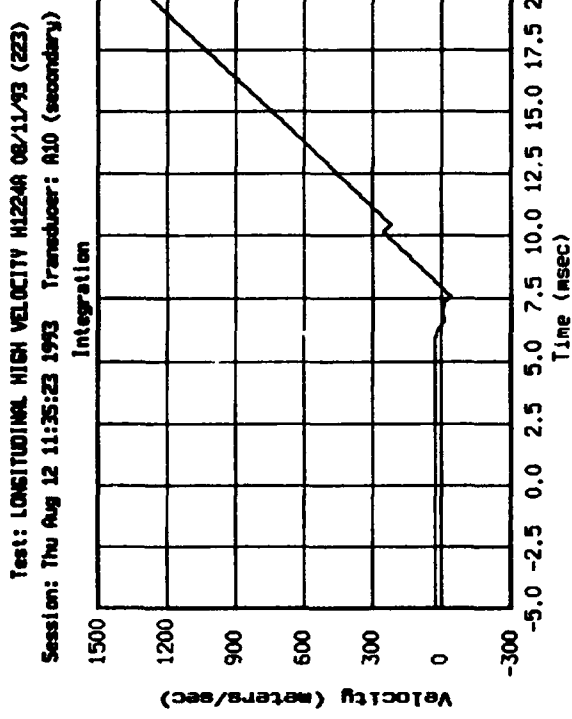
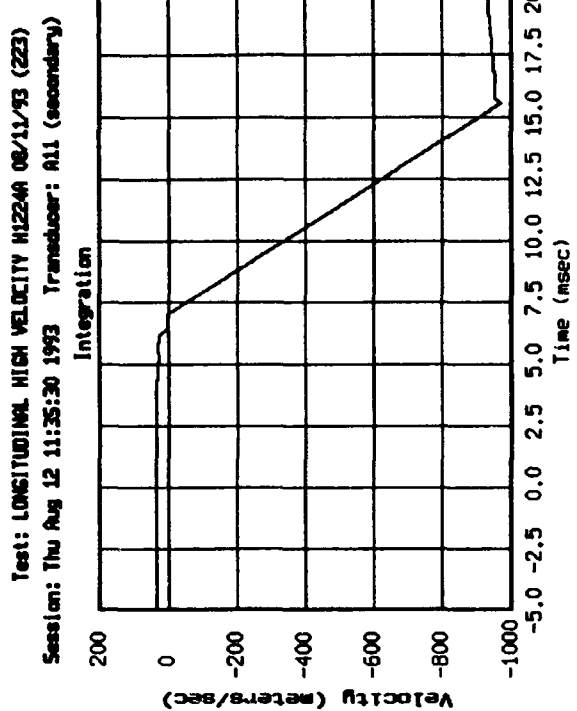
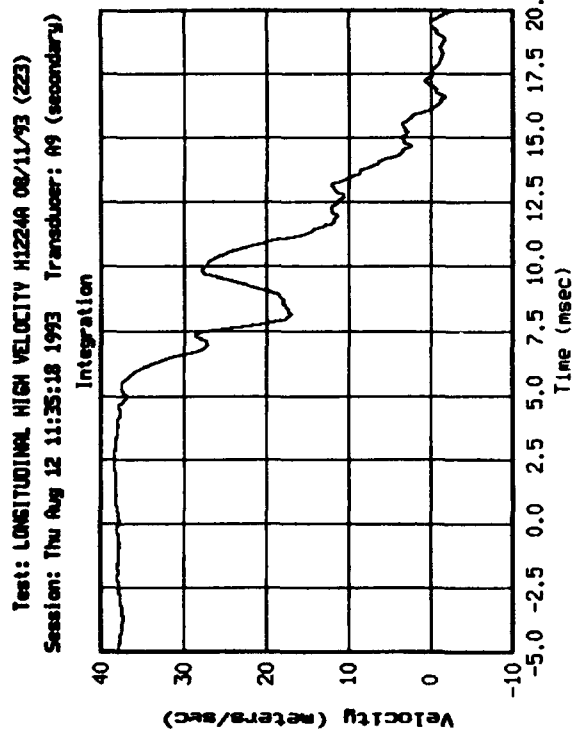


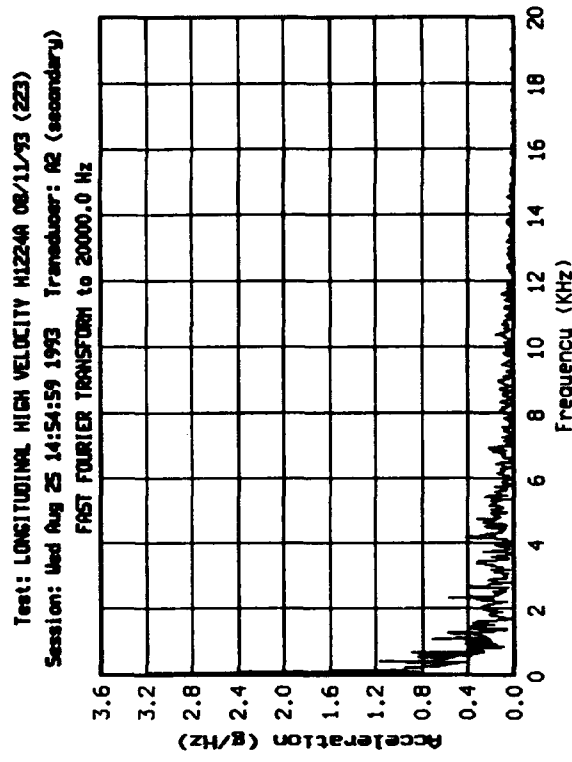
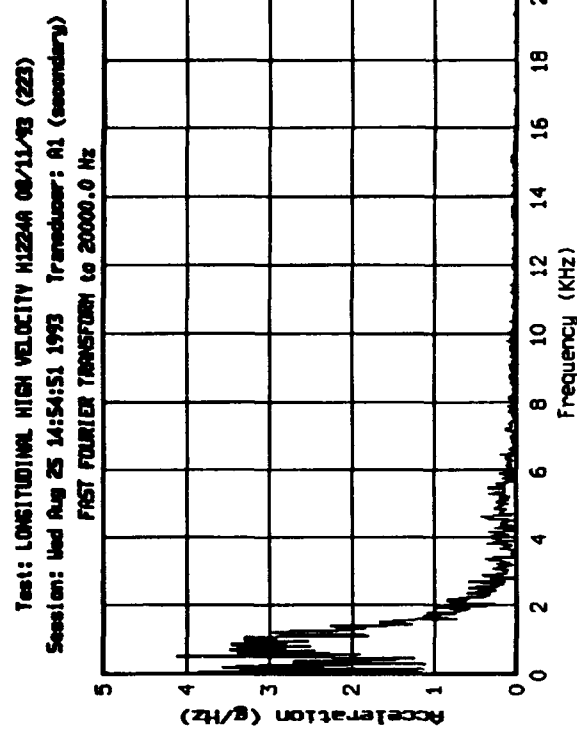


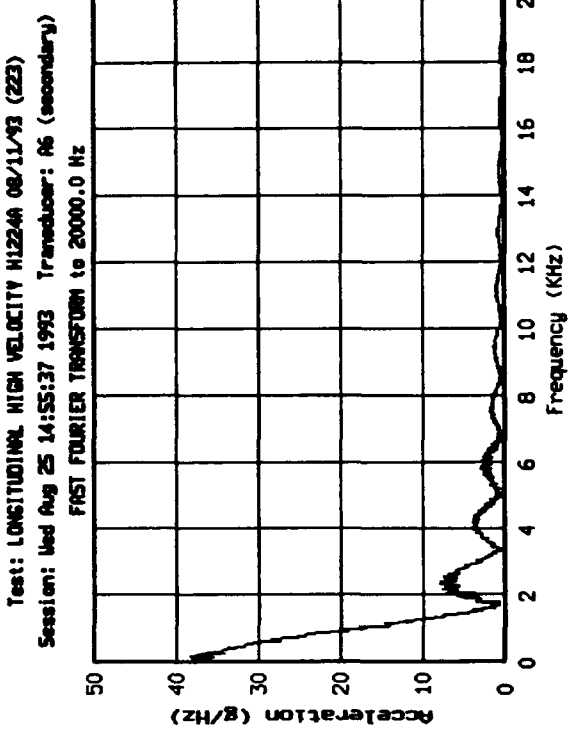
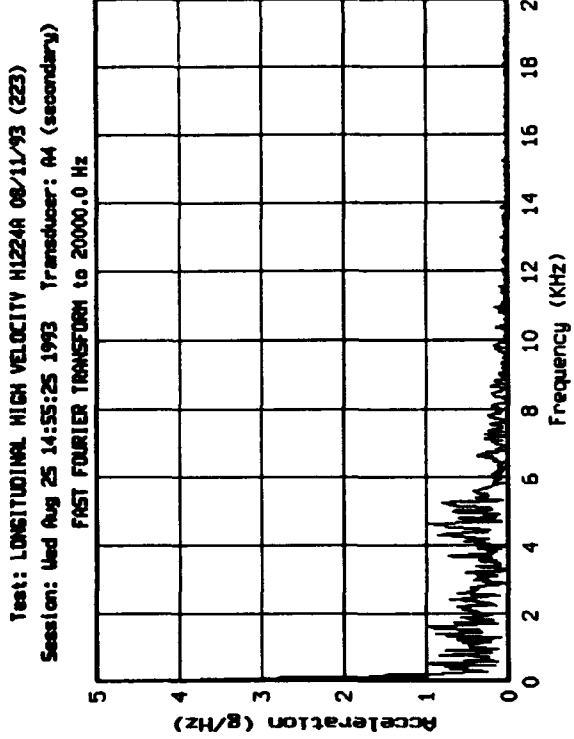
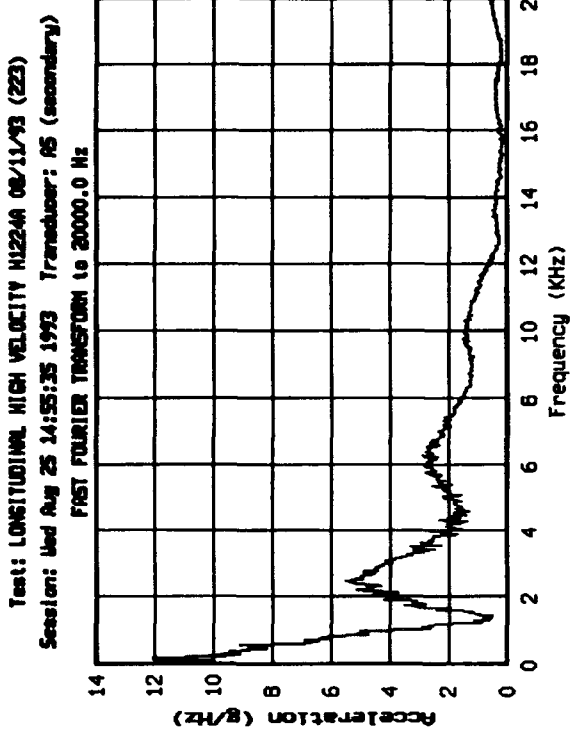
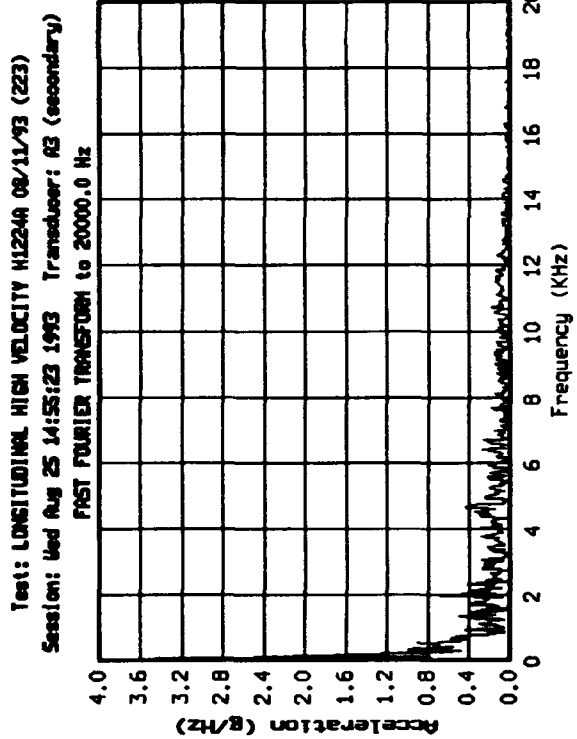


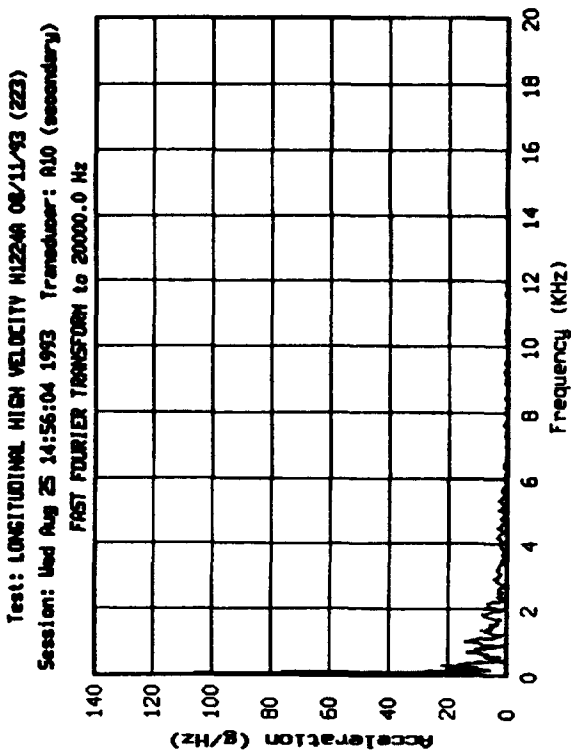
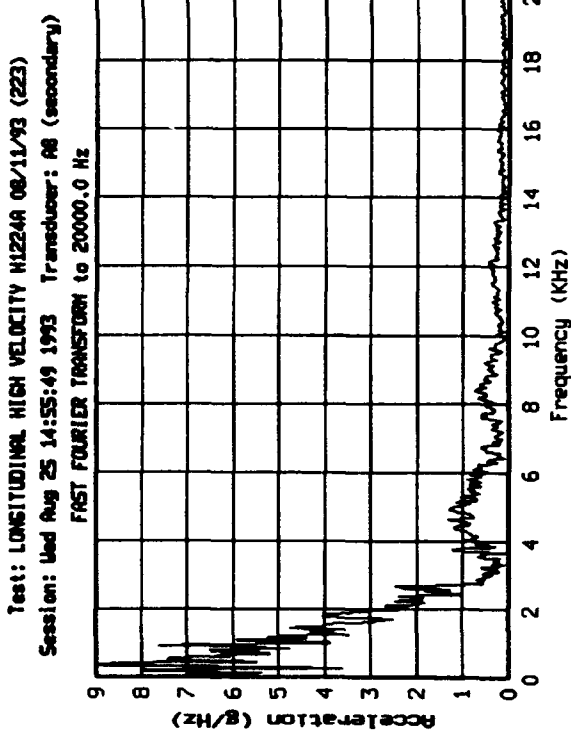
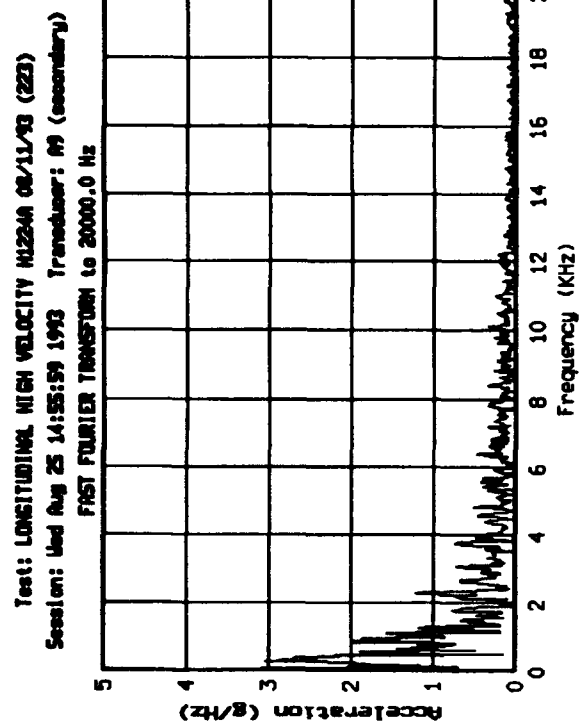
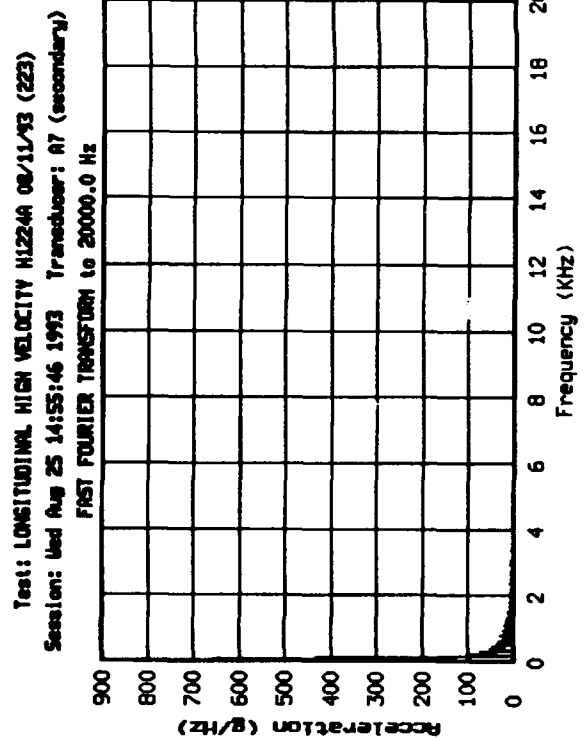


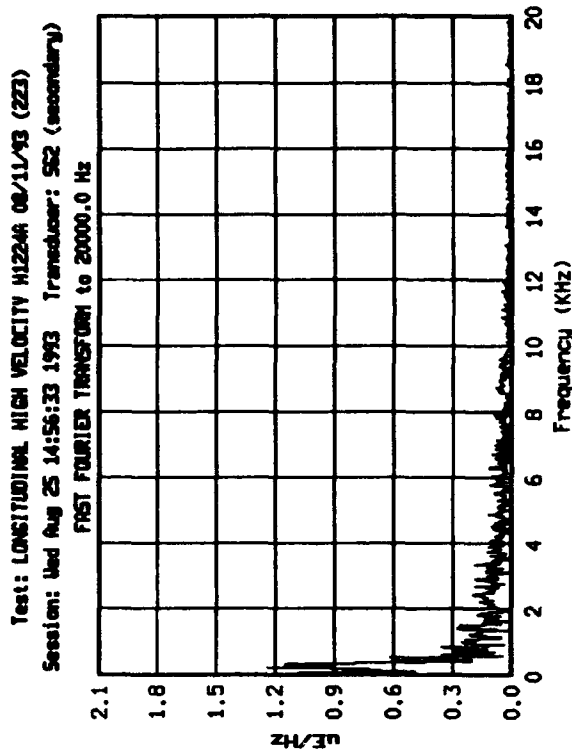
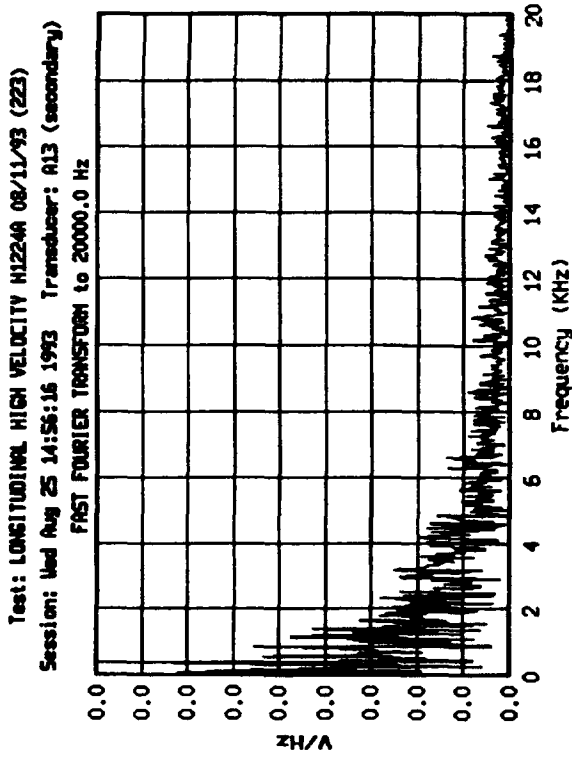
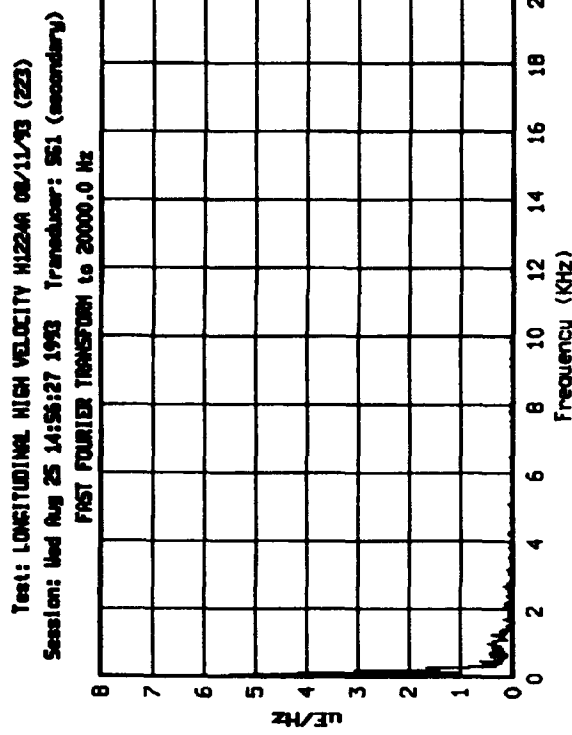
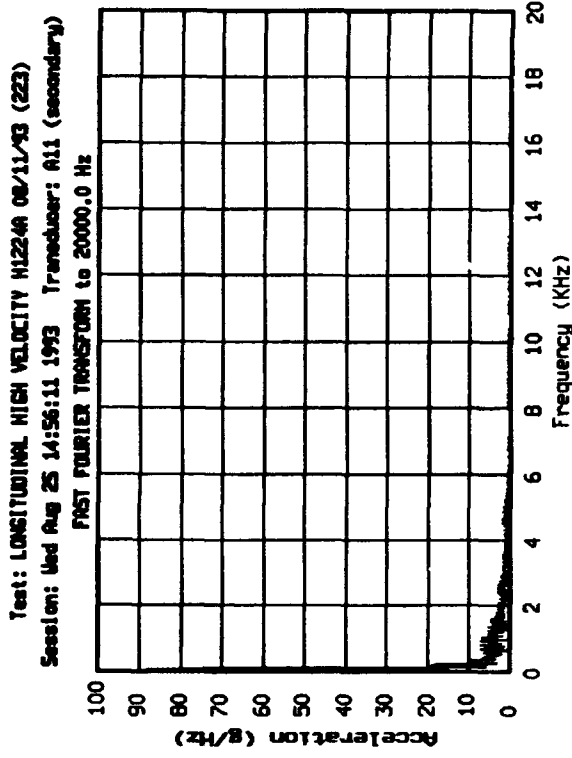


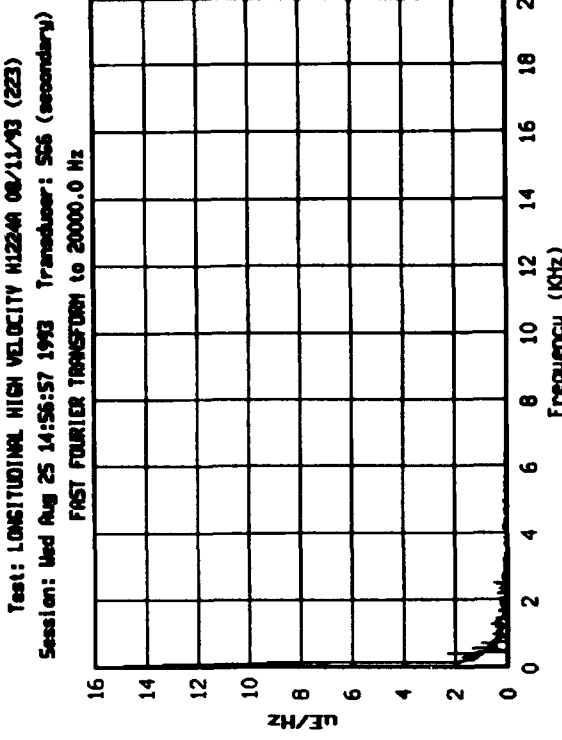
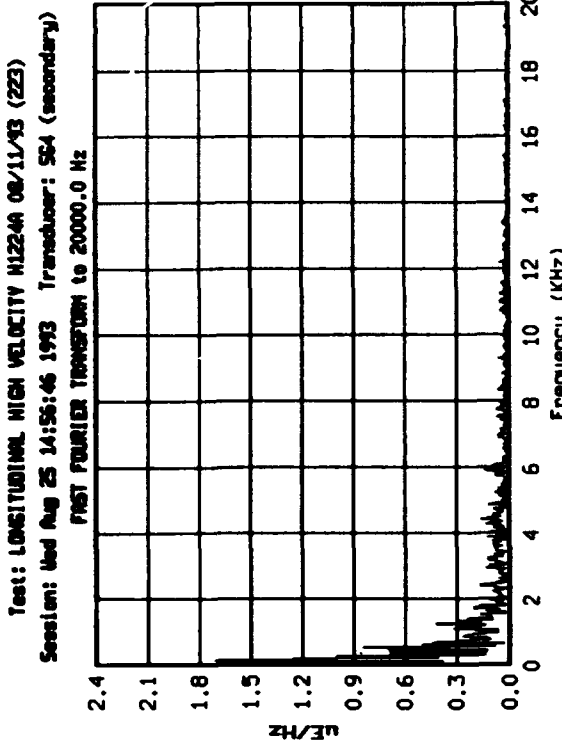
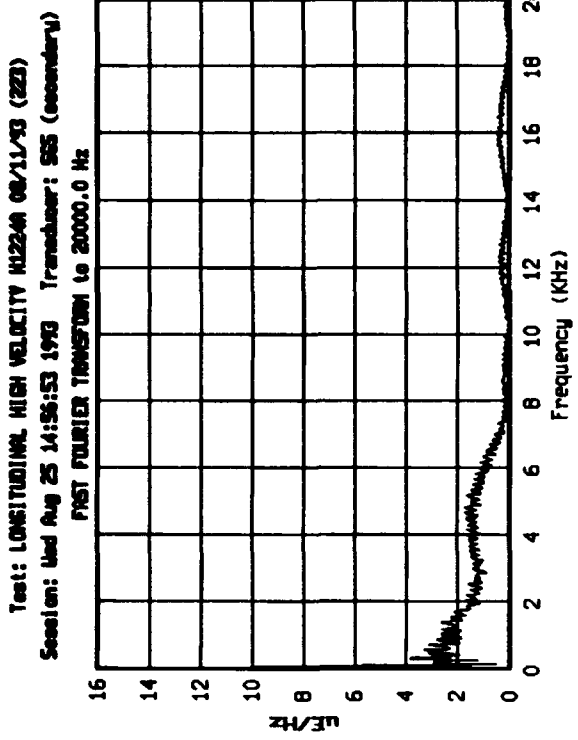
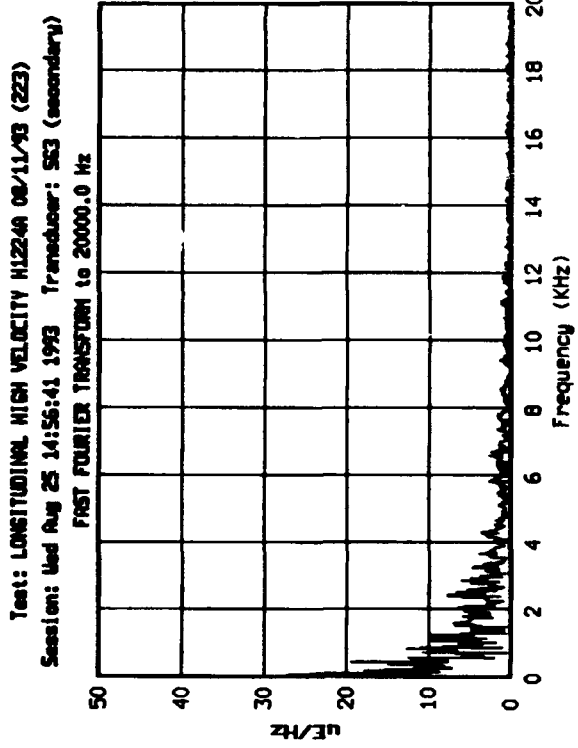


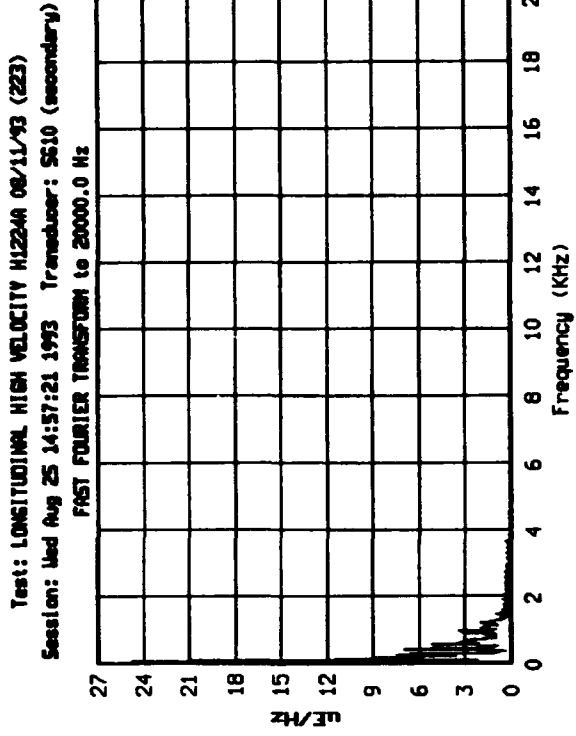
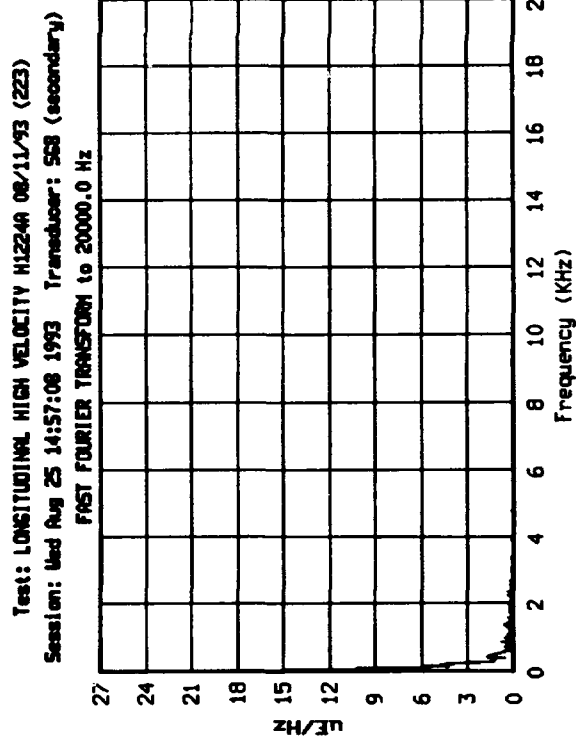
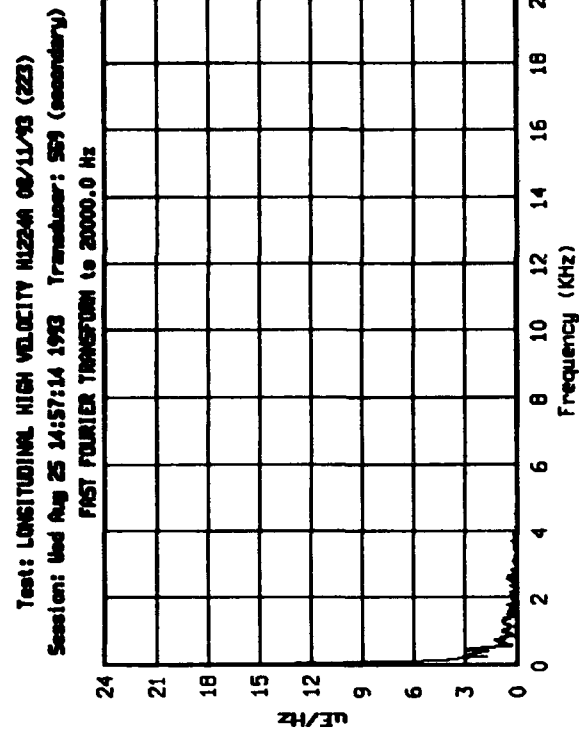
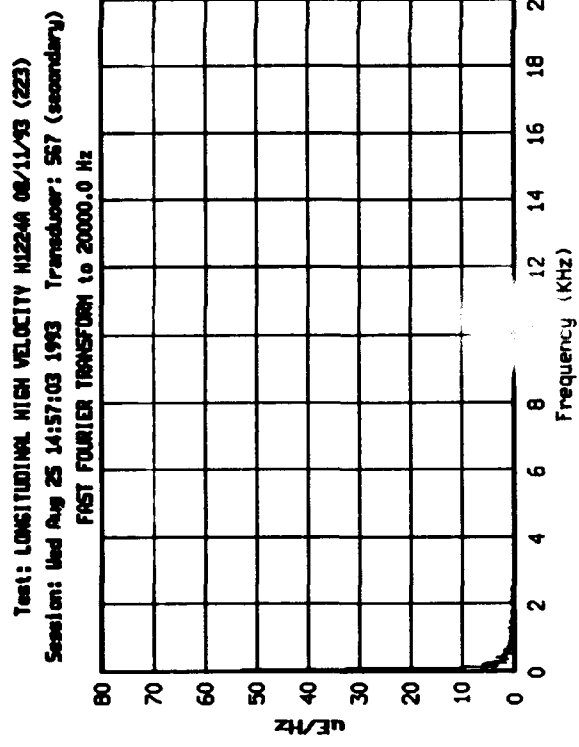


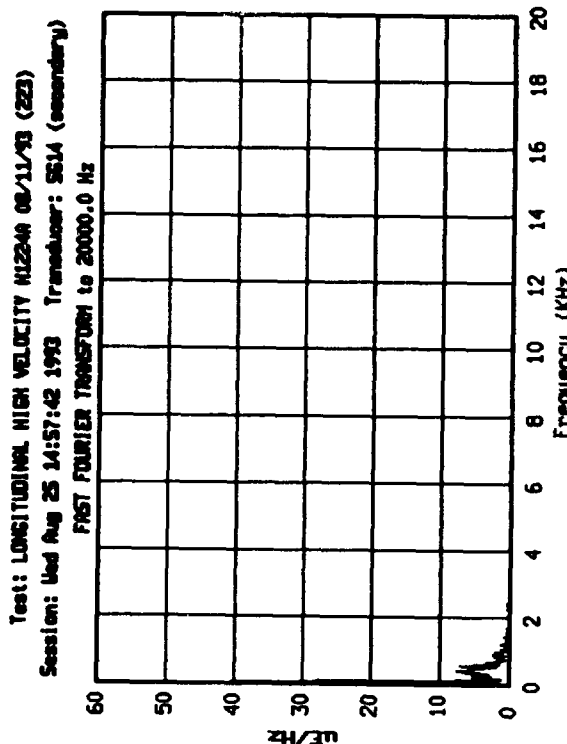
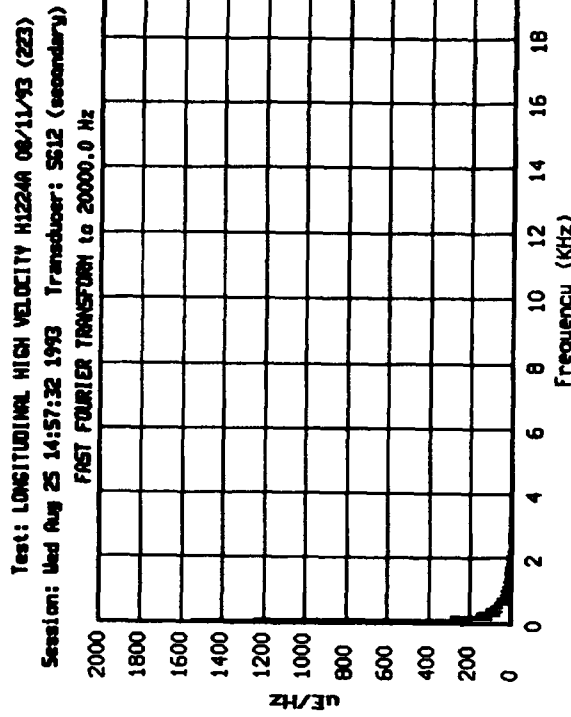
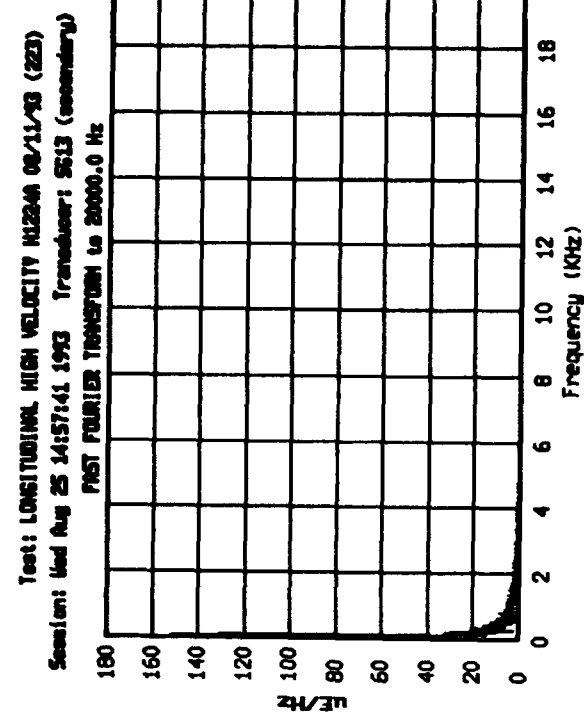
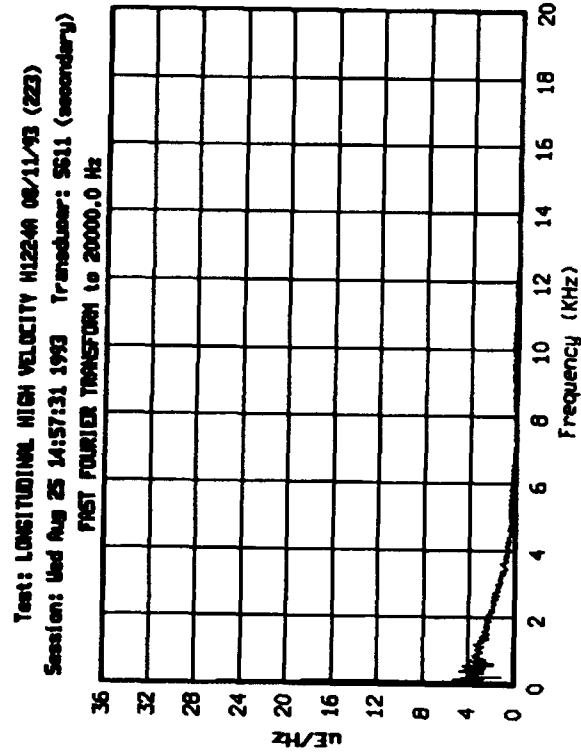


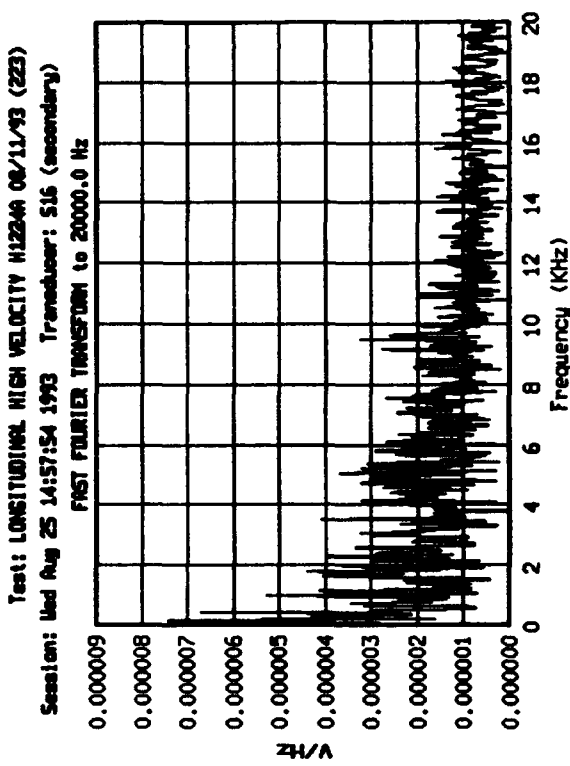
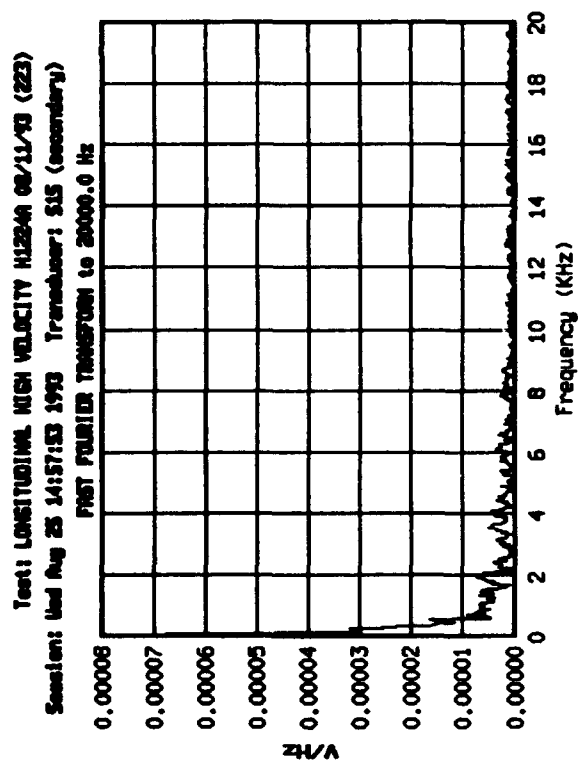






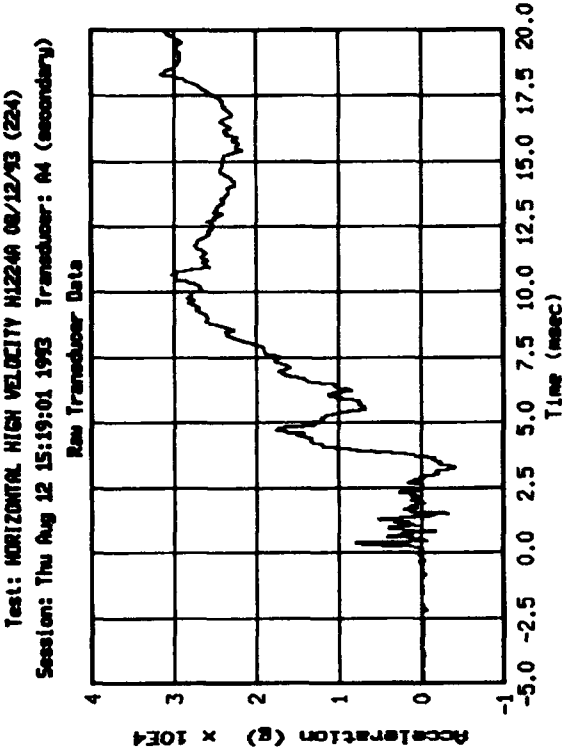
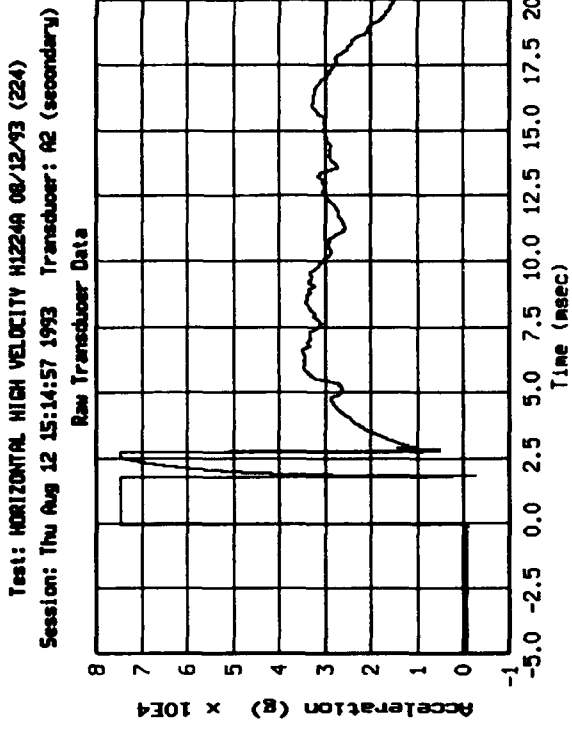
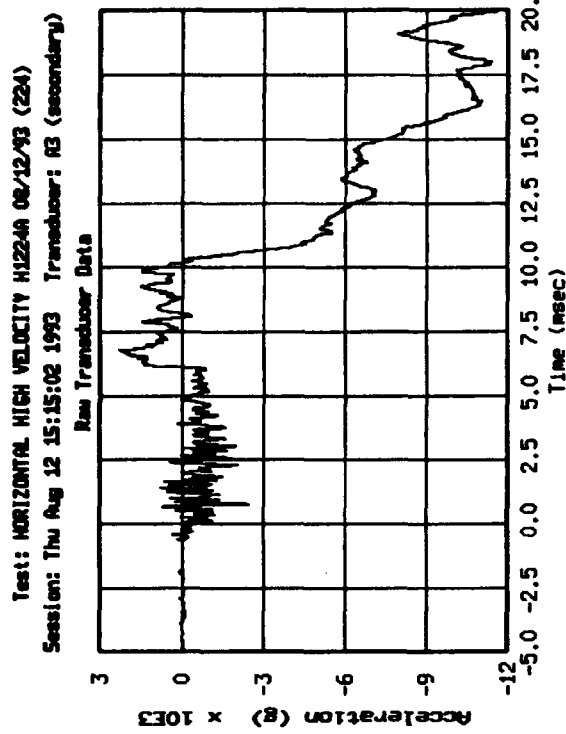
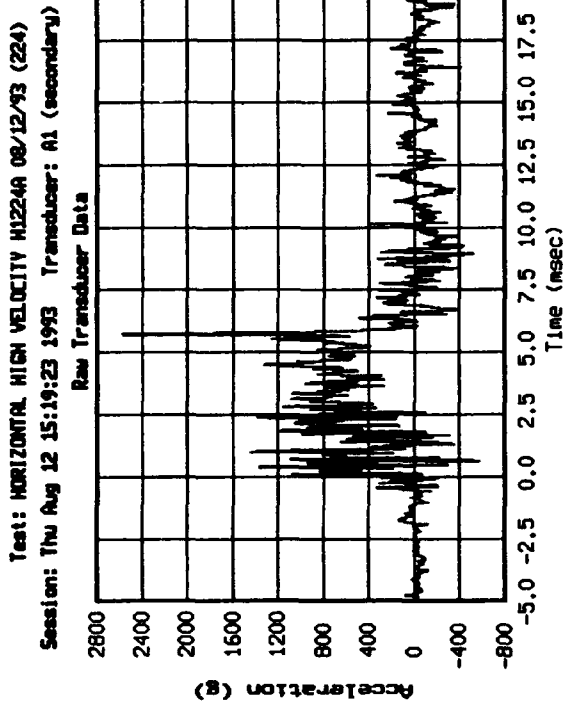


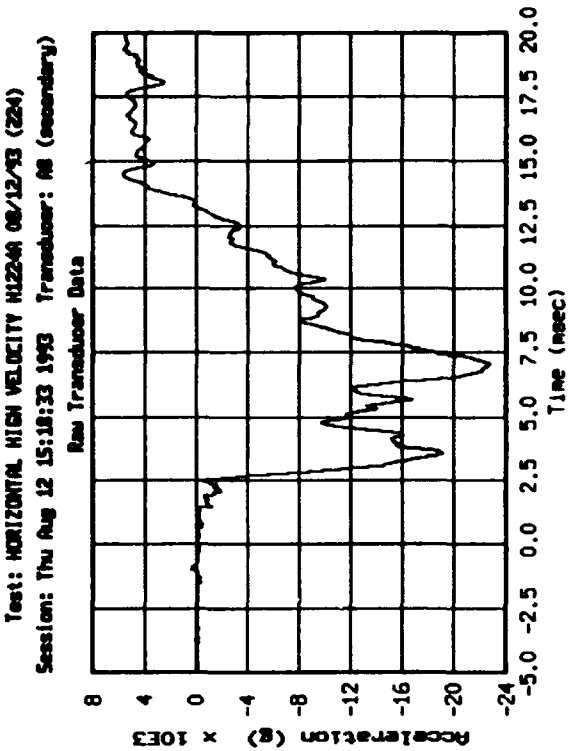
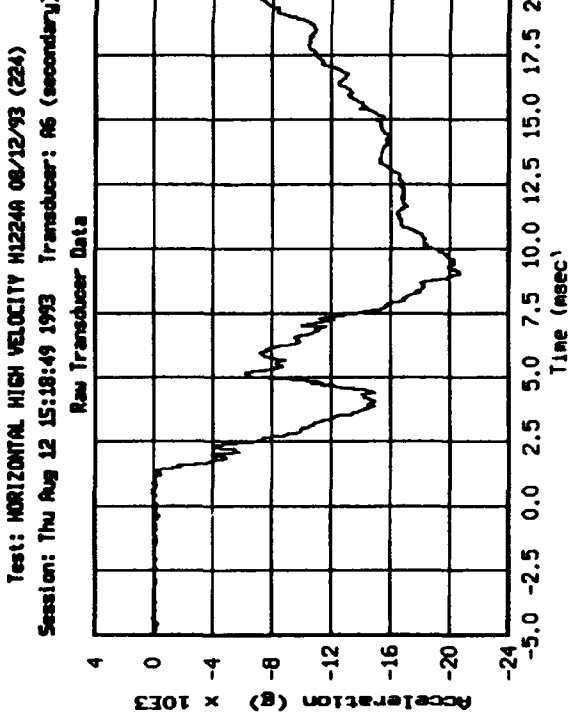
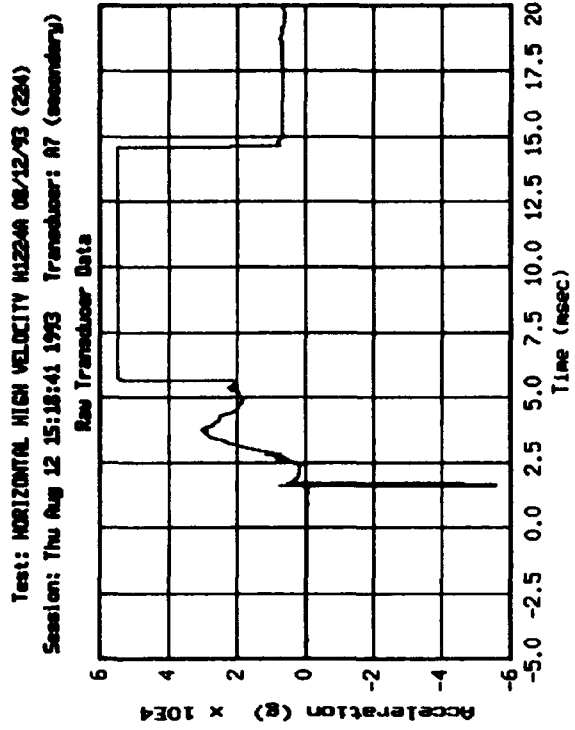
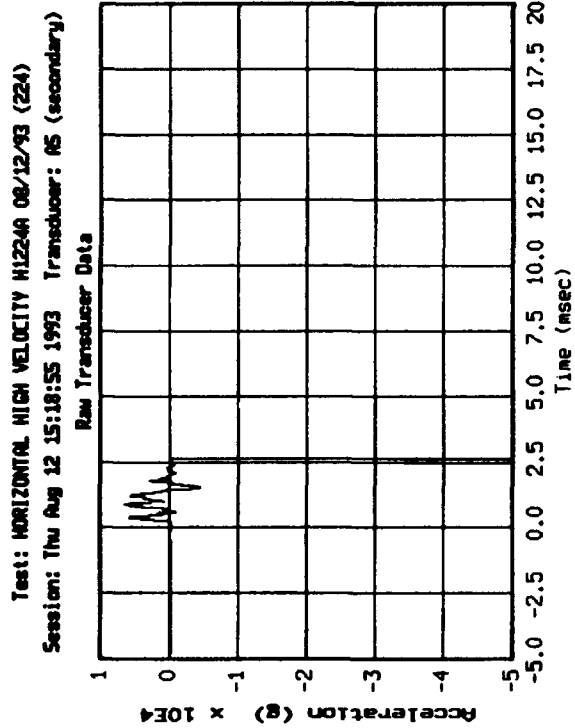


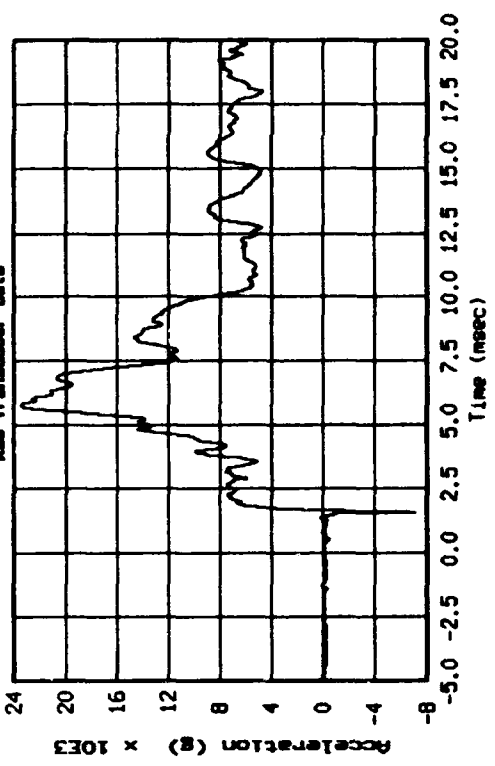
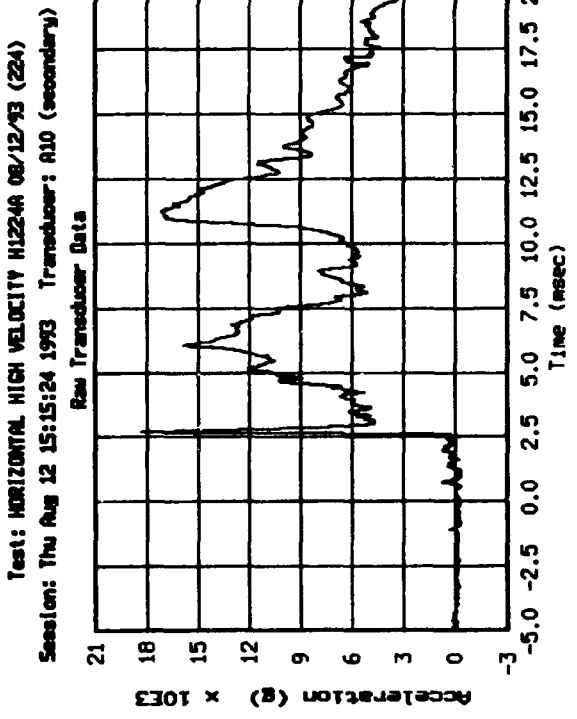
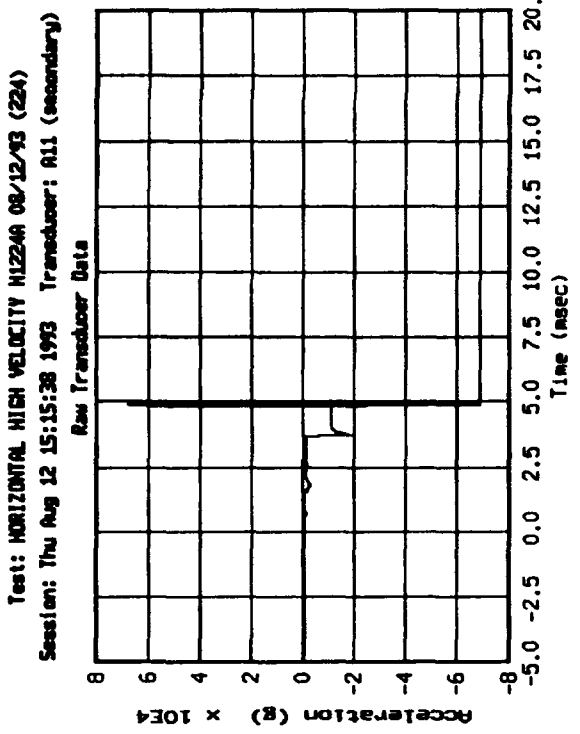
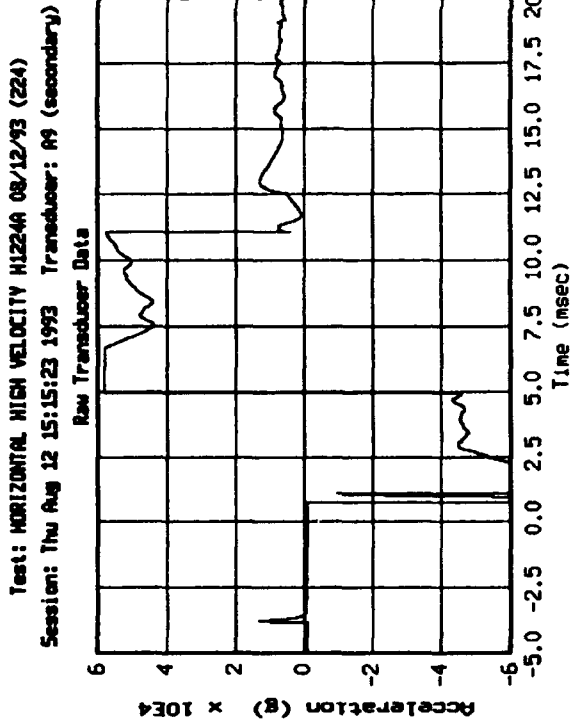


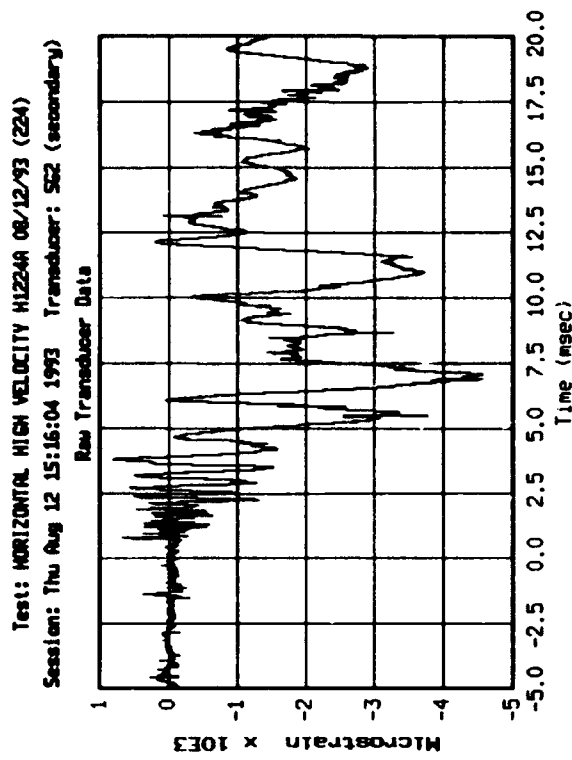
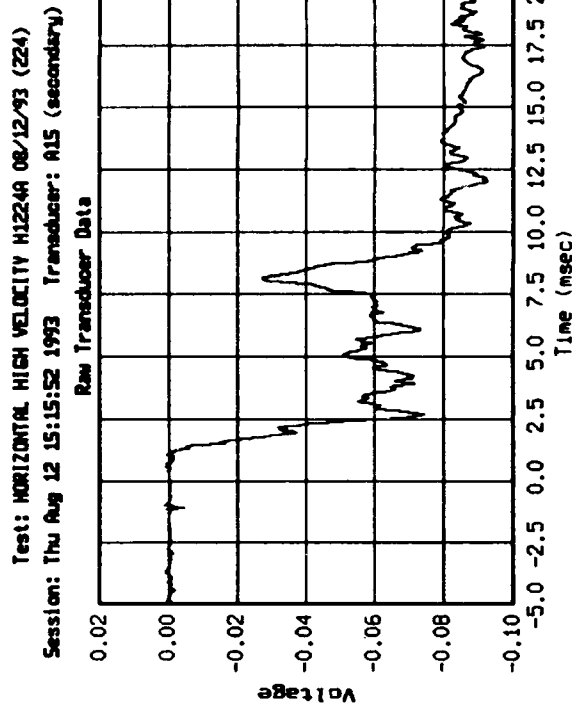
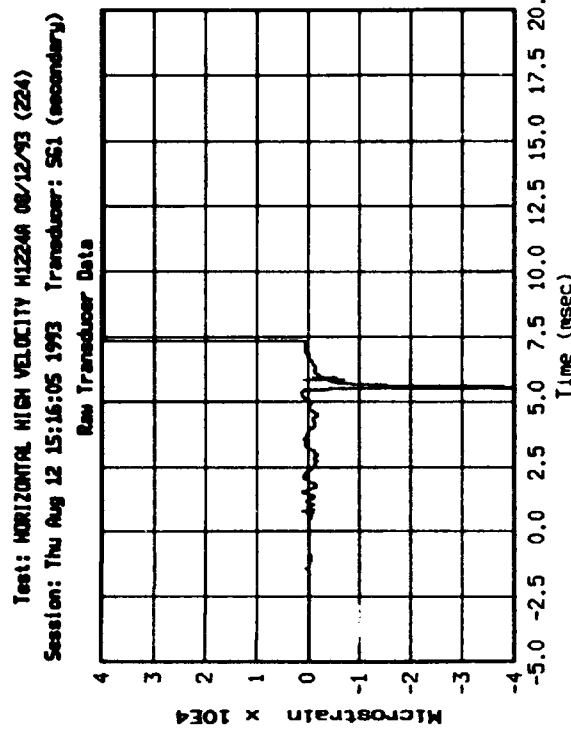
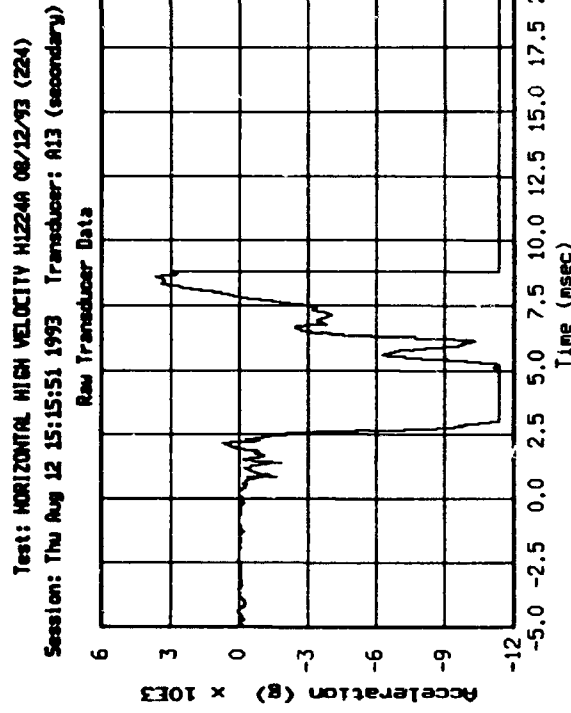
Appendix D. HHV Accelerometer and Strain Gage Data: Raw, Filtered, and Reduced

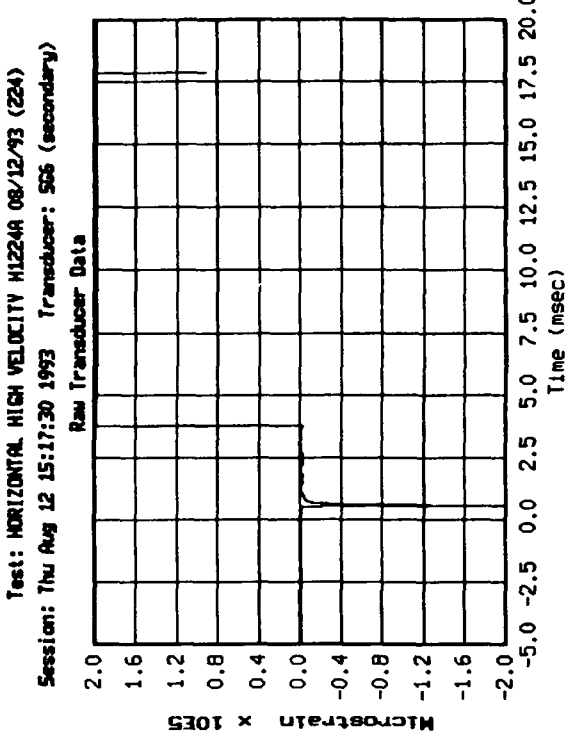
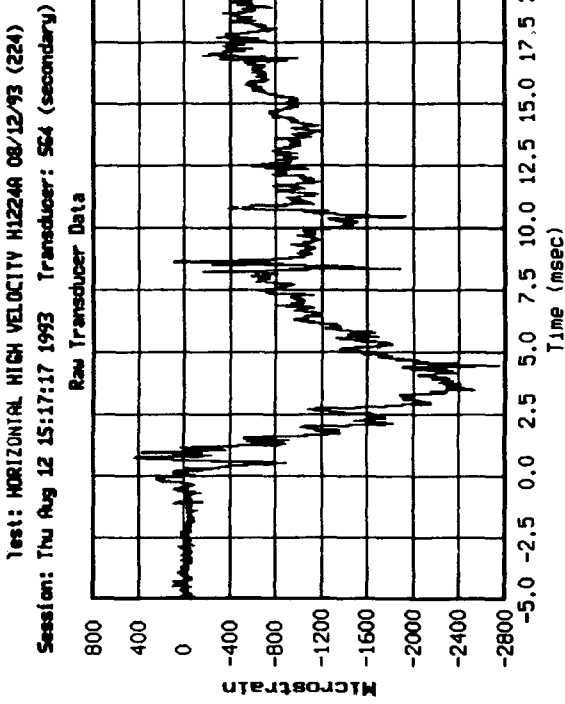
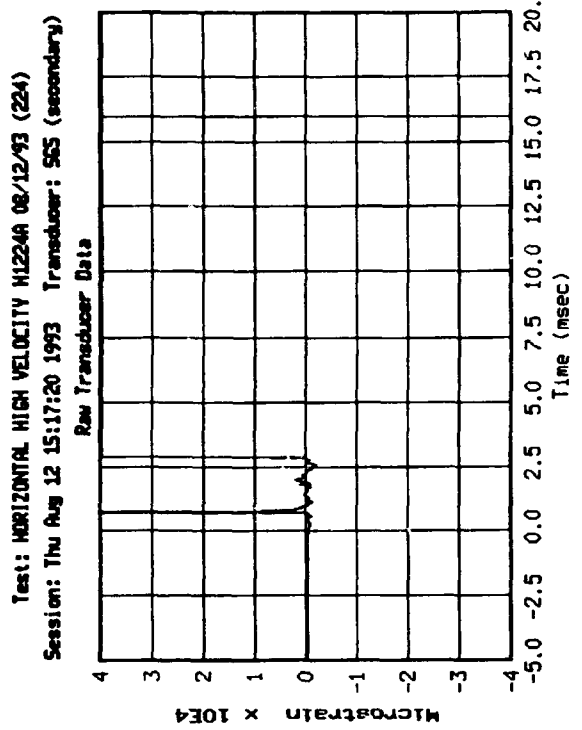
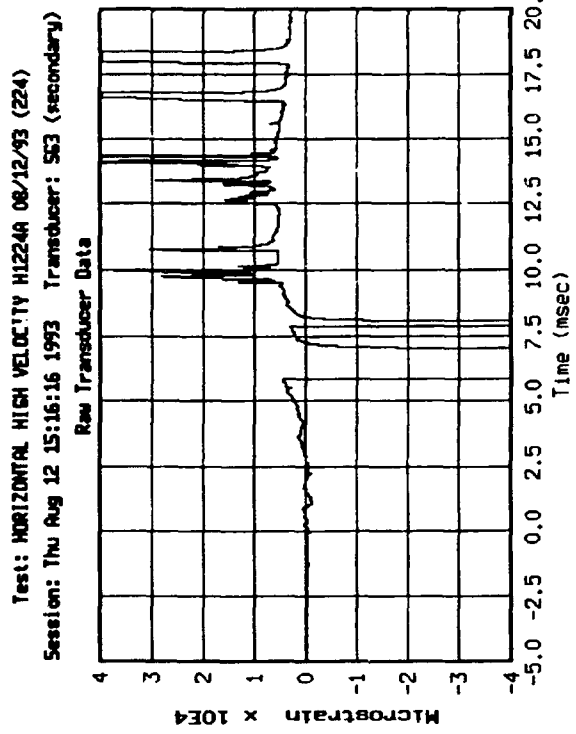
The following pages show raw (unfiltered) acceleration and strain gage data for the Horizontal High-Velocity (HHV) impact test. Following this raw data are plots of filtered data (using a low-pass Butterworth 6-stage filter) with cutoff frequencies of 250 Hz and 2,000 Hz. Integrated acceleration data, yielding velocity versus time plots, are presented to analyze kinetic energy values during the test. And finally, Fast Fourier Transforms (FFTs) for each raw data channel are included to analyze acceleration and strain amplitudes in the frequency domain.

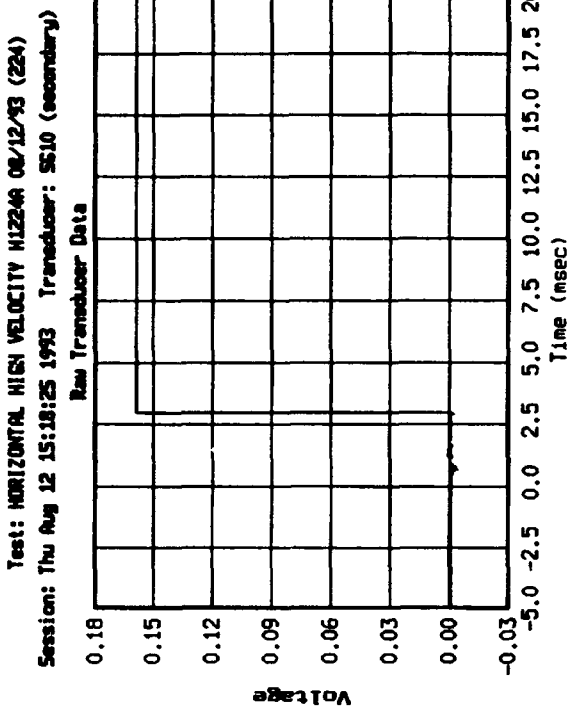
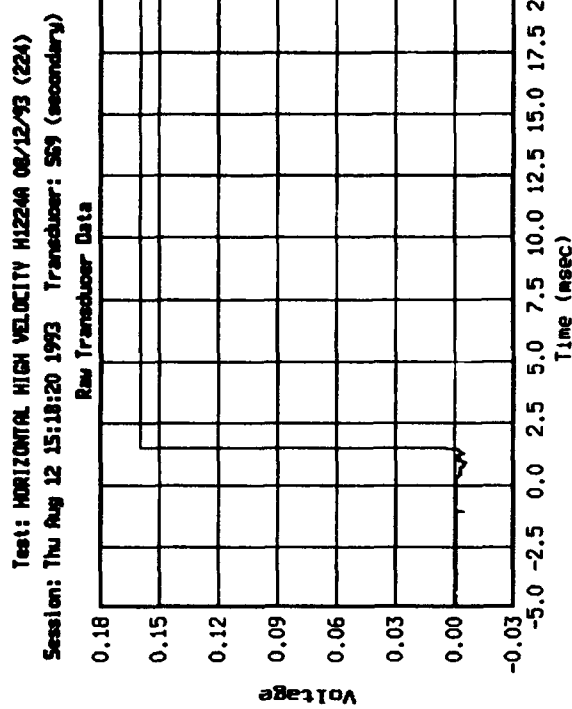
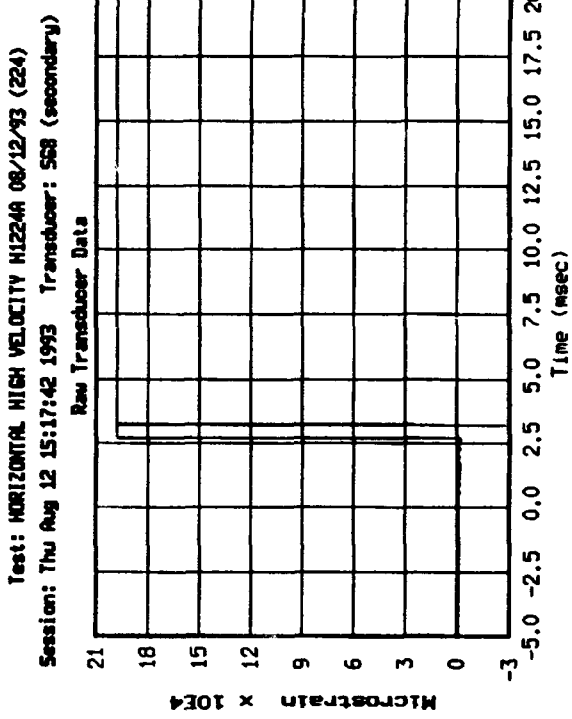
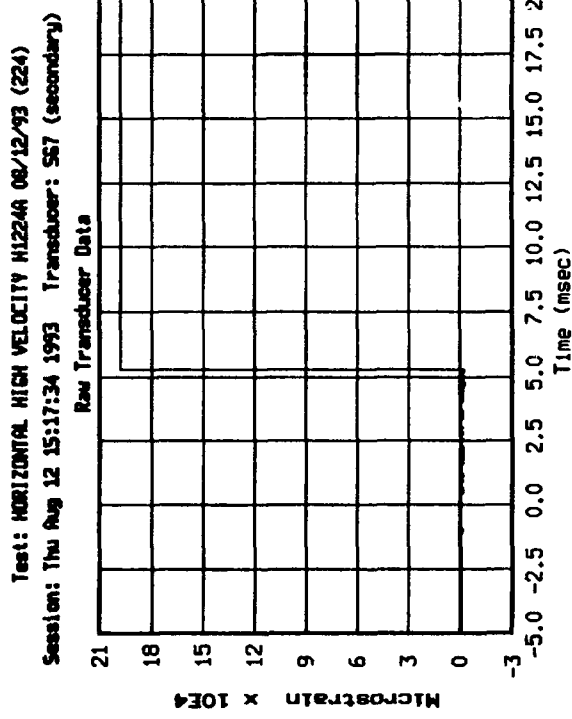


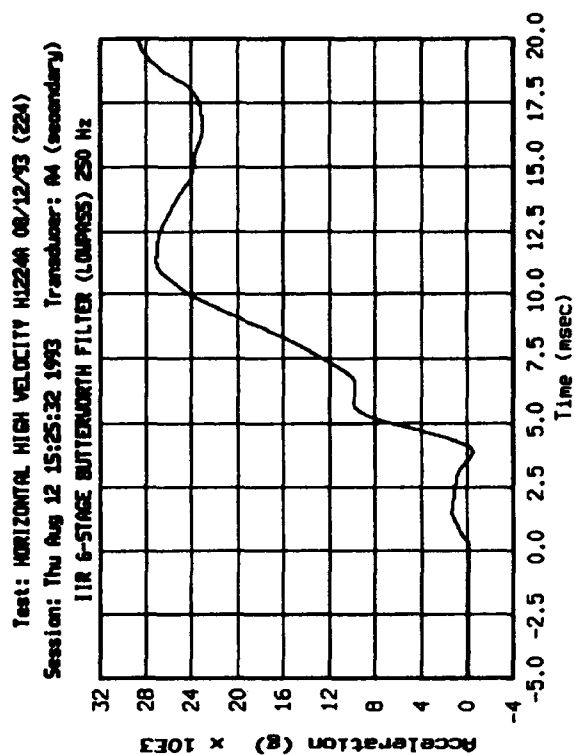
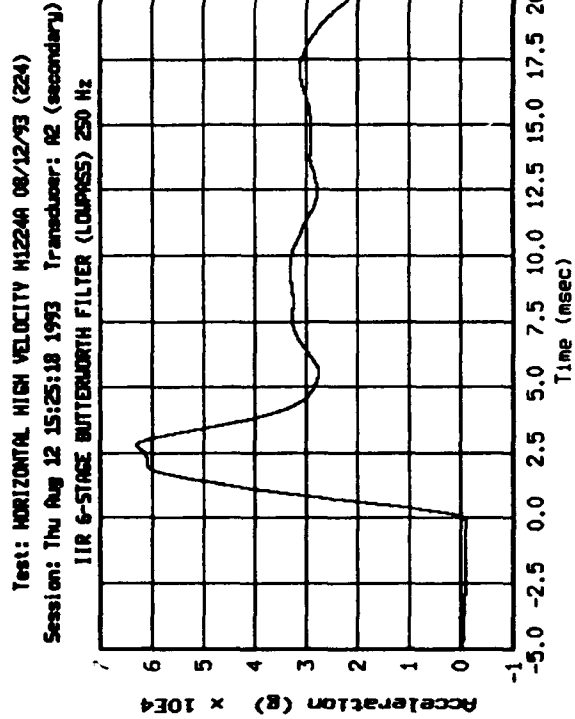
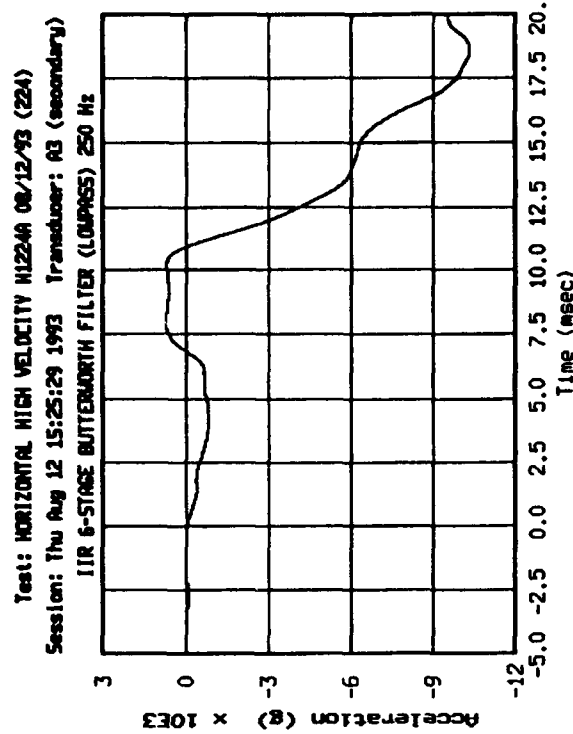
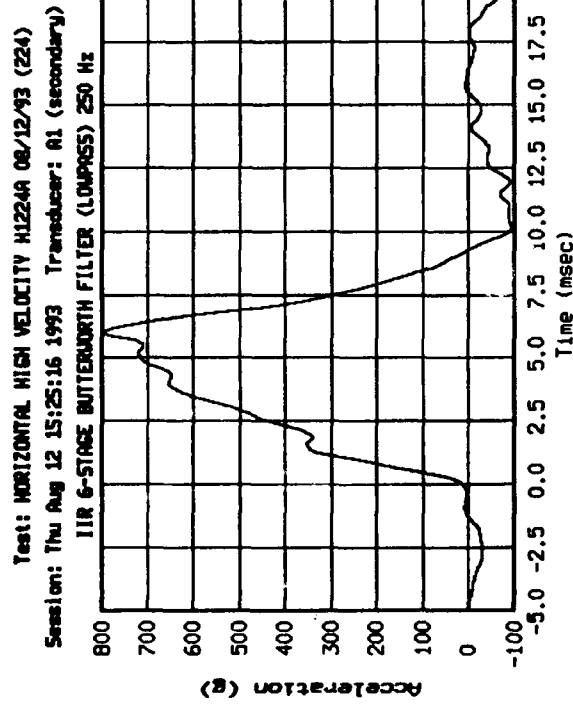


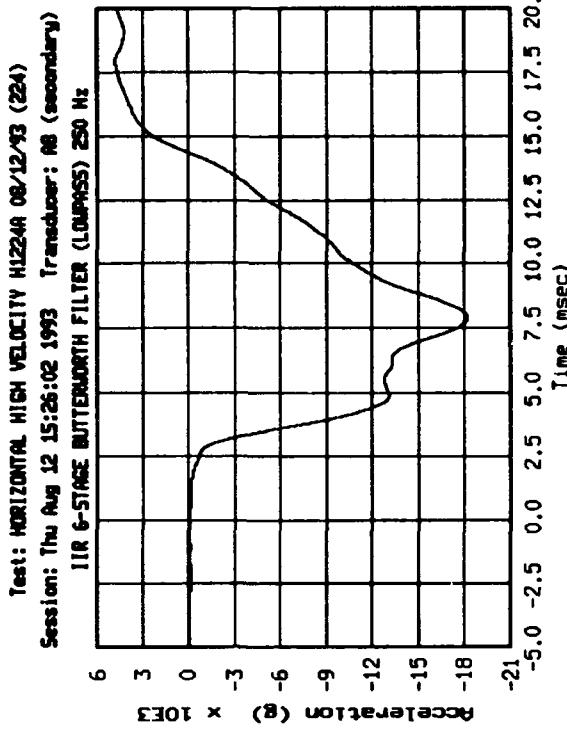
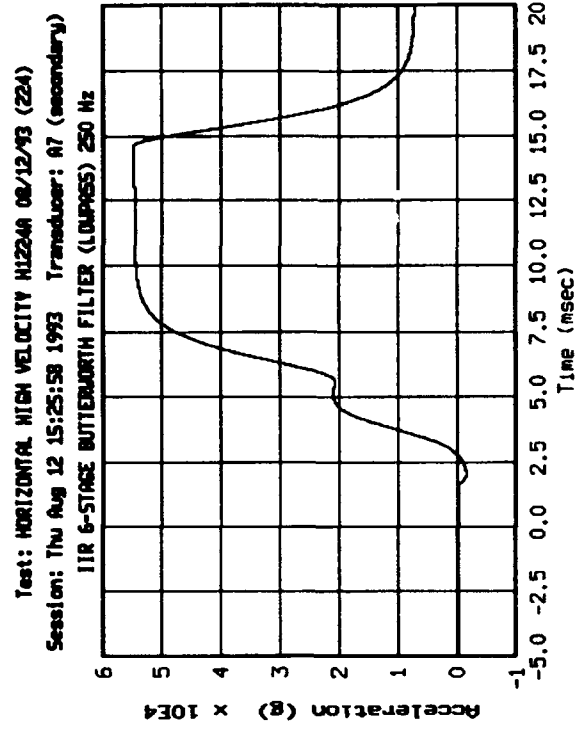
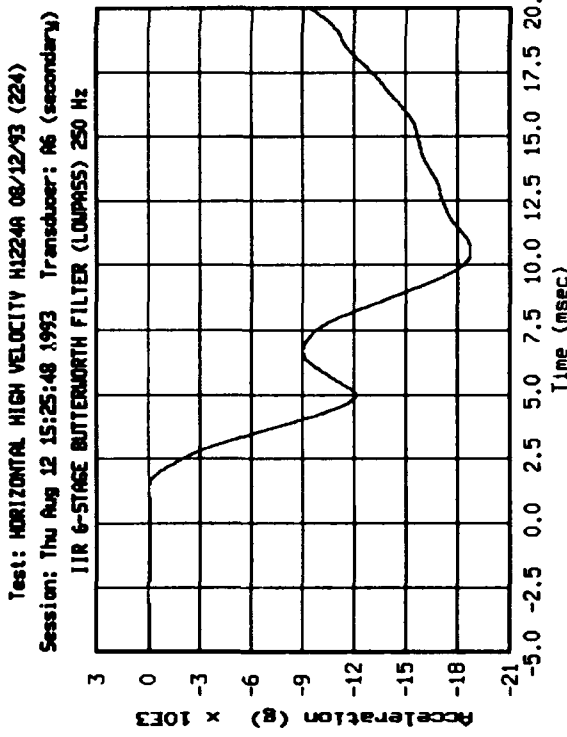
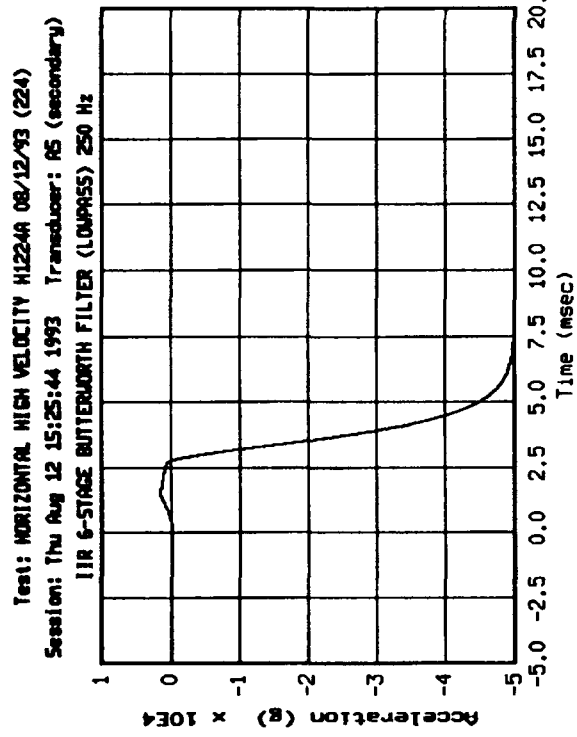


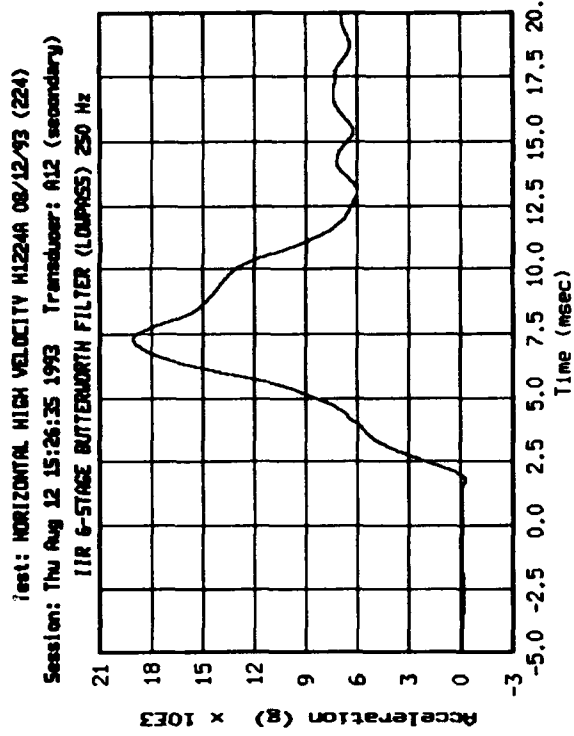
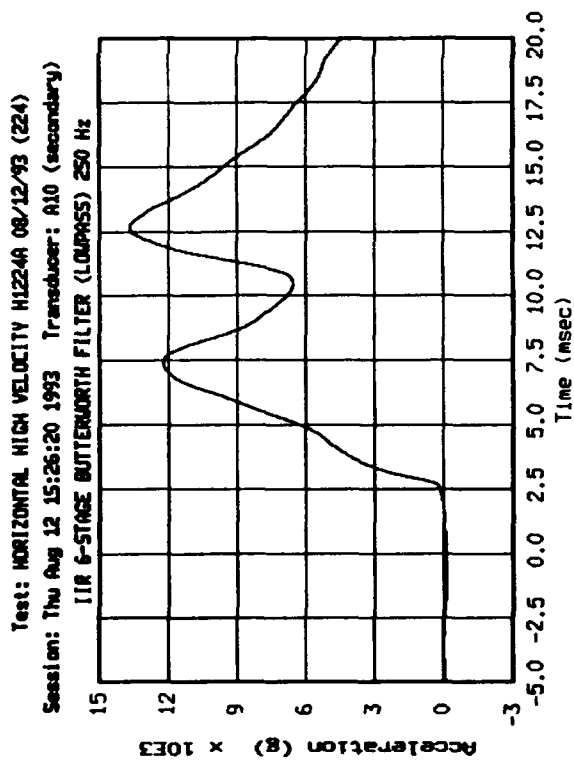
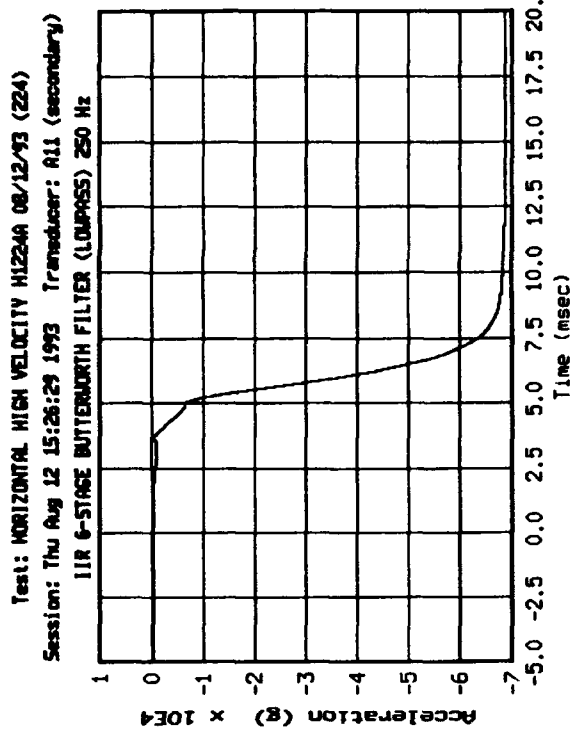
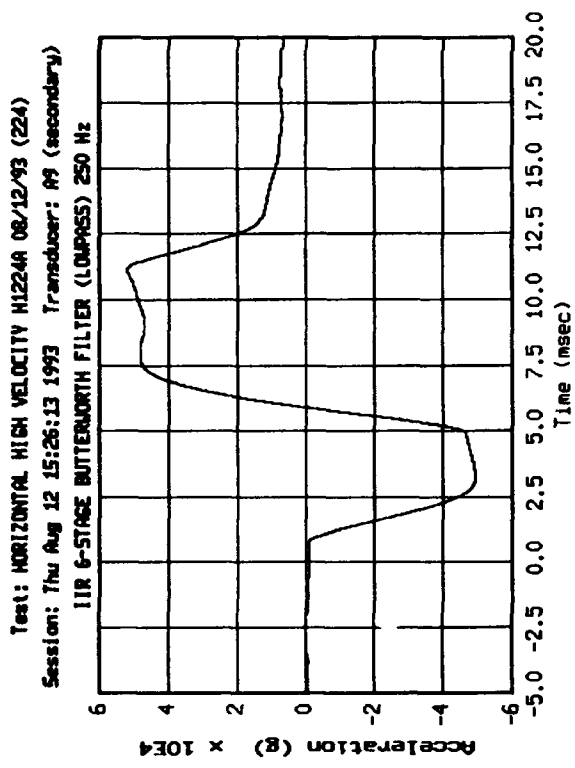


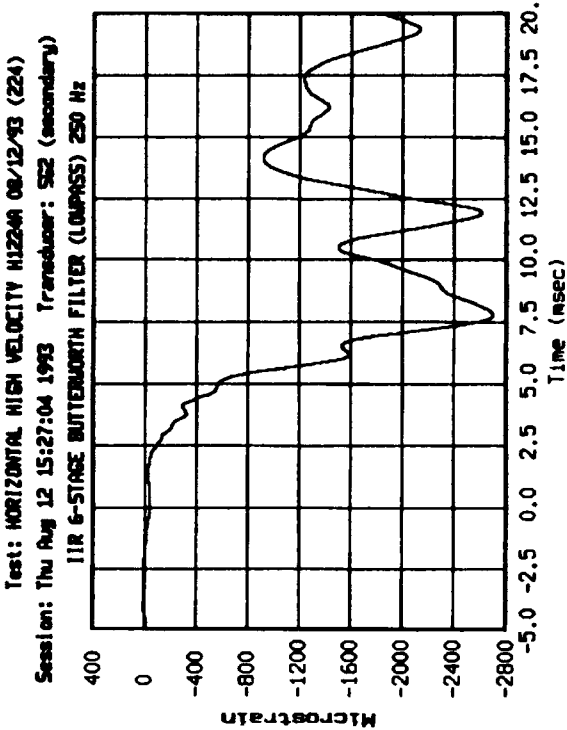
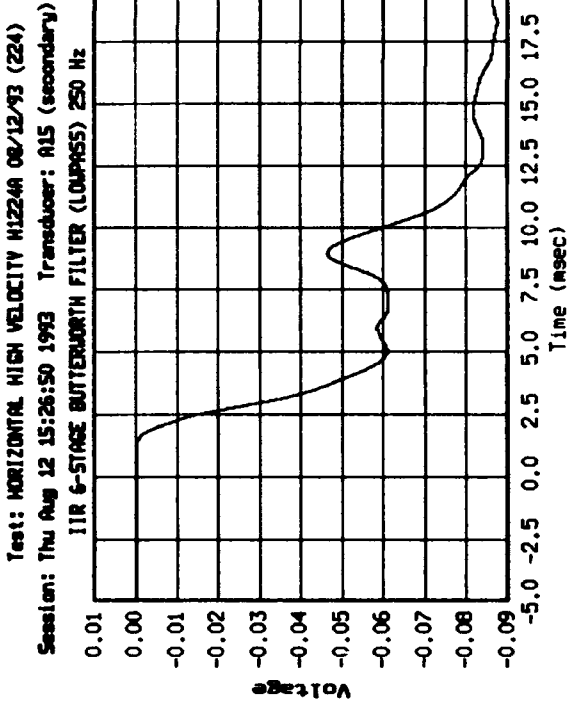
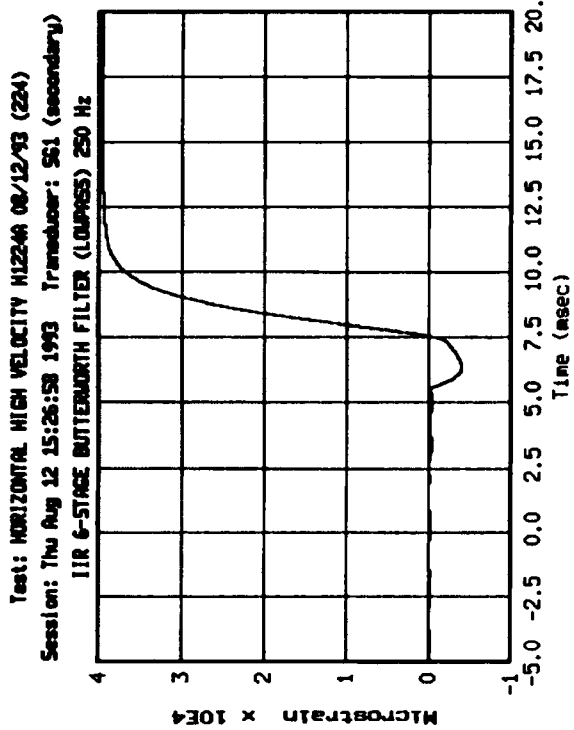
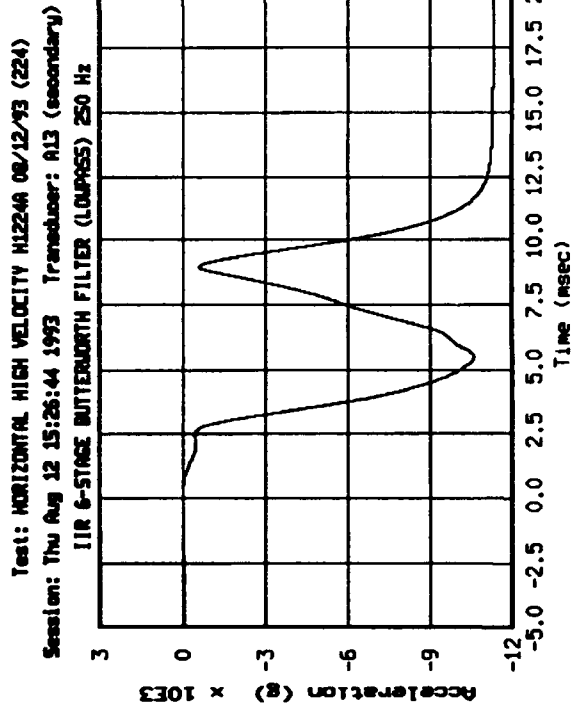


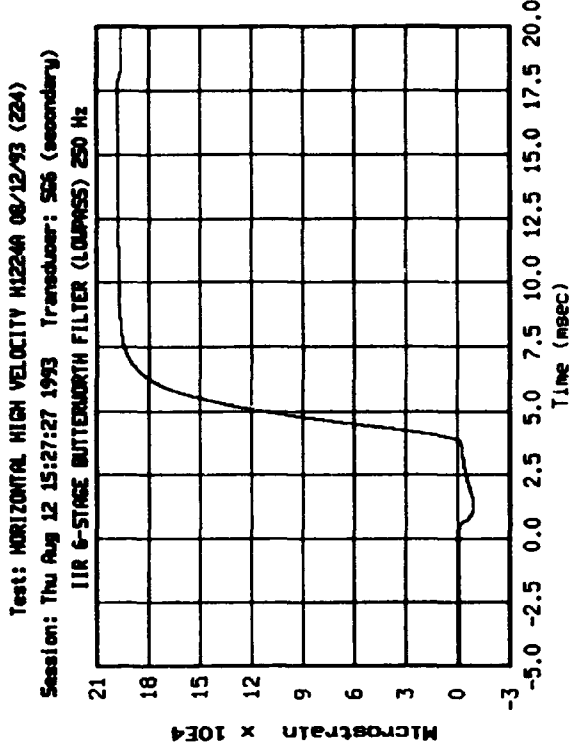
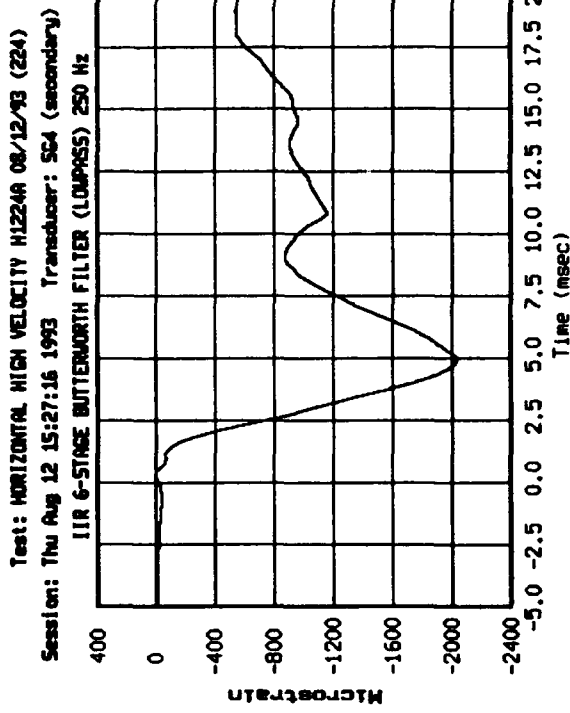
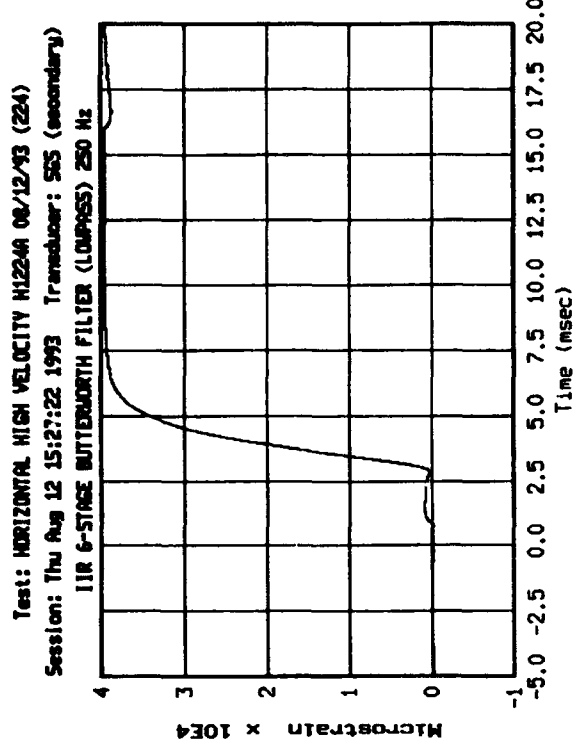
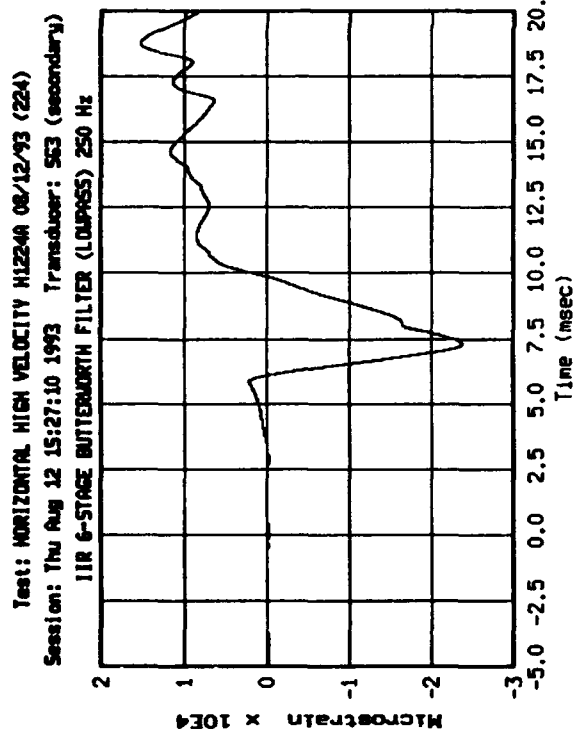


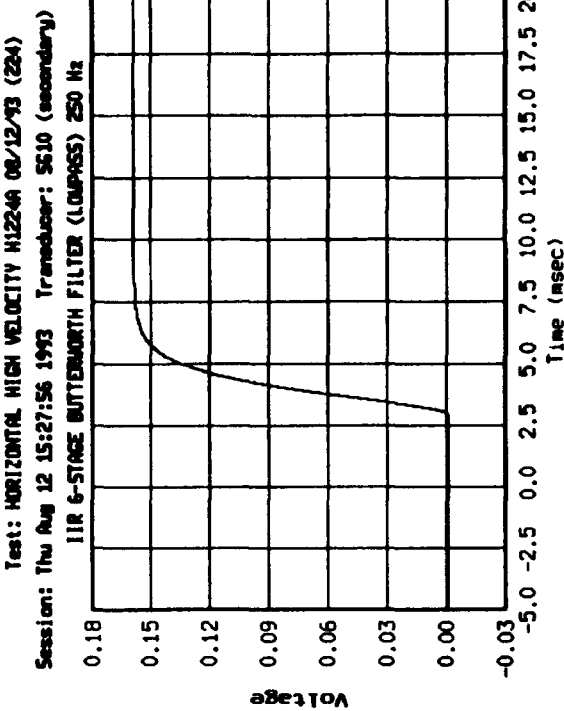
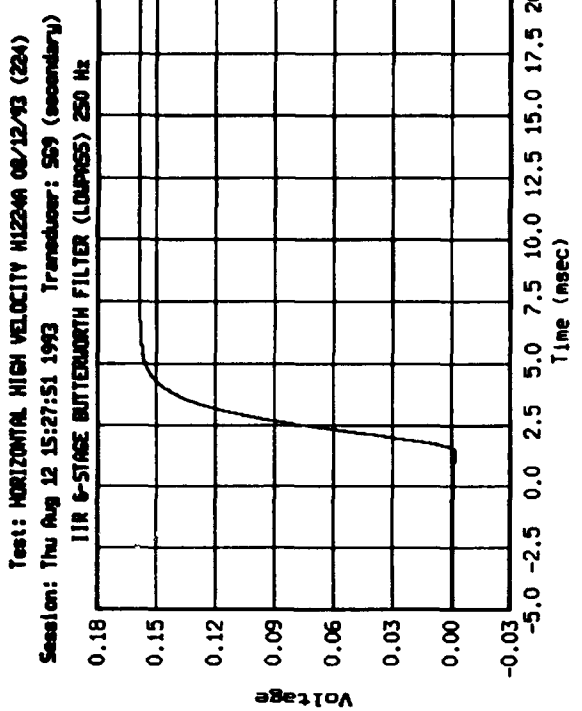
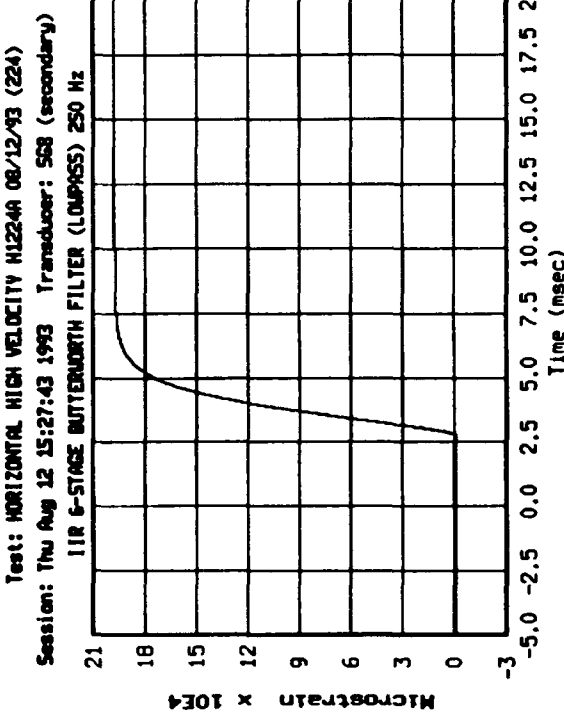
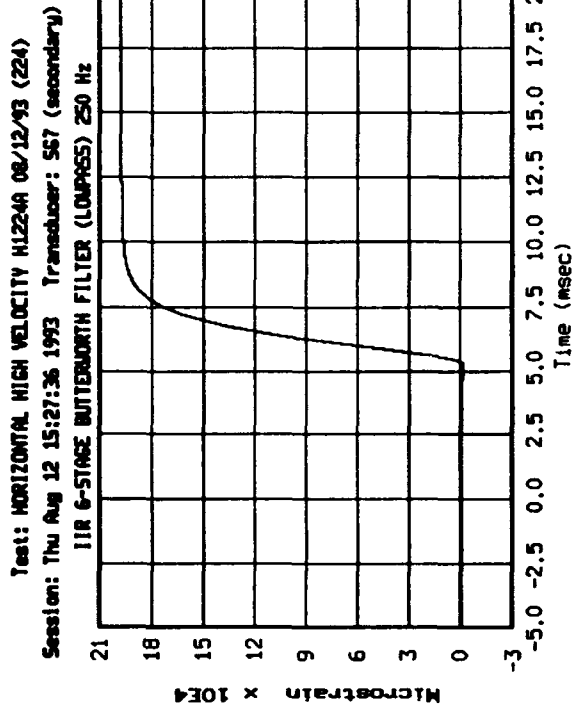


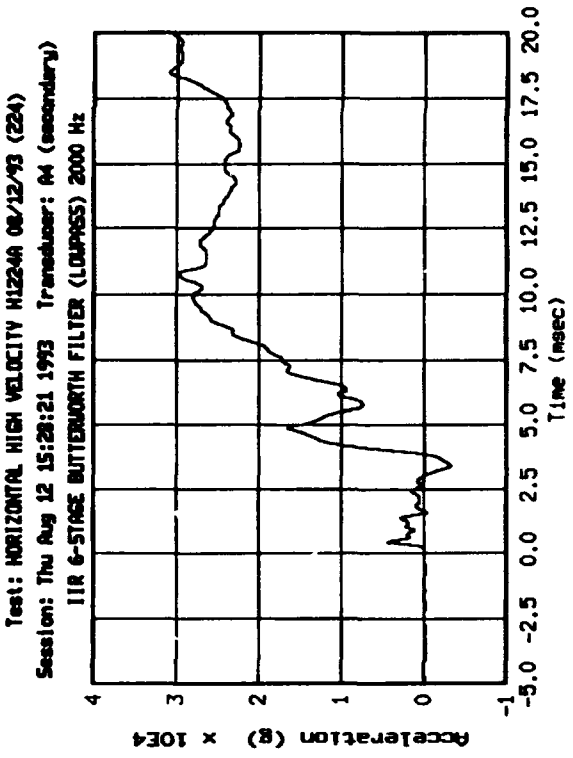
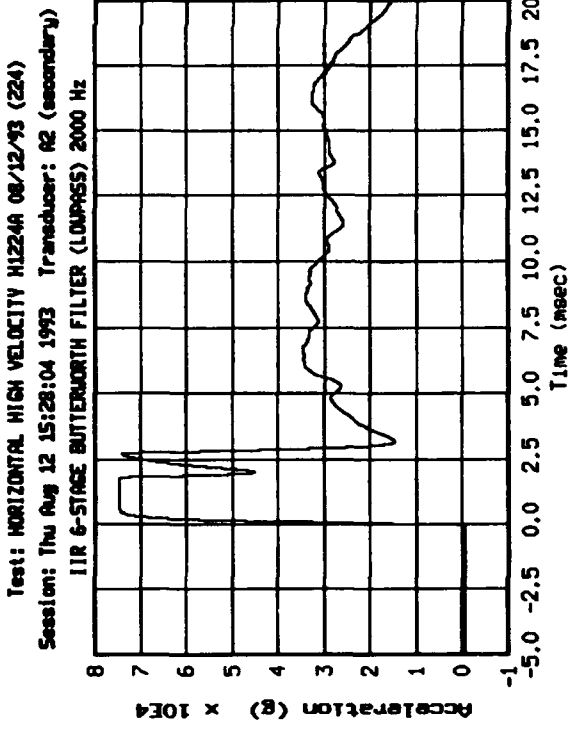
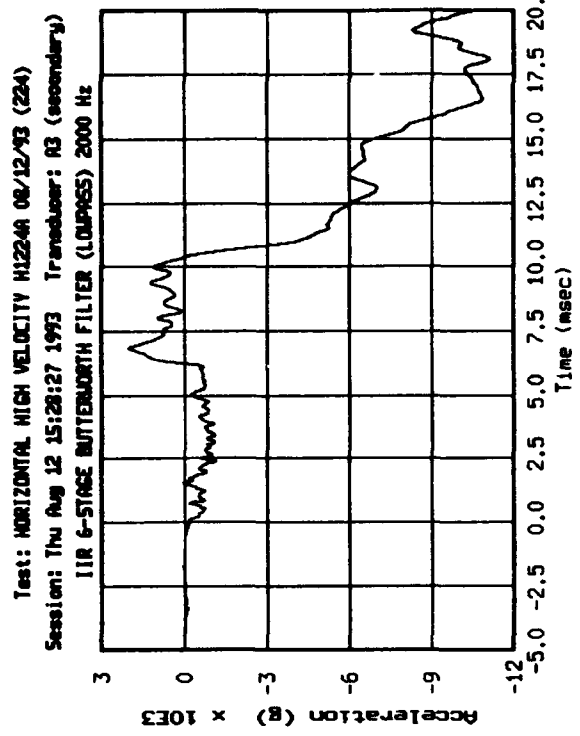
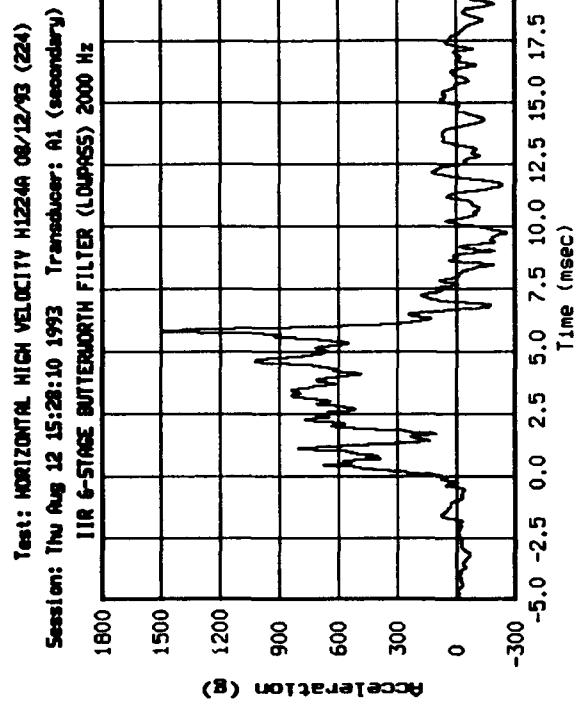


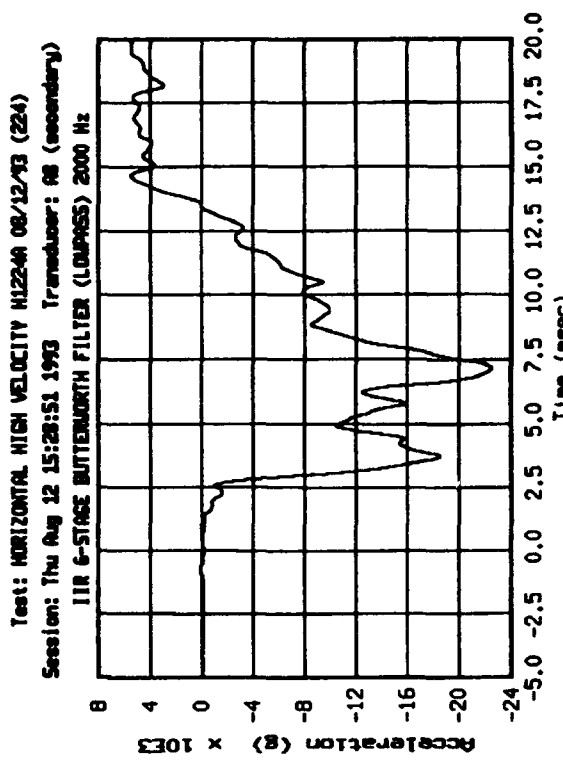
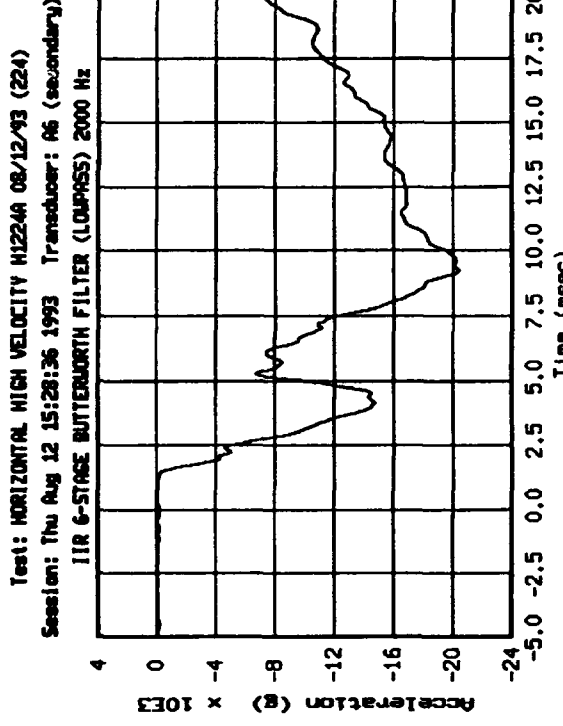
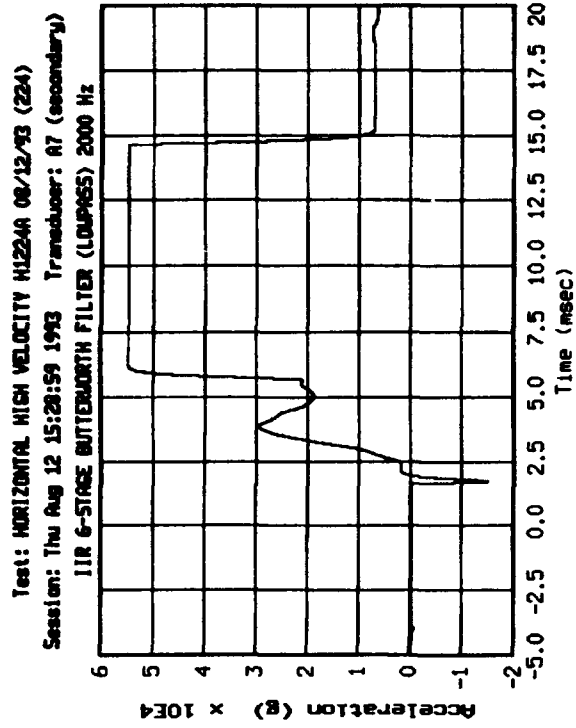
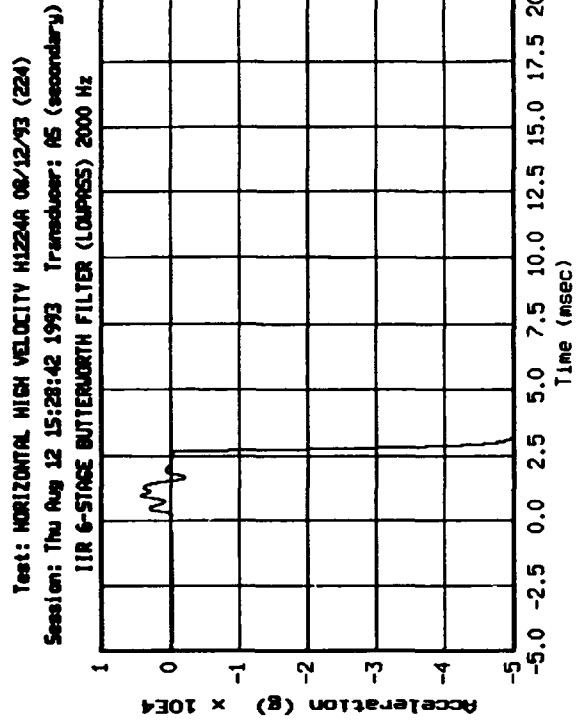


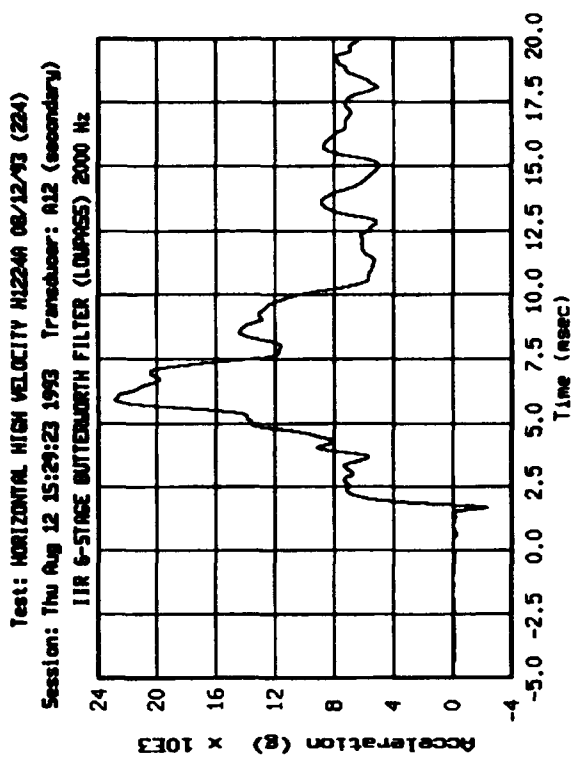
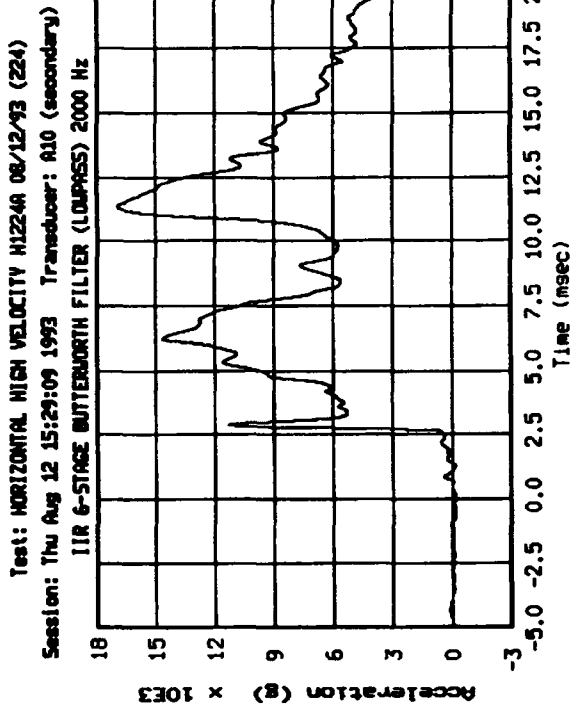
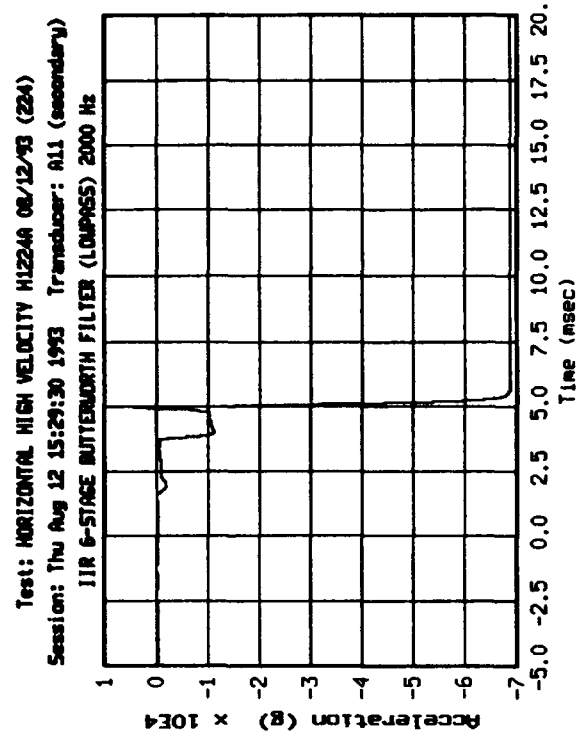
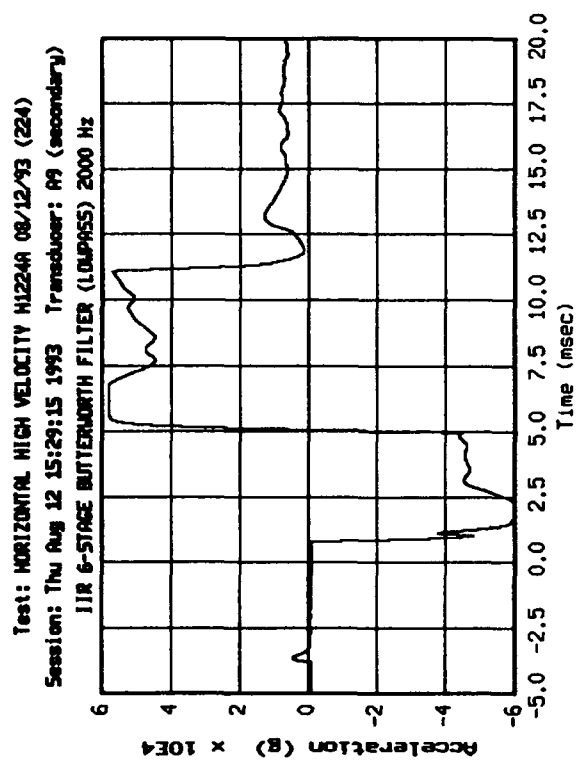


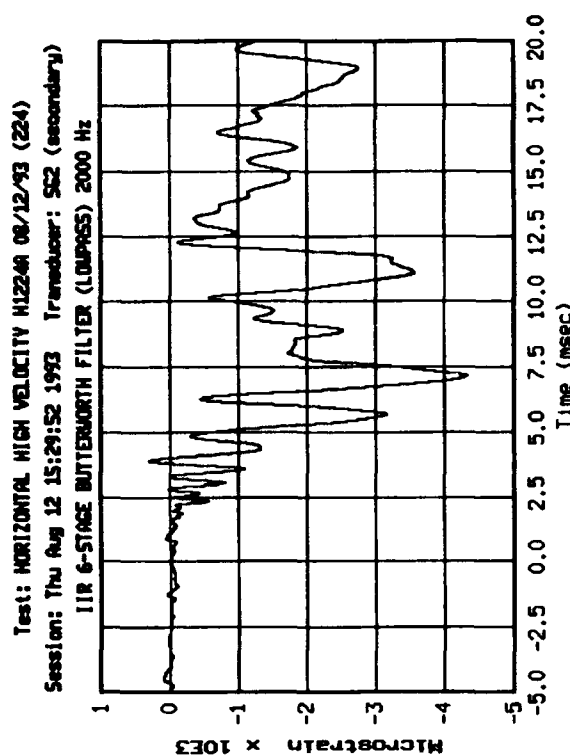
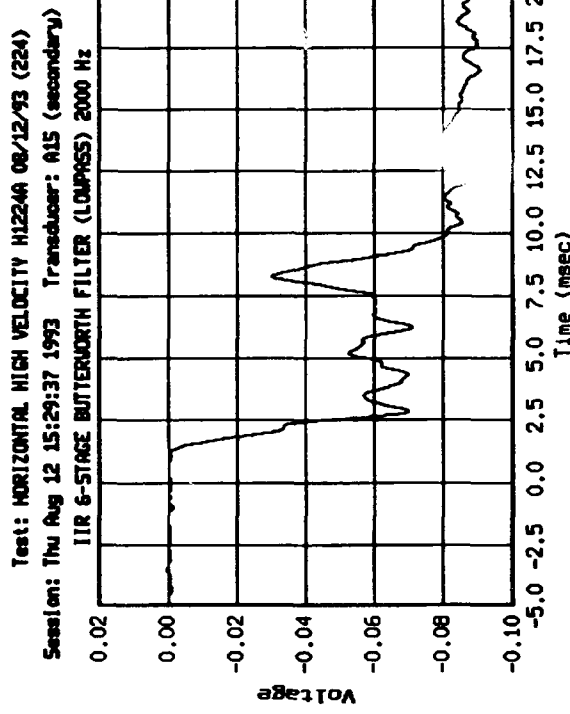
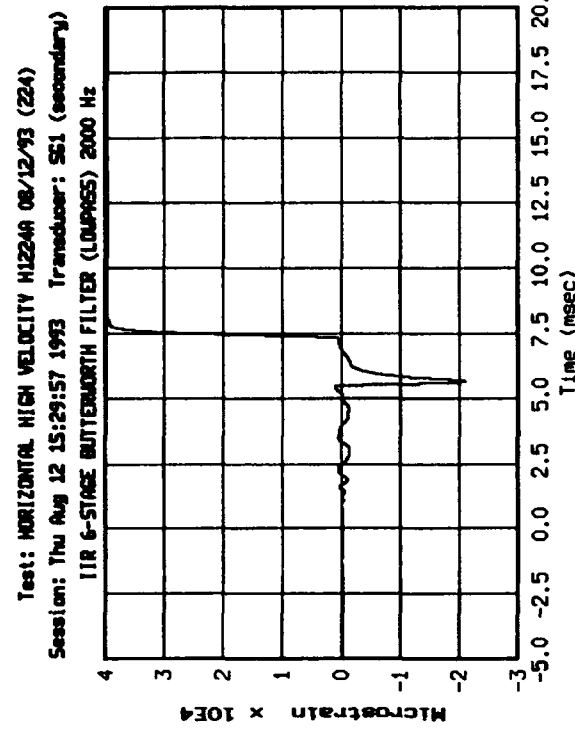
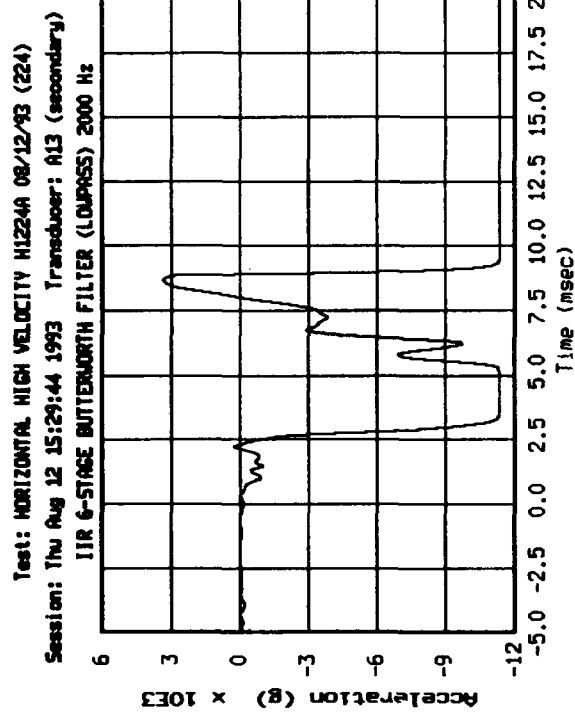


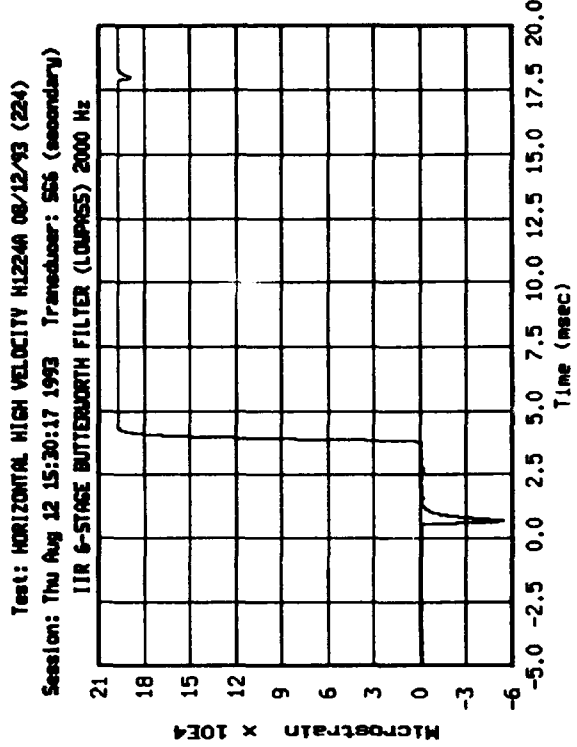
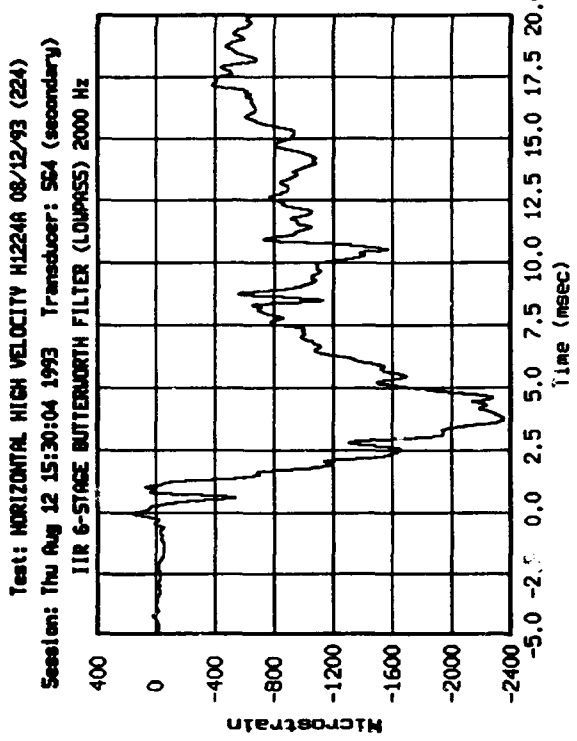
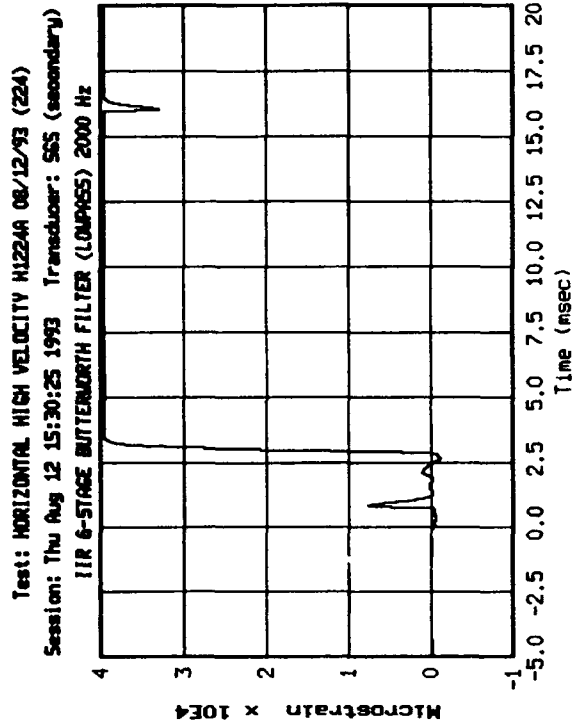
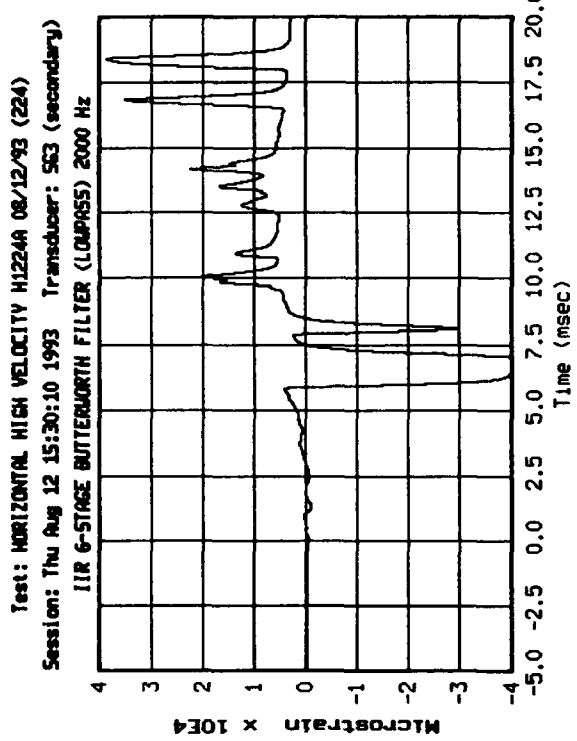


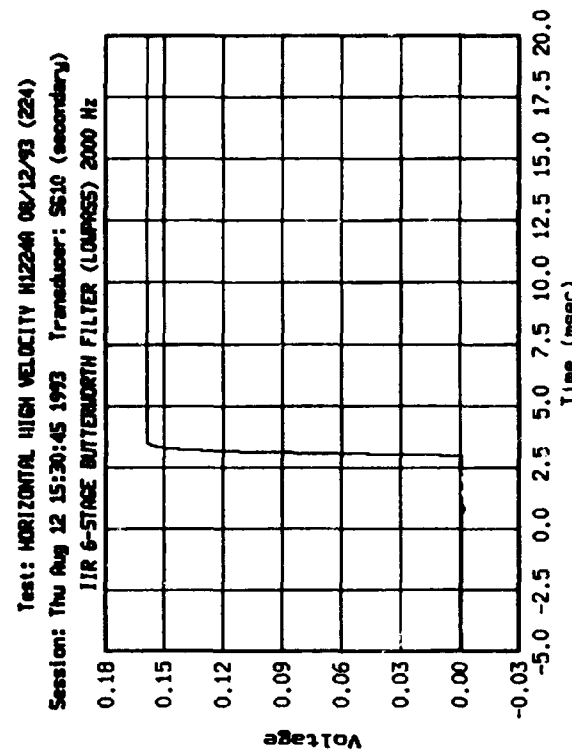
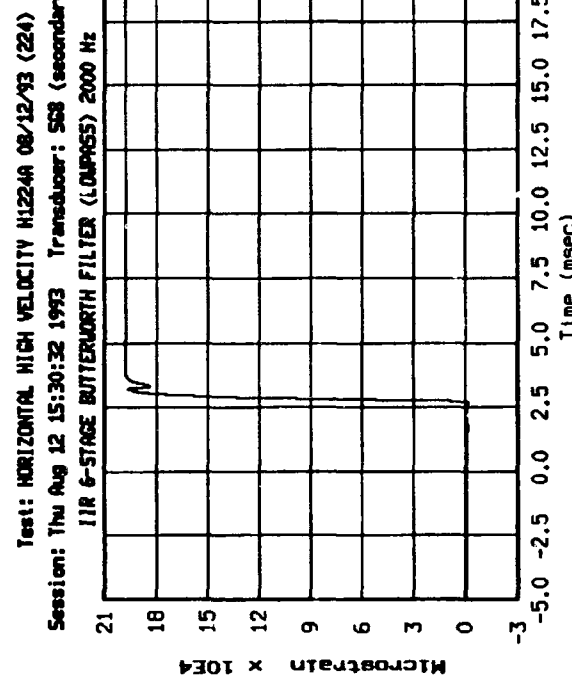
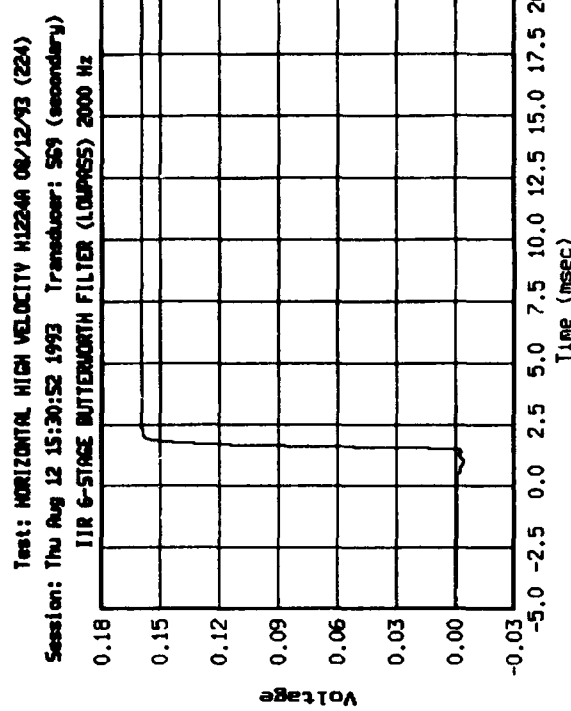
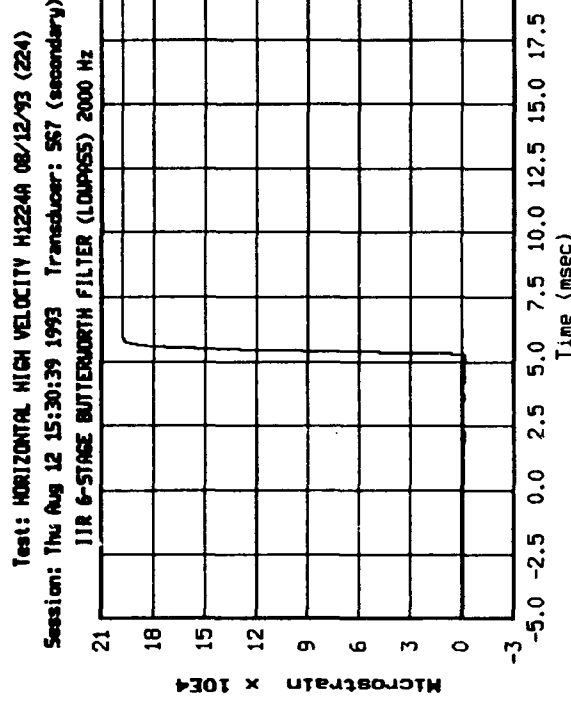


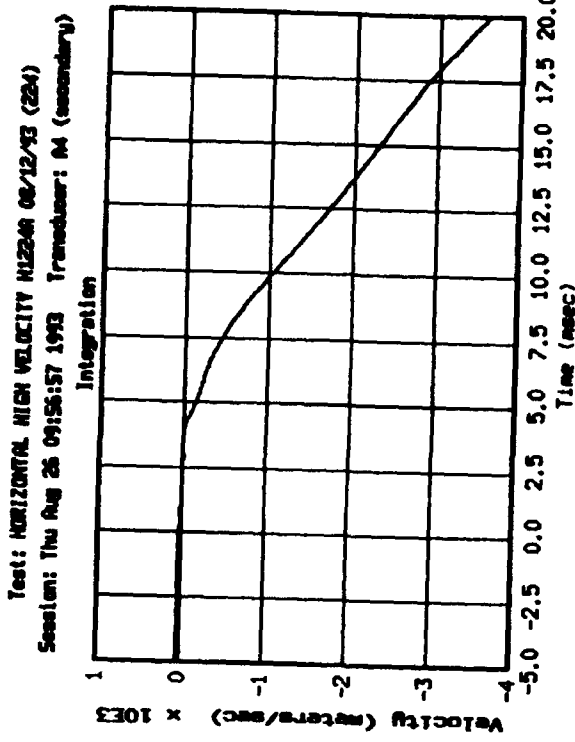
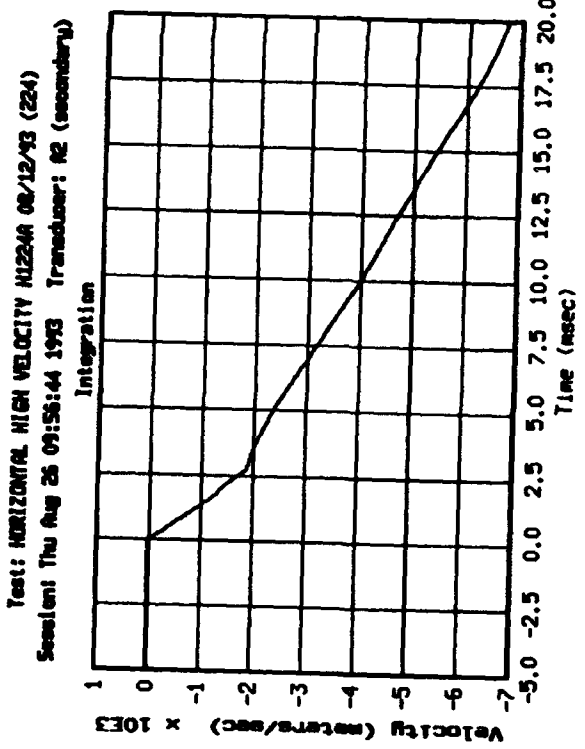
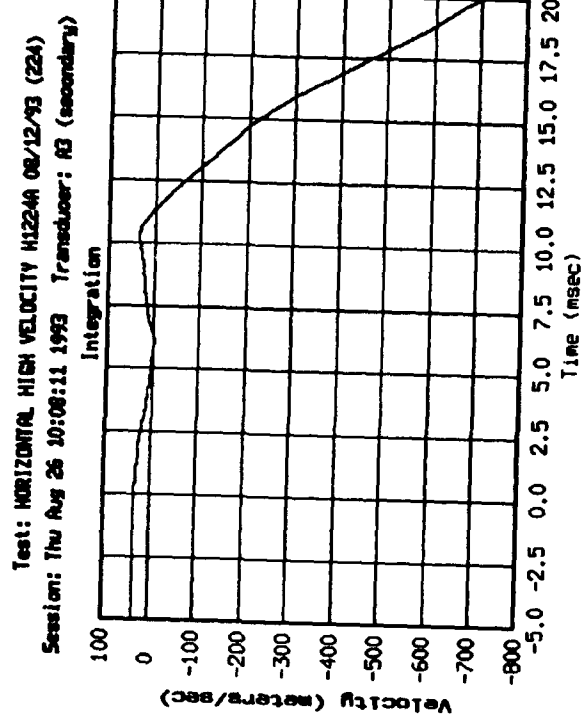
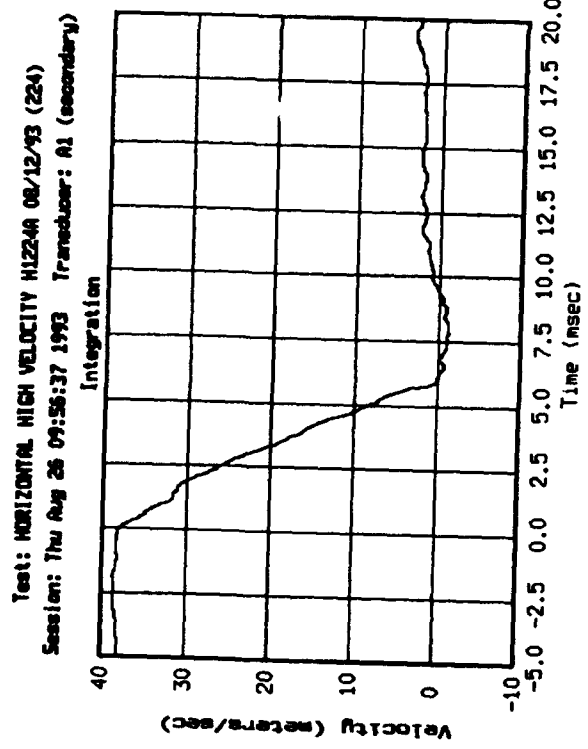


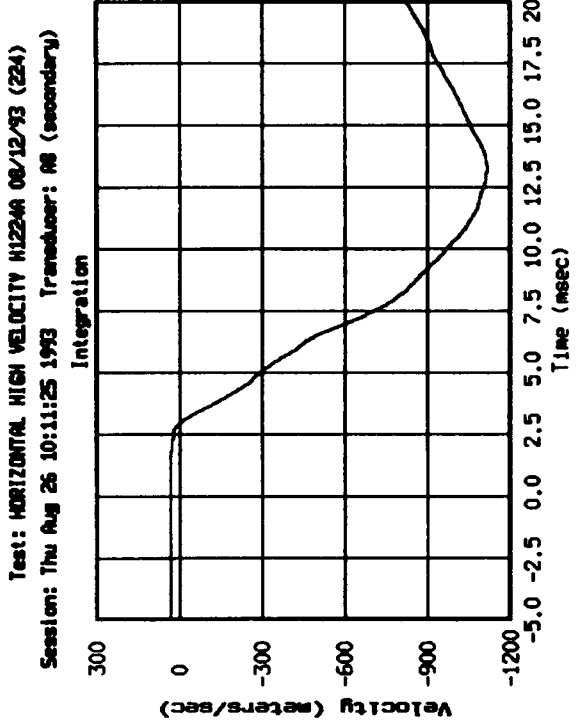
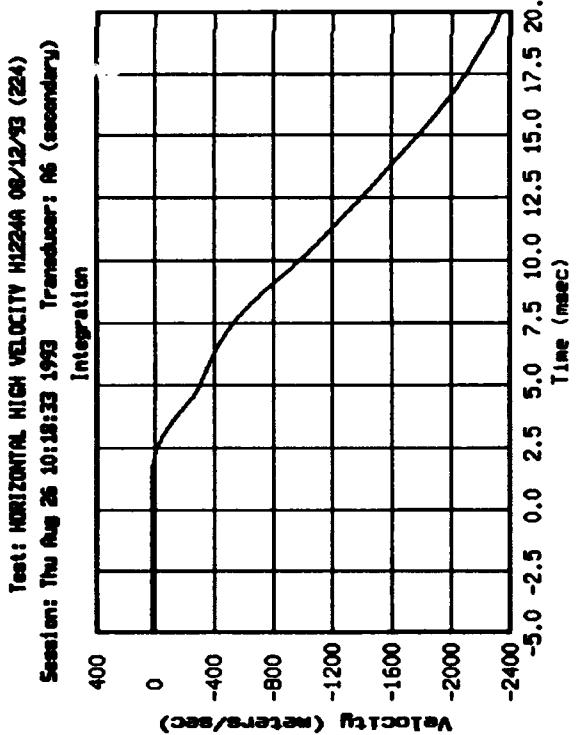
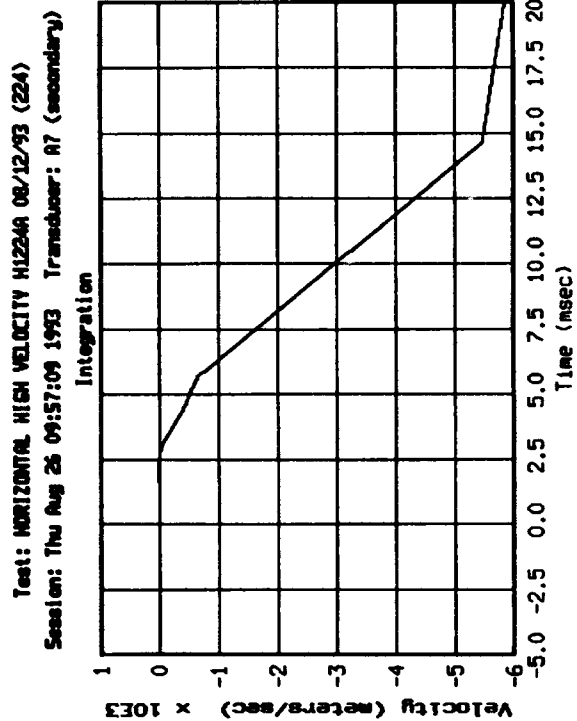
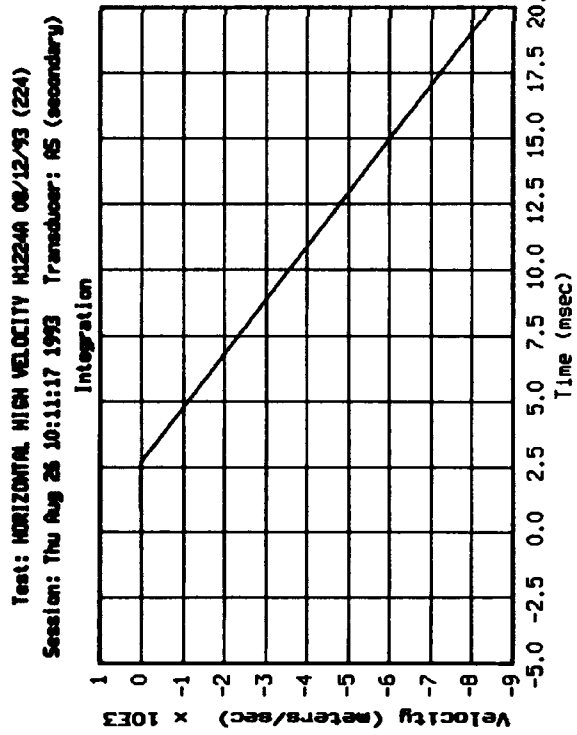


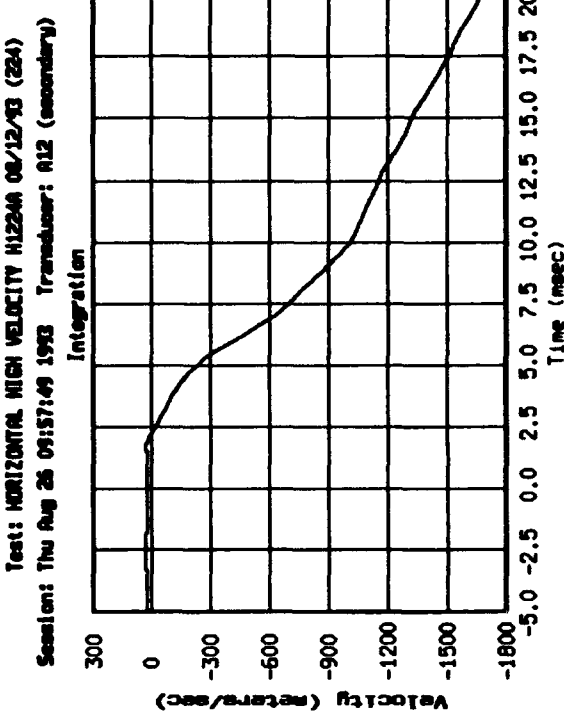
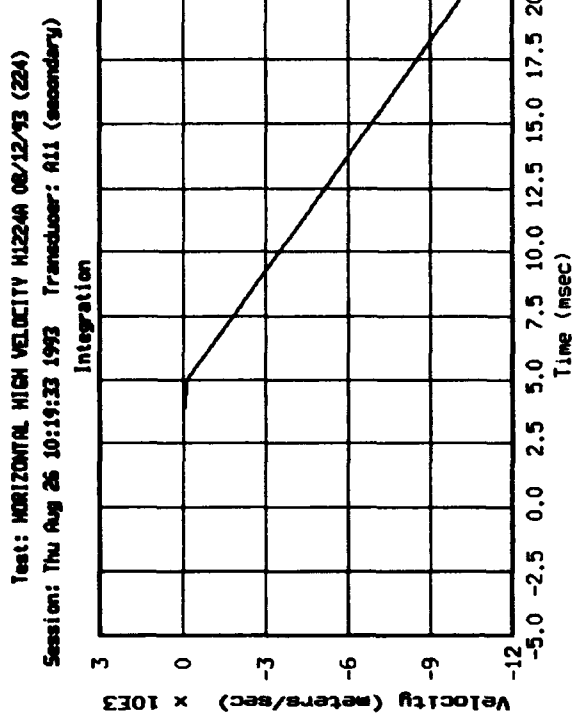
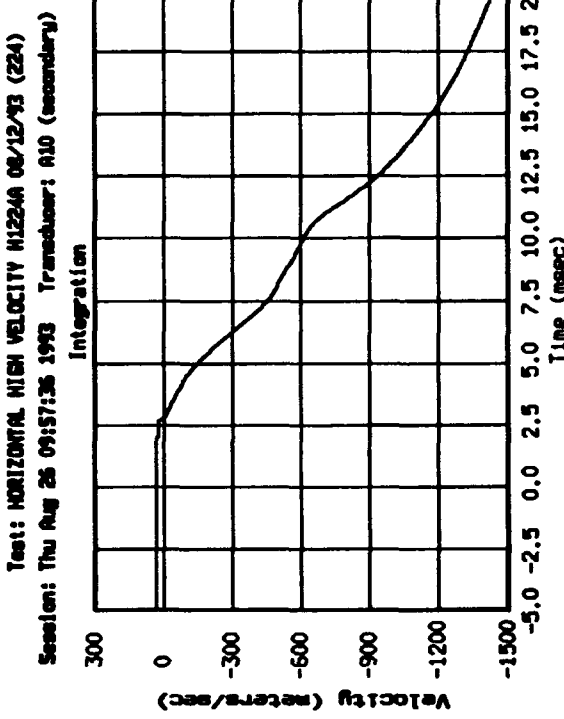
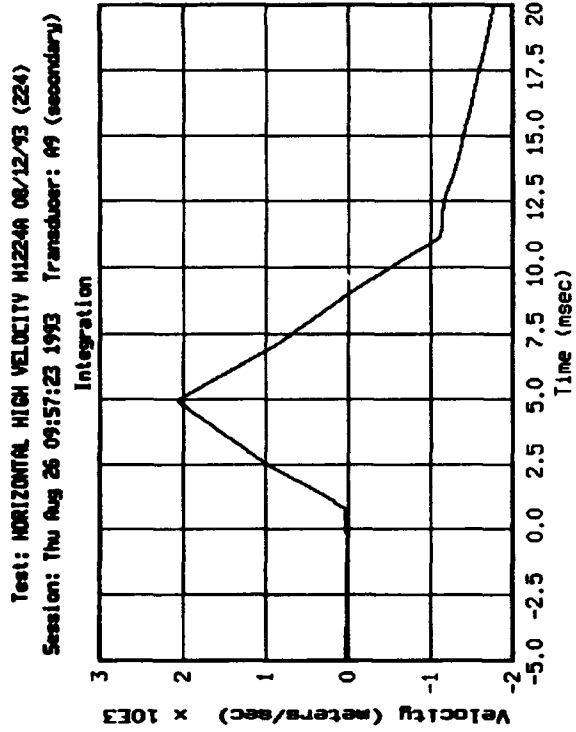


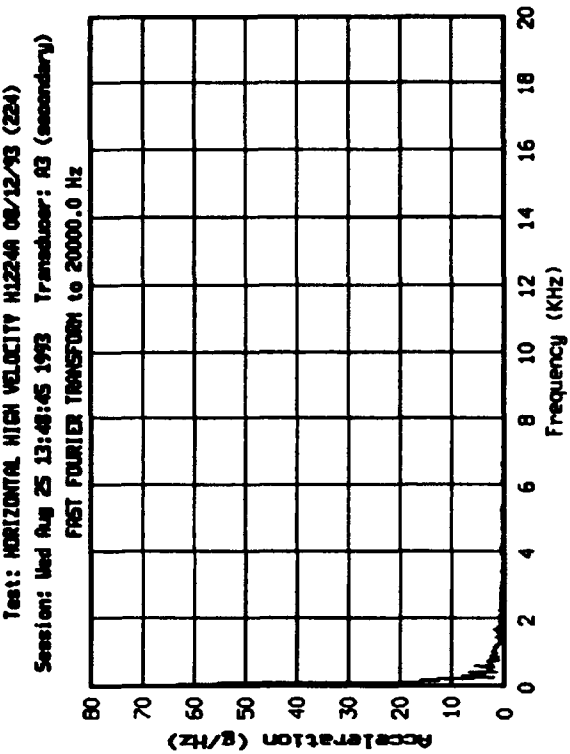
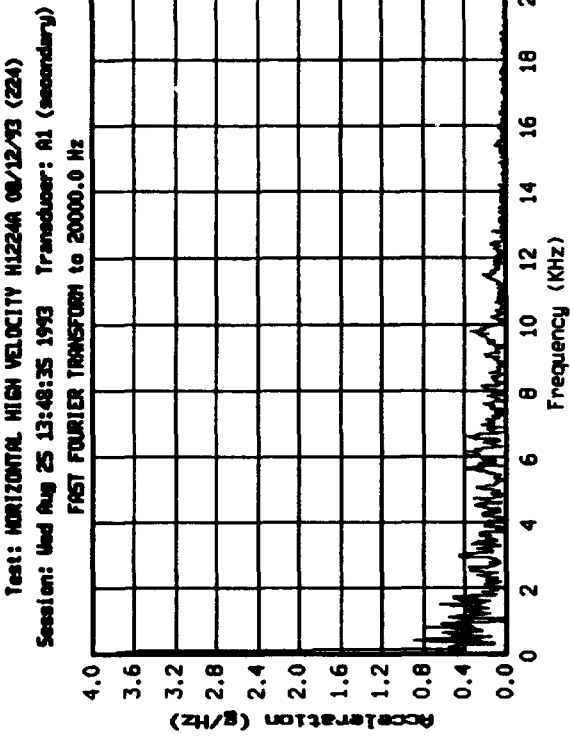
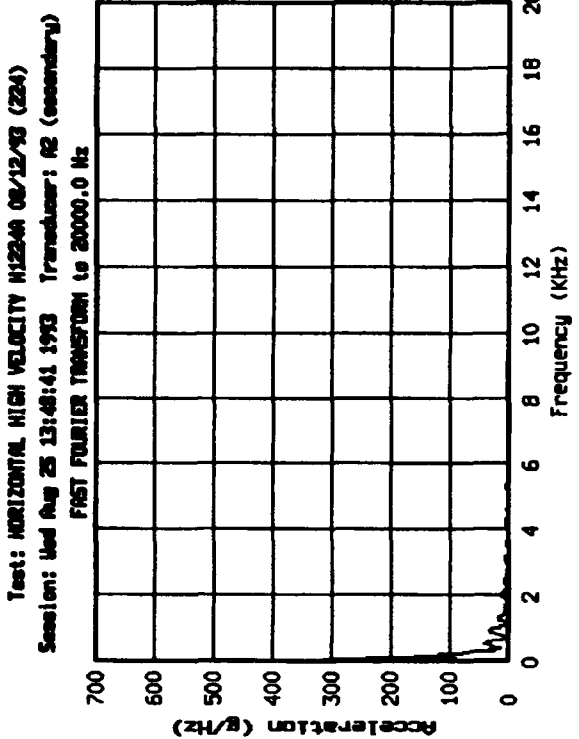
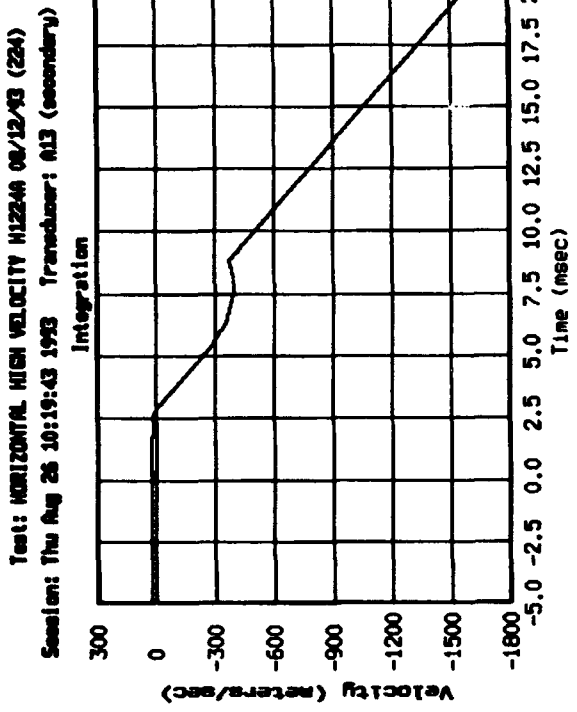


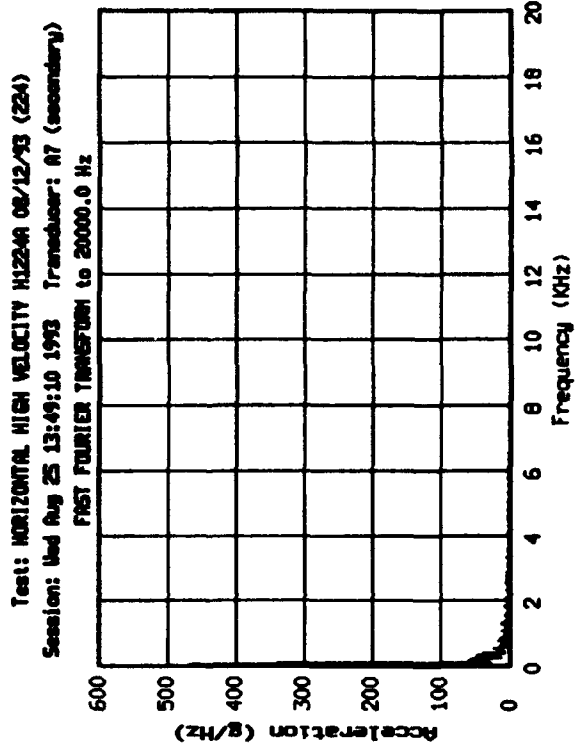
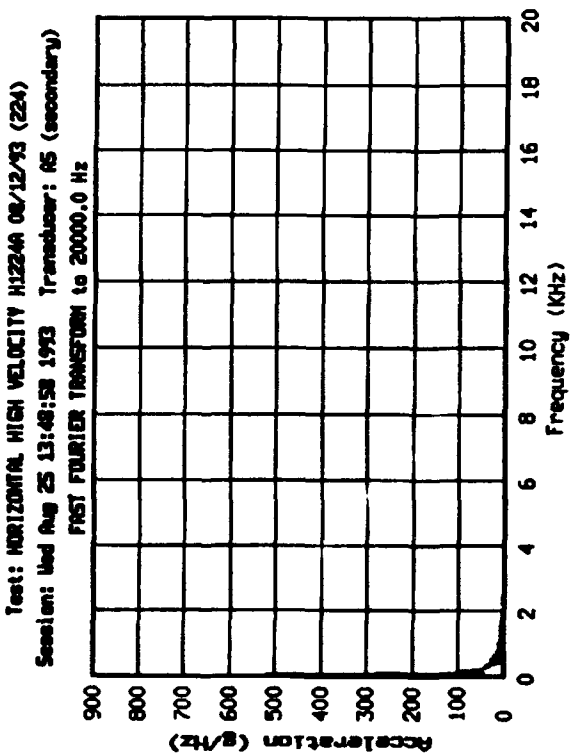
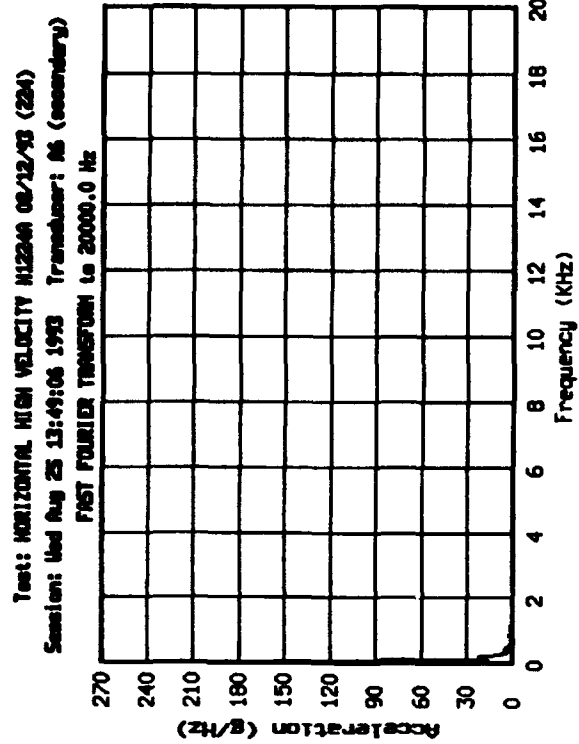
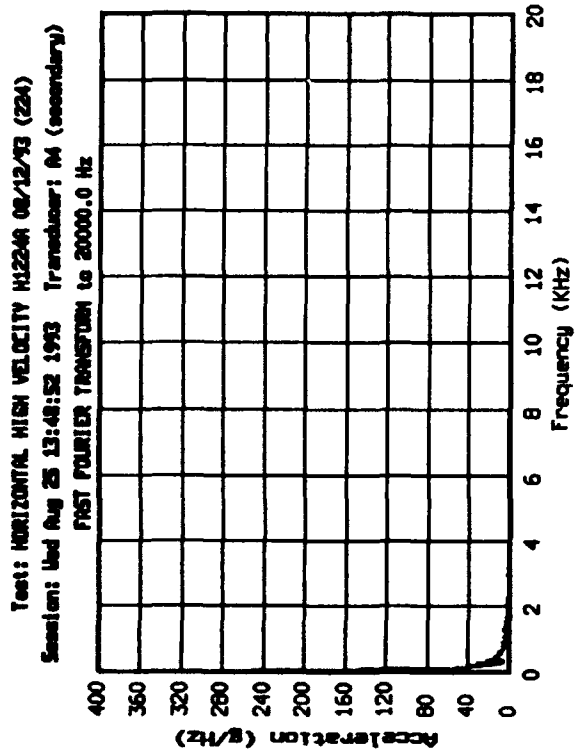


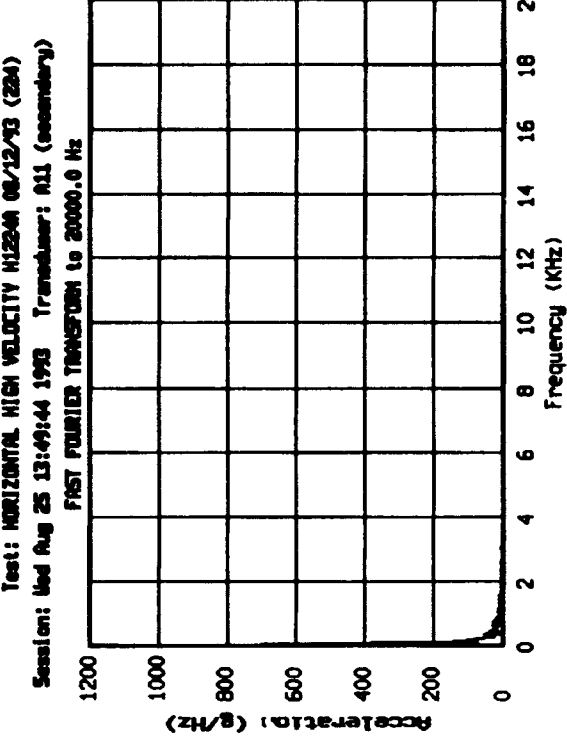
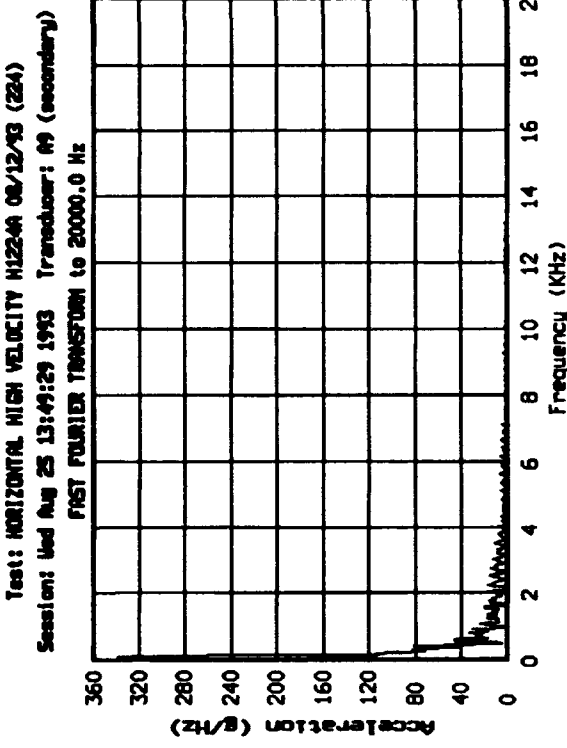
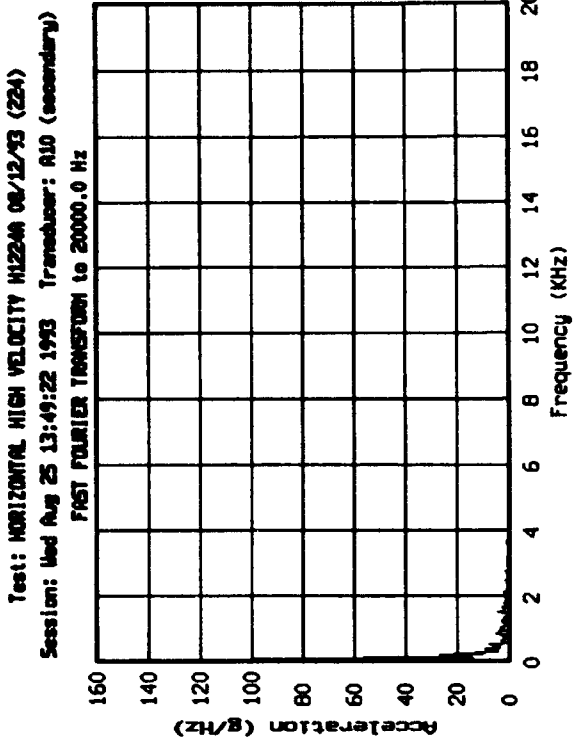
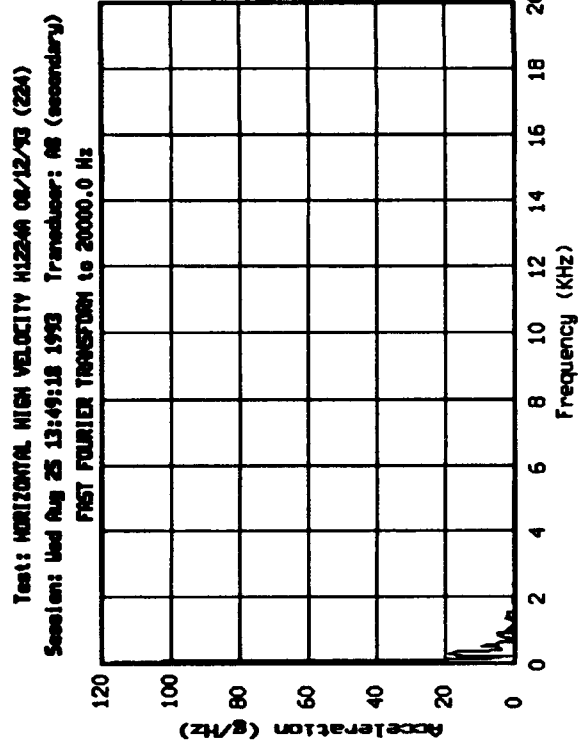


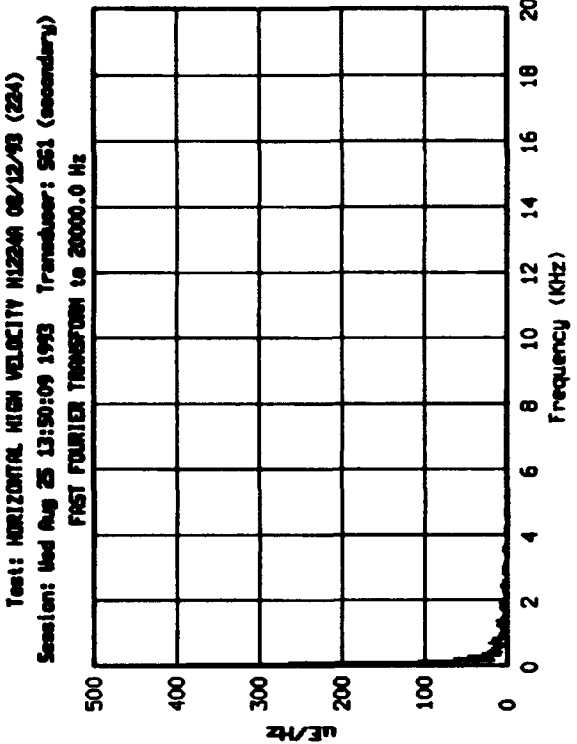
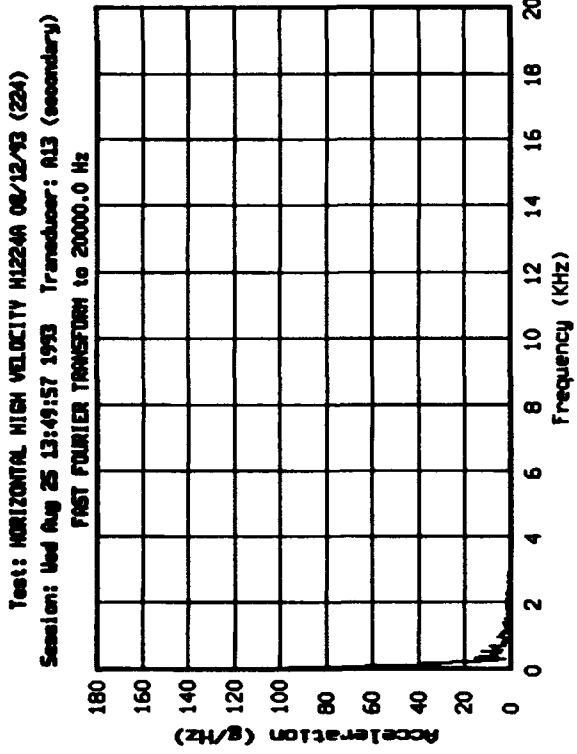
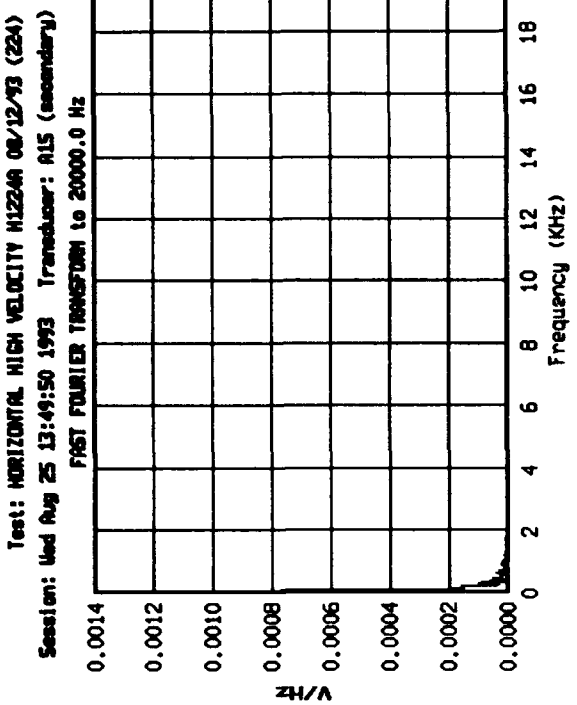
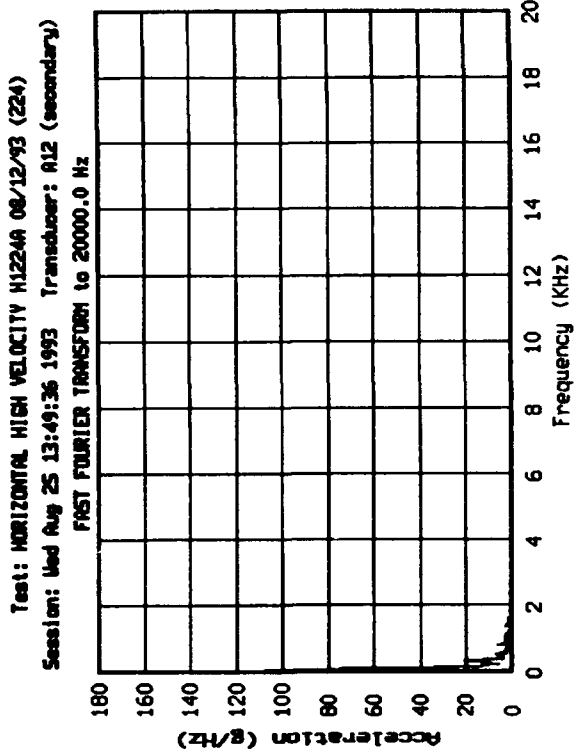


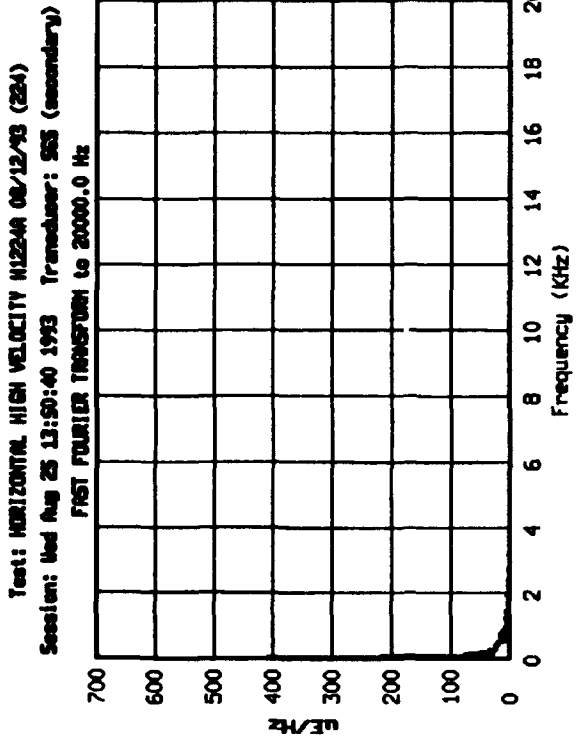
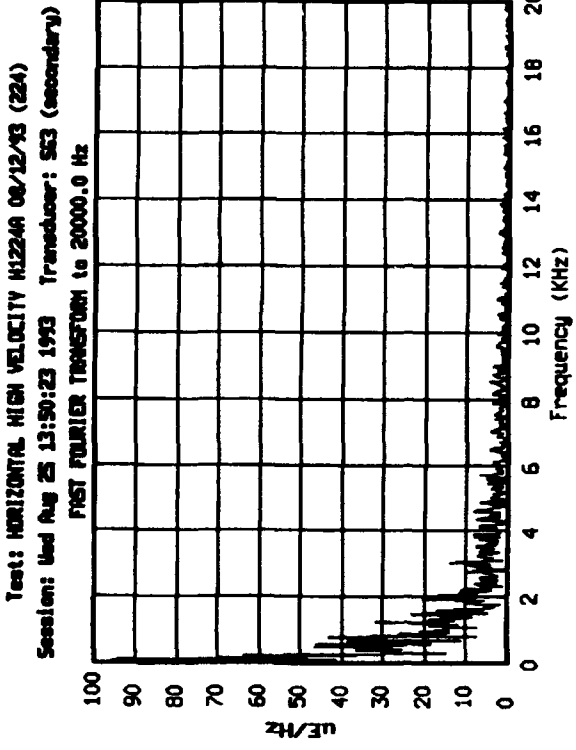
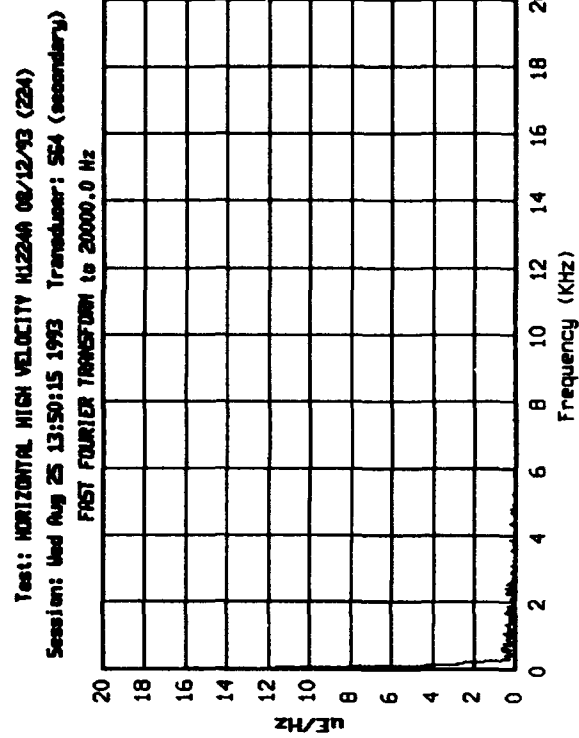
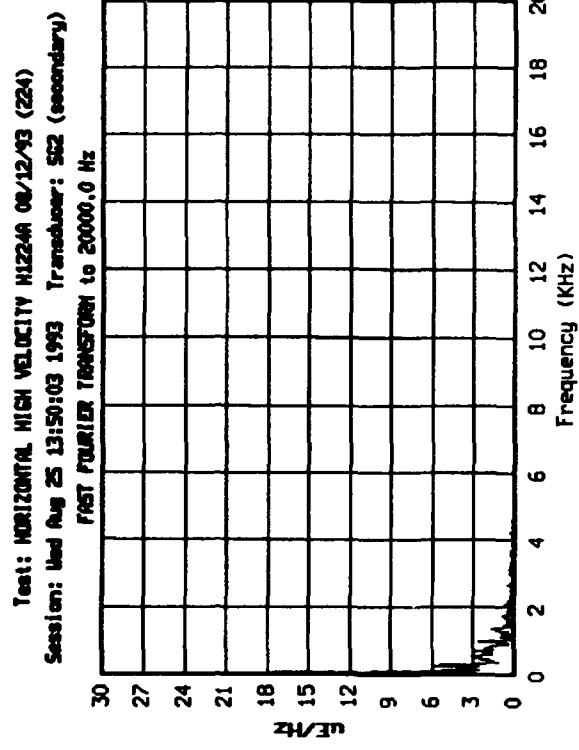


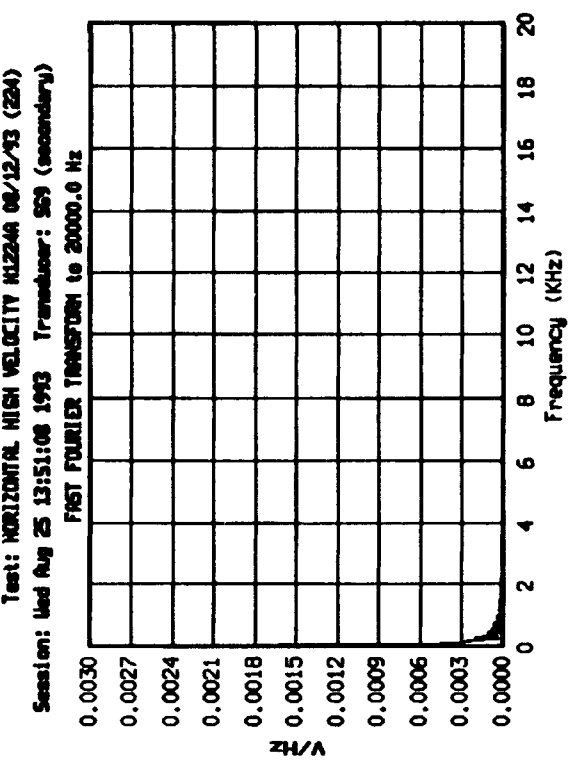
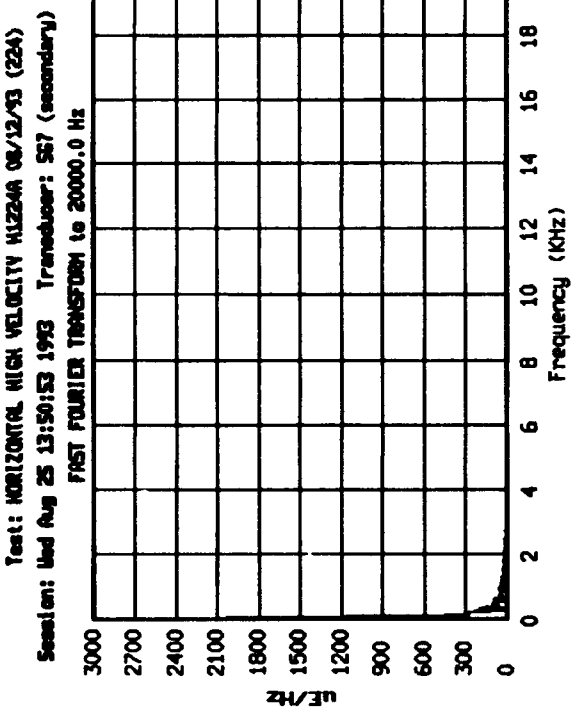
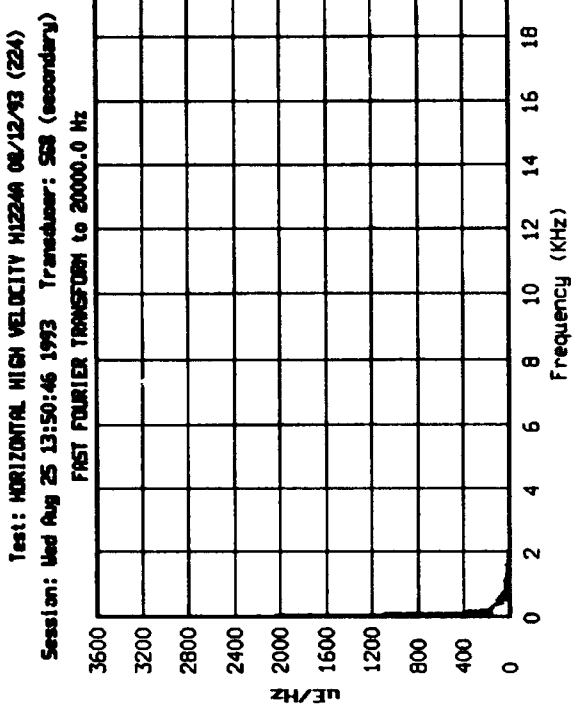
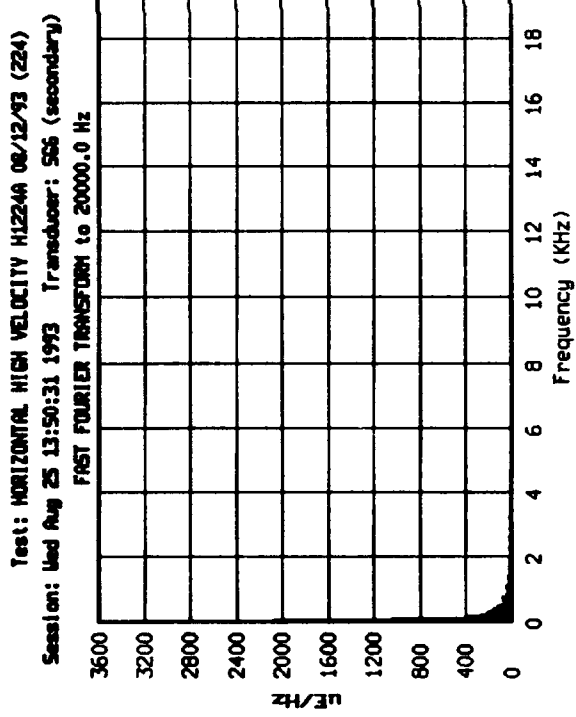




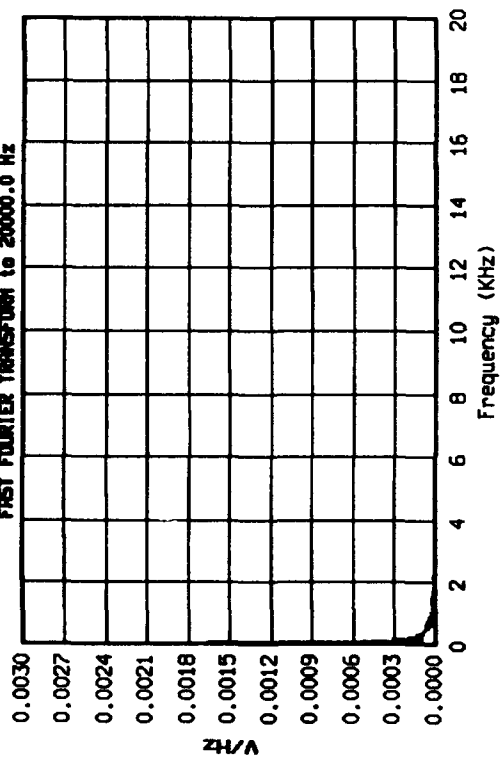








Test: HORIZONTAL HIGH VELOCITY H1224A 08/12/93 (224)
Session: Wed Aug 25 13:51:01 1993 Transducer: SS10 (secondary)



Appendix E. Inspection Data

The following tables present pre- and post-test H1224A container body, inner container, and RV and fore and aft cover inspection data at measurement locations designated in Figures 3.1, 3.2, and 3.3.

Table E 1.1: LLV H1224A Container Body Inspection Data

Measurement Designation	Pre-Test		Post-Test		Measurement Change	
	(mm)	(in.)	(mm)	(in.)	(mm)	(in.)
OD 0, 0°	825.70	32.508	825.09	32.484	0.61	0.024
OD 0, 45°	822.83	32.395	822.50	32.382	0.33	0.013
OD 0, 90°	821.77	32.353	821.41	32.339	0.36	0.014
OD 0, 135°	824.08	32.444	823.72	32.430	0.36	0.014
OD 1, 0°	824.61	32.465	824.38	32.456	0.23	0.009
OD 1, 45°	823.24	32.411	823.14	32.407	0.10	0.004
OD 1, 90°	821.77	32.353	821.72	32.351	0.05	0.002
OD 1, 135°	824.33	32.454	824.18	32.448	0.15	0.006
OD 20, 0°	822.33	32.375	824.33	32.454	-2.01	-0.079
OD 20, 45°	822.15	32.368	823.98	32.440	-1.83	-0.072
OD 20, 90°	822.91	32.398	822.96	32.400	-0.05	-0.002
OD 20, 135°	824.79	32.472	821.16	32.329	3.63	0.143
OD 21, 0°	851.84	33.537	855.68	33.688	-3.84	-0.151
OD 21, 45°	852.42	33.560	854.68	33.649	-2.26	-0.089
OD 21, 90°	853.67	33.609	853.49	33.602	0.18	0.007
OD 21, 135°	855.68	33.688	852.96	33.581	2.72	0.107
OD 22, 0°	822.12	32.367	824.97	32.479	-2.84	-0.112
OD 22, 45°	821.72	32.351	823.90	32.437	-2.18	-0.086
OD 22, 90°	822.91	32.398	822.81	32.394	0.10	0.004

Table E 1.1: LLV H1224A Container Body Inspection Data

Measurement Designation	Pre-Test		Post-Test		Measurement Change	
	(mm)	(in.)	(mm)	(in.)	(mm)	(in.)
OD 22, 135°	824.94	32.478	821.69	32.350	3.25	0.128
OD 24, 0°	820.60	32.307	824.15	32.447	-3.56	-0.140
OD 24, 45°	821.66	32.349	824.41	32.457	-2.74	-0.108
OD 24, 90°	823.24	32.411	821.92	32.359	1.32	0.052
OD 24, 135°	825.32	32.493	822.63	32.387	2.69	0.106
OD 25, 0°	820.80	32.315	824.15	32.447	-3.35	-0.132
OD 25, 45°	821.05	32.325	823.77	32.432	-2.72	-0.107
OD 25, 90°	822.91	32.398	821.31	32.335	1.60	0.063
OD 25, 135°	824.64	32.466	822.05	32.364	2.59	0.102
OD 26, 0°	912.47	35.924	913.43	35.962	-0.97	-0.038
OD 26, 45°	911.12	35.871	911.96	35.904	-0.84	-0.033
OD 26, 90°	909.22	35.796	908.20	35.756	1.02	0.040
OD 26, 135°	912.44	35.923	910.92	35.863	1.52	0.060
OD 27, 0°	822.83	32.395	823.85	32.435	-1.02	-0.040
OD 27, 45°	820.09	32.287	822.15	32.368	-2.06	-0.081
OD 27, 90°	818.77	32.235	816.81	32.158	1.96	0.077
OD 27, 135°	821.49	32.342	821.11	32.327	0.38	0.015
OD 28, 0°	813.97	32.046	814.27	32.058	-0.30	-0.012
OD 28, 45°	811.38	31.944	813.82	32.040	-2.44	-0.096
OD 28, 90°	809.42	31.867	806.02	31.733	3.40	0.134
OD 28, 135°	812.55	31.990	813.33	32.021	-0.79	-0.031
OD 37.75, 0°	812.80	32.000	810.39	31.905	2.41	0.095
OD 37.75, 45°	812.34	31.982	819.20	32.252	-6.86	-0.270
OD 37.75, 90°	807.34	31.785	790.12	31.107	17.22	0.678

Table E 1.1: LLV H1224A Container Body Inspection Data

Measurement Designation	Pre-Test		Post-Test		Measurement Change	
	(mm)	(in.)	(mm)	(in.)	(mm)	(in.)
OD 37.75, 135°	814.43	32.064	823.59	32.425	-9.17	-0.361
OD 38.75, 0°	812.80	32.000	808.94	31.848	3.86	0.152
OD 38.75, 45°	811.61	31.953	818.54	32.226	-6.93	-0.273
OD 38.75, 90°	806.83	31.765	788.19	31.031	18.64	0.734
OD 38.75, 135°	814.48	32.066	823.59	32.425	-9.12	-0.359
OD 39.75, 0°	843.71	33.217	852.32	33.556	-8.61	-0.339
OD 39.75, 45°	843.36	33.203	855.88	33.696	-12.52	-0.493
OD 39.75, 90°	838.89	33.027	832.71	32.784	6.17	0.243
OD 39.75, 135°	845.24	33.277	860.83	33.891	-15.60	-0.614
OD 40.75, 0°	812.67	31.995	817.98	32.204	-5.31	-0.209
OD 40.75, 45°	811.81	31.961	814.02	32.048	-2.21	-0.087
OD 40.75, 90°	806.53	31.753	789.71	31.091	16.81	0.662
OD 40.75, 135°	814.15	32.053	821.00	32.323	-6.86	-0.270
OD 41.75, 0°	812.16	31.975	818.74	32.234	-6.58	-0.259
OD 41.75, 45°	812.77	31.999	815.70	32.114	-2.92	-0.115
OD 41.75, 90°	807.21	31.780	792.40	31.197	14.81	0.583
OD 41.75, 135°	814.55	32.069	821.08	32.326	-6.53	-0.257
OD 50.5, 0°	811.10	31.933	814.17	32.054	-3.07	-0.121
OD 50.5, 45°	811.76	31.959	808.35	31.825	3.40	0.134
OD 50.5, 90°	811.53	31.950	798.30	31.429	13.23	0.521
OD 50.5, 135°	813.05	32.010	811.68	31.956	1.37	0.054
OD 51.5, 0°	815.90	32.122	813.03	32.009	2.87	0.113
OD 51.5, 45°	817.30	32.177	815.75	32.116	1.55	0.061
OD 51.5, 90°	815.82	32.119	803.73	31.643	12.09	0.476

Table E 1.1: LLV H1224A Container Body Inspection Data

Measurement Designation	Pre-Test		Post-Test		Measurement Change	
	(mm)	(in.)	(mm)	(in.)	(mm)	(in.)
OD 51.5, 135°	817.32	32.178	816.36	32.140	0.97	0.038
OD 52.5, 0°	815.52	32.107	809.07	31.853	6.45	0.254
OD 52.5, 45°	816.99	32.165	809.57	31.873	7.42	0.292
OD 52.5, 90°	816.31	32.138	809.73	31.879	6.58	0.259
OD 52.5, 135°	817.19	32.173	811.56	31.951	5.64	0.222
L1, 0°	1459.13	57.446	1428.04	56.222	31.09	1.224
L1, 45°	1460.68	57.507	1431.16	56.345	29.51	1.162
L1, 90°	1460.73	57.509	1442.03	56.773	18.69	0.736
L1, 135°	1460.53	57.501	1455.06	57.286	5.46	0.215
L1, 180°	1459.81	57.473	1463.70	57.626	-3.89	-0.153
L1, 225°	1459.92	57.477	1461.69	57.547	-1.78	-0.070
L1, 270°	1457.93	57.399	1449.40	57.063	8.53	0.336
L1, 315°	1458.47	57.420	1436.22	56.544	22.25	0.876
L2, 0°	1344.17	52.920	1320.50	51.988	23.67	0.932
L2, 45°	1344.78	52.944	1317.12	51.855	27.66	1.089
L2, 90°	1345.54	52.974	1326.29	52.216	19.25	0.758
L2, 135°	1344.19	52.921	1339.90	52.752	4.29	0.169
L2, 180°	1344.30	52.925	1346.83	53.025	-2.54	-0.100
L2, 225°	1342.95	52.872	1342.49	52.854	0.46	0.018
L2, 270°	1342.26	52.845	1332.53	52.462	9.73	0.383
L2, 315°	1343.18	52.881	1322.58	52.070	20.60	0.811

Table E 1.2: LLV Inner Container Inspection Data

Measurement Designation	Pre-Test		Post-Test		Measurement Change	
	(mm)	(in.)	(mm)	(in.)	(mm)	(in.)
OD 0, 0°	519.18	20.440	519.81	20.465	-0.64	-0.025
OD 0, 60°	514.48	20.255	513.08	20.200	1.40	0.055
OD 0, 120°	519.43	20.450	520.07	20.475	-0.64	-0.025
OD 11.38, 0°	518.87	20.428	518.69	20.421	0.18	0.007
OD 11.38, 60°	513.46	20.215	513.46	20.215	0.00	0.000
OD 11.38, 120°	519.10	20.437	519.23	20.442	-0.13	-0.005
OD 17.38, 0°	519.53	20.454	514.38	20.251	5.16	0.203
OD 17.38, 60°	516.10	20.319	516.89	20.350	-0.79	-0.031
OD 17.38, 120°	519.35	20.447	523.67	20.617	-4.32	-0.170
OD 23.38, 0°	518.29	20.405	517.40	20.370	0.89	0.035
OD 23.38, 60°	514.83	20.269	517.02	20.355	-2.18	-0.086
OD 23.38, 120°	518.21	20.402	516.13	20.320	2.08	0.082
OD 38.75, 0°	517.55	20.376	516.64	20.340	0.91	0.036
OD 38.75, 60°	517.83	20.387	519.51	20.453	-1.68	-0.066
OD 38.75, 120°	517.19	20.362	515.62	20.300	1.57	0.062
L1, 0°	987.02	38.859	987.45	38.876	-0.43	-0.017
L1, 60°	987.42	38.875	1002.59	39.472	-15.16	-0.597
L1, 120°	987.42	38.875	988.34	38.911	-0.91	-0.036
L1, 180°	987.15	38.864	989.43	38.954	-2.29	-0.090
L1, 240°	986.82	38.851	1002.16	39.455	-15.34	-0.604
L1, 300°	986.76	38.849	989.86	38.971	-3.10	-0.122

Table E 1.3: LLV RV, Fore, and Aft Cover Inspection Data

Measurement Designation	Pre-Test		Post-Test		Measurement Change	
	(mm)	(in.)	(mm)	(in.)	(mm)	(in.)
OD A, 0°	500.71	19.713	500.68	19.712	0.03	0.001
OD A, 60°	500.68	19.712	500.63	19.710	0.05	0.002
OD A, 120°	500.91	19.721	500.89	19.720	0.03	0.001
ID B, 0°	426.52	16.792	426.59	16.795	-0.08	-0.003
ID B, 60°	426.49	16.791	426.39	16.787	0.10	0.004
ID B, 120°	426.59	16.795	426.72	16.800	-0.13	-0.005
ID C, 0°	490.58	19.314	490.55	19.313	0.03	0.001
ID C, 60°	491.03	19.332	491.08	19.334	-0.05	-0.002
ID C, 120°	491.19	19.338	491.21	19.339	-0.03	-0.001
L2, 0°	236.30	9.303	236.19	9.299	~ 1 ~	0.004
L2, 60°	236.19	9.299	236.02	9.292	0.18	0.007
L2, 120°	235.84	9.285	235.79	9.283	0.05	0.002
L2, 180°	235.76	9.282	235.74	9.281	0.03	0.001
L2, 240°	235.84	9.285	235.76	9.282	0.08	0.003
L2, 300°	235.94	9.289	235.89	9.287	0.05	0.002
OD B, 0°	431.55	16.990	431.50	16.988	0.05	0.002
OD B, 60°	431.55	16.990	431.65	16.994	-0.10	-0.004
OD B, 120°	431.62	16.993	431.62	16.993	0.00	0.000
ID D, 0°	165.76	6.526	165.71	6.524	0.05	0.002
ID D, 60°	165.76	6.526	165.79	6.527	-0.03	-0.001
ID D, 120°	165.76	6.526	165.76	6.526	0.00	0.000
L1, 0°	883.51	34.784	872.79	34.362	10.72	0.422
L1, 60°	883.41	34.780	872.64	34.356	10.77	0.424

Table E 1.3: LLV RV, Fore, and Aft Cover Inspection Data

Measurement Designation	Pre-Test		Post-Test		Measurement Change	
	(mm)	(in.)	(mm)	(in.)	(mm)	(in.)
L1, 120°	883.46	34.782	872.49	34.350	10.97	0.432
L1, 180°	883.36	34.778	872.31	34.343	11.05	0.435
L1, 240°	883.36	34.778	872.54	34.352	10.82	0.426
L1, 300°	883.41	34.780	872.67	34.357	10.74	0.423
OD D, 0°	171.25	6.742	171.30	6.744	-0.05	-0.002
OD D, 60°	171.25	6.742	171.27	6.743	-0.03	-0.001
OD D, 120°	171.25	6.742	171.25	6.742	0.00	0.000
OD E, 0°	482.35	18.990	482.60	19.000	-0.25	-0.010
OD E, 60°	482.35	18.990	481.41	18.953	0.94	0.037
OD E, 120°	482.35	18.990	481.51	18.957	0.84	0.033

Table E 2.1: HLV H1224A Container Body Inspection Data

Measurement Designation	Pre-Test		Post-Test		Measurement Change	
	(mm)	(in.)	(mm)	(in.)	(mm)	(in.)
OD 0, 0°	822.60	32.386	807.21	31.780	15.39	0.606
OD 0, 45°	822.83	32.395	823.65	32.427	-0.81	-0.032
OD 0, 90°	818.34	32.218	816.46	32.144	1.88	0.074
OD 0, 135°	824.69	32.468	825.27	32.491	-0.58	-0.023
OD 1, 0°	822.86	32.396	808.51	31.831	14.35	0.565
OD 1, 45°	823.49	32.421	824.99	32.480	-1.50	-0.059
OD 1, 90°	819.91	32.280	819.76	32.274	0.15	0.006
OD 1, 135°	825.27	32.491	825.88	32.515	-0.61	-0.024
OD 20, 0°	822.20	32.370	773.28	30.444	48.92	1.926

Table E 2.1: HLV H1224A Container Body Inspection Data

Measurement Designation	Pre-Test		Post-Test		Measurement Change	
	(mm)	(in.)	(mm)	(in.)	(mm)	(in.)
OD 20, 45°	823.49	32.421	827.35	32.573	-3.86	-0.152
OD 20, 90°	823.75	32.431	854.61	33.646	-30.86	-1.215
OD 20, 135°	825.60	32.504	826.54	32.541	-0.94	-0.037
OD 21, 0°	853.85	33.616	799.95	31.494	53.90	2.122
OD 21, 45°	854.41	33.638	857.99	33.779	-3.58	-0.141
OD 21, 90°	855.60	33.685	887.12	34.926	-31.52	-1.241
OD 21, 135°	856.26	33.711	856.69	33.728	-0.43	-0.017
OD 22, 0°	822.50	32.382	760.55	29.943	61.95	2.439
OD 22, 45°	822.88	32.397	827.07	32.562	-4.19	-0.165
OD 22, 90°	824.97	32.479	859.46	33.837	-34.49	-1.358
OD 22, 135°	825.14	32.486	826.34	32.533	-1.19	-0.047
OD 24, 0°	822.02	32.363	748.69	29.476	73.33	2.887
OD 24, 45°	822.22	32.371	826.31	32.532	-4.09	-0.161
OD 24, 90°	824.43	32.458	862.89	33.972	-38.46	-1.514
OD 24, 135°	823.72	32.430	824.18	32.448	-0.46	-0.018
OD 25, 0°	820.93	32.320	738.66	29.081	82.27	3.239
OD 25, 45°	821.64	32.348	825.40	32.496	-3.76	-0.148
OD 25, 90°	823.87	32.436	863.30	33.988	-39.42	-1.552
OD 25, 135°	823.19	32.409	823.24	32.411	-0.05	-0.002
OD 26, 0°	910.59	35.850	833.70	32.823	76.89	3.027
OD 26, 45°	913.21	35.953	914.22	35.993	-1.02	-0.040
OD 26, 90°	912.75	35.935	960.30	37.807	-47.55	-1.872
OD 26, 135°	912.80	35.937	911.99	35.905	0.81	0.032
OD 27, 0°	819.15	32.250	739.04	29.096	80.11	3.154

Table E 2.1: HLV H1224A Container Body Inspection Data

Measurement Designation	Pre-Test		Post-Test		Measurement Change	
	(mm)	(in.)	(mm)	(in.)	(mm)	(in.)
OD 27, 45°	822.60	32.386	828.67	32.625	-6.07	-0.239
OD 27, 90°	822.12	32.367	960.22	37.804	-138.10	-5.437
OD 27, 135°	821.41	32.339	821.77	32.353	-0.36	-0.014
OD 28, 0°	810.46	31.908	734.97	28.936	75.49	2.972
OD 28, 45°	811.99	31.968	817.80	32.197	-5.82	-0.229
OD 28, 90°	813.61	32.032	858.90	33.815	-45.29	-1.783
OD 28, 135°	811.81	31.961	813.51	32.028	-1.70	-0.067
OD 37.75, 0°	812.90	32.004	778.13	30.635	34.77	1.369
OD 37.75, 45°	811.91	31.965	815.64	32.112	-3.73	-0.147
OD 37.75, 90°	812.22	31.977	838.50	33.012	-26.29	-1.035
OD 37.75, 135°	812.80	32.000	811.76	31.959	1.04	0.041
OD 38.75, 0°	812.52	31.989	779.48	30.688	33.05	1.301
OD 38.75, 45°	810.84	31.923	814.20	32.055	-3.35	-0.132
OD 38.75, 90°	811.71	31.957	835.94	32.911	-24.23	-0.954
OD 38.75, 135°	812.27	31.979	811.25	31.939	1.02	0.040
OD 39.75, 0°	841.76	33.140	808.74	31.840	33.02	1.300
OD 39.75, 45°	842.65	33.175	819.15	32.250	23.50	0.925
OD 39.75, 90°	842.77	33.180	865.23	34.064	-22.45	-0.884
OD 39.75, 135°	843.84	33.222	842.01	33.150	1.83	0.072
OD 40.75, 0°	809.65	31.876	786.00	30.945	23.65	0.931
OD 40.75, 45°	811.73	31.958	813.69	32.035	-1.96	-0.077
OD 40.75, 90°	810.59	31.913	830.68	32.704	-20.09	-0.791
OD 40.75, 135°	812.80	32.000	811.73	31.958	1.07	0.042
OD 41.75, 0°	809.73	31.879	788.87	31.058	20.85	0.821

Table E 2.1: HLV H1224A Container Body Inspection Data

Measurement Designation	Pre-Test		Post-Test		Measurement Change	
	(mm)	(in.)	(mm)	(in.)	(mm)	(in.)
OD 41.75, 45°	814.71	32.075	814.65	32.073	0.05	0.002
OD 41.75, 90°	810.59	31.913	830.07	32.680	-19.48	-0.767
OD 41.75, 135°	813.41	32.024	812.50	31.988	0.91	0.036
OD 50.5, 0°	807.72	31.800	802.56	31.597	5.16	0.203
OD 50.5, 45°	812.34	31.982	813.05	32.010	-0.71	-0.028
OD 50.5, 90°	812.34	31.982	817.52	32.186	-5.18	-0.204
OD 50.5, 135°	811.20	31.937	810.84	31.923	0.36	0.014
OD 51.5, 0°	813.23	32.017	809.88	31.885	3.35	0.132
OD 51.5, 45°	817.40	32.181	818.77	32.235	-1.37	-0.054
OD 51.5, 90°	816.97	32.164	819.99	32.283	-3.02	-0.119
OD 51.5, 135°	816.74	32.155	816.38	32.141	0.36	0.014
OD 52.5, 0°	815.01	32.087	811.94	31.966	3.07	0.121
OD 52.5, 45°	830.71	32.705	831.85	32.750	-1.14	-0.045
OD 52.5, 90°	817.88	32.200	819.38	32.259	-1.50	-0.059
OD 52.5, 135°	817.14	32.171	816.99	32.165	0.15	0.006
L1, 180°	1455.88	57.318	1468.27	57.806	-12.40	-0.488
L1, 0°	1457.96	57.400	1460.58	57.503	-2.62	-0.103
L1, 45°	1458.34	57.415	1463.80	57.630	-5.46	-0.215
L1, 90°	1458.82	57.434	1470.74	57.903	-11.91	-0.469
L1, 135°	1457.60	57.386	1470.38	57.889	-12.78	-0.503
L1, 0°	1457.96	57.400	1460.58	57.503	-2.62	-0.103
L1, 180°	1455.88	57.318	1468.27	57.806	-12.40	-0.488
L1, 225°	1455.32	57.296	1472.36	57.967	-17.04	-0.671
L1, 270°	1455.34	57.297	1472.13	57.958	-16.79	-0.661

Table E 2.1: HLV H1224A Container Body Inspection Data

Measurement Designation	Pre-Test		Post-Test		Measurement Change	
	(mm)	(in.)	(mm)	(in.)	(mm)	(in.)
L1, 315°	1455.75	57.313	1464.54	57.659	-8.79	-0.346
L2, 0°	1340.71	52.784	1336.14	52.604	4.57	0.180
L2, 45°	1340.76	52.786	1344.60	52.937	-3.84	-0.151
L2, 90°	1342.92	52.871	1354.76	53.337	-11.84	-0.466
L2, 135°	1339.93	52.753	1351.15	53.195	-11.23	-0.442
L2, 180°	1338.05	52.679	1346.10	52.996	-8.05	-0.317
L2, 225°	1337.77	52.668	1349.38	53.125	-11.61	-0.457
L2, 270°	1339.47	52.735	1353.24	53.277	-13.77	-0.542
L2, 315°	1337.61	52.662	1344.52	52.934	-6.91	-0.272

Table E 2.2: HLV Inner Container Inspection Data

Measurement Designation	Pre-Test		Post-Test		Measurement Change	
	(mm)	(in.)	(mm)	(in.)	(mm)	(in.)
OD 0, 0°	513.08	20.200	521.44	20.529	-8.36	-0.329
OD 0, 60°	512.24	20.167	520.88	20.507	-8.64	-0.340
OD 0, 120°	530.76	20.896	506.25	19.931	24.51	0.965
OD 11.38, 0°	514.02	20.237	519.05	20.435	-5.03	-0.198
OD 11.38, 60°	513.94	20.234	509.04	20.041	4.90	0.193
OD 11.38, 120°	526.52	20.729	511.73	20.147	14.78	0.582
OD 17.38, 0°	515.70	20.303	521.36	20.526	-5.66	-0.223
OD 17.38, 60°	516.15	20.321	521.21	20.520	-5.05	-0.199
OD 17.38, 120°	526.59	20.732	491.67	19.357	34.92	1.375
OD 23.38, 0°	516.03	20.316	525.86	20.703	-9.83	-0.387

Table E 2.2: HLV Inner Container Inspection Data

Measurement Designation	Pre-Test		Post-Test		Measurement Change	
	(mm)	(in.)	(mm)	(in.)	(mm)	(in.)
OD 23.38, 60°	516.61	20.339	525.88	20.704	-9.27	-0.365
OD 23.38, 120°	523.27	20.601	499.29	19.657	23.98	0.944
OD 38.75, 0°	517.22	20.363	517.53	20.375	-0.30	-0.012
OD 38.75, 60°	517.98	20.393	518.19	20.401	-0.20	-0.008
OD 38.75, 120°	519.68	20.460	517.07	20.357	2.62	0.103
L1, 0°	987.37	38.873	986.66	38.845	0.71	0.028
L1, 60°	987.17	38.865	986.49	38.838	0.69	0.027
L1, 120°	985.88	38.814	982.90	38.697	2.97	0.117
L1, 180°	986.43	38.836	986.49	38.838	-0.05	-0.002
L1, 240°	986.71	38.847	986.08	38.822	0.64	0.025
L1, 300°	986.82	38.851	986.76	38.849	0.05	0.002

Table E 2.3: HLV RV, Fore, and Aft Cover Inspection Data

Measurement Designation	Pre-Test		Post-Test		Measurement Change	
	(mm)	(in.)	(mm)	(in.)	(mm)	(in.)
OD A, 0°	502.29	19.775	502.87	19.798	-0.58	-0.023
OD A, 60°	502.34	19.777	500.48	19.704	1.85	0.073
OD A, 120°	502.21	19.772	502.97	19.802	-0.76	-0.030
ID B, 0°	502.87	19.798	426.54	16.793	76.33	3.005
ID B, 60°	502.89	19.799	425.45	16.750	77.44	3.049
ID B, 120°	502.89	19.799	428.09	16.854	74.80	2.945
ID C, 0°	490.60	19.315	492.07	19.373	-1.47	-0.058
ID C, 60°	490.30	19.303	486.64	19.159	3.66	0.144

Table E 2.3: HLV RV, Fore, and Aft Cover Inspection Data

Measurement Designation	Pre-Test		Post-Test		Measurement Change	
	(mm)	(in.)	(mm)	(in.)	(mm)	(in.)
ID C, 120°	490.86	19.325	492.56	19.392	-1.70	-0.067
L2, 0°	234.90	9.248	225.37	8.873	9.52	0.375
L2, 60°	235.36	9.266	226.34	8.911	9.02	0.355
L2, 120°	235.43	9.269	225.63	8.883	9.80	0.386
L2, 180°	235.31	9.264	225.86	8.892	9.45	0.372
L2, 240°	234.92	9.249	225.63	8.883	9.30	0.366
L2, 300°	234.62	9.237	224.92	8.855	9.70	0.382
OD B, 0°	431.29	16.980	431.80	17.000	-0.51	-0.020
OD B, 60°	431.67	16.995	430.15	16.935	1.52	0.060
OD B, 120°	431.95	17.006	431.95	17.006	0.00	0.000
ID D, 0°	165.86	6.530	155.65	6.128	10.21	0.402
ID D, 60°	165.86	6.530	155.70	6.130	10.16	0.400
ID D, 120°	165.86	6.530	155.70	6.130	10.16	0.400
L1, 0°	883.39	34.779	883.51	34.784	-0.13	-0.005
L1, 60°	883.36	34.778	883.82	34.796	-0.46	-0.018
L1, 120°	883.26	34.774	883.87	34.798	-0.61	-0.024
L1, 180°	883.28	34.775	883.64	34.789	-0.36	-0.014
L1, 240°	883.31	34.776	883.39	34.779	-0.08	-0.003
L1, 300°	883.34	34.777	883.28	34.775	0.05	0.002
OD D, 0°	171.32	6.745	171.22	6.741	0.10	0.004
OD D, 60°	171.32	6.745	171.20	6.740	0.13	0.005
OD D, 120°	171.32	6.745	171.22	6.741	0.10	0.004
OD E, 0°	482.40	18.992	482.45	18.994	-0.05	-0.002
OD E, 60°	482.37	18.991	482.37	18.991	0.00	0.000

Table E 2.3: HLV RV, Fore, and Aft Cover Inspection Data

Measurement Designation	Pre-Test		Post-Test		Measurement Change	
	(mm)	(in.)	(mm)	(in.)	(mm)	(in.)
OD E, 120°	482.40	18.992	482.40	18.992	0.00	0.000

Table E 3.1: LHV H1224A Container Body Inspection Data

Measurement Designation	Pre-Test		Post-Test		Measurement Change	
	(mm)	(in.)	(mm)	(in.)	(mm)	(in.)
OD 0, 0°	821.69	32.350	820.70	32.311	0.99	0.039
OD 0, 45°	820.95	32.321	819.56	32.266	1.40	0.055
OD 0, 90°	821.11	32.327	819.86	32.278	1.24	0.049
OD 0, 135°	821.28	32.334	818.16	32.211	3.12	0.123
OD 1, 0°	822.30	32.374	821.72	32.351	0.58	0.023
OD 1, 45°	821.54	32.344	819.81	32.276	1.73	0.068
OD 1, 90°	822.88	32.397	821.66	32.349	1.22	0.048
OD 1, 135°	821.84	32.356	815.34	32.100	6.50	0.256
OD 20, 0°	819.20	32.252	831.14	32.722	-11.94	-0.470
OD 20, 45°	819.45	32.262	802.26	31.585	17.20	0.677
OD 20, 90°	821.87	32.357	831.85	32.750	-9.98	-0.393
OD 20, 135°	819.05	32.246	807.62	31.796	11.43	0.450
OD 21, 0°	843.43	33.206	860.76	33.888	-17.32	-0.682
OD 21, 45°	843.81	33.221	836.68	32.940	7.14	0.281
OD 21, 90°	845.36	33.282	836.42	32.930	8.94	0.352
OD 21, 135°	843.13	33.194	813.69	32.035	29.44	1.159
OD 22, 0°	819.20	32.252	827.71	32.587	-8.51	-0.335
OD 22, 45°	818.97	32.243	802.87	31.609	16.10	0.634

Table E 3.1: LHV H1224A Container Body Inspection Data

Measurement Designation	Pre-Test		Post-Test		Measurement Change	
	(mm)	(in.)	(mm)	(in.)	(mm)	(in.)
OD 22, 90°	819.99	32.283	830.61	32.701	-10.62	-0.418
OD 22, 135°	818.18	32.212	803.99	31.653	14.20	0.559
OD 24, 0°	821.82	32.355	826.19	32.527	-4.37	-0.172
OD 24, 45°	822.43	32.379	812.24	31.978	10.19	0.401
OD 24, 90°	823.16	32.408	828.29	32.610	-5.13	-0.202
OD 24, 135°	821.99	32.362	816.15	32.132	5.84	0.230
OD 25, 0°	821.79	32.354	823.65	32.427	-1.85	-0.073
OD 25, 45°	822.53	32.383	814.20	32.055	8.33	0.328
OD 25, 90°	822.96	32.400	825.70	32.508	-2.74	-0.108
OD 25, 135°	822.10	32.366	818.29	32.216	3.81	0.150
OD 26, 0°	910.74	35.856	912.67	35.932	-1.93	-0.076
OD 26, 45°	911.96	35.904	913.56	35.967	-1.60	-0.063
OD 26, 90°	909.40	35.803	911.00	35.866	-1.60	-0.063
OD 26, 135°	909.45	35.805	903.76	35.581	5.69	0.224
OD 27, 0°	820.67	32.310	818.11	32.209	2.57	0.101
OD 27, 45°	822.96	32.400	825.35	32.494	-2.39	-0.094
OD 27, 90°	819.28	32.255	815.92	32.123	3.35	0.132
OD 27, 135°	819.56	32.266	815.67	32.113	3.89	0.153
OD 28, 0°	810.79	31.921	805.48	31.712	5.31	0.209
OD 28, 45°	815.09	32.090	820.17	32.290	-5.08	-0.200
OD 28, 90°	810.26	31.900	803.91	31.650	6.35	0.250
OD 28, 135°	810.64	31.915	809.07	31.853	1.57	0.062
OD 37.75, 0°	809.37	31.865	752.47	29.625	56.90	2.240
OD 37.75, 45°	815.11	32.091	843.38	33.204	-28.27	-1.113

Table E 3.1: LHV H1224A Container Body Inspection Data

Measurement Designation	Pre-Test		Post-Test		Measurement Change	
	(mm)	(in.)	(mm)	(in.)	(mm)	(in.)
OD 37.75, 90°	806.83	31.765	763.47	30.058	43.36	1.707
OD 37.75, 135°	812.62	31.993	835.79	32.905	-23.16	-0.912
OD 38.75, 0°	807.06	31.774	752.40	29.622	54.66	2.152
OD 38.75, 45°	813.00	32.008	837.74	32.982	-24.74	-0.974
OD 38.75, 90°	803.73	31.643	759.56	29.904	44.17	1.739
OD 38.75, 135°	810.54	31.911	832.28	32.767	-21.74	-0.856
OD 39.75, 0°	830.86	32.711	819.33	32.257	11.53	0.454
OD 39.75, 45°	836.47	32.932	874.27	34.420	-37.80	-1.488
OD 39.75, 90°	827.43	32.576	785.44	30.923	41.99	1.653
OD 39.75, 135°	834.59	32.858	879.53	34.627	-44.93	-1.769
OD 40.75, 0°	806.73	31.761	780.41	30.725	26.31	1.036
OD 40.75, 45°	812.75	31.998	805.43	31.710	7.32	0.288
OD 40.75, 90°	802.03	31.576	697.23	27.450	104.80	4.126
OD 40.75, 135°	811.73	31.958	829.26	32.648	-17.53	-0.690
OD 41.75, 0°	807.97	31.810	793.80	31.252	14.17	0.558
OD 41.75, 45°	814.71	32.075	819.53	32.265	-4.83	-0.190
OD 41.75, 90°	803.78	31.645	704.09	27.720	99.69	3.925
OD 41.75, 135°	814.17	32.054	835.94	32.911	-21.77	-0.857
OD 50.5, 0°	811.83	31.962	809.27	31.861	2.57	0.101
OD 50.5, 45°	813.84	32.041	818.79	32.236	-4.95	-0.195
OD 50.5, 90°	808.10	31.815	780.54	30.730	27.56	1.085
OD 50.5, 135°	813.38	32.023	813.74	32.037	-0.36	-0.014
OD 51.5, 0°	815.57	32.109	814.53	32.068	1.04	0.041
OD 51.5, 45°	817.17	32.172	815.95	32.124	1.22	0.048

Table E 3.1: LHV H1224A Container Body Inspection Data

Measurement Designation	Pre-Test		Post-Test		Measurement Change	
	(mm)	(in.)	(mm)	(in.)	(mm)	(in.)
OD 51.5, 90°	813.74	32.037	813.31	32.020	0.43	0.017
OD 51.5, 135°	817.40	32.181	818.39	32.220	-0.99	-0.039
OD 52.5, 0°	816.15	32.132	815.70	32.114	0.46	0.018
OD 52.5, 45°	829.69	32.665	814.17	32.054	15.52	0.611
OD 52.5, 90°	816.61	32.150	830.50	32.697	-13.89	-0.547
OD 52.5, 135°	817.98	32.204	812.04	31.970	5.94	0.234
L1, 0°	1454.76	57.274	1314.20	51.740	140.56	5.534
L1, 45°	1455.45	57.301	1326.39	52.220	129.06	5.081
L1, 90°	1454.12	57.249	1322.96	52.085	131.17	5.164
L1, 135°	1455.65	57.309	1303.96	51.337	151.69	5.972
L1, 180°	1455.24	57.293	1286.31	50.642	168.94	6.651
L1, 225°	1456.56	57.345	1274.95	50.195	181.61	7.150
L1, 270°	1455.85	57.317	1277.82	50.308	178.03	7.009
L1, 315°	1455.85	57.317	1294.77	50.975	161.09	6.342
L2, 0°	1340.38	52.771	*	*	N/A	N/A
L2, 45°	1340.43	52.773	*	*	N/A	N/A
L2, 90°	1339.21	52.725	*	*	N/A	N/A
L2, 135°	1340.28	52.767	*	*	N/A	N/A
L2, 180°	1340.21	52.764	*	*	N/A	N/A
L2, 225°	1339.80	52.748	*	*	N/A	N/A
L2, 270°	1339.34	52.730	*	*	N/A	N/A
L2, 315°	1339.27	52.727	*	*	N/A	N/A

* Part destroyed during test and measurement not possible.

Table E 3.2: LHV Inner Container Inspection Data

Measurement Designation	Pre-Test		Post-Test		Measurement Change	
	(mm)	(in.)	(mm)	(in.)	(mm)	(in.)
OD 0, 0°	520.47	20.491	528.68	20.814	-8.20	-0.323
OD 0, 60°	517.50	20.374	514.48	20.255	3.02	0.119
OD 0, 120°	516.81	20.347	508.48	20.019	8.33	0.328
OD 11.38, 0°	518.90	20.429	492.02	19.371	26.87	1.058
OD 11.38, 60°	517.68	20.381	521.64	20.537	-3.96	-0.156
OD 11.38, 120°	517.42	20.371	532.13	20.950	-14.71	-0.579
OD 17.38, 0°	520.17	20.479	449.71	17.705	70.46	2.774
OD 17.38, 60°	518.13	20.399	673.35	26.510	-155.22	-6.111
OD 17.38, 120°	517.98	20.393	712.47	28.050	-194.49	-7.657
OD 23.38, 0°	519.68	20.460	588.21	23.158	-68.53	-2.698
OD 23.38, 60°	517.45	20.372	477.52	18.800	39.93	1.572
OD 23.38, 120°	517.60	20.378	479.96	18.896	37.64	1.482
OD 38.75, 0°	519.48	20.452	531.22	20.914	-11.73	-0.462
OD 38.75, 60°	517.14	20.360	514.73	20.265	2.41	0.095
OD 38.75, 120°	517.78	20.385	509.52	20.060	8.26	0.325
L1, 0°	987.42	38.875	896.52	35.296	90.91	3.579
L1, 60°	987.93	38.895	879.91	34.642	108.03	4.253
L1, 120°	988.14	38.903	842.09	33.153	146.05	5.750
L1, 180°	987.12	38.863	814.65	32.073	172.47	6.790
L1, 240°	986.92	38.855	821.59	32.346	165.33	6.509
L1, 300°	986.97	38.857	873.30	34.382	113.67	4.475

Table E 3.3: LHV RV, Fore, and Aft Cover Inspection Data

Measurement Designation	Pre-Test		Post-Test		Measurement Change	
	(mm)	(in.)	(mm)	(in.)	(mm)	(in.)
OD A, 0°	500.68	19.712	500.63	19.710	0.05	0.002
OD A, 60°	500.63	19.710	500.91	19.721	-0.28	-0.011
OD A, 120°	500.89	19.720	500.94	19.722	-0.05	-0.002
ID B, 0°	426.59	16.795	426.47	16.790	0.13	0.005
ID B, 60°	426.39	16.787	426.67	16.798	-0.28	-0.011
ID B, 120°	426.72	16.800	426.59	16.795	0.13	0.005
ID C, 0°	490.55	19.313	490.27	19.302	0.28	0.011
ID C, 60°	491.08	19.334	491.13	19.336	-0.05	-0.002
ID C, 120°	491.21	19.339	490.86	19.325	0.36	0.014
L2, 0°	236.19	9.299	234.39	9.228	1.80	0.071
L2, 60°	236.02	9.292	235.99	9.291	0.03	0.001
L2, 120°	235.79	9.283	235.89	9.281	-0.10	-0.004
L2, 180°	235.74	9.281	234.29	9.224	1.45	0.057
L2, 240°	235.76	9.282	232.59	9.157	3.17	0.125
L2, 300°	235.89	9.287	232.56	9.156	3.33	0.131
OD B, 0°	431.50	16.988	431.83	17.001	-0.33	-0.013
OD B, 60°	431.65	16.994	431.47	16.987	0.18	0.007
OD B, 120°	431.62	16.993	431.80	17.000	-0.18	-0.007
ID D, 0°	165.71	6.524	*	*	N/A	N/A
ID D, 60°	165.79	6.527	*	*	N/A	N/A
ID D, 120°	165.76	6.526	*	*	N/A	N/A
L1, 0°	840.92	33.107	*	*	N/A	N/A
L1, 60°	840.89	33.106	*	*	N/A	N/A

Table E 3.3: LHV RV, Fore, and Aft Cover Inspection Data

Measurement Designation	Pre-Test		Post-Test		Measurement Change	
	(mm)	(in.)	(mm)	(in.)	(mm)	(in.)
L1, 120°	840.92	33.107	*	*	N/A	N/A
L1, 180°	840.94	33.108	*	*	N/A	N/A
L1, 240°	840.94	33.108	*	*	N/A	N/A
L1, 300°	840.92	33.107	*	*	N/A	N/A
OD D, 0°	171.30	6.744	173.33	6.824	-2.03	-0.080
OD D, 60°	171.27	6.743	171.81	6.764	-0.53	-0.021
OD D, 120°	171.25	6.742	171.96	6.770	-0.71	-0.028
OD E, 0°	482.60	19.000	499.44	19.663	-16.84	-0.663
OD E, 60°	481.41	18.953	442.57	17.424	38.84	1.529
OD E, 120°	481.51	18.957	465.79	18.338	15.72	0.619

* Part destroyed during test and measurement not possible.

Table E 4.1: HHV H1224A Container Body Inspection Data

Measurement Designation	Pre-Test		Post-Test		Measurement Change	
	(mm)	(in.)	(mm)	(in.)	(mm)	(in.)
OD 0, 0°	822.63	32.387	786.33	30.958	36.30	1.429
OD 0, 45°	824.18	32.448	842.01	33.150	-17.83	-0.702
OD 0, 90°	821.64	32.348	818.13	32.210	3.51	0.138
OD 0, 135°	823.19	32.409	815.04	32.088	8.15	0.321
OD 1, 0°	825.70	32.508	780.36	30.723	45.34	1.785
OD 1, 45°	826.82	32.552	838.48	33.011	-11.66	-0.459
OD 1, 90°	823.70	32.429	822.99	32.401	0.71	0.028
OD 1, 135°	823.06	32.404	809.14	31.856	13.92	0.548

Table E 4.1: HHV H1224A Container Body Inspection Data

Measurement Designation	Pre-Test		Post-Test		Measurement Change	
	(mm)	(in.)	(mm)	(in.)	(mm)	(in.)
OD 20, 0°	823.87	32.436	650.70	25.618	173.18	6.818
OD 20, 45°	825.68	32.507	820.93	32.320	4.75	0.187
OD 20, 90°	823.24	32.411	945.21	37.213	-121.97	-4.802
OD 20, 135°	822.02	32.363	797.64	31.403	24.38	0.960
OD 21, 0°	856.56	33.723	676.50	26.634	180.06	7.089
OD 21, 45°	858.27	33.790	858.24	33.789	0.03	0.001
OD 21, 90°	854.74	33.651	981.89	38.657	-127.15	-5.006
OD 21, 135°	853.74	33.612	825.58	32.503	28.17	1.109
OD 22, 0°	824.31	32.453	629.72	24.792	194.59	7.661
OD 22, 45°	827.00	32.559	813.89	32.043	13.11	0.516
OD 22, 90°	823.93	32.438	965.76	38.022	-141.83	-5.584
OD 22, 135°	822.66	32.388	791.92	31.178	30.73	1.210
OD 24, 0°	823.21	32.410	614.12	24.178	209.09	8.232
OD 24, 45°	826.26	32.530	807.59	31.795	18.67	0.735
OD 24, 90°	823.24	32.411	982.09	38.665	-158.85	-6.254
OD 24, 135°	822.53	32.383	782.70	30.815	39.83	1.568
OD 25, 0°	822.96	32.400	597.61	23.528	225.35	8.872
OD 25, 45°	825.45	32.498	798.78	31.448	26.67	1.050
OD 25, 90°	822.33	32.375	980.03	38.584	-157.71	-6.209
OD 25, 135°	822.07	32.365	779.42	30.686	42.65	1.679
OD 26, 0°	908.51	35.768	682.96	26.888	225.55	8.880
OD 26, 45°	910.44	35.844	782.70	30.815	127.74	5.029
OD 26, 90°	909.78	35.818	1059.05	41.695	-149.28	-5.877
OD 26, 135°	907.49	35.728	907.03	35.710	0.46	0.018

Table E 4.1: HHV H1224A Container Body Inspection Data

Measurement Designation	Pre-Test		Post-Test		Measurement Change	
	(mm)	(in.)	(mm)	(in.)	(mm)	(in.)
OD 27, 0°	819.81	32.276	585.09	23.035	234.72	9.241
OD 27, 45°	821.87	32.357	747.67	29.436	74.19	2.921
OD 27, 90°	820.55	32.305	978.53	38.525	-157.99	-6.220
OD 27, 135°	818.54	32.226	828.42	32.615	-9.88	-0.389
OD 28, 0°	810.39	31.905	591.41	23.284	218.97	8.621
OD 28, 45°	813.51	32.028	745.95	29.368	67.56	2.660
OD 28, 90°	810.92	31.926	968.32	38.123	-157.40	-6.197
OD 28, 135°	814.22	32.056	818.59	32.228	-4.37	-0.172
OD 37.75, 0°	809.60	31.874	634.90	24.996	174.70	6.878
OD 37.75, 45°	811.68	31.956	775.28	30.523	36.40	1.433
OD 37.75, 90°	806.86	31.766	951.56	37.463	-144.70	-5.697
OD 37.75, 135°	816.89	32.161	809.83	31.883	7.06	0.278
OD 38.75, 0°	808.05	31.813	634.52	24.981	173.53	6.832
OD 38.75, 45°	808.43	31.828	775.67	30.538	32.77	1.290
OD 38.75, 90°	804.24	31.663	947.62	37.308	-143.38	-5.645
OD 38.75, 135°	816.33	32.139	806.15	31.738	10.19	0.401
OD 39.75, 0°	833.27	32.806	649.63	25.576	183.64	7.230
OD 39.75, 45°	832.36	32.770	798.53	31.438	33.83	1.332
OD 39.75, 90°	829.23	32.647	961.97	37.873	-132.74	-5.226
OD 39.75, 135°	833.70	32.823	834.59	32.858	-0.89	-0.035
OD 40.75, 0°	809.02	31.851	641.25	25.246	167.77	6.605
OD 40.75, 45°	809.57	31.873	787.10	30.988	22.48	0.885
OD 40.75, 90°	803.22	31.623	938.48	36.948	-135.26	-5.325
OD 40.75, 135°	816.81	32.158	806.78	31.763	10.03	0.395

Table E 4.1: HHV H1224A Container Body Inspection Data

Measurement Designation	Pre-Test		Post-Test		Measurement Change	
	(mm)	(in.)	(mm)	(in.)	(mm)	(in.)
OD 41.75, 0°	810.77	31.920	644.80	25.386	165.96	6.534
OD 41.75, 45°	812.24	31.978	791.54	31.163	20.70	0.815
OD 41.75, 90°	805.51	31.713	935.94	36.848	-130.43	-5.135
OD 41.75, 135°	818.24	32.214	808.69	31.838	9.55	0.376
OD 50.5, 0°	811.61	31.953	614.32	24.186	197.28	7.767
OD 50.5, 45°	812.42	31.985	809.96	31.888	2.46	0.097
OD 50.5, 90°	807.82	31.804	851.87	33.538	-44.04	-1.734
OD 50.5, 135°	817.24	32.175	806.70	31.760	10.54	0.415
OD 51.5, 0°	816.13	32.131	762.00	30.000	54.13	2.131
OD 51.5, 45°	817.17	32.172	*	*	N/A	N/A
OD 51.5, 90°	815.01	32.087	833.45	32.813	-18.44	-0.726
OD 51.5, 135°	825.32	32.493	*	*	N/A	N/A
OD 52.5, 0°	816.66	32.152	764.54	30.100	52.12	2.052
OD 52.5, 45°	831.09	32.720	*	*	N/A	N/A
OD 52.5, 90°	817.91	32.201	828.04	32.600	-10.13	-0.399
OD 52.5, 135°	825.32	32.493	*	*	N/A	N/A
L1, 0°	1458.04	57.403	*	*	N/A	N/A
L1, 45°	1454.76	57.274	*	*	N/A	N/A
L1, 90°	1454.89	57.279	*	*	N/A	N/A
L1, 135°	1456.18	57.330	*	*	N/A	N/A
L1, 180°	1457.55	57.384	*	*	N/A	N/A
L1, 225°	1457.88	57.397	*	*	N/A	N/A
L1, 270°	1457.58	57.385	*	*	N/A	N/A
L1, 315°	1458.52	57.422	*	*	N/A	N/A

Table E 4.1: HHV H1224A Container Body Inspection Data

Measurement Designation	Pre-Test		Post-Test		Measurement Change	
	(mm)	(in.)	(mm)	(in.)	(mm)	(in.)
L2, 0°	1343.10	52.878	*	*	N/A	N/A
L2, 45°	1338.61	52.701	*	*	N/A	N/A
L2, 90°	1338.58	52.700	*	*	N/A	N/A
L2, 135°	1340.31	52.768	*	*	N/A	N/A
L2, 180°	1342.06	52.837	*	*	N/A	N/A
L2, 225°	1341.09	52.799	*	*	N/A	N/A
L2, 270°	1341.35	52.809	*	*	N/A	N/A
L2, 315°	1341.70	52.823	*	*	N/A	N/A

* Part destroyed during test and measurement not possible.

Table E 4.2: HHV Inner Container Inspection Data

Measurement Designation	Pre-Test		Post-Test		Measurement Change	
	(mm)	(in.)	(mm)	(in.)	(mm)	(in.)
OD 0, 0°	520.83	20.505	527.51	20.768	-6.68	-0.263
OD 0, 60°	517.53	20.375	528.32	20.800	-10.80	-0.425
OD 0, 120°	517.63	20.379	513.97	20.235	3.66	0.144
OD 11.38, 0°	518.57	20.416	470.05	18.506	48.51	1.910
OD 11.38, 60°	517.42	20.371	528.35	20.801	-10.92	-0.430
OD 11.38, 120°	517.58	20.377	539.39	21.236	-21.82	-0.859
OD 17.38, 0°	520.22	20.481	400.53	15.769	119.68	4.712
OD 17.38, 60°	518.08	20.397	507.90	19.996	10.19	0.401
OD 17.38, 120°	518.24	20.403	506.91	19.957	11.33	0.446
OD 23.38, 0°	519.05	20.435	469.52	18.485	49.53	1.950

Table E 4.2: HHV Inner Container Inspection Data

Measurement Designation	Pre-Test		Post-Test		Measurement Change	
	(mm)	(in.)	(mm)	(in.)	(mm)	(in.)
OD 23.38, 60°	517.17	20.361	465.66	18.333	51.51	2.028
OD 23.38, 120°	517.09	20.358	502.21	19.772	14.88	0.586
OD 38.75, 0°	518.74	20.423	483.46	19.034	35.28	1.389
OD 38.75, 60°	517.53	20.375	595.58	23.448	-78.05	-3.073
OD 38.75, 120°	517.63	20.379	531.24	20.915	-13.61	-0.536
L1, 0°	986.23	38.828	982.68	38.688	3.56	0.140
L1, 60°	986.71	38.847	974.72	38.375	11.99	0.472
L1, 120°	987.12	38.863	971.55	38.250	15.57	0.613
L1, 180°	987.15	38.864	960.45	37.813	26.70	1.051
L1, 240°	987.04	38.860	966.80	38.063	20.24	0.797
L1, 300°	987.04	38.860	979.50	38.563	7.54	0.297

Table E 4.3: HHV RV, Fore, and Aft Cover Inspection Data

Measurement Designation	Pre-Test		Post-Test		Measurement Change	
	(mm)	(in.)	(mm)	(in.)	(mm)	(in.)
OD A, 0°	502.72	19.792	*	*	N/A	N/A
OD A, 60°	502.92	19.800	508.97	20.038	-6.05	-0.238
OD A, 120°	502.56	19.786	507.11	19.965	-4.55	-0.179
ID B, 0°	426.21	16.780	345.44	13.600	80.77	3.180
ID B, 60°	426.26	16.782	441.96	17.400	-15.70	-0.618
ID B, 120°	426.36	16.786	462.28	18.200	-35.92	-1.414
ID C, 0°	490.88	19.326	454.18	17.881	36.70	1.445
ID C, 60°	490.68	19.318	520.85	20.506	-30.18	-1.188

Table E 4.3: HHV RV, Fore, and Aft Cover Inspection Data

Measurement Designation	Pre-Test		Post-Test		Measurement Change	
	(mm)	(in.)	(mm)	(in.)	(mm)	(in.)
ID C, 120°	490.32	19.304	514.60	20.260	-24.28	-0.956
L2, 0°	234.87	9.247	227.20	8.945	7.67	0.302
L2, 60°	235.25	9.262	210.31	8.280	24.94	0.982
L2, 120°	235.48	9.271	226.70	8.925	8.79	0.346
L2, 180°	235.25	9.262	224.41	8.835	10.85	0.427
L2, 240°	234.87	9.247	224.16	8.825	10.72	0.422
L2, 300°	234.62	9.237	227.08	8.940	7.54	0.297
OD B, 0°	431.55	16.990	*	*	N/A	N/A
OD B, 60°	431.50	16.988	433.43	17.064	-1.93	-0.076
OD B, 120°	431.32	16.981	432.54	17.029	-1.22	-0.048
ID D, 0°	165.74	6.525	166.47	6.554	-0.74	-0.029
ID D, 60°	165.74	6.525	169.95	6.691	-4.22	-0.166
ID D, 120°	165.74	6.525	170.21	6.701	-4.47	-0.176
L1, 0°	840.77	33.101	*	*	N/A	N/A
L1, 60°	840.74	33.100	846.33	33.320	-5.59	-0.22
L1, 120°	840.74	33.100	841.07	33.113	-0.033	-0.013
L1, 180°	840.79	33.102	*	*	N/A	N/A
L1, 240°	840.79	33.102	838.99	33.031	1.80	0.071
L1, 300°	840.74	33.100	842.54	33.171	-1.80	-0.071
OD D, 0°	171.20	6.740	170.87	6.727	0.33	0.013
OD D, 60°	171.20	6.740	171.40	6.748	-0.20	-0.008
OD D, 120°	171.17	6.739	171.45	6.750	-0.28	-0.011
OD E, 0°	482.88	19.011	470.41	18.520	12.47	0.491
OD E, 60°	482.85	19.010	483.29	19.027	-0.43	-0.017

Table E 4.3: HHV RV, Fore, and Aft Cover Inspection Data

Measurement Designation	Pre-Test		Post-Test		Measurement Change	
	(mm)	(in.)	(mm)	(in.)	(mm)	(in.)
OD E, 120°	482.85	19.010	483.41	19.032	-0.56	-0.022

* Part destroyed during test and measurement not possible.

Distribution List

No. of
Copies

- | | | | |
|---|---|---|--|
| 1 | Director, Defense Nuclear Agency
ATTN: CSTI
6801 Telegraph Road
Alexandria, VA 22310-3398 | 1 | Director, Defense Nuclear Agency
ATTN: Wayne Andrews
6801 Telegraph Road
Alexandria, VA 22310-3398 |
| 1 | Director, Defense Nuclear Agency
ATTN: Kenneth Stein
6801 Telegraph Road
Alexandria, VA 22310-3398 | 1 | Director, Defense Nuclear Agency
ATTN: Jack Deplitch
6801 Telegraph Road
Alexandria, VA 22310-3398 |
| 1 | Director, Defense Nuclear Agency
ATTN: Martin Fuentes
6801 Telegraph Road
Alexandria, VA 22310-3398 | 1 | DASAIC
816 State Street
P.O. Drawer QQ
Santa Barbara, CA 93102 |
| 1 | Weidlinger Associates
ATTN: J. Isenberg and H. Levine
4410 El Camino Real, Suite 110
Los Altos, CA 94022 | 1 | U. S. Department of Energy
Albuquerque Operations Office
Albuquerque Headquarters
Attn: H. T. Season
R. O. Gergen
P. O. Box 5400
Albuquerque, NM 87115 |
| 1 | Logicon RDA
ATTN: Steve Woodford
6940 South Kings Highway, Suite 210
Alexandria, VA 22310 | 1 | Defense Technical Information Center
Cameron Station
Alexandria, VA 22304-6145 |

Internal Distribution:

<u>No. of</u>	<u>Copies</u>	
1	MS 0631	R. L. Schwoebel, 12300
1	MS 0490	P. E. D'Antonio, 12324
1	MS 0491	R. E. Smith, 12333
1	MS 0491	C. G. Shirley, 12333
1	MS 0490	NSIC File SGD-8d2a[Container Testing]
1	MS 0479	D. C. Tipton, 5151
1	MS 0479	R. E. Davis, 5151
1	MS 0479	M. L. Kargel, 5151
1	MS 0724	D. L. Hartley, 6000
1	MS 0405	T. R. Jones, 6411
1	MS 0726	J. B. Woodard, 6600
1	MS 0726	L. E. Martin, 6600
1	MS 0715	R. E. Luna, 6603 Attn: TTC Master File
15	MS 0715	TTC Library, 6603
1	MS 0718	H. R. Yoshimura, 6641
1	MS 0718	J. D. Whitlow, 6641
1	MS 0717	G. F. Hohnstreiter, 6642
1	MS 0717	D. J. Ammerman, 6642
1	MS 0717	M. Arviso, 6642
1	MS 0717	J. G. Bobbe, 6642
15	MS 0717	D. C. Harding, 6642
1	MS 0717	J. D. Pierce, 6642
1	MS 0717	W. L. Uncapher, 6642
1	MS 0716	M. C. Brady, 6643
1	MS 0716	D. R. Stenberg, 6643
5	MS 0899	Technical Library, 7141
1	MS 0619	Technical Publications, 7151
1	MS 9018	Central Technical Files, 8523-2
10	MS 0100	Document Processing for DOE/OSTI, 7613-2